UNIVERSIDAD DE BUENOS AIRES
Facultad de Ciencias Exactas y Naturales
Departamento de Matemática

Métodos algebraicos para el estudio de redes bioquímicas

Tesis presentada para optar al título de Doctor de la Universidad de Buenos Aires en el área Ciencias Matemáticas

Mercedes Soledad Pérez Millán

Director de tesis: Dra. Alicia Dickenstein
Consejero de estudios: Dra. Alicia Dickenstein

Buenos Aires, noviembre 2011

Métodos algebraicos para el estudio de redes bioquímicas

Resumen

El principal objetivo de este trabajo es aplicar y desarrollar herramientas de álgebra (computacional) para estudiar redes bioquímicas. Empezamos encontrando invariantes que se satisfacen en los estados de equilibrio. Luego estudiamos sistemas cuyos estados de equilibrio se describen por binomios y los llamamos "sistemas con estados de equilibrio tóricos". Mostramos que el importante mecanismo enzimático de fosforilaciones secuenciales distributivas tiene esta característica. Después establecemos la relación, en el espacio de las constantes de reacción, entre sistemas con "complejos balanceados" y sistemas con microrreversibilidad, cuyos estados de equilibrio positivos satisfacen relaciones binomiales particulares. Finalizamos este enfoque continuo incorporando resultados computacionales para estados de equilibrio positivos desde la persectiva de la geometría algebraica real.

Finalmente, presentamos un modelo discreto del módulo de regulación del factor nuclear NF-κB, por medio de un sistema polinomial dinámico discreto. Este enfoque permite estudiar redes cuya información disponible es poco detallada, con la idea de proveer una primera descripción de las interacciones de la red a través de métodos de álgebra computacional.

Palabras clave: redes de reacciones químicas, cinética de acción de masas, sistemas polinomiales, modelado discreto, álgebra computacional.

Algebraic methods for the study of biochemical networks

Abstract

The main goal of this work is to apply and develop (computational) algebraic tools for the study of biochemical networks. We start by finding invariants that are satisfied at steady state. We then study systems whose steady states are described by binomials, and call them "systems with toric steady states". We show that the important enzymatic mechanism of sequential and distributive phosphorylations has this feature. Afterwards, we state the relationship, in rate constant space, between "complex balanced" and "detailed balanced" systems, whose positive steady states satisfy special binomial relations. We end this continuous approach by expanding on computational results for positive steady states from a real algebraic geometry perspective.

Finally, we present a discrete model for the NF-κB regulatory module, by means of a discrete polynomial dynamical system. This approach allows to study networks with poorly detailed data available, with the idea of providing a first description of the interactions of the network through computational algebra methods.

Key words: chemical reaction networks, mass–action kinetics, polynomial systems, discrete modeling, computational algebra.

Agradecimientos

Quisiera agradecerles a todos aquellos que, directa o indirectamente, contribuyeron a que esta tesis llegara a concretarse en tiempo y forma.

Antes que nada, a Alicia, por haberme dado tantas oportunidades y por haberme presentado este tema tan lindo. Por todas las experiencias, con las que he podido crecer mucho en mi aspecto académico. Y por todos los consejos y el tiempo invertido en mí.

A mis hermanos académicos, Nico, Fede y Enrique, porque sin ellos no habría podido sobrevivir a las dificultades de esta etapa doctoral. Por las horas de catarsis, las ayudas matemáticas, lingüísticas e informáticas, los bailes, los cantos, etc.

A mis colaboradores, por toda la ayuda y paciencia que han tenido. Y por todo lo que me han enseñado. Especialmente agradezco a Anne y a Jeremy por haberme invitado a sus lugares de trabajo para avanzar en nuestros proyectos conjuntos.

A todos aquellos que nos han brindado algún dato que nos ayudó a avanzar. A Daniel Perrucci, Martín Mereb, Teresa Krick, Pablo Solernó, Martin Feinberg. A los organizadores del "2008-09 Program on Algebraic Methods in Systems Biology and Statistics" en SAMSI, por la gran oportunidad que me dieron para conocer a muchos especialistas en este tema. Y a todos los organizadores del Biomat, por el esfuerzo que han hecho y siguen haciendo para impulsar la interdisciplina en nuestro país. También gracias a Damián Álvarez Paggi, y especialmente a Florencia Molinas, por ayudarme desde el lado biológico/químico.

A Gabriela Gil, mi profesora de matemática del IMA y principal responsable de que haya seguido esta carrera, por toda la confianza que me tuvo desde el primer momento.

A mis compañeros de oficina, quienes han hecho muy llevadero mi tránsito por esta etapa, me han ayudado con muchas cuestiones académicas, y se han convertido en muy buenos amigos, que han estado en las buenas y en las malas: Nico, Fede, Fer, Fran, Juan Pablo, Juanjo, Leandro, Mari, Nico C., Pablo, Vero, Tertu. Y también a mis compañeros "de pasillo" y afines: Mariano, Santiago y, especialmente, Alexandra.

También agradezco a mis compañeros de clase en el CBC y a los coordinadores, por las oportunidades que me han dado y por mostrarme que mis esfuerzos valen la pena.

A las chicas y a los chicos del DM por todo lo compartido; en especial a Ani, Caro e Isa, que me supieron acompañar tanto en los momentos buenos como en los difíciles.

A mis compañeros del taller de tango. Ese espacio que me ha dado tanto en mi vida. Un lugar lleno de gente preciosa, que me ha enseñado mucho más que el baile.

A Lucas, quien ha sabido ganar mi corazón. Quien me ha enseñado a compartir la vida, escuchando y comprometiéndose, y me ha soportado y ayudado en los momentos más atareados.

Y, por supuesto, a mi familia. A mi mamá, a mi papá y a mi Buba, que siempre han estado ahí. Apoyándome, comprendiéndome, escuchándome, y que sin ellos nunca habría podido llegar a esta instancia de mi vida.

Introducción

La matemática es una herramienta importante para abordar muchos de los problemas que surgen hoy en día en la biología, a la vez que la biología es una nueva puerta para el desarrollo de futuras teorías matemáticas. El objetivo principal de este trabajo es aplicar y desarrollar herramientas algebraicas (computacionales) para el estudio de redes de reacciones bioquímicas.

Mayormente abordamos estas redes bioquímicas con un modelado dinámico continuo. En general, las no linealidades encontradas en las redes moleculares impiden el análisis matemático del comportamiento de la red, el cual ha sido ampliamente estudiado por medio de simulaciones numéricas, para las cuales los detalles bioquímicos y los valores numéricos de todos los parámetros se deben especificar de antemano. Esto ha hecho difícil, si no imposible, "ver el bosque en lugar del árbol" y discernir principios generales entre la apabullante complejidad molecular de los procesos celulares. Sin embargo, las redes moleculares dan lugar, a través de la cinética de acción de masas, a sistemas polinomiales dinámicos, cuyos estados de equilibrio son ceros de un conjunto de ecuaciones polinomiales. Estas ecuaciones se pueden analizar por medio de métodos algebraicos, en los cuales los parámetros son tratados como expresiones simbólicas cuyos valores numéricos no tienen que ser sabidos de antemano.

Karin Gatermann introdujo la conexión entre cinética de acción de masas y el álgebra computacional a comienzos de la última década [54–56]. Gunawardena también empezó a abordar estos resultados de la Teoría de Redes de Reacciones Químicas (CRNT, por sus iniciales en inglés) con herramientas algebraicas [63, 64, 112, 164]. En [30], Craciun et ál. estudiaron los sistemas dinámicos tóricos (o sistemas de acción de masas con "complejos balanceados"), cuya característica principal es que el locus de sus estados de equilibrio es una variedad tórica, con una perspectiva álgebro-geométrica. Ellos coinciden con Gatermann en que "las ventajas de las variedades tóricas son bien conocidas", y desarrollan la teoría básica de sistemas dinámicos tóricos en el contexto de la geometría algebraica computacional.

Desde ese entonces, se han introducido más herramientas algebraicas, aunque la mayoría de ellas todavía son básicas. Trabajamos a lo largo de esta tesis sobre la dirección algebraica, con la intención de incorporar más herramientas del álgebra, la matemática discreta, la combinatoria, el álgebra computacional, la geometría algebraica y la geometría algebraica real. Aplicamos algunos de nuestros resultados a redes biológicas bien conocidas.

En los primeros capítulos de este trabajo tratamos con resultados sobre sistemas de reacciones químicas. Nuestro foco está mayormente sobre los estados de equilibrio de sistemas de reacciones químicas. Primero encontramos invariantes (lineales en los complejos) que se satisfacen en los estados de equilibrio. Estos invariantes son útiles para verificar la idoneidad del sistema. Luego nos movemos a sistemas cuyos estados de equilibrio se describen por binomios. Decimos que estos sistemas tienen estados de equilibrio tóricos. Mostramos

que el importante mecanismo de fosforilaciones y defosforilaciones secuenciales por un par de enzimas quinasa/fosfatasa tiene esta propiedad. Después establecemos la relación, en el espacio de las constantes de reacción, entre sistemas con "complejos balanceados" y sistemas con microrreversibilidad, cuyos estados de equilibrio positivos satisfacen relaciones binomiales particulares. Finalizamos este enfoque continuo incorporando resultados computacionales para estados de equilibrio positivos desde la perspectiva de la geometría algebraica real.

En el último capítulo incorporamos un nuevo tipo de modelado, concretamente un modelo algebraico discreto y determinístico para describir un sistema biológico específico: proponemos y estudiamos un modelo discreto para el módulo de regulación del factor nuclear NF-κB. Este último enfoque fue introducido por primera vez en la década de 1960 con modelos de redes Booleanas. Los modelos cualitativos de las redes moleculares, como los modelos lógicos, no requieren parámetros cinéticos pero igual pueden proveer información sobre la dinámica de la red y sirven como herramientas para generar hipótesis. El análisis estructural y cualitativo está emergiendo como una alternativa viable y útil [124,134,171]. Además, los modelos discretos tienen la ventaja de ser más intuitivos que los modelos basados en ecuaciones diferenciales, así que le han añadido cierto atractivo para los investigadores sin una formación matemática sólida. En Hinkelmann et ál. [75], los autores proponen un marco de trabajo matemático de sistemas polinomiales dinámicos sobre un cuerpo finito, el cual provee acceso a herramientas teóricas y computacionales de álgebra y matemática discreta, que nosotros perseguimos.

Invitamos al lector a inspeccionar la introducción de cada capítulo de esta tesis para una visión más profunda de nuestro trabajo y la bibliografía relacionada. En la página 139, se puede encontrar una lista con la notación del trabajo.

Para una mejor comprensión del esquema de este trabajo, introducimos brevemente algo de terminología en los siguientes párrafos.

Una *red de reacciones químicas* es un grafo dirigido finito cuyos vértices están etiquetados por complejos y cuyas aristas representan las reacciones. El digrafo G tiene m vértices, y el vértice i de G representa el i-ésimo complejo químico, al cual le asociamos el monomio $x^{y_i} = x_1^{y_{i1}} x_2^{y_{i2}} \cdots x_s^{y_{is}}$. Las incógnitas $x_1, x_2, \ldots, x_s$ representan las concentraciones de las s especies en la red, y las consideramos funciones $x_i(t)$ del tiempo t. Estas redes de reacciones químicas usualmente se asumen bajo cinética de acción de masas y la dinámica se describe a través de un sistema de ecuaciones diferenciales autónomas, $\frac{d\mathbf{x}}{dt} = f(\mathbf{x})$, donde $\mathbf{x} = (x_1, x_2, \ldots, x_s)$. Un aspecto importante de la dinámica es estudiar los estados de equilibrio del sistema, es decir, los valores de $\mathbf{x}$ para los cuales $f(\mathbf{x}) = 0$. Bajo cinética de acción de masas, las funciones coordenadas $f_1, \ldots, f_s$ son polinomios en las concentraciones de las especies $x_1, \ldots, x_s$ y los estados de equilibrio del sistema forman la variedad (real no negativa) del ideal $I = \langle f_1, \ldots, f_s \rangle$.

Generalmente, los sistemas de cinética de acción de masas se descomponen en $f(\mathbf{x}) = \Sigma\Psi(\mathbf{x})$, donde Σ es una matriz $s \times m$ que guarda los coeficientes del sistema polinomial, y $\Psi(\mathbf{x})$ guarda los monomios. La matriz Σ de estos sistemas particulares de cinética de acción de masas tiene muchas características interesantes. Se puede decir mucho a partir de esta generosa linealidad, y muchos de los resultados en esta área explotan esta característica del sistema. Incluso para describir los estados de equilibrio, las propiedades de la matriz Σ son muy útiles, y tomamos ventaja de ellas en los Capítulos 3, 4 y 5. Sin embargo, como mencionamos en el párrafo anterior, encontrar los estados de equilibrio del sistema es equivalente a resolver el

sistema polinomial $f_1(\mathbf{x}) = \cdots = f_s(\mathbf{x}) = 0$, que a su vez es equivalente a describir la variedad del ideal $I = \langle f_1, \ldots, f_s \rangle$. Más aún, uno está interesado en buscar los ceros *positivos* del ideal I, y esto invita a la *geometría algebraica real* a jugar un rol importante en esta búsqueda. Presentamos en los Capítulos 4 y 5 algunas herramientas de la geometría algebraica, y le abrimos la puerta a la geometría algebraica real en el Capítulo 6. Además introducimos algunas condiciones semialgebraicas para las constantes de reacción en el Capítulo 4.

Otro enfoque para modelar redes biológicas se presenta en el Capítulo 7, donde trabajamos con un modelo discreto de un sistema biológico específico: el módulo de regulación del factor nuclear NF-κB. NF-κB es una familia de factores de transcripción de expresión ubicua que regula la expresión de numerosos genes que juegan roles importantes en respuestas celulares, crecimiento celular, supervivencia y respuestas inflamatorias e inmunes. Los modelos discretos han surgido como una alternativa a los modelos continuos cuando la intención es estudiar redes con información disponible poco detallada, con la idea de proveer una primera descripción de las interacciones de la red por medio de métodos del álgebra computacional. Una de las ventajas de este tipo de modelado es que es independiente de parámetros como constantes de afinidad y catalíticas específicas, las cuales en muchos casos son muy difíciles de determinar y requieren un profundo conocimiento del sistema (lo cual, salvo para el módulo de regulación de NF–κB y algún otro caso particular, es muy poco frecuente). Además, aunque tuviéramos datos experimentales con precisión perfecta y resolución temporal ilimitada, los modelos de sistemas dinámicos continuos suelen ser no identificables (es decir, dos redes de reacciones diferentes pueden generar sistemas dinámicos continuos idénticos, lo que hace imposible discriminar entre ellos).

Reconstruimos la red como un *sistema dinámico discreto*, con un enfoque cualitativo determinístico. Para ser más precisos, es un sistema polinomial dinámico sobre el cuerpo base $\mathbb{F}_3$. El camino de transducción de señales de NF-κB también ha sido abordado con modelos de ecuaciones diferenciales. Nuestro modelo se basa en uno de estos modelos continuos y además en información experimental de la literatura.

Outline y contribución

En el Capítulo 2 comenzamos presentando algunos preliminares de la teoría de redes de reacciones químicas. Recolectamos definiciones de la literatura, principalmente de [48, 80] y preparamos el escenario para nuestros resultados presentes en los capítulos subsiguientes.

En el Capítulo 3, explotamos la teoría de redes reacciones químicas para desarrollar un procedimiento eficiente para calcular invariantes que son combinaciones lineales simbólicas de "complejos", o los monomios provenientes de cinética de acción de masas. Recuperamos, como un caso especial, el Teorema de Shinar y Feinberg [144], que da condiciones estructurales para que una red de deficiencia uno tenga "robustez de concentración absoluta" (ACR por sus iniciales en inglés). Luego usamos invariantes lineales en los complejos para analizar dos ejemplos de bifuncionalidad enzimática, el regulador de osmolaridad bacteriano EnvZ/OmpR, que tiene deficiencia dos, y el regulador glicolítico fosfofructoquinasa-2-fructosa-2 ,6-bisfosfatasa de mamíferos, que tiene deficiencia cuatro, mostrando cómo los métodos desarrollados en ese capítulo se pueden utilizar para el análisis algebraico de los estados de equilibrio de redes realistas.

En el Capítulo 4, nos enfocamos en sistemas donde el ideal de los estados de equilibrio es un ideal binomial. Decimos que tales sistemas tienen estados de equilibrio tóricos. Damos condiciones suficientes para que un sistema de reacciones químicas tenga estados de equilibrio tóricos (Teoremas 4.2.2 y 4.2.4) y mostramos en este caso que el locus de estados de equilibrio tiene una buena parametrización monomial (Teoremas 4.2.3 y 4.2.5). Además analizamos la capacidad de estos sistemas de exhibir estados de equilibrio positivos y multiestacionaridad. Una aplicación importante de nuestro trabajo se refiere a las redes que describen la fosforilación en varios sitios de una proteína por un par quinasa/fosfatasa en un mecanismo secuencial distributivo. El Teorema 4.3.1 resume nuestros resultados en estos sistemas.

En el Capítulo 5, clarificamos la relación entre las condiciones algebraicas que deben satisfacer las constantes de reacción en sistemas de cinética (de acción de masas) generalizada para la existencia de estados de equilibrio microrreversibles ("detailed balancing") o con "complejos balanceados" ("complex balancing"). Estos sistemas tienen una amplia aplicación en química y biología [32, 60, 64, 112, 142, 146]. Sus propiedades principales han sido establecidas por Horn, Jackson y Feinberg [45, 49, 50, 79–82]. El principal resultado se presenta en el Teorema 5.1.1.

En el Capítulo 6, usamos herramientas del álgebra computacional, la geometría algebraica y la geometría algebraica real para detectar si un sistema de reacciones químicas muestra robustez de concentración absoluta para una cierta especie (definida en [144]). Comentamos sobre las dificultades para un algoritmo general y presentamos algunas condiciones suficientes para que un sistema tenga robustez de concentración absoluta.

El último capítulo de este trabajo, el Capítulo 7, presenta un *modelo algebraico discreto, cualitativo y determinístico* para el módulo de regulación del factor nuclear NF-κB. Para describir la dinámica entre los componentes del sistema del camino de transducción de señales de NF-κB, construimos un modelo discreto mayormente basado en la información molecular presente en Lee et ál. [109] y Hoffmann et ál. [76], y el modelo continuo desarrollado por Lipniacki et ál. [110]. Concebimos estos componentes en una red con once nodos que pueden tomar a lo sumo tres niveles (es decir, discretizamos la información en tres niveles $\{0, 1, 2\}$) y luego construimos un sistema polinomial dinámico $f : \mathbb{F}_3^{11} \to \mathbb{F}_3^{11}$. La estrategia utilizada se basa en un enfoque de abajo hacia arriba, comenzando con un extenso repaso de datos moleculares publicados para reconstruir la red biológica subyacente. Formamos las once funciones correspondientes a cada nodo usando el sistema de álgebra computacional Singular [35]. Finalmente, pudimos reproducir la dinámica observada en el tipo silvestre con estímulo persistente y también en el caso A20 knockout. Este modelo se puede construir con la información que usualmente manejan los biólogos: IκB se une a NF–κB y evita que entre al núcleo, IKKa induce la degradación de IκB, etc. Y a pesar de simplemente requerir este tipo de información, puede brindar más información, como predicciones en casos mutantes.

Publicaciones

El trabajo presentado en esta tesis se basa mayormente en artículos previamente publicados o enviados a publicación. La mayor parte del trabajo se ha hecho en estrecha colaboración con varios coautores.

El Capítulo 3 está basado en

Complex–linear invariants of biochemical networks. Karp R., Pérez Millán M., Dasgupta T., Dickenstein A. and Gunawardena J., 2011. Enviado. [92].

Esencialmente trabajé en todo el artículo. Especialmente, participé en la producción del resultado teórico.

El Capítulo 4 está basado en

Chemical reaction systems with toric steady states. Pérez Millán M., Dickenstein A., Shiu A., Conradi C., 2011. Aceptado para su publicación en el Bulletin of Mathematical Biology.

Disponible en línea en DOI: 10.1007/s11538-011-9685-x. [126].

Aunque trabajé en todo el artículo, particularmente generé un análisis detallado y las pruebas para el sistema para la fosforilación en varios sitios de una proteína por un par quinasa/fosfatasa en un mecanismo secuencial distributivo, lo que fue el punto de partida para producir los resultados más generales de las primeras secciones del artículo.

El Capítulo 5 está basado en

How far is complex balancing from detailed balancing?. Dickenstein A. and Pérez Millán M, 2011. Bulletin of Mathematical Biology, 73:4, pp. 811–828.

Disponible en línea en DOI:10.1007/s11538-010-9611-7. [39].

Mis contribuciones más importantes al artículo fueron los enunciados y pruebas de los resultados principales. También redacté gran parte del trabajo.

El artículo *A discrete model of the nuclear factor NF–κB regulatory network* está en preparación y es trabajo conjunto con J. I. Fuxman Bass y A. S. Jarrah. Se presenta en el Capítulo 7. Mis contribuciones a este trabajo fueron la construcción y el análisis matemáticos del modelo. Establecí las conexiones entre los resultados de este modelo y la teoría de redes de reacciones químicas. Diseñé e implementé los algoritmos, y asistí a J.I.F.B. en la construcción de las tablas.

Contents

1 Introduction **1**
- 1.1 Outline and contribution . . . 3
- 1.2 Publications . . . 4

2 Chemical Reaction Network Theory **7**
- 2.1 Chemical Reaction Systems . . . 7
  - 2.1.1 Mass–action kinetics systems . . . 10
- 2.2 Steady States . . . 14
- 2.3 Stoichiometric Compatibility Class . . . 17
- 2.4 Deficiency . . . 20
- 2.5 Generalized mass–action kinetics . . . 20
  - 2.5.1 The Michaelis-Menten formula . . . 24

3 Invariants of biochemical networks **25**
- 3.1 CRNT and the graphical framework . . . 27
- 3.2 Generating complex-linear invariants . . . 27
  - 3.2.1 Invariants that are not of type 1 . . . 28
- 3.3 Duality and the structure of $\mathcal{I}_k$ . . . 29
- 3.4 Haldane relationships and the S-F Theorem . . . 30
- 3.5 Bifunctional enzymes . . . 32

4 CRS with toric steady states **41**
- 4.1 Toric Steady States . . . 41
- 4.2 Sufficient conditions for toric steady states . . . 44
  - 4.2.1 More general sufficient conditions . . . 52
- 4.3 The n-site phosphorylation system . . . 55
  - 4.3.1 The n-site phosphorylation system . . . 55
  - 4.3.2 Results . . . 57
  - 4.3.3 Proof of Theorem 4.3.1 . . . 59
- 4.4 Multistationarity . . . 63
  - 4.4.1 Second representation of a chemical reaction system . . . 64
  - 4.4.2 Main result on multistationarity . . . 66
  - 4.4.3 Related results . . . 68

5 How far is complex from detailed balancing? 71
5.1 Setting and results . . . 71
5.2 Preliminaries for this chapter . . . 76
5.2.1 Detailed balanced systems . . . 77
5.2.2 The minors of $\mathcal{L}(G)$ . . . 77
5.2.3 The linear relations . . . 78
5.3 Formally and complex balanced systems . . . 79
5.3.1 Formally balanced systems . . . 79
5.3.2 Complex balanced systems . . . 79
5.4 Proof of Theorem 5.1.1 . . . 81
5.5 General kinetic systems . . . 83

6 Finding ACR with tools from computational algebra 87
6.1 Setting . . . 87
6.2 Some basic algebraic notions . . . 88
6.3 First sufficient conditions for ACR . . . 89
6.4 ACR vs. CACR . . . 91
6.5 ACR with tools from real algebraic geometry . . . 93

7 A discrete model for the NF-κB module 101
7.1 Introduction . . . 101
7.2 Background on modeling tools . . . 102
7.3 A continuous model for the NF-κB module . . . 107
7.4 Algebraic modeling of the network . . . 110
7.4.1 A toy model . . . 110
7.4.2 Coming back to NF-κB: our model . . . 113
7.5 Results . . . 117
7.5.1 Comparison with experimental data and the continuous model . . . 117
7.5.2 Conservation and final states . . . 119
7.6 Discussion for this chapter and future work . . . 121

Notation 139

Appendix 1: The functions 143

Appendix 2: Fixed points for S=0 151

Chapter 1

Introduction

Mathematics is an important tool for addressing many of the problems that nowadays arise in biology, while biology is a new gate to the development of future mathematical theories. The main goal of this work is to apply and develop (computational) algebraic tools for the study of biochemical networks.

We mainly approach these biochemical networks by a continuous dynamical modeling. In general, the nonlinearities found in molecular networks prevent mathematical analysis of network behavior, which has largely been studied by numerical simulation, for which the biochemical details and the numerical values of all parameters must be specified in advance. This has made it difficult, if not impossible, to "see the wood for the trees" and to discern general principles within the overwhelming molecular complexity of cellular processes. However, molecular networks give rise, through mass–action kinetics, to polynomial dynamical systems, whose steady states are zeros of a set of polynomial equations. These equations may be analyzed by algebraic methods, in which parameters are treated as symbolic expressions whose numerical values do not have to be known in advance.

Karin Gatermann introduced the connection between mass–action kinetics and computational algebra at the beginning of the last decade [54–56]. Gunawardena also started approaching results from Chemical Reaction Network Theory (CRNT) with algebraic tools [63, 64, 112, 164]. In [30], Craciun et al. studied toric dynamical systems (or complex balanced mass–action systems), whose main feature is that the steady state locus is a toric variety, with an algebro-geometric perspective. They agree with Gatermann in that "the advantages of toric varieties are well-known", and develop the basic theory of toric dynamical systems in the context of computational algebraic geometry.

Since then, more algebraic tools have been introduced, although most of them are still basic. We work throughout this thesis in the algebraic direction, with the intention of incorporating more tools from algebra, discrete mathematics, combinatorics, computational algebra, algebraic geometry and real algebraic geometry. We apply some of our results to well known biological networks.

The first chapters of this work deal with results on chemical reaction systems. Our focus is mainly on steady states of chemical reaction systems. Firstly we find (complex-linear) invariants that are satisfied at steady state. These invariants are useful for verifying the suitability of the model. We then move to systems whose steady states are described by binomials. We say that such systems have toric steady states. We show that the important enzymatic mech-

anism of sequential phosphorylations and dephosphorylations by a pair of kinase/phosphatase enzymes has this feature. Afterwards, we concentrate on systems whose positive steady states satisfy special binomials. They are called in the literature "complex balanced" and "detailed balanced" systems, and we describe the relationship between them. To end this continuous approach, we expand on results for positive steady states.

In the last chapter we incorporate a new type of modeling, namely a discrete deterministic algebraic model for describing a specific biological system: we propose and study a discrete model for the NF-κB regulatory module. This last approach was first introduced in the 1960s with Boolean network models. Qualitative models of molecular networks such as logical models, do not require kinetic parameters but can still provide information about network dynamics and serve as tools for hypothesis generation. Structural and qualitative analysis is emerging as a feasible and useful alternative [124, 134, 171]. Moreover, discrete models have the advantage of being more intuitive than models based on differential equations, so they have added appeal for researchers without a strong mathematical background. In Hinkelmann et al. [75], the authors propose the mathematical framework of polynomial dynamical systems over a finite field, which provides access to theoretical and computational tools from computer algebra and discrete mathematics, which we pursue.

We invite the reader to survey the introduction of each chapter of the thesis for a deeper insight of our work and the related bibliography. On page 139, a list of notations can be found.

For a better understanding of the outline of this work, we briefly introduce some terminology in the following paragraphs.

A *chemical reaction network* is a finite directed graph whose vertices are labeled by complexes and whose edges represent the reactions. The digraph G has m vertices, and the vertex i of G stands for the i-th chemical complex, to which we associate the monomial $x^{y_i} = x_1^{y_{i1}} x_2^{y_{i2}} \cdots x_s^{y_{is}}$. The unknowns $x_1, x_2, \ldots, x_s$ represent the concentrations of the s species in the network, and we regard them as functions $x_i(t)$ of time t. These chemical reaction networks are usually assumed under mass–action kinetics and the dynamics is described through an autonomous system of differential equations, $\frac{d\mathbf{x}}{dt} = f(\mathbf{x})$, where $\mathbf{x} = (x_1, x_2, \ldots, x_s)$. An important aspect of the dynamics is the study of the steady states of the system, i.e. the values of $\mathbf{x}$ for which $f(\mathbf{x}) = 0$. Under mass–action kinetics, the coordinate functions $f_1, \ldots, f_s$ are polynomials in the species concentrations $x_1, \ldots, x_s$ and the steady states of the system form the (real nonnegative) variety of the ideal $I = \langle f_1, \ldots, f_s \rangle$.

Generally, mass–action kinetics systems are decomposed as $f(\mathbf{x}) = \Sigma\Psi(\mathbf{x})$, where Σ is an $s \times m$ matrix that keeps the coefficients of the polynomial system, and $\Psi(\mathbf{x})$ keeps the monomials. The matrix Σ of these particular mass–action kinetics systems has many nice features. Much can be said from this generous linearity, and most of the results in the area exploit this characteristic of the system. Even for describing the steady states, the properties of the matrix Σ are very helpful, and we take advantage of them in Chapters 3, 4 and 5. However, as we mentioned in the previous paragraph, finding the steady states of the system is equivalent to solving the polynomial system $f_1(\mathbf{x}) = \cdots = f_s(\mathbf{x}) = 0$, which is in turn equivalent to describing the variety of the ideal $I = \langle f_1, \ldots, f_s \rangle$. Moreover, one is interested in pursuing the *positive* zeros of the ideal I, and this invites *real algebraic geometry* to play an important role in this search. We introduce in Chapters 4 and 5 some tools from algebraic geometry, and we open the door for real algebraic geometry in Chapter 6. We also introduce some semialgebraic

conditions for the reaction constants in Chapter 4.

Another approach to model biological networks is presented in Chapter 7, where we work with a discrete model of a specific biological system: the NF-κB regulatory module. NF-κB is a ubiquitously expressed family of transcription factors that regulates the expression of numerous genes that play important roles in cellular responses, cell growth, survival and inflammatory and immune responses. Discrete models have emerged as an alternative to continuous models when the intention is to study networks with poorly detailed data available, with the idea of providing a first description of the interactions of the network by means of computational algebra methods. One of the advantages of this type of modeling is that it does not depend on specific affinity and catalytic constants, which are usually difficult to determine and require a deep understanding of the system (which, except for the NF–κB regulatory module and some other special cases, is rare). Moreover, even if we were given experimental data of perfect accuracy and unlimited temporal resolution, continuous dynamical system models are sometimes unidentifiable (i.e.two different reaction networks might generate identical continuous dynamical systems, making it impossible to discriminate between them).

We reconstruct the network as a *discrete dynamical system*, with a qualitative deterministic approach. To be more precise, it is a polynomial dynamical system over the ground field $\mathbb{F}_3$. The NF-κB signaling pathway has also been approached with models of differential equations. Our model is based on one of these continuous models and also on experimental data from the literature.

1.1 Outline and contribution

In Chapter 2 we start by presenting some preliminaries on Chemical Reaction Network Theory. We collect definitions from the literature, mainly form [48, 80] and prepare the setting for our results in the subsequent chapters.

In Chapter 3, we exploit Chemical Reaction Network Theory (CRNT) to develop an efficient procedure for calculating invariants that are symbolic linear combinations of "complexes", or the monomials coming from mass action. We recover, as a special case, the Shinar-Feinberg Theorem [144], that gives structural conditions for a network of deficiency one to have "absolute concentration robustness" (ACR). We then use complex-linear invariants to analyze two examples of enzyme bifunctionality, the bacterial EnvZ/OmpR osmolarity regulator, having deficiency two, and the mammalian phosphofructokinase-2-fructose-2,6-bisphosphatase glycolytic regulator, having deficiency four, showing how the methods developed in that chapter can be used for steady-state algebraic analysis of realistic networks.

In Chapter 4, we focus on systems where the steady state ideal is a binomial ideal. We say that such systems have toric steady states. We give sufficient conditions for a chemical reaction system to have toric steady states (Theorems 4.2.2 and 4.2.4) and show in this case that the steady state locus has a nice monomial parametrization (Theorems 4.2.3 and 4.2.5). Furthermore, we analyze the capacity of such a system to exhibit positive steady states and multistationarity. An important application of our work concerns the networks that describe the multisite phosphorylation of a protein by a kinase/phosphatase pair in a sequential and distributive mechanism. Theorem 4.3.1 summarizes our results on these systems.

In Chapter 5, we clarify the relation between the algebraic conditions that must be satisfied by the reaction constants in general (mass–action) kinetics systems for the existence of detailed or complex balancing equilibria. These systems have a wide range of applications in chemistry and biology [32, 60, 64, 112, 142, 146]. Their main properties have been set by Horn, Jackson and Feinberg [45, 49, 50, 79–82]. The main result is presented in Theorem 5.1.1.

In Chapter 6, we use tools from computational algebra, algebraic geometry and real algebraic geometry to detect if a chemical reaction system shows absolute concentration robustness for a certain chemical species (defined in [144]). We comment on the difficulties for a general algorithm and present some sufficient conditions for a system to have ACR.

The last chapter of this work, Chapter 7, presents a *discrete qualitative deterministic algebraic model* for the NF-κB regulatory module. In order to describe the dynamics between the components of the NF-κB signaling pathway, we construct a discrete model mostly based upon the molecular data present at Lee et al. [109] and Hoffmann et al. [76], and the continuous model developed by Lipniacki et al. [110]. We conceive these components in a network with eleven nodes which can take at most three levels (i.e., we discretize the data into the levels $\{0, 1, 2\}$) and we then build a polynomial dynamical system $f : \mathbb{F}_3^{11} \to \mathbb{F}_3^{11}$. The strategy used is based on a bottom-up approach, starting with an extensive overview of published molecular data to reconstruct the underlying biological network. We formed the eleven functions corresponding to each node using the computer algebra system Singular [35]. Eventually, we could reproduce the dynamics observed in the wild-type case with persistent stimulation and also in the A20 knock-out. This model can be built with the information biologists normally handle: IκB binds to NF–κB and prevents it from entering the nucleus, IKKa induces IκB degradation, etc. And despite it simply requires this kind of data, it can render even more information, such as predictions in mutant cases.

1.2 Publications

The work presented in this thesis is largely based on previously published or submitted articles. Note that most work has been done in close collaboration with various authors.

Chapter 3 is based on

Complex–linear invariants of biochemical networks. Karp R., Pérez Millán M., Dasgupta T., Dickenstein A. and Gunawardena J., 2011. Submitted. [92].

I essentially worked all throughout the paper. Specially, I participated in producing the theoretical result.

Chapter 4 is based on

Chemical reaction systems with toric steady states. Pérez Millán M., Dickenstein A., Shiu A., Conradi C., 2011. Accepted for publication at the Bulletin of Mathematical Biology.

Available online at DOI: 10.1007/s11538-011-9685-x. [126].

Although I worked on all the article, I particularly generated a detailed analysis and the proofs for the system for the multisite phosphorylation of a protein by a kinase/phosphatase pair in a sequential and distributive mechanism, which was the starting point for producing the more general results in the first sections of the article.

Chapter 5 is based on

How far is complex balancing from detailed balancing?. Dickenstein A. and Pérez Millán M, 2011. Bulletin of Mathematical Biology, 73:4, pp. 811–828.

Available online at DOI:10.1007/s11538-010-9611-7. [39].

My main contributions to the paper were the statements and proofs of the main results. I also redacted great part of the article.

The article *A discrete model of the nuclear factor NF–κB regulatory network* is in preparation and is joint work with J. I. Fuxman Bass and A. S. Jarrah. It is presented in Chapter 7. My contributions to this work were the mathematical construction and analysis of the model. I established the connections between the results in this model and Chemical Reaction Network Theory. I designed and implemented the algorithms, and I assisted J.I.F.B. in building the tables.

Chapter 2

Chemical Reaction Network Theory

Chemical Reaction Network Theory (CRNT) has been developed over the last 40 years, initially through the work of Horn and Jackson and subsequently by Martin Feinberg and his students. The CRNT connects qualitative properties of ordinary differential equations (ODEs) corresponding to a reaction network to the network structure. In particular, its assertions are independent of specific parameter values and it generally assumes that all kinetics are of the mass–action form. The theory introduces new concepts, such as the deficiency of a reaction network, and gives conditions on such networks for the existence, uniqueness, multiplicity and stability of fixed points. As conclusions try to disregard the values of the parameters in the system, this theory should be of interest to those who associate such behavior with biological robustness [4, 169].

In this chapter we review the basic concepts of CRNT that will serve useful for the subsequent chapters. Most of the ideas and definitions below are inspired in the seminal works of Feinberg and Horn and Jackson [48, 80].

2.1 Chemical Reaction Systems

An example of a *chemical reaction*, as it usually appears in the literature, is the following:

$$A + B \longrightarrow 3A + C \tag{2.1}$$

In this reaction, one unit of chemical *species* A and one of B react to form three units of A and one of C. The *educt* (or *reactant* or *source*) $A + B$ and the *product* $3A + C$ are called *complexes*. We will refer to complexes such as $A + B$ that are the educt of a reaction as *educt complexes*. The molar concentrations of the three species, denoted by $x_A = [A]$, $x_B = [B]$, and $x_C = [C]$, will change in time as the reaction occurs (in fact it is the temporal evolution of the composition that we wish to investigate). A molar concentration, say x_A, specifies the number of A molecules per unit volume of mixture. More precisely, x_A is the number of A molecules per unit volume divided by Avogadro's number, 6.023×10^{23}.

We define a *chemical reaction network* as a finite directed graph whose vertices are labeled by complexes and whose edges represent the reactions. Specifically, the digraph is denoted $G = (V, \mathscr{R})$, with vertex set $V$and cardinality $\#V = m$, and edge set $\mathscr{R} \subseteq V \times V$ without

any self-loops. Throughout this work, the integer unknowns m, s, and r denote the numbers of complexes, species, and edges (reactions), respectively.

The vertex i of G represents the i-th chemical complex, and we associate to it the monomial

$$x^{y_i} \;=\; x_1^{(y_i)_1} x_2^{(y_i)_2} \cdots x_s^{(y_i)_s} \,.$$

More precisely, if the i-th complex is $(y_i)_1 A + (y_i)_2 B + \cdots$ (where the j-th coordinate $(y_i)_j$is in $\mathbb{Z}_{\geq 0}$ for $j = 1, 2, \ldots, s$), then it defines the monomial $x_A^{(y_i)_1} x_B^{(y_i)_2} \cdots$.

For example, the two complexes in network (2.1) give rise to the monomials $x_A x_B$ and $x_A^3 x_C$, which determine two vectors $y_1 = (1, 1, 0)$ and $y_2 = (3, 0, 1)$. We will refer to $y_1, \ldots, y_m$ as the complexes in the network. The component $(y_i)_j$ (corresponding to the j-th species, $\mathfrak{s}_j$) of the vector y_i is usually called by chemists the *stoichiometric coefficient* of $\mathfrak{s}_j$ in complex y_i. When the context is clear, will denote $(y_i)_j$ as y_{ij}, and we will sometimes use y or y' for arbitrary complexes. We record the complexes by an $s \times m$-matrix of non-negative integers $Y = (y_{ji})$, which contains these stoichiometric coefficients. The i-th column of the matrix is then $((y_i)_1, \cdots, (y_i)_s)^\dagger$. Here, and all throughout this work, † denotes transpose.

As we regard the complexes to be vectors in $\mathbb{R}^s$ (in particular, they lie in $\mathbb{Z}^s_{\geq 0}$), it makes sense to add two complexes, to subtract one complex from another, to multiply a complex by a number, and to take the scalar product of a complex with any other vector of $\mathbb{R}^s$. Moreover, it makes sense to speak of the support of a complex, that is, the nonzero entries of the corresponding vector. The support of the complex y_i will be denoted $\mathrm{supp}(y_i)$.

A *chemical reaction network*, then, consists of three sets:

(i) a finite set $\mathscr{S} = \{\mathfrak{s}_1, \ldots, \mathfrak{s}_s\}$, elements of which are called the *species* of the network.

(ii) a finite set $\mathscr{C}$ of distinct vectors in $\mathbb{Z}^s_{\geq 0}$ called the *complexes* of the network. They must satisfy that each element of $\mathscr{S}$ "appears in" at least one complex; that is, $\mathscr{S}$ contains no superfluous species.

(iii) a relation $\mathscr{R} \subset \mathscr{C} \times \mathscr{C}$ such that

  (a) $(y, y) \notin \mathscr{R}$, for all $y \in \mathscr{C}$. That is, no complex reacts to itself.

  (b) For each $y \in \mathscr{C}$ there exists a $y' \in \mathscr{C}$ such that $(y, y') \in \mathscr{R}$ or such that $(y', y) \in \mathscr{R}$.

  Elements of $\mathscr{R}$ are called the *reactions* of the network. For each $(y, y') \in \mathscr{R}$ we say that complex y reacts to complex y' (which will also be written as $y \to y'$). Then the last condition here means that each element of $\mathscr{C}$ is the product complex of some reaction or is the educt complex of some reaction.

The notation $\mathbb{R}^{\mathscr{S}}$ (or $\mathbb{Z}^{\mathscr{S}}$) is sometimes introduced in the literature [45] in order to avoid the numbering of the species.

We would like to write down differential equations that describe the evolution of the molar concentrations. Since chemical reactions are the source of changes in the concentrations of the species, the key to understanding how to write down differential equations lies in knowing how rapidly each of the several reactions occurs. What is generally assumed is that the instantaneous occurrence rate of each reaction depends on its own way on the vector $\mathbf{x} = (x_1, \ldots, x_s)$. Thus,

we presume, for example, the existence of a non–negative real valued rate function $\mathcal{K}_{y\to y'}(\cdot)$ such that $\mathcal{K}_{y\to y'}(\mathbf{x})$ is the instantaneous occurrence rate of reaction $y \to y'$ (per unit volume of mixture) when the instantaneous mixture composition (i.e., the concentration of the species in the mixture) is given by the vector $\mathbf{x}$.

Definition 2.1.1. *A* kinetics *for a reaction network $G = (V, \mathscr{R}, Y)$ is an assignment to each reaction $(y, y') \in \mathscr{R}$ of a continuous rate function $\mathcal{K}_{y\to y'} : \mathbb{R}^s_{\geq 0} \to \mathbb{R}_{\geq 0}$ such that*

$$\mathcal{K}_{y\to y'}(\mathbf{x}) > 0 \quad \textit{if and only if} \quad \operatorname{supp}(y) \subseteq \operatorname{supp}(\mathbf{x}).$$

We are now ready to define what a chemical reaction system is.

Definition 2.1.2. *A* chemical reaction system *$G = (V, \mathscr{R}, \mathcal{K}, Y)$ is a chemical reaction network $G = (V, \mathscr{R}, Y)$ endowed with a kinetics $\mathcal{K}$.*

Suppose that, at some instant, the concentration of the species is represented in $\mathbf{x}$. Let us begin by thinking about the instantaneous rate of change of x_A. Every time the reaction $A + B \to 3A + C$ occurs, we gain two molecules of A, and that reaction has an occurrence rate $\mathcal{K}_{A+B\to 3A+C}(\mathbf{x})$. Thus we write

$$\frac{dx_A}{dt} = 2\mathcal{K}_{A+B\to 3A+C}(\mathbf{x}). \tag{2.2}$$

If we turn our attention to species B we notice that whenever reaction $A+B \to 3A+C$ occurs, we lose one molecule of B. Thus, we write

$$\frac{dx_B}{dt} = -\mathcal{K}_{A+B\to 3A+C}(\mathbf{x}). \tag{2.3}$$

Continuing in this way we have

$$\frac{dx_C}{dt} = \mathcal{K}_{A+B\to 3A+C}(\mathbf{x}). \tag{2.4}$$

Definition 2.1.3. *Let $G = (V, \mathscr{R}, Y)$ be a reaction network. The* reaction vector *corresponding to reaction $(y, y') \in \mathscr{R}$ is the vector $y' - y \in \mathbb{R}^s$.*

Note that the component of $y' - y$ corresponding to the i-th species in $\mathscr{S}$ is just $(y')_i - (y)_i$, the difference between the stoichiometric coefficient of $\mathfrak{s}_i$ in the product complex y' and its stoichiometric coefficient in the educt complex y. This difference is the net number of molecules of $\mathfrak{s}_i$ produced with each occurrence of the reaction $y \to y'$. Consider, for example, the reaction in (2.1); the corresponding reaction vector is $(2, -1, 1)$.

Definition 2.1.4. *For a reaction system $G = (V, \mathscr{R}, \mathcal{K}, Y)$ the* species formation rate function *$f : \mathbb{R}^s_{\geq 0} \to \mathbb{R}^s$ is defined by*

$$f(\mathbf{x}) := \sum_{\mathscr{R}} \mathcal{K}_{y\to y'}(\mathbf{x})(y' - y).$$

That is, $f(\cdot)$ is obtained by summing the reaction vectors for the network, each multiplied by the corresponding reaction rate function.

Interpretation: If, in a homogeneous reactor, the concentrations are represented by $\mathbf{x} \in \mathbb{R}^s_{\geq 0}$ then, for each $i \in \{1, \ldots, s\}$, $f_i(\mathbf{x})$ gives the instantaneous rate of generation (per unit volume of mixture) of moles of the i-th species due to the simultaneous occurrence of all reactions in $\mathscr{R}$. Note that

$$f_i(\mathbf{x}) = \sum_{\mathscr{R}} \mathcal{K}_{y \to y'}(\mathbf{x})((y)'_i - (y)_i),$$

so that $f_i(\mathbf{x})$ is obtained by summing all the reaction occurrence rates, each weighted by the net number of molecules of $\mathfrak{s}_i$ produced with each occurrence of the corresponding reaction.

By the differential equation for a reaction system we mean

$$\dot{\mathbf{x}} = f(\mathbf{x}), \tag{2.5}$$

where the dot denotes time differentiation and $f(\cdot)$ is the species formation rate function. That is, for a reaction system $G = (V, \mathscr{R}, \mathcal{K}, Y)$ the corresponding differential equation is

$$\dot{\mathbf{x}} = \sum_{\mathscr{R}} \mathcal{K}_{y \to y'}(\mathbf{x})(y' - y).$$

2.1.1 Mass–action kinetics systems

If we regard a single elementary reaction as representing an encounter and interaction between reactant molecules, kinetic theory suggests the familiar mass–action form for the rate function.

A *chemical reaction system under mass–action kinetics* is a finite directed graph $G = (V, \mathscr{R}, \kappa, Y)$ endowed with a kinetics such that each reaction takes place at a rate that is proportional to the product of the concentrations of the species being consumed in that reaction.

Definition 2.1.5. *A kinetics $\mathcal{K}$ for a reaction network $G = (V, \mathscr{R}, Y)$ is* mass–action *if, for each $(y, y') \in \mathscr{R}$, there exists a positive number $\kappa_{y \to y'}$ such that*

$$\mathcal{K}_{y \to y'}(\mathbf{x}) := \kappa_{y \to y'} \mathbf{x}^y.$$

The positive number $\kappa_{y \to y'}$ is called the rate constant *for the reaction (y, y').*

For the reaction $A + B \to 3A + C$, an occurrence requires that a molecule of A meet a molecule of B in the reactor, and we take the probability of such an encounter to be proportional to the product $x_A x_B$. We take the occurrence rate of $A + B \to 3A + C$ to be given by

$$\mathcal{K}_{A+B \to 3A+C}(\mathbf{x}) = \kappa x_A x_B,$$

where κ is a positive constant.

Usually, when a reaction network is considered under mass–action kinetics, the rate constants are indicated alongside the corresponding reaction arrows in the network diagram. That is, the edges of the directed graph G are labeled by parameters (reaction rate constants).

Recalling reaction (2.1) with mass–action kinetics, we have:

$$A + B \xrightarrow{\kappa} 3A + C \tag{2.6}$$

We can rewrite equations (2.2), (2.3) and (2.4) as

$$\begin{aligned} \frac{dx_A}{dt} &= 2\kappa x_A x_B \ , \\ \frac{dx_B}{dt} &= -\kappa x_A x_B \ , \\ \frac{dx_C}{dt} &= \kappa x_A x_B \ . \end{aligned} \tag{2.7}$$

The species formation rate function for a mass–action system takes the form

$$f(\mathbf{x}) := \sum_{\mathscr{R}} \kappa_{y\to y'} \mathbf{x}^y (y' - y).$$

And the corresponding differential equations are then

$$\dot{\mathbf{x}} = \sum_{\mathscr{R}} \kappa_{y\to y'} \mathbf{x}^y (y' - y),$$

represented in the vector $\dot{\mathbf{x}} = (\dot{x}_1, \ldots, \dot{x}_s)^\dagger = \left(\frac{dx_1}{dt}, \ldots, \frac{dx_s}{dt}\right)^\dagger$.

Observe that the function f, in the case of mass–action kinetics is polynomial in each coordinate. The variables are the concentrations x_i, and the coefficients belong to $\mathbb{Q}[\kappa]$ (that is, the coefficients are polynomials in the reaction rate constants).

Before we move on, we will make a simple but important observation due to V. Hárs, J. Tóth, 1979 [68]. It tells us when a polynomial system can come from a mass–action kinetics system.

Lemma 2.1.1 (Hungarian)**.** *A polynomial system of s real polynomials $f_1, \ldots, f_s$ in s variables arises from a mass–action kinetics dynamical system if and only if there exist real polynomials $p_k, q_k,\ k = 1, \ldots, s$ with non negative coefficients such that $f_k = p_k - x_k q_k$ for all $k \in \{1, \ldots, s\}$.*

From here we can deduce that the dynamics that arises from the Lorenz equations

$$\begin{aligned} \frac{dx}{dt} &= \sigma y - \sigma x \\ \frac{dy}{dt} &= \rho x - y - \mathbf{xz} \\ \frac{dz}{dt} &= xy - \beta z, \end{aligned}$$

cannot come from a mass–action kinetics modeling since the last term on the right-hand side of the second equation has a negative coefficient and the monomial does not involve the corresponding variable y.

Let us see in an example from [68] how a chemical reaction network can be constructed from a system of equations of the form described in the statement of Lemma 2.1.1:

Example 2.1.1.

$$\begin{aligned} \dot{x_A} &= -2\alpha x_A^2 x_D + 2\gamma x_C^4 \\ \dot{x_B} &= 3\alpha x_A^2 x_D - 3\beta x_B^3 x_D^2 \\ \dot{x_C} &= 4\beta x_B^3 x_D^2 - 4\gamma x_C^4 \\ \dot{x_D} &= \alpha x_A^2 x_D - 2\beta x_B^3 x_D^2 + \gamma x_C^4 \end{aligned} \tag{2.8}$$

We can build the following reaction network corresponding to this dynamics:

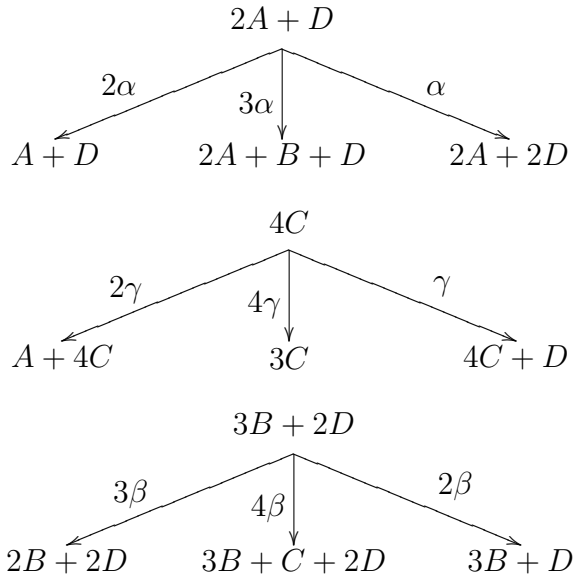

On the other hand, the kinetic differential equation of the mechanism

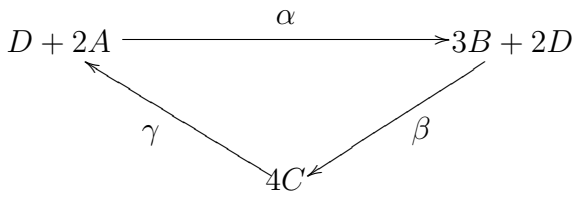

is also (2.8).

Although there is nonlinearity in mass–action, arising from the pattern of substrate stoichiometry (this is reflected in the monomials $\mathbf{x}^y$), the differential equations come from linear processes on complexes . This observation is the starting point of CRNT and reveals that biochemical networks conceal much linearity behind their nonlinearity, [48,63,66, and see below]. This arises from the underlying network of chemical reactions, which define a directed graph on the complexes that participate in the chemical reactions. The existence of this underlying structure limits the nonlinearity that can appear, which is why the strong results of CRNT are possible.

Working at the level of complexes serves to disentangle the interactions between individual chemical species. For example, the steady states (see Section 2.2 below) of the system fall into two categories: those that arise at the level of complexes and those that arise from the way in which different complexes contain the same chemical species. The deficiency of a network, which we define below as the dimension of a certain vector space (see Section 2.4), measures the extent of the second possibility. However, one of the most interesting discoveries of CRNT has to do with steady states of the first kind.

We now rebuild the dynamics from a different perspective. Given a directed graph, G, with labels in $\mathbb{R}_{>0}$ it will give rise to an abstract dynamics in which each edge is treated as if it

were a first-order chemical reaction with its label as rate constant (a first-order reaction is one that depends on the concentration of only one reactant). Since the rates are all first-order, the dynamics are linear and may therefore be written in matrix terms as $dy/dt = \mathcal{L}(G).y$, where $y \in \mathbb{R}^m$ is a column vector, consisting of an abstract concentration y_i at each node i of G, and $\mathcal{L}(G)$ is a $m \times m$ matrix called the Laplacian matrix of G (an $m \times m$-matrix whose off-diagonal entries are the κ_{ji} and whose column sums are zero). In the literature, $\mathcal{L}(G)$ is also noted as A_κ. Here, "." signifies matrix multiplication, regarding vectors as matrices of one row or one column.

For example, with network 2.6

$$A + B \xrightarrow{\kappa} 3A + C,$$

we can form the network

$$y_1 \xrightarrow{\kappa} y_2,$$

for which the differential equations are

$$\begin{bmatrix} \frac{dy_1}{dt} \\ \frac{dy_2}{dt} \end{bmatrix} = \begin{bmatrix} -\kappa y_1 \\ \kappa y_1 \end{bmatrix} = \begin{bmatrix} -\kappa & 0 \\ \kappa & 0 \end{bmatrix} \begin{bmatrix} y_1 \\ y_2 \end{bmatrix}.$$

For CRNT, the Laplacian, $\mathcal{L}(G) : \mathbb{R}^m \to \mathbb{R}^m$, is a linear analogue for complexes of the nonlinear function, $f : \mathbb{R}^s \to \mathbb{R}^s$, for species, in the following sense. Let $\Psi : \mathbb{R}^s \to \mathbb{R}^m$ be the nonlinear function that lists the monomials for each complex, $\Psi(x) = (x^{y_1}, \cdots, x^{y_m})^\dagger$. Let Y be as before. We can think of it as $Y : \mathbb{R}^m \to \mathbb{R}^s$, the linear function that associates to each complex, considered as a basis element of $\mathbb{R}^m$, its corresponding stoichiometry pattern. With these definitions, it may be checked that $f(x) = Y.\mathcal{L}(G).\Psi(x)$, for any $x \in \mathbb{R}^s$.

This fundamental observation, which originates in the pioneering work of Horn and Jackson, [80], is the starting point of CRNT. It shows that the the nonlinear rate function f can be decomposed into a purely linear part, $Y.\mathcal{L}(G)$, that includes the Laplacian, and the essential nonlinearity, Ψ, coming from the complex monomials.

Now we define the *complex-to-species rate matrix* of size $s \times m$ to be

$$\Sigma \;:=\; Y \cdot \mathcal{L}(G)\,. \tag{2.9}$$

The reaction network G defines, then, the following dynamical system:

$$\frac{d\mathbf{x}}{dt} \;=\; \left(\frac{dx_1}{dt}, \frac{dx_2}{dt}, \ldots, \frac{dx_s}{dt}\right)^\dagger \;=\; \Sigma \cdot \Psi(x)\,. \tag{2.10}$$

Example 2.1.2. *The following chemical reaction network is the 1-site phosphorylation system. We will study generalizations of this network all throughout this work. The notation comes from Wang and Sontag 2008 ([170]).*

$$S_0 + E \underset{k_{\mathrm{off}_0}}{\overset{k_{\mathrm{on}_0}}{\rightleftarrows}} ES_0 \overset{k_{\mathrm{cat}_0}}{\to} S_1 + E \tag{2.11}$$

$$S_1 + F \underset{l_{\mathrm{off}_0}}{\overset{l_{\mathrm{on}_0}}{\rightleftarrows}} FS_1 \overset{l_{\mathrm{cat}_0}}{\to} S_0 + F\,.$$

The key players in this network are a kinase enzyme (E), a phosphatase enzyme (F), and two substrates (S_0 and S_1). The substrate S_1 is obtained from the unphosphorylated protein S_0 by attaching a phosphate group to it via an enzymatic reaction involving E. Conversely, a reaction involving F removes the phosphate group from S_1 to obtain S_0. The intermediate complexes ES_0 and ES_1 are the bound enzyme-substrate complexes. Under the ordering of the 6 species as $(S_0, S_1, ES_0, FS_1, E, F)$ and the 6 complexes as $(S_0 + E, S_1 + E, ES_0, S_0 + F, S_1 + F, FS_1)$, the matrices whose product defines the dynamical system (2.10) follow:

$$\Psi(x) = (x_{S_0}x_E,\ x_{S_1}x_E,\ x_{ES_0},\ x_{S_0}x_F,\ x_{S_1}x_F,\ x_{FS_1})^\dagger = (x_1x_5, x_2x_5, x_3, x_1x_6, x_2x_6, x_4)^\dagger,$$

$$Y = \begin{bmatrix} 1 & 0 & 0 & 1 & 0 & 0 \\ 0 & 1 & 0 & 0 & 1 & 0 \\ 0 & 0 & 1 & 0 & 0 & 0 \\ 0 & 0 & 0 & 0 & 0 & 1 \\ 1 & 1 & 0 & 0 & 0 & 0 \\ 0 & 0 & 0 & 1 & 1 & 0 \end{bmatrix}, \text{ and}$$

$$\mathcal{L}(G) := \begin{bmatrix} -k_{\mathrm{on}_0} & 0 & k_{\mathrm{off}_0} & 0 & 0 & 0 \\ 0 & 0 & k_{\mathrm{cat}_0} & 0 & 0 & 0 \\ k_{\mathrm{on}_0} & 0 & -k_{\mathrm{off}_0} - k_{\mathrm{cat}_0} & 0 & 0 & 0 \\ 0 & 0 & 0 & 0 & 0 & l_{\mathrm{cat}_0} \\ 0 & 0 & 0 & 0 & -l_{\mathrm{on}_0} & l_{\mathrm{off}_0} \\ 0 & 0 & 0 & 0 & l_{\mathrm{on}_0} & -l_{\mathrm{cat}_0} - l_{\mathrm{off}_0} \end{bmatrix}.$$

2.2 Steady States

By an equilibrium for a reaction system $G = (V, \mathscr{R}, \mathcal{K}, Y)$ we mean a vector of concentrations $\mathbf{x} \in \mathbb{R}^s_{\geq 0}$ at which the species formation function takes the value zero. By a positive equilibrium we mean an equilibrium in $\mathbb{R}^s_{>0}$; that is, an equilibrium at which all species concentrations are positive.

Some reaction networks (e.g., $A \to 2B$) have the property that, when taken with mass–action kinetics, the induced differential equations admit no positive equilibria for some or even for any assignments of the rate constants. Any equilibria that do exist are characterized by the "extinction" of one or more species.

On the other hand, some networks (e.g. , $A \leftrightarrows 2B$) taken with mass–action kinetics admit at least one equilibrium in each positive stoichiometric compatibility class, regardless of the values that the rate constants take (see Section 2.3).

Even if we grant that the existence or non–existence of positive equilibria is easy to decide for simple networks, this is not true for complicated networks. Ultimately one is confronted with a large system of polynomial equations in many variables (species concentrations) in which many parameters (rate constants) appear.

The nonlinearities in (2.7) usually preclude mathematical analysis of the dynamical behavior of such ODE systems, which are customarily studied by numerical simulation. This requires that the rate constants be given numerical values, which in most cases are neither known nor readily measurable. The resulting "parameter problem" remains a major difficulty in exploiting mathematical models, [65]. However, the steady states of such ODEs are zeros of a set of

polynomial equations, $f_1(x,\kappa) = 0, \cdots, f_s(x,\kappa) = 0$. Computational algebra and algebraic geometry provide powerful tools for studying these solutions, [28], and these have recently been used to gain new biological insights, [30, 34, 112, 126, 164, 165]. The rate constants can now be treated as symbolic parameters, whose numerical values do not need to be known in advance. The capability to rise above the parameter problem allows more general results to be obtained than can be expected from numerical simulation, [165].

The focus on steady states, rather than transient dynamics, is still of substantial interest. For instance, in time-scale separation, which has been a widespread method of simplification in biochemistry and molecular biology, a fast sub-system is assumed to be at steady state with respect to a slower environment and steady-state analysis is used to eliminate the internal complexity in the sub-system, [66]. Approximate or quasi-steady states have also been shown to exist under various cellular conditions and can now be engineered *in vivo*, [103, 108]. Finally, steady states provide the skeleton around which the transient dynamics unfolds, so knowledge of the former can be helpful for understanding the latter.

A formal definition of steady states within this context is given below.

Definition 2.2.1. *Consider a polynomial dynamical system $dx_i/dt = f_i(x)$, for $i = 1, 2, \ldots, s$, with $f_1, f_2, \ldots, f_s \in \mathbb{R}[x_1, x_2, \ldots, x_s]$. We are interested in the* nonnegative *zeros of the* steady state ideal*:*

$$J_{\Sigma\Psi} \;=\; \langle f_1, f_2, \ldots, f_s \rangle = \left\{ \sum_{i=1}^{s} h_i(x) f_i(x) \quad | \quad h_i(x) \in \mathbb{R}[x_1, \ldots, x_s] \text{ for } 1 \leq i \leq s \right\}.$$

The nonnegative zeros of $J_{\Sigma\Psi}$ are called steady states*, and the term* steady state locus *is used to denote the set of nonnegative zeros of $J_{\Sigma\Psi}$:*

$$\left\{ \tilde{\mathbf{x}} \in \mathbb{R}^s_{\geq 0} \quad | \quad f_1(\tilde{\mathbf{x}}) = f_2(\tilde{\mathbf{x}}) \cdots = f_s(\tilde{\mathbf{x}}) = 0 \right\}.$$

Hence, the steady states of the chemical reaction system form the *nonnegative real variety* of the ideal $J_{\Sigma\Psi}$.

Note that in the case of mass–action kinetics chemical reaction systems, the polynomials $f_1, f_2, \ldots, f_s$ correspond to the rows of the system (2.10).

In order to exploit the linearity mentioned before, we note that the steady states of the Laplacian dynamics are elements of the kernel of $\mathcal{L}(G)$: $\ker \mathcal{L}(G) = \{y \in \mathbb{R}^m \mid \mathcal{L}(G).y = 0\}$.

Once we introduce the stoichiometry, we must study the kernel of Σ. Before concentrating on this, we must define what linkage classes, strong linkage classes and terminal strong linkage classes are.

Definition 2.2.2. *A* linkage class *refers to a connected component of a network.*

In graph theory a directed graph is called strongly connected if for every pair of nodes y and y' there is a path from y to y' and vice versa. The strong linkage classes *(or strongly connected components) are the maximal strongly connected subgraphs of a directed graph. If no edge from a node inside a strong linkage class to a node outside exists, we have a* terminal strong linkage class*.*

Now, the kernel of Σ can be calculated in two stages, [46, 66]. First, if G is strongly connected, then $\dim(\ker \mathcal{L}(G)) = 1$. Following [30], we introduce the following definition:

Definition 2.2.3. *Consider any directed subgraph T of G such that the underlying undirected graph of T is a spanning tree of the underlying undirected graph of G. We denote the set of vertices of T by $V(T)$ and its set of edges by $\mathscr{R}(T)$. Thus, $\mathscr{R}(T)$ consists of $m-1$ edges. Write κ^T for the product of the $m-1$ rate constants which correspond to all edge labels of the edges in $\mathscr{R}(T)$. Let i be one of the nodes of G. The directed tree is called an i-tree if the node i is its unique sink, i.e., all edges are directed towards node i. We introduce the following constants, which are polynomials in the (κ_{ij}):*

$$K_i = \sum_{T\ an\ i-tree} \kappa^T. \tag{2.12}$$

Note that each K_i is a nonempty sum of positive terms because, as G is strongly connected, there exists at least one i-tree for every vertex i and each $\kappa_{uv} > 0$ for $(u, v) \in \mathscr{R}$.

It follows from the Matrix-Tree Theorem [149] that for any $i \in V$, the absolute value of the determinant of the submatrix of $\mathcal{L}(G)$ obtained by deleting the i-th column and any one of the rows, equals K_i. This (non-zero) minor is independent (up to sign) of the choice of rows because the column sums of $\mathcal{L}(G)$ are zero.

Example 2.2.1. *We will introduce a mathematical example to make the calculations more transparent. Let G be the following connected chemical reaction system:*

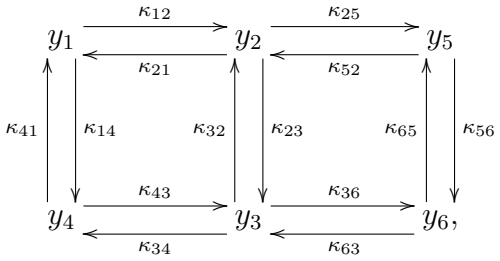

For example, $K_1 = \sum_{T\ an\ 1-tree} \kappa^T = \kappa_{21}\kappa_{32}\kappa_{63}\kappa_{41}\kappa_{52} + \kappa_{21}\kappa_{32}\kappa_{63}\kappa_{41}\kappa_{56} + \kappa_{21}\kappa_{32}\kappa_{63}\kappa_{43}\kappa_{52}$
$+\kappa_{21}\kappa_{32}\kappa_{63}\kappa_{43}\kappa_{56} + \kappa_{21}\kappa_{52}\kappa_{65}\kappa_{32}\kappa_{41} + \kappa_{21}\kappa_{52}\kappa_{65}\kappa_{32}\kappa_{43} + \kappa_{21}\kappa_{52}\kappa_{65}\kappa_{34}\kappa_{41} + \kappa_{21}\kappa_{52}\kappa_{65}\kappa_{36}\kappa_{41}$
$+\kappa_{21}\kappa_{52}\kappa_{65}\kappa_{36}\kappa_{43} + \kappa_{41}\kappa_{63}\kappa_{34}\kappa_{21}\kappa_{52} + \kappa_{41}\kappa_{63}\kappa_{34}\kappa_{21}\kappa_{56} + \kappa_{41}\kappa_{63}\kappa_{34}\kappa_{23}\kappa_{52} + \kappa_{41}\kappa_{63}\kappa_{34}\kappa_{23}\kappa_{56}$
$+\kappa_{41}\kappa_{63}\kappa_{34}\kappa_{25}\kappa_{56} + \kappa_{41}\kappa_{52}\kappa_{23}\kappa_{34}\kappa_{65}$.

The Matrix-Tree Theorem then provides an explicit construction of a basis element, $\rho_G \in \mathbb{R}^m$, in terms of the spanning trees of G: $\ker \mathcal{L}(G) = \langle\, \rho_G \,\rangle = \langle (K_1, \ldots, K_m)^\dagger \rangle$. The components $(\rho_G)_i$ are then polynomials in the symbolic labels.

If G is not strongly connected, it can be partitioned into its maximal strongly-connected sub-graphs, or "strong linkage classes". These inherit from G a directed graph structure, $\overline{G}$, in which there is an edge in $\overline{G}$ from the strong linkage class G_u to the strong linkage class G_v whenever there is an edge in G from some node in G_u to some node in G_v. $\overline{G}$ cannot have any directed cycles and so always has terminal strong linkage classes, with no edges leaving them. Let these be $G_1, \cdots, G_{\mathfrak{t}}$. For each $1 \le t \le \mathfrak{t}$, let $\rho^t \in \mathbb{R}^m$ be the vector which, for vertices of G that lie in G_t, agrees with the vector ρ_{G_t}, coming from the Matrix-Tree Theorem applied to G_t as an isolated graph, and, for all other vertices, j, $(\rho^t)_j = 0$. Then, the ρ^t form a basis for $\ker \mathcal{L}(G)$:

$$\ker \mathcal{L}(G) = \langle\, \rho^1, \cdots, \rho^{\mathfrak{t}} \,\rangle\,. \tag{2.13}$$

Note that ρ^t may be very sparse, being non-zero only for vertices in the single strong linkage class G_t.

2.3 Stoichiometric Compatibility Class

The essential idea here is that, *regardless of the kinetics*, reaction network structure *alone* imposes restrictions on the way that composition trajectories can look. In particular, a trajectory that passes through $\mathbf{x} \in \mathbb{R}^s_{\geq 0}$ can eventually reach $\mathbf{x}' \in \mathbb{R}^s_{\geq 0}$ only if the pair $(\mathbf{x}', \mathbf{x})$ is compatible with certain "stoichiometrical" conditions the reaction network imposes.

To see this, we consider a reaction system $G = (V, \mathscr{R}, \mathcal{K}, Y)$. The species formation rate function is given by

$$f(\mathbf{x}) = \sum_{\mathscr{R}} \mathcal{K}_{y \to y'}(\mathbf{x})(y' - y).$$

From Definition 2.1.1, we have the following well known lemma:

Lemma 2.3.1. *Let $G = (V, \mathscr{R}, \mathcal{K}, Y)$ be a reaction system with species formation rate function $f(\cdot)$. Then, for every $i \in \{1, \ldots, s\}$ and every $\mathbf{x} \in \mathbb{R}^s_{\geq 0}$, $x_i = 0$ implies that $f_i(\mathbf{x}) \geq 0$.*

Thus, for each $\mathbf{x} \in \mathbb{R}^s_{\geq 0}$, $f(\mathbf{x})$ is a non–negative linear combination of the reaction vectors for the network $G = (V, \mathscr{R}, Y)$. In particular, for $\mathbf{x} \in \mathbb{R}^s_{> 0}$, $f(\mathbf{x})$ is a positive linear combination of the reaction vectors. In any case $f(\mathbf{x})$ must point along the cone generated by the reaction vectors and must certainly lie in the linear subspace of $\mathbb{R}^s$ spanned by them. This last idea serves as motivation for our next definition.

Definition 2.3.1. *The* stoichiometric subspace *for a reaction network $G = (V, \mathscr{R}, Y)$ is the linear subspace $\mathcal{S} \subset \mathbb{R}^s$ defined by*

$$\mathcal{S} := \mathit{span}\{y' - y \in \mathbb{R}^s : (y, y') \in \mathscr{R}\}.$$

A vector $\mathbf{x}' \in \mathbb{R}^s_{\geq 0}$ can follow a vector $\mathbf{x} \in \mathbb{R}^s_{\geq 0}$ along a solution of $\dot{\mathbf{x}} = \sum_{\mathscr{R}} \mathcal{K}_{y \to y'}(\mathbf{x})(y' - y)$ only if $\mathbf{x}' - \mathbf{x}$ lies in the stoichiometric subspace (and, in particular, in the stoichiometric cone: the set of all non–negative linear combinations of the reaction vectors of the stoichiometric subspace) for the network $G = (V, \mathscr{R}, Y)$. Thus, if $\mathbf{x} : I \subseteq \mathbb{R} \to \mathbb{R}^s_{\geq 0}$ is a solution of $\dot{\mathbf{x}} = \sum_{\mathscr{R}} \mathcal{K}_{y \to y'}(\mathbf{x})(y' - y)$ which passes through $\mathbf{x}^0$ then, for all $t \in I$, we must have

$$\mathbf{x}(t) \in (\mathbf{x}^0 + \mathcal{S}) \cap \mathbb{R}^s_{\geq 0},$$

where $\mathcal{S}$ is the stoichiometric subspace and

$$\mathbf{x}^0 + \mathcal{S} := \{\mathbf{x}^0 + \gamma \in \mathbb{R}^s : \gamma \in \mathcal{S}\}.$$

This is to say that a vector of concentrations $\mathbf{x}$ can lie on a trajectory passing through $\mathbf{x}^0$ only if $\mathbf{x}$ and $\mathbf{x}^0$ are "stoichiometrically compatible".

Definition 2.3.2. *Let $G = (V, \mathscr{R}, Y)$ be a reaction network, and let $\mathcal{S} \subset \mathbb{R}^s$ be its stoichiometric subspace. Two vectors $\mathbf{x} \in \mathbb{R}^s_{\geq 0}$ and $\mathbf{x}' \in \mathbb{R}^s_{\geq 0}$ are stoichiometrically compatible if $\mathbf{x}' - \mathbf{x}$ lies in $\mathcal{S}$. Stoichiometric compatibility is an equivalence relation that induces a partition of $\mathbb{R}^s_{\geq 0}$ (resp.$\mathbb{R}^s_{>0}$) into equivalence classes called the* stoichiometric compatibility classes *(resp.* positive stoichiometric compatibility classes*) for the network. In particular, the stoichiometric compatibility class containing $\mathbf{x} \in \mathbb{R}^s_{\geq 0}$ is the set $(\mathbf{x}+\mathcal{S}) \cap \mathbb{R}^s_{\geq 0}$, and the positive stoichiometric compatibility class containing $\mathbf{x} \in \mathbb{R}^s_{>0}$ is the set $(\mathbf{x} + \mathcal{S}) \cap \mathbb{R}^s_{>0}$.*

The stoichiometric compatibility class is also called the "invariant polyhedron", and we will denote it by

$$\mathcal{P}_{x^0} \;:=\; (x^0 + \mathcal{S}) \cap \mathbb{R}^s_{\geq 0}\,, \tag{2.14}$$

for all positive time. In other words, this set is forward-invariant with respect to the dynamics (2.10). It follows that any stoichiometric compatibility class of a network has the same dimension as the stoichiometric subspace.

Let us consider the following two examples from [48].

Example 2.3.1. *Consider the simple network*

$$A \leftrightarrows 2B \tag{2.15}$$

If we suppose that this network is endowed with mass–action kinetics, the appropriate differential equations are

$$\begin{array}{rcl} \dot{x}_A &=& \kappa_{2B\to A} x_B^2 - \kappa_{A\to 2B} x_A \\ \dot{x}_B &=& 2\kappa_{A\to 2B} x_A - 2\kappa_{2B\to A} x_B^2 \end{array} \tag{2.16}$$

The set of equilibrium points for (2.16) *is given by those $\mathbf{x} \in \mathbb{R}^s_{\geq 0}$ that satisfy*

$$x_A = \frac{\kappa_{2B\to A}}{\kappa_{A\to 2B}} x_B^2$$

The phase portrait for (2.16) *is sketched in Figure 2.1.*

Example 2.3.2. *Consider the network*

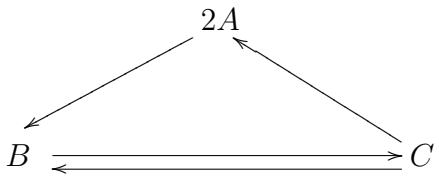

(2.17)

As the figure is intended to suggest, a composition trajectory must lie entirely within a stoichiometric compatibility class.

In the earlier example shown in (2.1), we have $y_2 - y_1 = (2, -1, 1)$, which means that with the occurrence of each reaction, two units of A and one of C are produced, while one unit of B is consumed. This vector $(2, -1, 1)$ spans the stoichiometric subspace $\mathcal{S}$ for the network (2.1).

The question of real interest is whether the differential equations for a reaction system can admit multiple positive equilibria *within a stoichiometric compatibility class*.

A chemical reaction system exhibits *multistationarity* if there exists a stoichiometric compatibility class $\mathcal{P}_{x^0}$ with two or more steady states in its relative interior. A system may admit multistationarity for all, some, or no choices of positive rate constants κ_{ij}; if such rate constants exist, then we say that the network *has the capacity for multistationarity*.

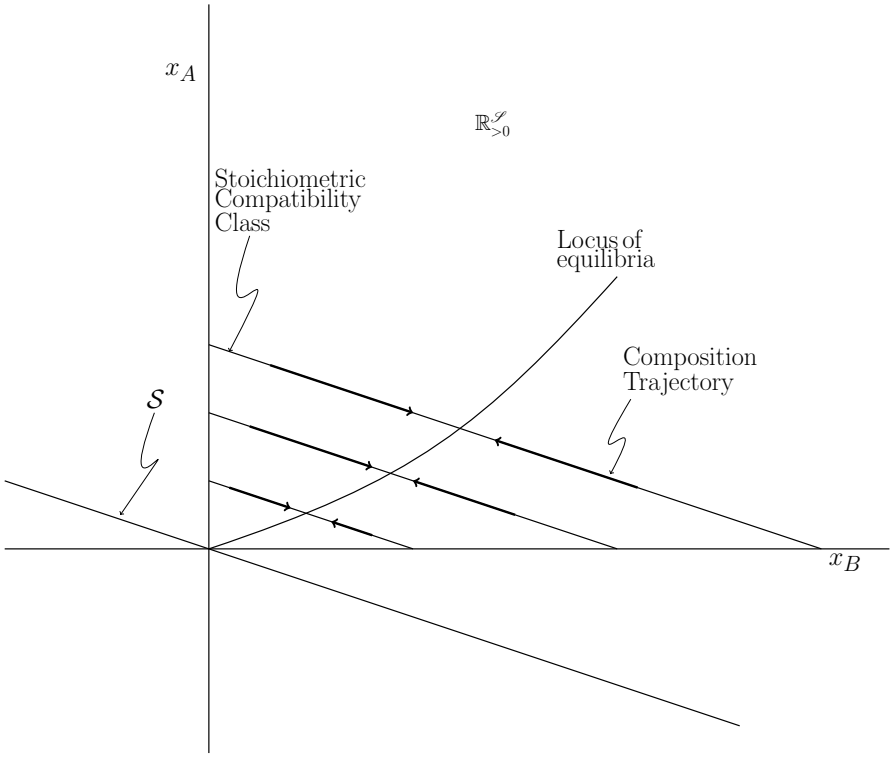

Figure 2.1: Stoichiometric compatibility class for network (2.15).

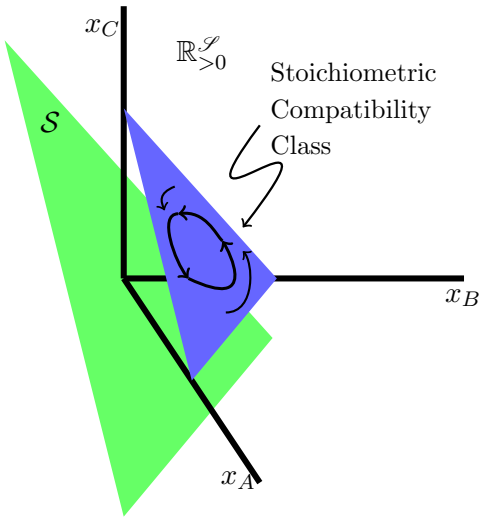

Figure 2.2: Stoichiometric compatibility class for network (2.17).

2.4 Deficiency

The deficiency of a chemical reaction network is an important invariant. Before we give any definition we focus on the fact that $\ker \Sigma$ contains the subspace $\ker \mathcal{L}(G)$ since $\Sigma = Y.\mathcal{L}(G)$. This directs our attention to the kernel of Y and more specifically to that part of the kernel of Y which lies in the image of $\mathcal{L}(G)$. This leads us to the following definition:

Definition 2.4.1. *The "dynamic deficiency" of a biochemical network, $\delta_D \in \mathbb{N}_{\geq 0}$, is the difference in dimension between the two subspaces: $\delta_D = \dim \ker \Sigma - \dim \ker \mathcal{L}(G)$, or, equivalently,*

$$\delta_D = \dim(\ker Y \cap \text{Image } \mathcal{L}(G)).$$

Note that the deficiency of a reaction network is non-negative because it can be interpreted as the dimension of a certain linear subspace [45].

The "dynamic deficiency" just defined is different from the "deficiency" as usually defined in CRNT, [48, 63], which we call the "structural deficiency", $\delta_S \in \mathbb{N}_{\geq 0}$:

$$\delta_S = m - \dim \mathcal{S} - l,$$

where m denotes the number of complexes, l is the number of linkage classes (connected components) and $\mathcal{S}$ is the stoichiometric subspace.

While δ_D may depend on the values of rate constants, δ_S is independent of them. However, the former will be more convenient for our purposes.

It is known that $\delta_D \leq \delta_S$. Furthermore, if there is only a single terminal strong linkage class in each linkage class of G, then $\delta_D = \delta_S$. Recall that a graph is connected if any two distinct nodes are linked by a path of contiguous edges, ignoring directions. A linkage class of G is then a maximal connected sub-graph. Distinct linkage classes are totally disconnected, with no edges between them.

For systems arising from zero-deficiency networks and networks whose linkage classes have deficiencies zero or one, there are many results due to Feinberg that concern the existence, uniqueness, and stability of steady states [45, 49–51].

2.5 Generalized mass–action kinetics

We can admit for consideration networks containing peculiar reactions like $A \to 2A$ or $0 \to A$ (zero reacts to A) which, at first glance, appear to be incompatible with the conservation of matter.

We would also like to study homogeneous (well-stirred) reactors that are open to the influx or efflux of at least certain species. There are varieties of open reactors for which the appropriate differential equations can be viewed as deriving from a reaction network obtained by modifying or augmenting the true chemical network in such a way as to model, by means of "pseudo–reactions", various non–chemical effects.

Obviously in open systems there is no longer any reason to require that the kinetic behavior be consistent with the requirements of thermodynamics applied to closed systems. Nevertheless, it is still of interest to identify classes of kinetic equations which behave as though the

laws of closed system thermodynamics applied, for we are then able to say something about the uniqueness and stability of their equilibrium states.

Biological systems suffer many further complexities, some of which appear to be accommodated within CRNT. Experimental studies of biological systems like metabolic pathways are often carried out by by buffering the concentration of certain substrates so that they remain approximately fixed over the duration of the experiment. With mass–action kinetics, these fixed concentrations can be incorporated into the rate constants of the reactions in which the substrates participate.

Following Horn and Jackson [80], we say that a network $G = (V, \mathscr{R}, Y)$ is *conservative* if there exists a (positive) vector contained in $\mathcal{S}^{\perp}$, the orthogonal complement of the stoichiometric subspace for the network.

One of the pleasant features of conservative networks is given by Horn and Jackson. They show that a network is conservative if and only if all its stoichiometric compatibility classes are compact (they call the stoichiometric compatibility classes *reaction simplices*).

In Appendix 1 of [80] it is shown that a stoichiometric compatibility class is bounded if and only if the system is conservative. Furthermore, if there is one bounded stoichiometric compatibility class, then all stoichiometric compatibility classes are bounded.

We may now assert that a kinetic description of chemical reactions in closed systems with ideal mixtures, completely consistent with the requirements of stoichiometry and thermodynamics, may be obtained by satisfying the following four requirements.

(a) The rate function of each elementary reaction is of the mass–action form.

(b) The stoichiometric coefficients are such that mass is conserved in each elementary reaction.

(c) The kinetic constants in the rate functions are constrained in such a way that the principle of detailed balancing is satisfied.

(d) The stoichiometric coefficients are non-negative integers.

There then arises the question whether anything might be gained by investigating the consequences of relaxing one or more of the conditions (b), (c) and (d); in other words, by studying *generalized mass–action kinetics*, in which only (a) need be satisfied.

In this work we are interested in the characteristics of some systems in which (b), (c) have been relaxed.

By relaxing condition (b), requiring mass conservation in each elementary reaction, many open systems can be drawn into the formal structure of mass–action kinetics.

Turning to condition (c), the principle of detailed balance stands for the condition that in case of equilibrium (= stationarity) the rate of each reaction equals the rate of the corresponding antireaction ($\kappa_{y\to y'}\mathbf{x}^{y} = \kappa_{y'\to y}\mathbf{x}^{y'}$). The detailed balancing requirement in closed systems is possibly less firmly rooted than the other requirements, and it is possible to find a more general class of kinetics which is fully consistent with the laws of thermodynamics. Furthermore, when the formal structure of generalized mass–action kinetics is used to describe open systems, in the manner just outlined, it would be quite inappropriate to require detailed balancing. For instance, in the following example:

$$A \to B,\ A \leftrightarrow 0,\ B \leftrightarrow 0,$$

detailed balancing would require the rate of addition of A (corresponding to $0 \to A$) to equal the rate of removal of A (corresponding to $A \to 0$) in the steady state. But clearly this cannot be so, because of the chemical reaction $A \to B$.

When establishing a setting for generalized mass–action kinetics systems, we seek to classify reaction networks according to their capacity to induce differential equations which admit behavior of a specified type.

In practice, complete sets of rate constants for intricate networks are hardly ever known with great precision. It is often the case that chemists have a very good sense of what reactions are occurring but can estimate or measure rate constants only to within a considerable margin of uncertainty. See [45, 47, 102].

Moreover, even though a great variety of computational methods have been developed for the identification of chemical reaction networks and their reaction rate constants from time-dependent measurements of chemical species concentrations, two different reaction networks might generate identical dynamical system models, making it impossible to discriminate between them, even if we are given experimental data of perfect accuracy and unlimited temporal resolution. In [33], Craciun and Pantea describe necessary and sufficient conditions for two reaction networks to give rise to the same dynamical system model. Also, they show that, even if we know the reaction network that gives rise to the chemical dynamics under study, there might exist multiple sets of reaction rate constants that provide perfect fit for the data since they give rise to identical dynamical system models.

In this new context of generalized mass–action kinetics, it is possible to find equilibria which are not detailed balance.

Definition 2.5.1. *A* complex balanced *mass–action kinetics system is a dynamical system for which the algebraic equations $\mathcal{L}(G)\Psi(\mathbf{x}) = 0$ admit a strictly positive solution $\mathbf{x}_0 \in \mathbb{R}^s_{>0}$. Such a solution $\mathbf{x}_0$ is a steady state of the system, i.e., the s coordinates of $Y\mathcal{L}(G)\Psi(\mathbf{x}_0)$ vanish.*

Clearly, a mass–action kinetics system (5.3) being complex balanced depends on both the digraph G and the rate constants κ_{ij}. A main property of complex balanced systems is that *all* strictly positive steady states $\mathbf{x}$ satisfy $\mathcal{L}(G)\Psi(\mathbf{x}) = 0$.

Complex balanced systems are shown to satisfy the "quasithermostatic" (QTS) and "quasithermodynamic" (QTD) conditions [80] (in the terminology of [30], "quasithermostatic" means that the positive steady state variety is toric). QTS and QTD roughly mean that a Lyapunov function of a certain form exists, for a unique interior steady state in each invariant polyhedron (stoichiometric compatibility class).

We introduce here an example of a system that is complex balanced and not detailed balanced.

Example 2.5.1. *This reaction network diagram represents a nonsequential multisite phosphorylation system with two sites, under mass–action kinetics. This network models, for example,*

the MEK-MKP3-ERK2 system [14, 52, 112, 113]:

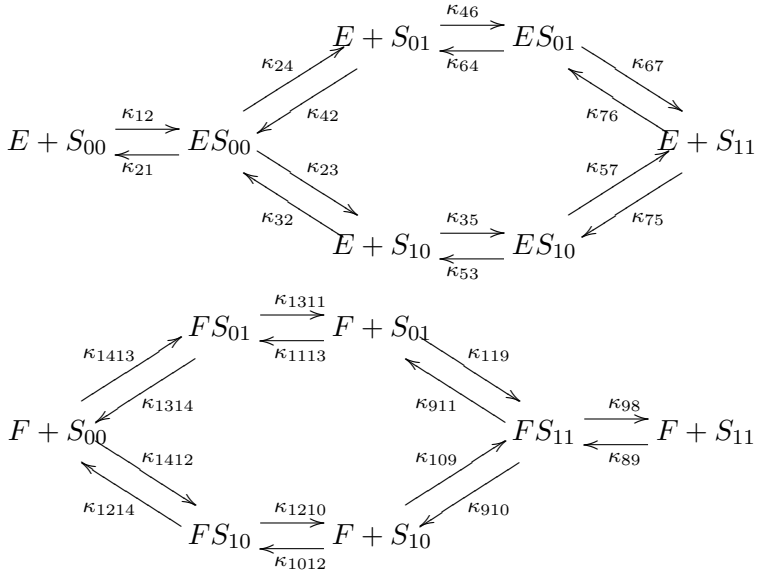

(2.18)

The four phosphoforms, S_{00}, S_{10}, S_{01}, S_{11}, are interconverted by the kinase E and the phosphatase F. There are other six species $ES_{00}, ES_{10}, ES_{01}, FS_{11}, FS_{10}, FS_{01}$. [1]

Under mass–action kinetics, although the rate constants κ_{32}, κ_{42}, κ_{75}, κ_{76}, κ_{109}, κ_{119}, κ_{1412}, κ_{1413}, are usually taken to be very small and so the corresponding reactions are omitted, we will not ignore them in this example because we are interested in special properties of the reaction constants in reversible networks.

Assuming for any *choice of first order rate constant κ_1 and second order rate constant κ_2 for which the value of κ_1 equals the value of κ_2 regardless of the corresponding units, the rate constants of the mass–action kinetics system satisfy:*

$$
\begin{aligned}
&\kappa_{12} = \kappa_{46} = \kappa_{89} = \kappa_{1012} = \kappa_2\\
&\kappa_{24} = \kappa_{53} = \kappa_{67} = \kappa_{910} = \kappa_{1214} = \kappa_{1311} = \kappa_1\\
&\kappa_{32} = \kappa_{42} = \kappa_{75} = \kappa_{76} = \kappa_{109} = \kappa_{119} = \kappa_{1412} = \kappa_{1413} = \frac{1}{4}\kappa_2\\
&\kappa_{35} = \kappa_{1113} = \frac{3}{4}\kappa_2,\ \ \kappa_{23} = \kappa_{57} = \kappa_{64} = \kappa_{911} = \kappa_{1314} = \frac{3}{4}\kappa_1,\\
&\kappa_{21} = \frac{23}{4}\kappa_1,\ \ \kappa_{98} = \frac{47}{4}\kappa_1,\ \ \kappa_{1210} = \frac{69}{22}\kappa_1.
\end{aligned}
\tag{2.19}
$$

Then, for any $\alpha \in \mathbb{R}_{>0}$, the real vector in $\mathbb{R}^{12}_{>0}$ of the values of the molar concentrations of the different species $\mathbf{x}_{0,\alpha} = \alpha\,(23, 17, 11, 47, 1, 2, 4, 8, 14, 11, 13, 16)$ is a positive steady state of the system. Moreover, it satisfies $\mathcal{L}(G)\Psi(\mathbf{x}_{0,\alpha}) = 0$, that is, it is a complex balancing equilibrium ([80], [30], see definition 2.5.1 below). On the other hand, for this choice of rate constants the system is not *detailed balanced since the requirement of the rate of each*

[1] In the MEK-MKP3-ERK2 system, E would stand for MEK, F for MKP3, S_{00} for ERK2, S_{11} for the doubly phosphorylated ERK2 (ppERK2) and S_{10} and S_{01} for the two monophosphorylated forms of ERK2 (the form phosphorylated on tyrosine, p_YERK2, or threonine, p_TERK2, alone); also $ES_{00}, ES_{10}, ES_{01}, FS_{11}, FS_{10}, FS_{01}$ represent MEK·ERK2, MEK·p_YERK2, MEK·p_TERK2, MKP3·ppERK2, MKP3·p_YERK2, MKP3·p_TERK2, respectively.

reaction equaling the rate of the corresponding antireaction does not hold, for instance, for both $i_1 = 1,\ j_1 = 2$ *and* $i_2 = 10,\ j_2 = 12$ *simultaneously that is, for the pairs of reactions*

$$E + S_{00} \underset{\frac{23}{4}\kappa_1}{\overset{\kappa_2}{\rightleftarrows}} ES_{00}\,, \qquad FS_{10} \underset{\kappa_2}{\overset{\frac{69}{22}\kappa_1}{\rightleftarrows}} F + S_{10}.$$

In Chapter 5 we clarify the relation between complex and detailed balanced systems.

2.5.1 The Michaelis-Menten formula

One case worth mentioning (although it is not entirely related to generalized mass–action kinetics) is the Michaelis-Menten formula which usually arises while studying enzymes. Biochemists usually describe the kinetics of enzyme catalyzed reactions by formulae which look much more complex than mass–action rules like. The well-known Michaelis-Menten kinetics for a reaction $A \to B$, catalyzed by an enzyme E,

$$\frac{dx_B}{dt} = \frac{V_{max} x_A}{K_M + x_A},$$

is a rational, and not linear, function of the concentration x_A. However, the Michaelis-Menten formula is derived from the reaction network

$$A + E \rightleftarrows EA \to B + E$$

under mass–action, assuming that the transitional enzyme-substrate complex, EA, is in steady state, x_B is small and x_E is much smaller than x_A , ([27], §2.2). Michaelis-Menten kinetics may hence be incorporated into the CRNT framework by appropriately modifying the underlying reaction network.

We are now ready to focus on some new results on this area.

Chapter 3

Invariants of biochemical networks

As we mentioned in the Introduction of this work, the nonlinearities found in molecular networks usually prevent mathematical analysis of network behavior, which has largely been studied by numerical simulation. This can lead to difficult problems of parameter determination. However, molecular networks give rise, through mass-action kinetics, to polynomial dynamical systems, whose steady states are zeros of a set of polynomial equations. These equations may be analyzed by algebraic methods, in which parameters are treated as symbolic expressions whose numerical values do not have to be known in advance. For instance, an "invariant" of a network is a polynomial expression on selected state variables that is satisfied in any steady state. Invariants have been found that encode key network properties and that discriminate between different network structures. Although invariants may be calculated by computational algebraic methods, such as Gröbner bases, these become computationally infeasible for biologically realistic networks. In this chapter, we exploit Chemical Reaction Network Theory (CRNT) to develop an efficient procedure for calculating invariants that are linear combinations of "complexes", or the monomials coming from mass action. Complex-linear invariants form a limited subset of all invariants but, as shown here, they have biological significance and can be efficiently calculated for realistic networks. Our work clarifies and subsumes many previous results and provides a new tool for symbolic, steady-state analysis of molecular networks. For instance, we recover as a special case the Shinar-Feinberg Theorem, that gives structural conditions for a network of deficiency one to have "absolute concentration robustness" (ACR). We also apply our method to enzyme bifunctionality, analyzing two examples, the bacterial EnvZ/OmpR osmolarity regulator, having deficiency two, and the mammalian phosphofructokinase-2-fructose-2,6-bisphosphatase glycolytic regulator, having deficiency four. As we said, complex-linear invariants provide a tool for systematically analyzing the steady-state properties of complex networks, without knowledge of parameter values.

The focus on steady states, rather than transient dynamics, is still of substantial interest. For instance, in time-scale separation, which has been a widespread method of simplification in biochemistry and molecular biology, a fast sub-system is assumed to be at steady state with respect to a slower environment and steady-state analysis is used to eliminate the internal complexity in the sub-system, [66]. Approximate or quasi-steady states have also been shown to exist under various cellular conditions and can now be engineered *in vivo*, [103, 108]. Finally, steady states provide the skeleton around which the transient dynamics unfolds, so knowledge

of the former can be helpful for understanding the latter.

The present chapter focuses on the algebraic concept of an "invariant": a polynomial expression on selected state variables that is zero in any steady state, with the coefficients of the expression being rational expressions in the symbolic rate constants, [112]. Recall that a rational expression is a quotient of two polynomials; an example of such being the classical Michaelis-Menten constant of an enzyme, [27]. (A more general definition of an invariant allows the coefficients to include conserved quantities, [173], but this extension is not discussed here.) Since each of the rate functions, $f_i(x;\kappa)$, is zero in any steady state, the force of the definition comes from the restriction to "selected state variables". It is possible that, by performing appropriate algebraic operations on $f_1, \cdots, f_s$, non-selected variables can be eliminated, leaving a polynomial expression on only the selected variables that must be zero in any steady state.

Invariants turn out to be surprisingly useful. They have been shown to characterize the biochemical networks underlying multisite protein phosphorylation, [112], suggesting that different network architectures can be identified through experimental measurements at steady state. If an invariant has only a single selected variable that appears linearly, this variable has the same value in any steady state since it is determined solely by the rate constants. In particular, its value is unaffected by changes to the initial conditions or to the total amounts of any species. This is "absolute concentration robustness" (ACR), as introduced in [144], which accounts for experimental findings in some bacterial bifunctional enzymes, [8, 141, 143]. The mammalian bifunctional enzyme, phosphofructokinase-2-fructose-2,6-bisphosphatase (PFK2-F2,6BPase), which has a more complex enzymatic network, also yields invariants, with implications for regulation of glycolysis, [34]. The methods developed here provide a systematic way to analyze such bifunctional enzymes, as explained below.

Computational algebra exploits the method of Gröbner bases to provide an Elimination Theorem, [28], that permits variables to be systematically eliminated among the rate equations, $f_1, \cdots, f_s$, [112]. Algorithms for calculating Gröbner bases are available in general-purpose tools like Mathematica, Matlab and Maple and in specialized mathematical packages such as Singular [35] and Macaulay2 [61].However, these algorithms are computationally expensive for the task at hand. They have been developed for general sets of polynomials and have not been optimized for those coming from biochemical networks. For instance, Mathematica's Gröbner basis algorithm does not terminate on the network for PFK2-F2,6BPase. If invariants are to be exploited further, alternative approaches are needed.

Aside from this nonlinearity, the defining rate equations come from linear processes on complexes. This observation is the starting point of CRNT and reveals that biochemical networks conceal much linearity behind their nonlinearity, [48, 63, 66, and see below]. This suggests the possibility of using fast linear methods, in preference to slow polynomial algorithms, to construct a subset of invariants: those that are symbolic linear combinations of the complex monomials, x^y. As before, this definition acquires substance by restricting the complexes that can appear. If $y_1, \ldots, y_k$ are the selected complexes, then a complex-linear invariant is a polynomial expression of the form $a_1 x^{y_1} + \cdots + a_k x^{y_k}$, that is zero in any steady state, where $a_1, \cdots, a_k$ may be rational expressions in the symbolic rate constants.

In this chapter, based on joint work with R. Karp, T. Dasgupta, A. Dickenstein and J. Gunawardena, we examine a large class of complex-linear invariants that we call "type 1". We determine the dimension of the space of type 1 invariants (Proposition 3.3.1) and provide a lin-

ear algorithm for calculating them (Theorem 3.3.1). We recover the Shinar-Feinberg Theorem for ACR, [144], as Corollary 3.4.2. We then apply the method to contrast two examples of enzymatic bifunctionality, the bacterial EnvZ/OmpR osmolarity regulator and the mammalian PFK2-F2,6BPase glycolytic regulator. The method is sufficiently straightforward that the invariants for networks of this kind can be found by manual inspection of an appropriate matrix. This provides a foundation for the steady-state algebraic analysis of a broad class of relevant biochemical networks.

3.1 CRNT and the graphical framework

It is assumed that there are s species, $\mathscr{S} = \{\mathfrak{s}_1, \cdots, \mathfrak{s}_s\}$, whose concentrations are $x_1, \cdots, x_s \in \mathbb{R}$, respectively, and m complexes, $\mathscr{C} = \{y_1, \ldots, y_m\}$.

Recall that the reactions in the network define a directed graph on the complexes, with an edge $y_i \to y_j$ whenever there is a reaction with substrate stoichiometry given by y_i and product stoichiometry given by y_j. This graph may be studied using a graphical framework for analyzing steady states that underpins many crucial analyses in biochemistry and systems biology. This is fully explained in [66] and briefly reviewed here.

As we saw in Chapter 2, the kernel of $\mathcal{L}(G)$ can be calculated as follows: Let $G_1, \cdots, G_{\mathfrak{t}}$ be the terminal strong linkage classes of G. For each $1 \leq t \leq \mathfrak{t}$, let $\rho^t \in \mathbb{R}^m$ be the vector which, for vertices of G that lie in G_t, agrees with the vector ρ_{G_t}, coming from the Matrix-Tree Theorem applied to G_t as an isolated graph, and, for all other vertices, j, $(\rho^t)_j = 0$. Then, the ρ^t form a basis for $\ker \mathcal{L}(G)$:

$$\ker \mathcal{L}(G) = \langle\, \rho^1, \cdots, \rho^{\mathfrak{t}} \,\rangle\,. \tag{3.1}$$

This graphical, linear framework provides a way to rewrite certain nonlinear biochemical systems as linear, at steady state. It has many applications, [66]. For CRNT, the Laplacian, $\mathcal{L}(G) : \mathbb{R}^m \to \mathbb{R}^m$, is a linear analogue for complexes of the nonlinear function, $f : \mathbb{R}^s \to \mathbb{R}^s$, for species. With the definitions given in Section 2.1 it may be checked that $f(x) = Y.\mathcal{L}(G).\Psi(x)$, for any $x \in \mathbb{R}^s$.

This fundamental observation, which originates in the pioneering work of Horn and Jackson, [80], is the starting point of CRNT. It shows that the the nonlinear rate function f can be decomposed into a purely linear part, $Y.\mathcal{L}(G)$, that includes the Laplacian, and the essential nonlinearity, Ψ, coming from the complex monomials. This decomposition is the basis for what follows.

3.2 Generating complex-linear invariants

Depending on the application, invariants may be required that involve only certain complexes, $y_{i_1}, \ldots, y_{i_k}$. Since the indices can be permuted so that the complexes of interest appear first in the ordering, it can be assumed that invariants are sought on $y_1, \ldots, y_k$. Let Σ be the $s \times m$ matrix representing the linear part of the CRNT decomposition, $\Sigma = Y.\mathcal{L}(G)$. A simple way to construct a complex-linear invariant on $y_1, \ldots, y_k$ is to find a vector, $a^\dagger \in \mathbb{R}^k$, such that, if $(a, 0)^\dagger \in \mathbb{R}^m$ is a extended with $m - k$ zeros, $(a, 0) = (a_1, \cdots, a_k, 0, \cdots, 0)$, then $(a, 0)$ is in

the rowspan of Σ. That is, it is a linear combination of the rows of Σ. If $x \in \mathbb{R}^s$ is any steady state of the system, so that $f(x) = 0$, then $\Psi(x) \in \ker \Sigma$ because $\Sigma.\Psi(x) = Y.\mathcal{L}(G).\Psi(x) = f(x) = 0$. Since $(a, 0)$ is in the rowspan of Σ, $(a, 0).\Psi(x) = 0$. Hence, by definition of Ψ, $a_1 x^{y_1} + \cdots + a_k x^{y_k} = 0$, giving a complex-linear invariant on $y_1, \ldots, y_k$.

Not all such invariants may arise in this way. For that to happen, it is necessary not just for $(a, 0).\Psi(x) = 0$ whenever x is a steady state but for $(a, 0).v = 0$ for all $v \in \ker \Sigma$. The relationship between $\{\Psi(x) \mid x \text{ is a steady state}\}$ and $\ker \Sigma$ is not straightforward. To sidestep this problem, we focus here only on those invariants, $a_1 x^{y_1} + \cdots + a_k x^{y_k}$, in which $(a, 0)$ is in the rowspan of Σ. We call these type 1 complex-linear invariants. Non-type 1 invariants do exist, as we show in Subsection 3.2.1. The type 1 invariants form a vector space that we abbreviate $\mathcal{I}_k$; note that $\mathcal{I}_k$ depends on $y_1, \ldots, y_k$ and not just on k. Two basic problems are, first, to determine the dimension of $\mathcal{I}_k$ and, second, to generate its elements.

A simple solution to the second problem is to break the matrix Σ into the $s \times k$ sub-matrix K consisting of the first k columns of Σ and the $s \times (m - k)$ sub-matrix $\widetilde{\Sigma}$ consisting of the remaining $m - k$ columns, so that $\Sigma = K \,|\, \widetilde{\Sigma}$. Any vector $b^\dagger \in \mathbb{R}^s$ which is in the left null space of $\widetilde{\Sigma}$, $b \in \mathcal{N}_L(\widetilde{\Sigma})$, so that $b.\widetilde{\Sigma} = 0$, gives an $(a, 0) = b.\Sigma$ that is in the rowspan of Σ. The assignment $b \to b.\Sigma$ thereby defines a surjection, $\mathcal{N}_L(\widetilde{\Sigma}) \to \mathcal{I}_k$. Moreover, $b_1.\Sigma = b_2.\Sigma$, if, and only if, $(b_1 - b_2) \in \mathcal{N}_L(\Sigma) \subseteq \mathcal{N}_L(\widetilde{\Sigma})$. Hence, there is an isomorphism $\mathcal{I}_k \cong \mathcal{N}_L(\widetilde{\Sigma})/\mathcal{N}_L(\Sigma)$. If X is any $s \times r$ matrix, $\dim \mathcal{N}_L(X) = n - \mathrm{rank} X$. We conclude that $\dim \mathcal{I}_k = \mathrm{rank}\Sigma - \mathrm{rank}\widetilde{\Sigma}$, which yields a convenient way to determine the dimension of $\mathcal{I}_k$ by Gaussian elimination.

This method amounts to eliminating the complexes $y_{k+1}, \ldots, y_m$ by taking linear combinations of the defining rate functions, $f_1, \cdots, f_s$. This can be biologically informative because it suggests which rate functions, and, hence, which species at steady state, determine the invariant, [34]. An alternative approach, based on duality, allows the sparsity of (3.1) to be exploited. We will develop it in Section 3.3, but first we will make some comments on non-type 1 invariants.

3.2.1 Invariants that are not of type 1

Consider the hypothetical reaction network in Figure 3.1A. While such chemistry is unlikely, it illustrates the mathematical issues. The network has three species, $\mathfrak{s}_1, \mathfrak{s}_2, \mathfrak{s}_3$ and nine complexes $y_1, \ldots, y_9$, ordered as in Figure 3.2C. The ODEs are

$$\begin{aligned} \frac{dx_1}{dt} &= k_1 x_1 \\ \frac{dx_2}{dt} &= k_4 x_1 x_3 - k_2 x_2^2 \\ \frac{dx_3}{dt} &= k_5 x_1 x_2 - k_3 x_3^2 \,. \end{aligned} \tag{3.2}$$

With the given ordering, the matrix $\Sigma = Y.\mathcal{L}(G)$ is

$$\begin{bmatrix} k_1 & 0 & 0 & 0 & 0 & 0 & 0 & 0 & 0 \\ 0 & 0 & -k_2 & 0 & 0 & 0 & k_4 & 0 & 0 \\ 0 & 0 & 0 & 0 & -k_3 & 0 & 0 & k_5 & 0 \end{bmatrix} .$$

A

$$\begin{aligned} \mathfrak{s}_1 &\to 2\mathfrak{s}_1 \\ 2\mathfrak{s}_2 &\to \mathfrak{s}_2 \\ 2\mathfrak{s}_3 &\to \mathfrak{s}_3 \\ \mathfrak{s}_1+\mathfrak{s}_3 &\to \mathfrak{s}_1+\mathfrak{s}_2+\mathfrak{s}_3 \\ \mathfrak{s}_1+\mathfrak{s}_2 &\to \mathfrak{s}_1+\mathfrak{s}_2+\mathfrak{s}_3 \end{aligned}$$

B

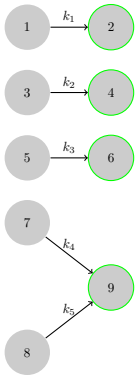

C

$$\begin{aligned} y_1 &\quad \mathfrak{s}_1 \\ y_2 &\quad 2\mathfrak{s}_1 \\ y_3 &\quad 2\mathfrak{s}_2 \\ y_4 &\quad \mathfrak{s}_2 \\ y_5 &\quad 2\mathfrak{s}_3 \\ y_6 &\quad \mathfrak{s}_3 \\ y_7 &\quad \mathfrak{s}_1+\mathfrak{s}_3 \\ y_8 &\quad \mathfrak{s}_1+\mathfrak{s}_2 \\ y_9 &\quad \mathfrak{s}_1+\mathfrak{s}_2+\mathfrak{s}_3 \end{aligned}$$

Figure 3.1: Network with complex-linear invariants that are not of type 1. **A** Hypothetical reaction network. **B** Labeled, directed graph on the complexes, with the terminal strong linkage classes outlined in green. **C** Numbering scheme for the complexes.

Focusing on the complexes y_1, y_3, y_5, y_7, y_8, Proposition 3.3.1 shows that the space of type 1 complex-linear invariants has dimension three. However, it is easy to see from (3.2) that the only steady state of the network is when $x_1 = x_2 = x_3 = 0$. Hence, for any values of $a, b, c, d, e \in \mathbb{R}$, the polynomial expression

$$ax^{y_1} + bx^{y_3} + cx^{y_5} + dx^{y_7} + ex^{y_8}$$

always vanishes in any steady state. Hence, the space of complex-linear invariants on y_1, y_3, y_5, y_7, y_8 has dimension five.

3.3 Duality and the structure of $\mathcal{I}_k$

Let $d = \dim\ker\Sigma$ and let B be any $m \times d$ matrix whose columns form a basis of $\ker\Sigma$. Then, $\Sigma.B = 0$ and the rowspan of Σ and the columnspan of B are dual spaces of each other. If $a^\dagger \in \mathbb{R}^k$, then $(a, 0)$ is in the rowspan of Σ if, and only if, $(a, 0).B = 0$. If B' is the $k \times d$ sub-matrix of B consisting of the first k rows, then $(a, 0).B = 0$ if, and only if, $a.B' = 0$. Hence, type 1 invariants form the dual space to the columns of B'.

Proposition 3.3.1. *The space $\mathcal{I}_k$ of type 1 complex-linear invariants on $y_1, \ldots, y_k$ satisfies* $\dim\mathcal{I}_k = \mathrm{rank}\Sigma - \mathrm{rank}\widetilde{\Sigma} = k - \mathrm{rank}B'$.

Let $\mathfrak{d} = \mathrm{rank}B'$. Note that $\mathfrak{d} \leq \min(k, d)$. If $\mathfrak{d} = k$, then $\dim\mathcal{I}_k = 0$ and there are no type 1 invariants on $y_1, \ldots, y_k$. If, however, $\mathfrak{d} < k$, then the original matrix B can be simplified in two

steps. First the columns. Since the column rank of B' is $\mathfrak{d}$, elementary column operations—interchange of two columns, multiplication of a column by a scalar, addition of one column to another—can be applied to the columns of B', to bring the last $d - \mathfrak{d}$ columns to zero. If exactly the same elementary column operations are applied to the full matrix B, a new matrix is obtained, which we still call B, whose columns still form a basis for $\ker \Sigma$. B is now in lower-triangular block form,

$$B = \left[\begin{array}{c|c} B' & 0 \\ \hline * & * \end{array}\right] \tag{3.3}$$

where, as before, B' is the $k \times \mathfrak{d}$ sub-matrix consisting of the first k rows and $\mathfrak{d}$ columns.

For the rows, since the row rank of B' is still $\mathfrak{d}$, there are $\mathfrak{d}$ rows of B' that are linearly independent. Let $U \subseteq \{1, \cdots, k\}$ be the corresponding subset of $\mathfrak{d}$ indices and let $V \subseteq \{1, \cdots, k\}$ be the subset of $k - \mathfrak{d}$ remaining indices. This defines a partition of the row indices of B': $U \cap V = \emptyset$ and $U \cup V = \{1, \cdots, k\}$. Let B'_U be the $\mathfrak{d} \times \mathfrak{d}$ sub-matrix of B' consisting of the rows with indices in U and B'_V be the $(k-\mathfrak{d}) \times \mathfrak{d}$ sub-matrix consisting of the remaining rows of B'. Using the same notation for $a^\dagger \in \mathbb{R}^k$, $a.B' = 0$ if, and only if, $a_U.(B'_U) + a_V.(B'_V) = 0$. Since, by construction, B'_U has full rank and is hence invertible, this may be rewritten as

$$a_U = -a_V.(B'_V).(B'_U)^{-1}\,. \tag{3.4}$$

This gives a non-redundant procedure for generating all elements of $\mathcal{I}_k$ by choosing $a^\dagger_V \in \mathbb{R}^{k-\mathfrak{d}}$ arbitrarily and $a^\dagger_U \in \mathbb{R}^{\mathfrak{d}}$ to satisfy 3.4. The resulting $a^\dagger \in \mathbb{R}^k$ satisfy $a.B' = 0$ and give exactly the type 1 complex-linear invariants on $y_1, \ldots, y_k$.

Using the same notation for $\Psi(x) \in \mathbb{R}^m$, the invariants themselves are given by $a_U.\Psi(x)_U + a_V.\Psi(x)_V = 0$, for any steady state $x \in \mathbb{R}^s$. Substituting 3.4 and rearranging gives $a_V.(\Psi(x)_V - (B'_V).(B'_U)^{-1}.\Psi(x)_U) = 0$. Since a_V can be chosen arbitrarily in the dual space, we conclude that

$$\Psi(x)_V = (B'_V).(B'_U)^{-1}.\Psi(x)_U\,, \tag{3.5}$$

which we summarize as follows.

Theorem 3.3.1. *Each of the $k - \mathfrak{d}$ rows of the matrix equation in 3.5 gives an independent type 1 complex-linear invariant on $y_1, \ldots, y_k$.*

All the calculations above are linear and can be readily undertaken in any computer algebra system with the rate constants treated as symbols. (Mathematica was used for the calculations in the SI.) The coefficients are then rational expressions in the symbolic rate constants.

3.4 Haldane relationships and the Shinar-Feinberg Theorem

Since $\Sigma = Y.\mathcal{L}(G)$, $\ker \Sigma$ contains the subspace $\ker \mathcal{L}(G)$. Since the structure of the latter is known from 3.1, this should assist in the calculation of invariants. Recall the definitions of dynamic deficiency, δ_D, and structural deficiency, δ_S, from §2.4. While δ_D may depend on the values of rate constants, δ_S is independent of them. However, the former is more convenient for our purposes.

As we mentioned before, $\delta_D \leq \delta_S$, and if there is only a single terminal strong linkage class in each linkage class of G, which holds for the graph in Figure 3.2C but not for that in

Figure 3.4A, then $\delta_D = \delta_S$, [48, 63]. Recall that a graph is connected if any two distinct nodes are linked by a path of contiguous edges, ignoring directions. A linkage class of G is then a maximal connected sub-graph. Distinct linkage classes are totally disconnected, with no edges between them.

Suppose first that $\delta_D = 0$ and that there is a positive steady state $x \in (\mathbb{R}_{>0})^s$. Since $\mathcal{L}(G).\Psi(x) = 0$, x is a "complex-balanced" steady state, in the terminology of Horn and Jackson, [80]. According to 3.1, the vectors ρ^t provide a basis for $\ker \Sigma = \ker \mathcal{L}(G)$ and, furthermore, $(\rho^t)_j \neq 0$ if, and only if, $y_j \in G_t$. Choose any terminal strong linkage class of G, which we may suppose to be G_1, and suppose that $y_1, \ldots, y_k$ are the complexes in G_1. Choose the matrix B so that ρ^1 is its first column and the other ρ^t for $t > 1$ are assigned to columns arbitrarily. By construction, B is already in lower-triangular block form and $\mathfrak{d} = 1$. Setting $U = \{1\}$ and $V = \{2, \cdots, k\}$ the $k-1$ type 1 invariants coming from 3.5 are $x^{y_i} = ((\rho^1)_i/(\rho^1)_1)x^{y_1}$ for $2 \leq i \leq k$. It is not difficult to see from the structure of B that these are the only type 1 invariants.

These invariants may be rewritten $x^{y_i}/x^{y_1} = (\rho^1)_i/(\rho^1)_1$ to resemble the Haldane relationships that hold between substrates and products of a reaction at equilibrium, [27]. Horn and Jackson introduced the concept of a complex-balanced steady state, in part, to recover generalized Haldane relationships for networks of reactions that might be in steady state but not at thermodynamic equilibrium, [66, 80].

Corollary 3.4.1. *If a network has $\delta_D = 0$ and a positive steady state, $x \in (\mathbb{R}_{>0})^s$, then the type 1 complex-linear invariants correspond to generalized Haldane relationships between complexes in the same terminal strong linkage class.*

Now suppose that $\delta_D = 1$. Then, $\ker \Sigma = \langle\, \chi, \rho^1, \cdots, \rho^{\mathfrak{t}} \,\rangle$, where $\chi \in \mathbb{R}^m$ is any vector in $\ker \Sigma$ that is not in $\ker \mathcal{L}(G)$. Choose B to have columns in the same order. Suppose that there are k complexes that are not in any terminal strong linkage class and that indices are chosen so that these are $y_1, \ldots, y_k$. Then, $(\rho^t)_i = 0$ for $1 \leq i \leq k$ and $1 \leq t \leq \mathfrak{t}$, so that B is already in lower-triangular block form with $\mathfrak{d} = 1$. If $x \in (\mathbb{R}_{>0})^s$ is a positive steady state, then $\Psi(x) \in \ker \Sigma$ and $\Psi(x)_i \neq 0$ for $1 \leq i \leq m$. If follows that $\chi_i \neq 0$ for $1 \leq i \leq k$. We may therefore choose $U = \{1\}$ and $V = \{2, \cdots, k\}$ and deduce from 3.5 that $x^{y_i} = (\chi_i/\chi_1)x^{y_1}$ for $2 \leq i \leq k$. These type 1 complex-linear invariants imply the following.

Corollary 3.4.2. [144, Theorem] *Suppose a network has $\delta_S = 1$ and that y_1 and y_2 are two complexes that are not in any terminal strong linkage class, whose stoichiometry differs only in species $\mathfrak{s}_q$. If the network has a positive steady state, $x \in (\mathbb{R}_{>0})^s$, then $\mathfrak{s}_q$ exhibits ACR.*

Proof: It is known that $\delta_D \leq \delta_S$ so either $\delta_D = 0$ or $\delta_D = 1$. Suppose the former. The ρ^t then form a basis for $\ker \Sigma$. Because y_1 is not in any non-terminal strong linkage class, $v_1 = 0$ for any $v \in \ker \Sigma$. However, $\Psi(x) \in \ker \Sigma$ and, since $x \in (\mathbb{R}_{>0})^s$, $\Psi(x)_1 \neq 0$. This contradiction shows that $\delta_D = 1$. Using the type 1 invariant above and the assumption that the stoichiometry of y_1 and y_2 differ only in the species $\mathfrak{s}_q$, we find that $(x_q)^{y_{2q} - y_{1q}} = \chi_2/\chi_1$, showing that the steady-state concentration of $\mathfrak{s}_q$ depends only on the rate constants, as required.

□

3.5 Bifunctional enzymes

Corollaries 3.4.1 and 3.4.2 only exploited Theorem 3.3.1 when $\mathfrak{d} = 1$. We now consider examples with $\mathfrak{d} > 1$. The examples concern enzyme bifunctionality. Enzymes are known for being highly specific but some exhibit multiple activities. One form of this arises when a protein catalyzes both a forward phosphorylation—covalent addition of phosphate, with ATP as the donor—and its reverse dephosphorylation—hydrolysis of the phosphate group. What advantage does such bifunctionality bring over having two separate enzymes?

We discuss one bacterial and one mammalian example. In *Escherichia coli*, osmolarity regulation is implemented in part by the EnvZ/OmpR two-component system (Figure 3.2A); for references, see [141]. Here, the sensor kinase, EnvZ, autophosphorylates on a histidine residue and catalyzes the transfer of the phosphate group to the aspartate residue of the response regulator, OmpR, which then acts as an effector. Bifunctionality arises because EnvZ, when ATP is bound, also catalyzes hydrolysis of phosphorylated OmpR-P.

It was suggested early on that the unusual design of the EnvZ/OmpR system might keep the absolute concentration of OmpR-p stable, [132]. This was later supported by experimental and theoretical analysis, [8], and the theoretical analysis was extended to other bifunctional two-component systems, [141]. These *ad-hoc* calculations were clarified when a core network for EnvZ/OmpR was found to have $\delta_S = 1$ and Corollary 3.4.2 could be applied to confirm ACR for OmpR-p, [144]. Attempts were made to broaden the analysis by extending the core network to include additional reactions thought to be present. For instance, EnvZ bound to ADP may also dephosphorylate OmpR-P. Adding these reactions to the core gives a network (Figure 3.2B) with $\delta_S = 2$, so that Corollary 3.4.2 can no longer be applied. However, it was shown by direct calculation in [141, Supplementary Information] that this network also satisfies ACR for OmpR-p.

Here, we use complex-linear invariants to confirm ACR and to find a formula for the absolute concentration value of OmpR-p in terms of the rate constants. The labeled, directed graph on the complexes has thirteen nodes and fifteen edges (Figure 3.2C). Each linkage class has only a single terminal strong linkage class and $\delta_D = \delta_S = 2$. We can apply Theorem 3.3.1 to systematically find two new invariants.

Corollary 3.5.1. *If the complexes in the reaction network in Figure 3.2B are ordered as shown in Figure 3.2D, then the space of type 1 complex-linear invariants on the complexes y_1, y_3, y_8, y_{11} has dimension 2 and the following are independent invariants,*

$$\left(\frac{k_1 k_3}{k_2}\right) x^{y_1} - (k_4 + k_5) x^{y_3} = 0$$
$$k_5 x^{y_3} - \left(\frac{k_{12} k_{10}}{k_{11} + k_{12}}\right) x^{y_8} - \left(\frac{k_{15} k_{13}}{k_{14} + k_{15}}\right) x^{y_{11}} = 0\,.$$

Proof. The nine species and thirteen complexes in the EnvZ/OmpR network in Figure 3.2 are

ordered as follows.

$\mathfrak{s}_1$	EnvZ-P-OmpR	y_1	$\mathfrak{s}_8$	EnvZ-ADP
$\mathfrak{s}_2$	EnvZ-ATP-OmpR-P	y_2	$\mathfrak{s}_4$	EnvZ
$\mathfrak{s}_3$	EnvZ-ADP-OmpR-P	y_3	$\mathfrak{s}_7$	EnvZ-ATP
$\mathfrak{s}_4$	EnvZ	y_4	$\mathfrak{s}_9$	EnvZ-P
$\mathfrak{s}_5$	OmpR	y_5	$\mathfrak{s}_9 + \mathfrak{s}_5$	EnvZ-P + OmpR
$\mathfrak{s}_6$	OmpR-P	y_6	$\mathfrak{s}_1$	EnvZ-P-OmpR
$\mathfrak{s}_7$	EnvZ-ATP	y_7	$\mathfrak{s}_4 + \mathfrak{s}_6$	EnvZ + OmpR-P
$\mathfrak{s}_8$	EnvZ-ADP	y_8	$\mathfrak{s}_7 + \mathfrak{s}_6$	EnvZ-ATP + OmpR-P
$\mathfrak{s}_9$	EnvZ-P	y_9	$\mathfrak{s}_2$	EnvZ-ATP-OmpR-P
		y_{10}	$\mathfrak{s}_7 + \mathfrak{s}_5$	EnvZ-ATP + OmpR
		y_{11}	$\mathfrak{s}_8 + \mathfrak{s}_6$	EnvZ-ADP + OmpR-P
		y_{12}	$\mathfrak{s}_3$	EnvZ-ADP-OmpR-P
		y_{13}	$\mathfrak{s}_8 + \mathfrak{s}_5$	EnvZ-ADP + OmpR

With this ordering and with the rate constants as in Figure 3.2C, the matrix $\Sigma = Y.\mathcal{L}(G)$ is

$$\begin{bmatrix} 0 & 0 & 0 & 0 & k_6 & -k_7-k_8 & k_9 & 0 & 0 & 0 & 0 & 0 & 0 \\ 0 & 0 & 0 & 0 & 0 & 0 & 0 & k_{10} & -k_{11}-k_{12} & 0 & 0 & 0 & 0 \\ 0 & 0 & 0 & 0 & 0 & 0 & 0 & 0 & 0 & 0 & k_{13} & -k_{14}-k_{15} & 0 \\ k_1 & -k_2-k_3 & k_4 & 0 & 0 & k_8 & -k_9 & 0 & 0 & 0 & 0 & 0 & 0 \\ 0 & 0 & 0 & 0 & -k_6 & k_7 & 0 & 0 & k_{12} & 0 & 0 & k_{15} & 0 \\ 0 & 0 & 0 & 0 & 0 & k_8 & -k_9 & -k_{10} & k_{11} & 0 & -k_{13} & k_{14} & 0 \\ 0 & k_3 & -k_4-k_5 & 0 & 0 & 0 & 0 & -k_{10} & k_{11}+k_{12} & 0 & 0 & 0 & 0 \\ -k_1 & k_2 & 0 & 0 & 0 & 0 & 0 & 0 & 0 & 0 & -k_{13} & k_{14}+k_{15} & 0 \\ 0 & 0 & k_5 & 0 & -k_6 & k_7 & 0 & 0 & 0 & 0 & 0 & 0 & 0 \end{bmatrix}$$

A basis for the kernel of Σ can then be calculated to make up the columns of a matrix B.

$$\begin{bmatrix} 0 & \frac{k_2(k_4+k_5)k_{15}}{k_1k_3k_5} & 0 & \frac{k_2(k_4+k_5)k_{12}}{k_1k_3k_5} & 0 & 0 \\ 0 & \frac{(k_4+k_5)k_{15}}{k_3k_5} & 0 & \frac{(k_4+k_5)k_{12}}{k_3k_5} & 0 & 0 \\ 0 & \frac{k_{15}}{k_5} & 0 & \frac{k_{12}}{k_5} & 0 & 0 \\ 0 & 0 & 0 & 0 & 0 & 1 \\ 0 & \frac{(k_7+k_8)k_{15}}{k_6k_8} & 0 & \frac{(k_7+k_8)k_{12}}{k_6k_8} & \frac{k_7k_9}{k_6k_8} & 0 \\ 0 & \frac{k_{15}}{k_8} & 0 & \frac{k_{12}}{k_8} & \frac{k_9}{k_8} & 0 \\ 0 & 0 & 0 & 0 & 1 & 0 \\ 0 & 0 & 0 & \frac{k_{11}+k_{12}}{k_{10}} & 0 & 0 \\ 0 & 0 & 0 & 1 & 0 & 0 \\ 0 & 0 & 1 & 0 & 0 & 0 \\ 0 & \frac{k_{14}+k_{15}}{k_{13}} & 0 & 0 & 0 & 0 \\ 0 & 1 & 0 & 0 & 0 & 0 \\ 1 & 0 & 0 & 0 & 0 & 0 \end{bmatrix}$$

Corollary 3.5.1 focuses on the complexes y_1, y_3, y_8, y_{11}, so that $k = 4$. These are not the first four complexes in the ordering, as was assumed for convenience before. We can imagine that the columns of Σ and the rows of B have been permuted so that these complexes are now the

first in the ordering but we will not bother to write out these new matrices. We note that columns 2 and 4 of B have non-zero entries in the relevant four rows, while the remaining columns have zero entries. We can undertake elementary column operations on B, as described before (in fact, only interchange of columns is required), to bring B into lower-triangular block form. The resulting 4×2 sub-matrix, B', in Equation (3.3), is then given by

$$\begin{bmatrix} \frac{k_2(k_4+k_5)k_{15}}{k_1k_3k_5} & \frac{k_2(k_4+k_5)k_{12}}{k_1k_3k_5} \\ \frac{k_{15}}{k_5} & \frac{k_{12}}{k_5} \\ 0 & \frac{k_{11}+k_{12}}{k_{10}} \\ \frac{k_{14}+k_{15}}{k_{13}} & 0 \end{bmatrix}$$

The columns of this are linearly independent, so that $\mathrm{rank}B' = 2$. It follows from Proposition 3.3.1 that the dimension of the space of type 1 complex-linear invariants on y_1, y_3, y_8, y_{11} is 2, as claimed. To generate the invariants, we note that rows 2 and 3 of B' are linearly independent, so that we can follow the prescription above and take $U = \{2, 3\}$ and $V = \{1, 4\}$. Then

$$B'_U = \begin{bmatrix} \frac{k_{15}}{k_5} & \frac{k_{12}}{k_5} \\ 0 & \frac{k_{11}+k_{12}}{k_{10}} \end{bmatrix}, \qquad B'_V = \begin{bmatrix} \frac{k_2(k_4+k_5)k_{15}}{k_1k_3k_5} & \frac{k_2(k_4+k_5)k_{12}}{k_1k_3k_5} \\ \frac{k_{14}+k_{15}}{k_{13}} & 0 \end{bmatrix}$$

Since $\Psi(x)_U = (x^{y_3}, x^{y_8})^\dagger$ and $\Psi(x)_V = (x^{y_1}, x^{y_{11}})^\dagger$, the two linearly independent type 1 complex-linear invariants may be read off from Equation (3.5),

$$\begin{bmatrix} x^{y_1} \\ x^{y_{11}} \end{bmatrix} = \begin{bmatrix} \frac{k_2(k_4+k_5)}{k_1k_3} & 0 \\ \frac{k_5(k_{14}+k_{15})}{k_{13}k_{15}} & -\frac{k_{10}k_{12}(k_{14}+k_{15})}{k_{13}k_{15}(k_{11}+k_{12})} \end{bmatrix} \begin{bmatrix} x^{y_3} \\ x^{y_8} \end{bmatrix}$$

to yield the expressions in Corollary 3.5.1, as claimed. □

Using the expressions for the complexes in Figure 3.2D, it can be seen that

$$x^{y_8} = x^{y_3}[\text{OmpR-P}], \quad x^{y_{11}} = x^{y_1}[\text{OmpR-P}].$$

Provided that $[\text{EnvZ-ATP}] = x^{y_3} \neq 0$, the invariants can be combined and simplified to yield the following expression

$$[\text{OmpR-P}] = \frac{k_1k_3k_5(k_{11}+k_{12})(k_{14}+k_{15})}{k_1k_3k_{10}k_{12}(k_{14}+k_{15}) + k_2k_{13}k_{15}(k_4+k_5)(k_{11}+k_{12})}. \tag{3.6}$$

This confirms that, as long as there is a positive steady state, the steady-state concentration of OmpR-P is not affected by changes in either the amount of OmpR or of EnvZ. The network exhibits ACR for OmpR-P, with the absolute value being given in terms of the rate constants by 3.6.

We now turn to our second example. Phosphofructokinase1 (PFK1) is one of the key regulatory enzymes in glycolysis, converting the small molecule fructose-6-phosphate to fructose-1,6-bisphosphate (Figure 3.3A); for references, see [34]. In mammalian cells, the bifunctional PFK2-F2,6BPase has two domains. PFK2 has the same substrate as PFK1 but produces fructose-2,6-bisphosphate. This is a terminal metabolite that is not consumed by other

metabolic processes. Instead, it acts as an allosteric effector, activating PFK1 and inhibiting fructose-1,6-bisphosphatase, the reverse enzyme present in gluconeogenic cells, such as hepatocytes. The other domain, F2,6BPase, catalyzes the dephosphorylation of F2,6BP and produces F6P.

Biochemical studies lead to the reaction network in Figure 3.3B. The kinase domain has an ordered, sequential mechanism and the kinase and phosphatase domains operate simultaneously; for more details, see [34]. The corresponding labeled, directed graph on the complexes has fourteen nodes and nineteen edges (Figure 3.4A). One of the linkage classes has two terminal strong linkage classes, $\delta_D = 4$ and $\delta_S = 5$.

Corollary 3.5.2. *If the complexes in the reaction network in Figure 3.3B are ordered as shown in Figure 3.4B, then the space of type 1 complex-linear invariants on the complexes y_1, y_2, y_4, y_6, y_8, y_{11} has dimension 2 and the following are the independent invariants,*

$$k_1 x^{y_1} - k_2 x^{y_2} + (k_{10} - k_8) x^{y_6} - (k_9 + k_{11}) x^{y_8} - k_{19} x^{y_{11}} = 0$$
$$k_5 x^{y_4} - k_8 x^{y_6} - k_{11} x^{y_8} + (k_{18} - k_{19}) x^{y_{11}} = 0\,.$$

Proof. The eight species and fourteen complexes of the PFK2-F2,6BPase network in Figures 3.3 and 3.4 are ordered as follows.

$\mathfrak{s}_1$	F2,6BP	y_1	$\mathfrak{s}_5$	E
$\mathfrak{s}_2$	F6P	y_2	$\mathfrak{s}_7$	E-ATP
$\mathfrak{s}_3$	E-ATP-F6P	y_3	$\mathfrak{s}_7 + \mathfrak{s}_2$	E-ATP + F6P
$\mathfrak{s}_4$	E-ATP-F6P-F2,6BP	y_4	$\mathfrak{s}_3$	E-ATP-F6P
$\mathfrak{s}_5$	E	y_5	$\mathfrak{s}_5 + \mathfrak{s}_1$	E + F2,6BP
$\mathfrak{s}_6$	E-F2,6BP	y_6	$\mathfrak{s}_6$	E-F2,6BP
$\mathfrak{s}_7$	E-ATP	y_7	$\mathfrak{s}_5 + \mathfrak{s}_2$	E + F6P
$\mathfrak{s}_8$	E-ATP-F2,6BP	y_8	$\mathfrak{s}_8$	E-ATP-F2,6BP
		y_9	$\mathfrak{s}_7 + \mathfrak{s}_1$	E-ATP + F2,6BP
		y_{10}	$\mathfrak{s}_3 + \mathfrak{s}_1$	E-ATP-F6P + F2,6BP
		y_{11}	$\mathfrak{s}_4$	E-ATP-F6P-F2,6BP
		y_{12}	$\mathfrak{s}_8 + \mathfrak{s}_2$	E-ATP-F2,6BP + F6P
		y_{13}	$\mathfrak{s}_6 + \mathfrak{s}_1$	E-F2,6BP + F2,6BP
		y_{14}	$\mathfrak{s}_3 + \mathfrak{s}_2$	E-ATP-F6P + F6P

With this ordering and with the rate constants in Figure 3.4A, the matrix $\Sigma = Y.\mathcal{L}(G)$ is

$$\begin{bmatrix}
0 & 0 & 0 & k_5 & -k_6 & k_7 & 0 & k_{13} & -k_{12} & -k_{14} & k_{15}+k_{18} & 0 & 0 & 0 \\
0 & 0 & -k_3 & k_4 & 0 & k_8 & 0 & k_{11} & 0 & 0 & k_{17}+k_{19} & -k_{16} & 0 & 0 \\
0 & 0 & k_3 & -k_4-k_5 & 0 & 0 & 0 & 0 & 0 & -k_{14} & k_{15}+k_{19} & 0 & 0 & 0 \\
0 & 0 & 0 & 0 & 0 & 0 & 0 & 0 & 0 & k_{14} & -k_{15}-k_{17}-k_{18}-k_{19} & k_{16} & 0 & 0 \\
-k_1 & k_2 & 0 & k_5 & -k_6 & k_7+k_8 & 0 & 0 & 0 & 0 & 0 & 0 & 0 & 0 \\
0 & 0 & 0 & 0 & k_6 & -k_7-k_8-k_{10} & 0 & k_9 & 0 & 0 & k_{18} & 0 & 0 & 0 \\
k_1 & -k_2 & -k_3 & k_4 & 0 & 0 & 0 & k_{11}+k_{13} & -k_{12} & 0 & 0 & 0 & 0 & 0 \\
0 & 0 & 0 & 0 & 0 & k_{10} & 0 & -k_9-k_{11}-k_{13} & k_{12} & 0 & k_{17} & -k_{16} & 0 & 0
\end{bmatrix}$$

and a matrix B, whose columns form a basis for the kernel of Σ, can then be calculated as

$$\begin{bmatrix}
0 & 0 & \frac{k_8-k_{10}}{k_1k_{10}} & \frac{k_{19}}{k_1} & \frac{(-k_8+k_{10})k_{12}}{k_1k_{10}} & \frac{k_8k_9+k_{10}k_{11}}{k_1k_{10}} & 0 & \frac{k_2}{k_1} \\
0 & 0 & 0 & 0 & 0 & 0 & 0 & 1 \\
0 & 0 & \frac{-k_5k_{10}+(k_4+k_5)k_8}{k_3k_5k_{10}} & \frac{-k_4k_{18}+(k_4+k_5)k_{19}}{k_3k_5} & -\frac{(k_4+k_5)k_8k_{12}}{k_3k_5k_{10}} & \frac{(k_4+k_5)(k_8k_9+k_{10}k_{11})}{k_3k_5k_{10}} & 0 & 0 \\
0 & 0 & \frac{k_8}{k_5k_{10}} & \frac{-k_{18}+k_{19}}{k_5} & -\frac{k_8k_{12}}{k_5k_{10}} & \frac{k_8k_9+k_{10}k_{11}}{k_5k_{10}} & 0 & 0 \\
0 & 0 & \frac{k_7+k_8+k_{10}}{k_6k_{10}} & -\frac{k_{18}}{k_6} & -\frac{(k_7+k_8+k_{10})k_{12}}{k_6k_{10}} & \frac{(k_7+k_8)k_9}{k_6k_{10}} & 0 & 0 \\
0 & 0 & \frac{1}{k_{10}} & 0 & -\frac{k_{12}}{k_{10}} & \frac{k_9}{k_{10}} & 0 & 0 \\
0 & 0 & 0 & 0 & 0 & 0 & 1 & 0 \\
0 & 0 & 0 & 0 & 0 & 1 & 0 & 0 \\
0 & 0 & 0 & 0 & 1 & \frac{k_{11}+k_{13}}{k_{12}} & 0 & 0 \\
0 & 0 & -\frac{1}{k_{14}} & \frac{k_{15}+k_{18}+k_{19}}{k_{14}} & 0 & 0 & 0 & 0 \\
0 & 0 & 0 & 1 & 0 & 0 & 0 & 0 \\
0 & 0 & \frac{1}{k_{16}} & \frac{k_{17}}{k_{16}} & 0 & 0 & 0 & 0 \\
0 & 1 & 0 & 0 & 0 & 0 & 0 & 0 \\
1 & 0 & 0 & 0 & 0 & 0 & 0 & 0
\end{bmatrix}$$

Corollary 3.5.2 focuses on the complexes $y_1, y_2, y_4, y_6, y_8, y_{11}$, so that $k = 6$. As before, we can imagine that the columns of Σ and the rows of B have been permuted to make these complexes first in the ordering. Only columns $3, 4, 5, 6, 8$ of B have non-zero entries in the relevant rows and, when restricted to these rows, column 5 is a scalar multiple of column 3. As before, we can interchange columns to bring B into lower-triangular block form, with the resulting 6×4 sub-matrix, B', in Equation 3.3 given by

$$\begin{bmatrix}
\frac{k_8-k_{10}}{k_1k_{10}} & \frac{k_{19}}{k_1} & \frac{k_8k_9+k_{10}k_{11}}{k_1k_{10}} & \frac{k_2}{k_1} \\
0 & 0 & 0 & 1 \\
\frac{k_8}{k_5k_{10}} & \frac{-k_{18}+k_{19}}{k_5} & \frac{k_8k_9+k_{10}k_{11}}{k_5k_{10}} & 0 \\
\frac{1}{k_{10}} & 0 & \frac{k_9}{k_{10}} & 0 \\
0 & 0 & 1 & 0 \\
0 & 1 & 0 & 0
\end{bmatrix}$$

with B' evidently of full rank 4. It follows from Proposition 3.3.1 that the space of type 1 complex-linear invariants on $y_1, y_2, y_4, y_6, y_8, y_{11}$ has dimension two, as claimed. To generate the invariants, we can take $U = \{2, 4, 5, 6\}$ and $V = \{1, 3\}$ so that

$$B'_U = \begin{bmatrix}
0 & 0 & 0 & 1 \\
\frac{1}{k_{10}} & 0 & \frac{k_9}{k_{10}} & 0 \\
0 & 0 & 1 & 0 \\
0 & 1 & 0 & 0
\end{bmatrix}, \quad B'_V = \begin{bmatrix}
\frac{k_8-k_{10}}{k_1k_{10}} & \frac{k_{19}}{k_1} & \frac{k_8k_9+k_{10}k_{11}}{k_1k_{10}} & \frac{k_2}{k_1} \\
\frac{k_8}{k_5k_{10}} & \frac{-k_{18}+k_{19}}{k_5} & \frac{k_8k_9+k_{10}k_{11}}{k_5k_{10}} & 0
\end{bmatrix}$$

B'_U is evidently non-singular. The two linear-independent type 1 complex-linear invariants can then be read off from Equation (3.5),

$$\begin{bmatrix} x^{y_1} \\ x^{y_4} \end{bmatrix} = \begin{bmatrix}
\frac{k_2}{k_1} & \frac{(k_8-k_{10})}{k_1} & \frac{(k_9+k_{11})}{k_1} & \frac{k_{19}}{k_1} \\
0 & \frac{k_8}{k_5} & \frac{k_{11}}{k_5} & \frac{(-k_{18}+k_{19})}{k_5}
\end{bmatrix} \begin{bmatrix} x^{y_2} \\ x^{y_6} \\ x^{y_8} \\ x^{y_{11}} \end{bmatrix}$$

to yield the expressions in Corollary 3.5.2, as claimed.

□

The second invariant in Corollary 3.5.2 was originally discovered by *ad-hoc* algebraic calculation. It is used in [34] to show that, if the kinase dominates the phosphatase, in the sense that $k_{18} > k_{19}$, then the steady state concentration of F6P is held below a level that depends only on the rate constants and not on the amounts of the enzymes or the substrate. Conversely, if the phosphatase dominates the kinase, so that $k_{18} < k_{19}$, then the steady state concentration of F2,6BP is similarly constrained below a level that depends only on the rate constants and not on the amounts. Interestingly, regulation of PFK2-F2,6BPase by phosphorylation, under the influence of the insulin and glucagon, causes the kinase and phosphatase activities to be shifted between the regimes $k_{18} > k_{19}$ and $k_{18} < k_{19}$. The implications of this for control of glycolysis are discussed in [34].

Despite the considerable differences between the reaction networks in Figures 3.2 and 3.3, the bifunctionality in both cases serves to limit the steady state concentrations of the substrate forms. In the simpler bacterial case, the concentration of OmpR-p is held at a constant level at steady state, while in the more complex mammalian case, either the steady-state concentration of F2,6BP or that of F6P is held below a constant level, depending on regulatory choices. In all cases, the "constant" levels depend only on the rate constants and not on the amounts of substrate or enzyme. We speculate that this may be a design principle of those bifunctional enzymes that catalyze forward and reverse modifications. There are other forms of bifunctionality, such as enzymes that catalyze successive steps in a metabolic pathway, and preliminary studies suggest that these behave very differently. If modification bifunctionality did evolve to implement concentration control, different enzymes still have markedly different reaction networks and steady-state properties, as seen above. The complex-linear invariants introduced here provide a way to systematically analyze this for realistic networks, without becoming mired in problems of parameter determination.

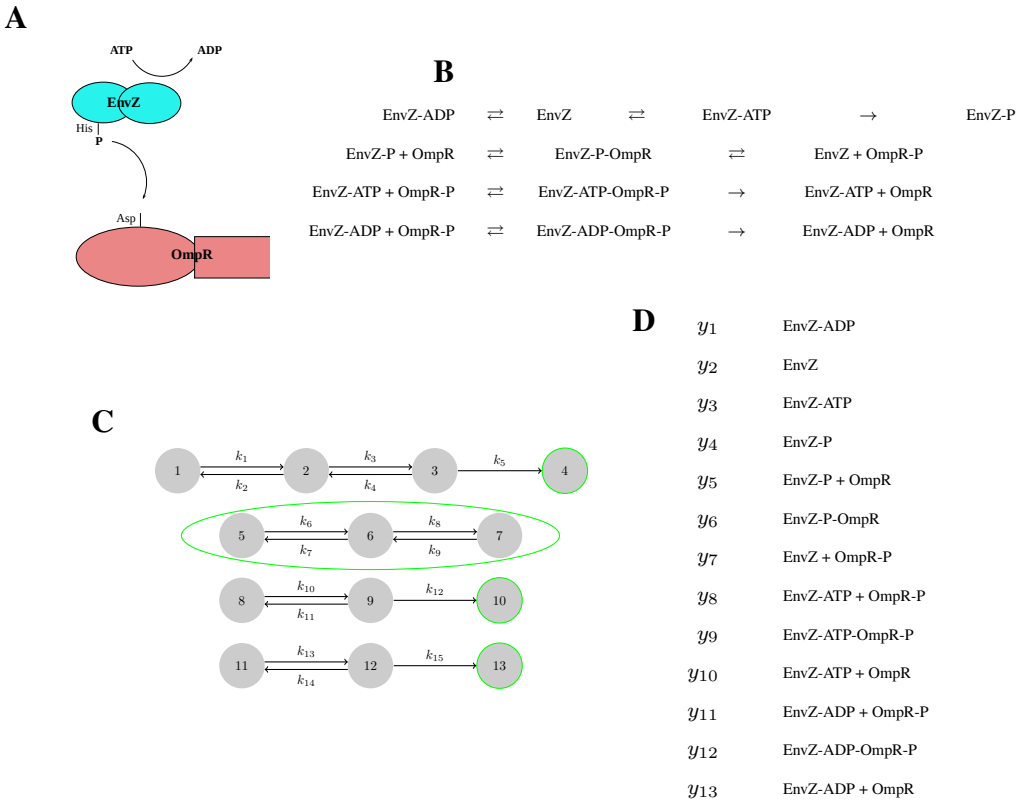

Figure 3.2: Two component signaling and the *E. coli* osmolarity network. **A** Schematic of two-component phospho-transfer between a histidine residue on the autophosphorylating sensor kinase and an aspartate on the response regulator. **B** Extended reaction network for the EnvZ/OmpR two-component osmoregulator in *E. coli*. Hyphens, as in EnvZ-ATP, indicate the formation of a biochemical complex between the components. **C** Corresponding labeled, directed graph on the complexes, with the terminal strong linkage classes outlined in yellow. Each linkage class has only a single terminal strong linkage class. **D** Numbering scheme for the complexes.

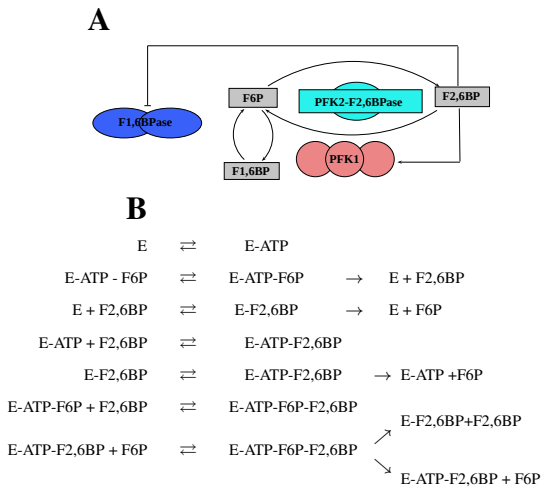

Figure 3.3: The bifunctional enzyme phosphofructokinase2-fructose-2,6-BPase (PFK2-F2,6BPase). **A** Schematic of glycolysis at the step involving phosphofructokinase1 (PFK1), that converts fructose-6-phosphate (F6P) into fructose-1,6-bisphosphate (F1,6BP), and fructose-1,6-bisphosphatase (F1,6BPase), that catalyzes the opposing reactions in gluconeogenic tissues. PFK2-F2,6BPase operates bifunctionally to produce and consume fructose-2,6-bisphosphate (F2,6BP), which allosterically regulates PFK1 and F1,6BPase. **B** The corresponding reaction network.

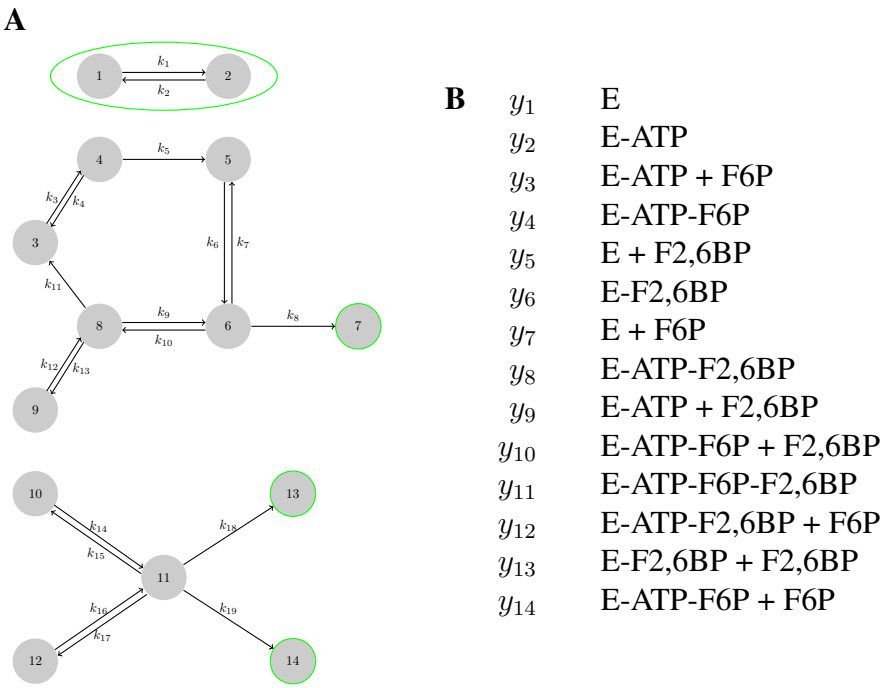

Figure 3.4: PFK2-F2,6BPase, as in Figure 3.3. **A** Labelled, directed graph on the complexes, with the terminal strong linkage classes outlined in yellow. The last linkage class has two terminal strong linkage classes. **B** Numbering scheme for the complexes.

Chapter 4

Chemical reaction systems with toric steady states

As we have already mentioned, the polynomial dynamical systems arising from mass–action chemical reaction systems are often large (consisting of tens or even hundreds of ordinary differential equations) and poorly parametrized (due to noisy measurement data and a small number of data points and repetitions). Therefore, it is often difficult to establish the existence of (positive) steady states or to determine whether more complicated phenomena such as multistationarity exist. If, however, the steady state ideal of the system is a binomial ideal, then we show that these questions can be answered easily. The focus of this chapter is on systems with this property, and we say that such systems have toric steady states. An example of these systems are those whose steady states are described by complex-linear invariants with two terms (recalling Chapter 3).

Our main result here gives sufficient conditions for a chemical reaction system to have toric steady states. Furthermore, we analyze the capacity of such a system to exhibit positive steady states and multistationarity. Examples of systems with toric steady states include weakly-reversible zero-deficiency chemical reaction systems. An important application of our work concerns the networks that describe the multisite phosphorylation of a protein by a kinase/phosphatase pair in a sequential and distributive mechanism. This chapter is based on joint work with A. Dickenstein, A. Shiu and C. Conradi.

4.1 Toric Steady States

Ordinary differential equations (ODEs) are an important modeling tool in Systems Biology and many other areas of Computational Biology. Due to the inherent complexity of biological systems, realistic models are often large, both in terms of the number of states and the (unknown) parameters. Moreover, models are often poorly parametrized, a consequence of noisy measurement data, a small number of data points, and a limited number of repetitions. Hence, for mass-action chemical reaction systems, the focus of the present chapter, simply establishing the existence of (positive) steady states can be demanding, as it requires the solution of a large polynomial system with unknown coefficients (usually the parameters). Moreover, due to the predominant parameter uncertainty, one is often not interested in establishing the existence of a

particular steady state, but rather in obtaining a parametrization of all steady states – preferably in terms of the system parameters [164]. Frequently one is also interested in the existence of multiple steady states (multistationarity), for example, in modeling the cell cycle [9, 19, 139], signal transduction [90, 113] or cellular differentiation [162, 163]. For general polynomial systems with unknown coefficients, the tasks of obtaining positive solutions or a parametrization of positive solutions, and deciding about multiple positive solutions, are clearly challenging. For the systems considered in this chapter – chemical reaction systems with *toric steady states* – these questions can be answered easily.

We say that a polynomial dynamical system $dx/dt = f(x)$ has *toric steady states* if the ideal generated by its steady state equations is a binomial ideal (see Definition 4.1.1). We give sufficient conditions for a chemical reaction system to have toric steady states (Theorems 4.2.2 and 4.2.4) and show in this case that the steady state locus has a nice monomial parametrization (Theorems 4.2.3 and 4.2.5). Furthermore, we show that the existence of positive steady states in this case is straightforward to check (Theorem 4.4.1).

There are several important classes of mass-action kinetics chemical reaction systems which have toric steady states. These include usual instances of detailed-balanced systems in the sense of Feinberg, Horn, and Jackson [45, 49, 79, 80], which show particularly nice dynamical behavior. These systems are weakly-reversible, a hypothesis we do not impose here.

A chemical reaction system with toric steady states of great biological importance is the *multisite phosphorylation system*; this network describes the n-site phosphorylation of a protein by a kinase/phosphatase pair in a sequential and distributive mechanism. Biochemically, these systems play an important role in signal transduction networks, cell cycle control, or cellular differentiation: for example, members of the family of mitogen-activated kinase cascades consist of several such phosphorylation systems with $n = 2$ or $n = 3$ (see e.g. [83, 140]), the progression from G1 to S phase in the cell cycle of budding yeast is controlled by a system with $n = 9$ (by way of the protein Sic1, see e.g. [37]), and a system with $n = 13$ plays an important role in T-cell differentiation (by way of the protein NFAT [74, 77, 111]).

Consequently there exists a body of work on the mathematics of phosphorylation systems and the more general class of post-translational modification systems: for example, Conradi *et al.* [25], Wang and Sontag [170], Manrai and Gunawardena [112], and Thomson and Gunawardena [164, 165]. While the first two references are concerned with the number of steady states and multistationarity, the references of Gunawardena *et al.* deal with parametrizing all positive steady states. The present chapter builds on these earlier results. In fact, the family of monomial parametrizations obtained here for multisite phosphorylation systems (Theorem 4.3.1) is a specific instance of a rational parametrization theorem due to Thomson and Gunawardena, and one parametrization of the family was analyzed earlier by Wang and Sontag. Furthermore, we show that by using results from [25] one can determine whether multistationarity exists for systems with toric steady states by analyzing certain linear inequality systems. In this sense our results can be seen as a generalization of [25].

Our main results on toric steady states appear in Section 4.2: Theorems 4.2.2 and 4.2.4 give sufficient criteria for a system to exhibit toric steady states, and Theorems 4.2.3 and 4.2.5 give parametrizations for the steady state locus. As an application of this work, we analyze the steady state loci of multisite phosphorylation systems in Section 4.3. Theorem 4.3.1 summarizes our results: we show that these systems have toric steady states for any choice of reaction rate constants, and we give an explicit parametrization of the steady state locus. Section 4.4

focuses on multiple steady states for chemical reaction systems with toric steady states. Theorem 4.4.1 gives a criterion for such a system to exhibit multistationarity, and we make the connection to a related criterion due to Feinberg.

Definition 4.1.1. *Consider a polynomial dynamical system $dx_i/dt = f_i(x)$, for $i = 1, 2, \ldots, s$, with $f_1, f_2, \ldots, f_s \in \mathbb{R}[x_1, x_2, \ldots, x_s]$. We are interested in the* nonnegative *zeros of the* steady state ideal*:*

$$J_{\Sigma\Psi} \;=\; \langle f_1, f_2, \ldots, f_s \rangle = \left\{ \sum_{i=1}^{s} h_i(x) f_i(x) \quad | \quad h_i(x) \in \mathbb{R}[x_1, \ldots, x_s] \text{ for } 1 \leq i \leq s \right\}.$$

The nonnegative zeros of $J_{\Sigma\Psi}$ are called steady states*, and the term* steady state locus *is used to denote the set of nonnegative zeros of $J_{\Sigma\Psi}$:*

$$\left\{ \tilde{x} \in \mathbb{R}^s_{\geq 0} \quad | \quad f_1(\tilde{x}) = f_2(\tilde{x}) \cdots = f_s(\tilde{x}) = 0 \right\}.$$

We say that the polynomial dynamical system has toric steady states *if $J_{\Sigma\Psi}$ is a binomial ideal and it admits nonnegative zeros.*

We are interested in *positive steady states* $x \in \mathbb{R}^s_{>0}$ and will not be concerned with *boundary steady states* $x \in \left(\mathbb{R}^s_{\geq 0} \setminus \mathbb{R}^s_{>0}\right)$.

This chapter focuses on mass-action kinetics chemical reaction systems. In this case, the polynomials $f_1, f_2, \ldots, f_s$ correspond to the rows of the system (2.10). In general, having toric steady states depends both on the reaction network and on the particular rate constants, as the following simple example shows.

Example 4.1.1 (Triangle network)**.** *Let $s = 2$, $m = 3$, and let G be the following network:*

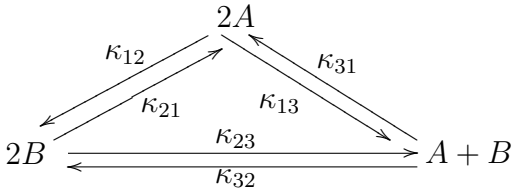

We label the three complexes as $x^{y_1} = x_1^2$, $x^{y_2} = x_2^2$, $x^{y_3} = x_1 x_2$, and we define κ_{ij} to be the (real positive) rate constant of the reaction from complex x^{y_i} to complex x^{y_j}. The resulting mass-action kinetics system (2.10) *equals*

$$\frac{dx_1}{dt} \quad = \quad -\frac{dx_2}{dt} \quad = \quad (-2\kappa_{12} - \kappa_{13})x_1^2 + (2\kappa_{21} + \kappa_{23})x_2^2 + (\kappa_{31} - \kappa_{32})x_1 x_2 \; .$$

Then, the steady state locus in $\mathbb{R}^2$ is defined by this single trinomial. As only the coefficient of $x_1 x_2$ can be zero, this system has toric steady states if and only if $\kappa_{31} = \kappa_{32}$.

A chemical reaction system exhibits *multistationarity* if there exists a stoichiometric compatibility class $\mathcal{P}_{x^0}$ (see Section 2.3) with two or more steady states in its relative interior. A system may admit multistationarity for all, some, or no choices of positive rate constants κ_{ij}; if such rate constants exist, then we say that the network *has the capacity for multistationarity*.

4.2 Sufficient conditions for the existence of toric steady states

The main results of this section, Theorems 4.2.1, 4.2.2, and 4.2.4, give sufficient conditions for a chemical reaction system to have toric steady states and state criteria for these systems to have positive toric steady states. Theorems 4.2.3 and 4.2.5 give a monomial parametrization of the steady state locus in this case.

We first state several conditions and intermediate results that will lead to Theorem 4.2.2. Recall that a *partition* of $\{1, 2, \ldots, m\}$ is a collection of nonempty disjoint subsets $I_1, I_2, \ldots, I_d$ with respective cardinalities $l_1, l_2, \ldots, l_d$ such that their union equals $\{1, 2, \ldots, m\}$ (or equivalently, such that $l_1 + l_2 + \cdots + l_d = m$). The support $\operatorname{supp}(b)$ of a real vector $b \in \mathbb{R}^m$ is the subset of indices corresponding to the nonzero entries of b. The following condition requires that a certain linear subspace has a basis with disjoint supports.

Condition 4.2.1. *For a chemical reaction system given by a network G with m complexes and reaction rate constants κ^*_{ij}, let Σ denote its complex-to-species rate matrix* (2.9)*, and set $d := \dim(\ker(\Sigma))$. We say that the chemical reaction system satisfies Condition 4.2.1, if there exists a partition $I_1, I_2, \ldots, I_d$ of $\{1, 2, \ldots, m\}$ and a basis $b^1, b^2, \ldots, b^d \in \mathbb{R}^m$ of $\ker(\Sigma)$ with $\operatorname{supp}(b^i) = I_i$.*

Remark 4.2.1. *Most of the networks considered in this chapter have the property that each linkage class contains a unique terminal strong linkage class. In this case, the dimension of the kernel of Σ satisfies $d := \dim(\ker(\Sigma)) = l + \delta_S$, where l denotes the number of linkage classes, and δ_S is the structural deficiency of the network; this result is due to Feinberg [50, Lemma 6.1.3].*

Remark 4.2.2. *Conditions 4.2.1, 4.2.2, and 4.2.3 in this chapter are simply linear algebra conditions. However, the objects of interest (such as the subspace in Condition 4.2.1) are parametrized by the unknown rate constants κ_{ij}, so verifying the conditions can become quite complicated for large networks.*

Condition 4.2.1 implies that the steady state ideal $J_{\Sigma\Psi}$ is binomial:

Theorem 4.2.1. *Consider a chemical reaction system with m complexes, and let d denote the dimension of $\ker(\Sigma)$. Assume that Condition 4.2.1 holds (i.e., there exists a partition $I_1, I_2, \ldots, I_d$ of $\{1, 2, \ldots, m\}$ and a basis $b^1, b^2, \ldots, b^d \in \mathbb{R}^m$ of $\ker(\Sigma)$ with $\operatorname{supp}(b^i) = I_i$). Then the steady state ideal $J_{\Sigma\Psi}$ is generated by the binomials*

$$b^j_{j_1} x^{y_{j_2}} - b^j_{j_2} x^{y_{j_1}}, \text{ for all } j_1,\ j_2 \in I_j, \text{ and for all } 1 \leq j \leq d. \tag{4.1}$$

Proof. Consider the vectors $\beta^j_{j_1,j_2} = b^j_{j_1} e_{j_2} - b^j_{j_2} e_{j_1} \in \mathbb{R}^m$ for all $j_1, j_2 \in I_j$, for all $1 \leq j \leq d$. It is straightforward to check that these vectors span the orthogonal complement $\ker(\Sigma)^\perp$ of the kernel of Σ. But by definition, this complement is spanned by the rows of the matrix Σ. Therefore, the binomials $b^j_{j_1} \Psi_{j_2}(x) - b^j_{j_2} \Psi_{j_1}(x)$ are $\mathbb{R}$-linear combinations of the polynomials $f_1(x), f_2(x), \ldots, f_s(x)$, and vice-versa. And so the binomials in (4.1) give another system of generators of $J_{\Sigma\Psi}$. □

Remark 4.2.3. *Under the assumptions of Theorem 4.2.1, we can present a smaller set of generators of the ideal $J_{\Sigma\Psi}$. Namely, let us call j_0 the first element of I_j, that is*

$$j_0 := \min I_j. \tag{4.2}$$

Then the steady state ideal $J_{\Sigma\Psi}$ is generated by the binomials

$$b^j_{j'}x^{y_{j_0}} - b^j_{j_0}x^{y_{j'}}, \text{ for all } j' \in I_j,\ j' \neq j_0, \text{ and for all } 1 \leq j \leq d. \tag{4.3}$$

Note that Theorem 4.2.1 does not provide any information about the existence of (toric) steady states (i.e. *nonnegative* solutions to the binomials (4.1), cf. Definition 4.1.1), let alone *positive steady states*. In general, this is a question of whether a parametrized family of polynomial systems has nonnegative solutions. For this purpose two further conditions are needed:

Condition 4.2.2. *Consider a chemical reaction system given by a network G with m complexes and reaction rate constants κ^*_{ij} that satisfies Condition 4.2.1 for the partition $I_1, I_2, \ldots, I_d$ of $\{1, 2, \ldots, m\}$ and a basis $b^1, b^2, \ldots, b^d \in \mathbb{R}^m$ of $\ker(\Sigma)$ (with $\operatorname{supp}(b^i) = I_i$). We say that this chemical reaction system **additionally** satisfies Condition 4.2.2, if for all $j \in \{1, 2, \ldots, d\}$, the nonzero entries of b^j have the same sign, that is, if*

$$\operatorname{sign}\left(b^j_{j_1}\right) = \operatorname{sign}\left(b^j_{j_2}\right), \text{ for all } j_1,\ j_2 \in I_j, \text{ for all } 1 \leq j \leq d. \tag{4.4}$$

The next result can be used to check the validity of Condition 4.2.2.

Lemma 4.2.1. *Consider a chemical reaction system with m complexes that satisfies Condition 4.2.1 for the partition $I_1, I_2, \ldots, I_d$ of $\{1, 2, \ldots, m\}$ and the basis $b^1, b^2, \ldots, b^d \in \mathbb{R}^m$ of $\ker(\Sigma)$. Let $j \in \{1, 2, \ldots, d\}$, There exists an $(l_j - 1) \times l_j$ submatrix Σ_j of Σ with columns indexed by the elements of I_j and linearly independent rows (that is, $rank(\Sigma_j) = l_j - 1$). Let Σ_j be any such matrix. For $i \in \{1, \ldots, l_j\}$, call $\Sigma_j(i)$ the submatrix of Σ_j obtained by deleting its i-th column. Then the system satisfies Condition 4.2.2 (that is, equations* (4.4) *are satisfied) if and only if, for all $j \in \{1, 2, \ldots, d\}$, the sign of $\det(\Sigma_j(i))$ is different from the sign of $\det(\Sigma_j(i+1))$ for $1 \leq i \leq l_j - 1$.*

Proof. First, note that the kernel of the submatrix of Σ formed by the columns indexed by I_j has dimension one and is spanned by the vector b'_j which consists of the l_j entries of b^j that are indexed by I_j. So there exist $l_j - 1$ rows that give a matrix Σ_j as in the statement.

By a basic result from Linear Algebra, the kernel of Σ_j is spanned by the vector v' with i-th entry equal to $(-1)^i \det(\Sigma_j(i))$. As the vector b'_j must be a multiple of v', it is immediate that (4.4) holds if and only if the sign of $\Sigma_j(i)$ is different from the sign of $\Sigma_j(i+1)$ for $1 \leq i \leq l_j - 1$. □

Condition 4.2.2 is necessary for the existence of positive real solutions to the system defined by setting the binomials (4.3) to zero. In working towards sufficiency, observe that the system can be rewritten as

$$x^{y_{j'} - y_{j_0}} \ = \ \frac{b^j_{j'}}{b^j_{j_0}}, \text{ for all } j' \in I_j,\ j' \neq j_0, \text{ and for all } 1 \leq j \leq d,$$

where j_0 is as in Equation (4.2).

Note that Condition 4.2.2 implies that the right-hand side of the above equation is positive. In addition, we are interested in positive solutions $x \in \mathbb{R}^s_{>0}$, so we now apply $\ln(\cdot)$ to both sides and examine the solvability of the resulting *linear system*:

$$\ln x \ (y_{j'} - y_{j_0})^\dagger \ = \ \ln \frac{b^j_{j'}}{b^j_{j_0}}, \text{ for all } j' \in I_j,\ j' \neq j_0, \text{ and for all } 1 \leq j \leq d,$$

where $\ln x = (\ln(x_1), \ln(x_2), \ldots, \ln(x_s))$. Now collect the differences $(y_{j'} - y_{j_0})^\dagger$ as columns of a matrix

$$\Delta := \left[(y_{j'} - y_{j_0})^\dagger\right]_{\forall j' \in I_j, j' \neq j_0, \forall 1 \leq j \leq d} , \tag{4.5}$$

and define the (row) vector

$$\Theta_\kappa := \left(\ln \frac{b^j_{j'}}{b^j_{j_0}} \right)_{\forall j' \in I_j, j' \neq j_0, \forall 1 \leq j \leq d} . \tag{4.6}$$

Observe that the basis vectors b^j and hence the vector Θ_κ depend on the rate constants. The binomials (4.1) admit a real positive solution (in the presence of Condition 4.2.2), if and only if the linear system

$$(\ln x)\, \Delta = \Theta_\kappa \tag{4.7}$$

has a real solution $(\ln x) \in \mathbb{R}^s$. This is the motivation for our final condition and Theorem 4.2.2 below:

Condition 4.2.3. *Consider a chemical reaction system given by a network G with m complexes and reaction rate constants κ^*_{ij} that satisfies both Condition 4.2.1 (i.e. there exists a partition $I_1, I_2, \ldots, I_d$ of $\{1, 2, \ldots, m\}$ and a basis $b^1, b^2, \ldots, b^d \in \mathbb{R}^m$ of $\ker(\Sigma)$ with $\operatorname{supp}(b^i) = I_i$) and Condition 4.2.2 (i.e., the coefficients of each binomial in equation (4.1) are of the same sign). Recall the matrix Δ and the vector Θ_κ (defined in equations (4.5) and (4.6), respectively). Let U be a matrix with integer entries whose columns form a basis of the kernel of Δ, that is, U is an integer matrix of maximum column rank such that the following matrix product is a zero matrix with s rows:*

$$\Delta\, U \;=\; \mathbf{0}\,.$$

*We say that this chemical reaction system **additionally** satisfies Condition 4.2.3 if the linear system* (4.7) *has a real solution $(\ln x) \in \mathbb{R}^s$. Equivalently, the Fundamental Theorem of Linear Algebra [151] implies that equation* (4.7) *has a solution, if and only if*

$$\Theta_\kappa\, U = 0\,. \tag{4.8}$$

Remark 4.2.4. *Conditions 4.2.2 and 4.2.3 impose semialgebraic constraints on the rate constants:*

- *If the matrix Δ defined in (4.5) has full column rank (i.e. the right kernel is trivial), then U is the zero vector. It follows that equation (4.8) holds, and hence, Condition 4.2.3 is trivially satisfied for any positive vector of rate constants. We will see that this is the case for multisite phosphorylation networks.*
- *If the matrix Δ does not have full column rank (i.e. there exists a nontrivial right kernel), then equation (4.8) evaluates to a system of polynomial equations in the rate constants.*

Now we can state sufficient conditions for a chemical reaction system to admit positive toric steady states:

Theorem 4.2.2 (Existence of positive toric steady states)**.** *Consider a chemical reaction system with m complexes which satisfies Condition 4.2.1 and hence has a binomial steady state ideal $J_{\Sigma\Psi}$. Then this chemical reaction system admits a positive toric steady state if and only if Conditions 4.2.2 and 4.2.3 hold.*

Proof. Assume that Conditions 4.2.1, 4.2.2, and 4.2.3 hold. Lemma 4.2.1 implies that the coefficients of the binomial system are of the same sign, hence Δ and Θ_κ given in equations (4.5) and (4.6) and the linear system (4.7) are well-defined. Then Condition 4.2.3 gives a solution $(\ln x)$ to the system (4.7), which immediately gives a positive steady state $x \in \mathbb{R}^s_{>0}$ of the chemical reaction system.

On the other hand, assume that Condition 4.2.1 holds and that the system admits a positive steady state, that is, the binomial system (4.1) has a positive real solution. In this case the coefficients of the binomials must be of the same sign, which implies that Condition 4.2.2 holds additionally. Again, positive real solutions of the binomial system imply solvability of the linear system (4.7) and thus, Condition 4.2.3 is satisfied as well. □

Remark 4.2.5 (Existence of steady states using fixed point arguments)**.** *In some cases, we can establish the existence of positive steady states by using fixed-point arguments. If the stoichiometric compatibility classes of a network are bounded and the chemical reaction system has no boundary steady states, then the Brouwer fixed point theorem guarantees that a positive steady state exists in each compatibility class. For example, the multisite phosphorylation networks that are studied in this chapter have this property.*

The focus of our results, however, is slightly different. We are more interested in parametrizing the steady state locus (and hence all positive steady states) and less with the actual number of steady states within a given stoichiometric compatibility class (apart from Section 4.4, where we are concerned with compatibility classes having at least two distinct positive steady states). Moreover, using fixed point arguments, the existence of positive steady states may only be deduced if the chemical reaction system has no boundary steady states, which is somewhat rare in examples from Computational Biology. Our results do not require any information about boundary steady states.

Example 4.2.1 (Triangle network, continued)**.** *We return to Example 4.1.1 to illustrate the three conditions. First,* $\ker(\Sigma)$ *is the plane in* $\mathbb{R}^3$ *orthogonal to the vector* $(-2\kappa_{12}-\kappa_{13}, 2\kappa_{21}+\kappa_{23}, \kappa_{31}-\kappa_{32})$*. It follows that the partition* $\{1,2\},\{3\}$ *works to satisfy Condition 4.2.1 if and only if* $\kappa_{31}=\kappa_{32}$*. Therefore, for a chemical reaction system arising from the Triangle network, Condition 4.2.1 holds (with partition* $\{1,2\},\{3\}$*) if and only if the system has toric steady states. The forward direction is an application of Theorem 4.2.1, while for general networks the reverse implication is false: we will see in Example 4.2.3 that there are networks with toric steady states that do not satisfy Condition 4.2.1 for any partition.*

Next, for those systems for which $\kappa_{31}=\kappa_{32}$*, Condition 4.2.2 comes down to verifying that the entries of the vector* $(-2\kappa_{12}-\kappa_{13}, 2\kappa_{21}+\kappa_{23})$ *have opposite signs, which is clearly true for positive rate constants. Finally, Condition 4.2.3 asks (again, in the* $\kappa_{31}=\kappa_{32}$ *setting) whether the following linear system has a real solution* $(\ln x_1,\ \ln x_2) \in \mathbb{R}^2$*:*

$$(\ln x_1,\ \ln x_2)\underbrace{\begin{pmatrix} 2 \\ -2 \end{pmatrix}}_{=\Delta} \;=\; \underbrace{\ln\left(\frac{2\kappa_{21}+\kappa_{23}}{2\kappa_{12}+\kappa_{13}}\right)}_{=\Theta_\kappa}\,,$$

which is clearly true. This linear equation arises from the binomial equation

$$(2\kappa_{12}+\kappa_{13})\,x_1^2-(2\kappa_{21}+\kappa_{23})\,x_2^2 \;=\; 0\,.$$

As Condition 4.2.3 holds, Theorem 4.2.2 implies that these systems admit positive steady states.

Under the hypothesis of Theorem 4.2.2, the following result shows how to parametrize the steady state locus.

Theorem 4.2.3. *Consider a chemical reaction system that satisfies Conditions 4.2.1, 4.2.2, and 4.2.3. Let $A \in \mathbb{Z}^{w\times s}$ be a matrix of maximal rank w such that $\ker(A)$ equals the span of all the differences $y_{j_2} - y_{j_1}$ for $j_1, j_2 \in I_j$, where $1 \leq j \leq d$. For $1 \leq i \leq s$, we let A_i denote the i-th column of A. Let $\tilde{x} \in \mathbb{R}^s_{>0}$ be a positive steady state of the chemical reaction system. Then all positive solutions $x \in \mathbb{R}^s_{>0}$ to the binomial system (4.1) can be written as*

$$x \;=\; \left(\tilde{x}_1\,\mathbf{t}^{A_1},\; \tilde{x}_2\,\mathbf{t}^{A_2},\; \ldots,\; \tilde{x}_s\,\mathbf{t}^{A_s}\right), \tag{4.9}$$

for some $\mathbf{t} \in \mathbb{R}^w$ (where we are using the standard notation for multinomial exponents). In particular, the positive steady state locus has dimension w and can be parametrized by monomials in the concentrations. Any two distinct positive steady states x^1 and x^2 satisfy

$$\ln x^2 - \ln x^1 \in \operatorname{im}\left(A^\dagger\right) \;=\; \operatorname{span}\left\{y_{j_2} - y_{j_1} \,|\, j_1, j_2 \in I_j, 1 \leq j \leq d\right\}^\perp. \tag{4.10}$$

Proof. By definition the rows of A span the orthogonal complement of the linear subspace spanned by the differences $y_{j_2} - y_{j_1}$ for $j_1, j_2 \in I_j$, $1 \leq j \leq d$. Let $\tilde{x} \in \mathbb{R}^s_{>0}$ be a positive steady state of the chemical reaction system; in other words, it is a particular positive solution for the following system of equations:

$$b^j_{j_1} x^{y_{j_2}} - b^j_{j_2} x^{y_{j_1}} \;=\; 0 \quad \text{for all } j_1, j_2 \in I_j, \text{ and for all } 1 \leq j \leq d\,.$$

(Here the b^j are the basis vectors of $\ker(\Sigma)$ with disjoint support.) Then it follows from basic results on binomial equations [38] that all positive solutions $x \in \mathbb{R}^s_{>0}$ to the above system of binomial equations can be written as

$$x \quad = \quad \left(\tilde{x}_1\,\mathbf{t}^{A_1},\; \tilde{x}_2\,\mathbf{t}^{A_2},\; \ldots,\; \tilde{x}_s\,\mathbf{t}^{A_s}\right),$$

for some $\mathbf{t} \in \mathbb{R}^w$. In particular, the positive steady state locus has w degrees of freedom.
For the convenience of the reader, we expand now the previous argument. In fact, it is easy to check that any vector of this shape is a positive solution. We first let x^* be a particular positive solution of the above binomials. Then $\frac{x^*}{\tilde{x}} \;:=\; \left(\frac{x^*_1}{\tilde{x}_1}, \frac{x^*_2}{\tilde{x}_2}, \ldots \frac{x^*_s}{\tilde{x}_s}\right)$ is a positive solution of the system of equations:

$$x^{y_{j_2}} - x^{y_{j_1}} = 0 \quad \text{for all } j_1, j_2 \in I_j, \text{ for all } 1 \leq j \leq d\,.$$

Therefore, $\left(\frac{x^*}{\tilde{x}}\right)^{y_{j_2} - y_{j_1}} \;=\; 1$. Or, equivalently, $\ln\left(\frac{x^*}{\tilde{x}}\right) \cdot (y_{j_2} - y_{j_1}) \;=\; 0$. This implies that $\ln\left(\frac{x^*}{\tilde{x}}\right)$ belongs to the rowspan of A, and this means there exist $\lambda_1, \lambda_2, \ldots, \lambda_w$ such that, if $\mathcal{A}_1, \mathcal{A}_2, \ldots, \mathcal{A}_w$ represent the rows of A, then we can write

$$\left(\ln\left(\frac{x^*}{\tilde{x}}\right)\right)_i = \lambda_1(\mathcal{A}_1)_i + \cdots + \lambda_w(\mathcal{A}_w)_i \quad \text{for all } 1 \leq i \leq s\,.$$

If we call $t_\ell := \exp(\lambda_\ell)$ for $1 \leq \ell \leq w$, then $x^*_i = \tilde{x}_i t^{A_i}$ for all $1 \leq i \leq s$, which is what we wanted to prove. □

We now turn to the case of a network for which Condition 4.2.1 holds with the *same* partition for all choices of rate constants. The following result, which follows immediately from Theorem 4.2.2, states that for such a network, the semialgebraic set of rate constants that give rise to systems admitting positive steady states is defined by Conditions 4.2.2 and 4.2.3.

Corollary 4.2.1. *Let G be a chemical reaction network with m complexes and r reactions, and assume that there exists a partition $I_1, I_2 \ldots, I_d$ of the m complexes such that for any choice of reaction rate constants, the resulting chemical reaction system satisfies Condition 4.2.1 with this partition. Then a vector of reaction rate constants $\kappa_{ij}^* \in \mathbb{R}^r_{>0}$ gives rise to a system that admits a positive steady state if and only if κ_{ij}^* satisfies Conditions 4.2.2 and 4.2.3.*

In the following example, we see that the 2-site phosphorylation network satisfies the hypothesis of Corollary 4.2.1. The 2-site system generalizes the 1-site system in Example 2.1.2, and we will consider general n-site systems in Section 4.3.

Example 4.2.2 (2-site phosphorylation system)**.** *The dual phosphorylation network arises from the 1-site network* (2.11) *by allowing a total of two phosphate groups to be added to the substrate of S_0 rather than only one. Again there are two enzymes (E and F), but now there are 3 substrates (S_0, S_1, and S_2). The substrate S_i is the substrate obtained from S_0 by attaching i phosphate groups to it. Each substrate can accept (via an enzymatic reaction involving E) or lose (via a reaction involving F) at most one phosphate; this means that the mechanism is "distributive". In addition, we say that the phosphorylation is "sequential" because multiple phosphate groups must be added in a specific order, and removed in a specific order as well.*

$$\begin{aligned} S_0 + E \underset{k_{\mathrm{off}_0}}{\overset{k_{\mathrm{on}_0}}{\rightleftarrows}} ES_0 \overset{k_{\mathrm{cat}_0}}{\to} S_1 + E \underset{k_{\mathrm{off}_1}}{\overset{k_{\mathrm{on}_1}}{\rightleftarrows}} ES_1 \overset{k_{\mathrm{cat}_1}}{\to} S_2 + E \\ S_2 + F \underset{l_{\mathrm{off}_1}}{\overset{l_{\mathrm{on}_1}}{\rightleftarrows}} FS_2 \overset{l_{\mathrm{cat}_1}}{\to} S_1 + F \underset{l_{\mathrm{off}_0}}{\overset{l_{\mathrm{on}_0}}{\rightleftarrows}} FS_1 \overset{l_{\mathrm{cat}_0}}{\to} S_0 + F \end{aligned} \tag{4.11}$$

We order the 9 species as $(S_0, S_1, S_2, ES_0, ES_1, FS_1, FS_2, E, F)$, and we order the 10 complexes as $(S_0 + E, S_1 + E, S_2 + E, ES_0, ES_1, S_0 + F, S_1 + F, S_2 + F, FS_1, FS_2)$. The 9×10-matrix Y and the 10×10-matrix $\mathcal{L}(G)$ for this system are the following:

$$Y = \begin{bmatrix} 1 & 0 & 0 & 0 & 0 & 1 & 0 & 0 & 0 & 0 \\ 0 & 1 & 0 & 0 & 0 & 0 & 1 & 0 & 0 & 0 \\ 0 & 0 & 1 & 0 & 0 & 0 & 0 & 1 & 0 & 0 \\ 0 & 0 & 0 & 1 & 0 & 0 & 0 & 0 & 0 & 0 \\ 0 & 0 & 0 & 0 & 1 & 0 & 0 & 0 & 0 & 0 \\ 0 & 0 & 0 & 0 & 0 & 0 & 0 & 0 & 1 & 0 \\ 0 & 0 & 0 & 0 & 0 & 0 & 0 & 0 & 0 & 1 \\ 1 & 1 & 1 & 0 & 0 & 0 & 0 & 0 & 0 & 0 \\ 0 & 0 & 0 & 0 & 0 & 1 & 1 & 1 & 0 & 0 \end{bmatrix}$$

$$\mathcal{L}(G) := \begin{bmatrix} -k_{\mathrm{on}_0} & 0 & 0 & k_{\mathrm{off}_0} & 0 & 0 & 0 & 0 & 0 & 0 \\ 0 & -k_{\mathrm{on}_1} & 0 & k_{\mathrm{cat}_0} & k_{\mathrm{off}_1} & 0 & 0 & 0 & 0 & 0 \\ 0 & 0 & 0 & 0 & k_{\mathrm{cat}_1} & 0 & 0 & 0 & 0 & 0 \\ k_{\mathrm{on}_0} & 0 & 0 & -k_{\mathrm{off}_0} - k_{\mathrm{cat}_0} & 0 & 0 & 0 & 0 & 0 & 0 \\ 0 & k_{\mathrm{on}_1} & 0 & 0 & -k_{\mathrm{off}_1} - k_{\mathrm{cat}_1} & 0 & 0 & 0 & 0 & 0 \\ 0 & 0 & 0 & 0 & 0 & 0 & 0 & 0 & l_{\mathrm{cat}_0} & 0 \\ 0 & 0 & 0 & 0 & 0 & 0 & -l_{\mathrm{on}_0} & 0 & l_{\mathrm{off}_0} & l_{\mathrm{cat}_1} \\ 0 & 0 & 0 & 0 & 0 & 0 & 0 & -l_{\mathrm{on}_1} & 0 & l_{\mathrm{off}_1} \\ 0 & 0 & 0 & 0 & 0 & 0 & l_{\mathrm{on}_0} & 0 & -l_{\mathrm{cat}_0} - l_{\mathrm{off}_0} & 0 \\ 0 & 0 & 0 & 0 & 0 & 0 & 0 & l_{\mathrm{on}_1} & 0 & -l_{\mathrm{cat}_1} - l_{\mathrm{off}_1} \end{bmatrix}$$

We will analyze the steady state locus of the resulting chemical reaction system by focusing on the structure of the kernel of the matrix $\Sigma = Y\mathcal{L}(G)$ of the system. Note that the network (4.11) has only two terminal strong linkage classes, $\{S_2 + E\}$ and $\{S_0 + F\}$. Also, $\mathrm{span}\{e_3, e_6\} \subseteq \ker(\Sigma)$, where e_i denotes the i-th canonical vector of $\mathbb{R}^{10}$. A partition of the 10 complexes that satisfies Condition 4.2.1 is given by $I_1 = \{1, 4, 7, 9\}$, $I_2 = \{2, 5, 8, 10\}$, $I_3 = \{3\}$, and $I_4 = \{6\}$. A corresponding basis of $\ker(\Sigma)$, that is, one in which the i-th basis vector has support I_i, is:

$$b^1 = \begin{bmatrix} (k_{\mathrm{off}_0} + k_{\mathrm{cat}_0})k_{\mathrm{on}_1}k_{\mathrm{cat}_1}l_{\mathrm{on}_1}l_{\mathrm{on}_0}l_{\mathrm{cat}_0} \\ 0 \\ 0 \\ k_{\mathrm{on}_0}k_{\mathrm{on}_1}k_{\mathrm{cat}_1}l_{\mathrm{on}_1}l_{\mathrm{on}_0}l_{\mathrm{cat}_0} \\ 0 \\ 0 \\ k_{\mathrm{on}_0}k_{\mathrm{cat}_0}k_{\mathrm{on}_1}k_{\mathrm{cat}_1}l_{\mathrm{on}_1}(l_{\mathrm{cat}_0} + l_{\mathrm{off}_0}) \\ 0 \\ k_{\mathrm{on}_0}k_{\mathrm{cat}_0}l_{\mathrm{on}_0}k_{\mathrm{on}_1}k_{\mathrm{cat}_1}l_{\mathrm{on}_1} \\ 0 \end{bmatrix},$$

$$b^2 = \begin{bmatrix} 0 \\ k_{\mathrm{on}_0}k_{\mathrm{cat}_0}l_{\mathrm{on}_0}(k_{\mathrm{off}_1} + k_{\mathrm{cat}_1})l_{\mathrm{on}_1}l_{\mathrm{cat}_1} \\ 0 \\ 0 \\ k_{\mathrm{on}_0}k_{\mathrm{cat}_0}l_{\mathrm{on}_0}k_{\mathrm{on}_1}l_{\mathrm{on}_1}l_{\mathrm{cat}_1} \\ 0 \\ 0 \\ k_{\mathrm{on}_0}k_{\mathrm{cat}_0}l_{\mathrm{on}_0}k_{\mathrm{on}_1}k_{\mathrm{cat}_1}(l_{\mathrm{cat}_1} + l_{\mathrm{off}_1}) \\ 0 \\ k_{\mathrm{on}_0}k_{\mathrm{cat}_0}l_{\mathrm{on}_0}k_{\mathrm{on}_1}k_{\mathrm{cat}_1}l_{\mathrm{on}_1} \end{bmatrix}, \quad b^3 = e_3\ ,\ b^4 = e_6\ .$$

The structure of this basis $\{b^i\}$ implies that for $v \in \mathbb{R}^{10}$, $v \in \ker(\Sigma)$ if and only if v satisfies the following binomial equations:

$$\begin{array}{ll} b^1_1 v_4 - b^1_4 v_1 = 0\ , & b^2_2 v_5 - b^2_5 v_2 = 0\ , \\ b^1_1 v_7 - b^1_7 v_1 = 0\ , & b^2_2 v_8 - b^2_8 v_2 = 0\ , \\ b^1_1 v_9 - b^1_9 v_1 = 0\ , & b^2_2 v_{10} - b^2_{10} v_2 = 0\ , \end{array} \tag{4.12}$$

Hence, any steady state of the 2-site phosphorylation system must satisfy the following equa-

tions in the species concentrations $x = (x_{S_0}, x_{S_1}, \ldots, x_E, x_F)$*:*

$$\begin{array}{ll} b_1^1 x_4 - b_4^1 x_8 x_1 = 0\,, & b_2^2 x_5 - b_5^2 x_8 x_2 = 0\,, \\ b_1^1 x_9 x_2 - b_7^1 x_8 x_1 = 0\,, & b_2^2 x_9 x_3 - b_8^2 x_8 x_2 = 0\,, \\ b_1^1 x_6 - b_9^1 x_8 x_1 = 0\,, & b_2^2 x_7 - b_{10}^2 x_8 x_2 = 0\,. \end{array} \tag{4.13}$$

To check Condition 4.2.3, we consider the matrix Δ *and the vector* Θ_κ*:*

$$\Delta = [e_4 - e_8 - e_1 \mid e_9 + e_2 - e_8 - e_1 \mid e_6 - e_8 - e_1 \mid e_5 - e_8 - e_2 \mid e_9 + e_3 - e_8 - e_2 \mid e_7 - e_8 - e_2]$$

$$\Theta_\kappa = \left(\ln \frac{b_4^1}{b_1^1}, \ln \frac{b_7^1}{b_1^1}, \ln \frac{b_9^1}{b_1^1}, \ln \frac{b_5^2}{b_2^2}, \ln \frac{b_8^2}{b_2^2}, \ln \frac{b_{10}^2}{b_2^2} \right)\,.$$

It is straightforward to check that Δ *has rank 6 and hence full rank. Thus Condition 4.2.3 is trivially satisfied and does not pose any constraints on the rate constants.*

Following the proof of Theorem 4.2.3, we first will parametrize the solution set of the following reduced system:

$$\begin{array}{ll} x_4 - x_8 x_1 = 0\,, & x_5 - x_8 x_2 = 0\,, \\ x_9 x_2 - x_8 x_1 = 0\,, & x_9 x_3 - x_8 x_2 = 0\,, \\ x_6 - x_8 x_1 = 0\,, & x_7 - x_8 x_2 = 0\,. \end{array} \tag{4.14}$$

We are interested in an integer matrix A *such that* $\ker(A) = \operatorname{im}(\Delta)$*. One such matrix is*

$$A \;=\; \begin{bmatrix} 0 & 1 & 2 & 1 & 2 & 1 & 2 & 1 & 0 \\ 0 & 0 & 0 & 1 & 1 & 1 & 1 & 1 & 1 \\ 1 & 1 & 1 & 1 & 1 & 1 & 1 & 0 & 0 \end{bmatrix}\,.$$

This provides the following 3-dimensional parametrization of the reduced system:

$$(t_1, t_2, t_3) \;\mapsto\; \left(t_3,\; t_1 t_3,\; t_1^2 t_3,\; t_1 t_2 t_3,\; t_1^2 t_2 t_3,\; t_1 t_2 t_3,\; t_1^2 t_2 t_3,\; t_1 t_2,\; t_2\right)\,,$$

where t_2 *is the concentration of the enzyme* F*,* t_1 *is the quotient of the concentration of the enzyme* E *divided by the concentration of the enzyme* F*, and* t_3 *is the concentration of the substrate* S_0*. Returning to the original binomials* (4.13)*, we have the following particular solution:*

$$x_1^* = x_8^* = x_9^* = 1,\; x_2^* = \frac{b_7^1}{b_1^1},\; x_3^* = \frac{b_8^2 b_7^1}{b_1^1 b_2^2},\; x_4^* = \frac{b_4^1}{b_1^1},\; x_5^* = \frac{b_5^2 b_7^1}{b_1^1 b_2^2},\; x_6^* = \frac{b_9^1}{b_1^1},\; x_7^* = \frac{b_{10}^2 b_7^1}{b_1^1 b_2^2}\,.$$

Therefore we obtain the following 3-dimensional parametrization of the steady state locus (4.13)*, as predicted in Theorem 4.2.3:*

$$\begin{aligned} &\mathbb{R}^3 \to \mathbb{R}^9 \\ &(t_1, t_2, t_3) \mapsto \left(t_3,\; \frac{b_7^1}{b_1^1} t_1 t_3,\; \frac{b_8^2 b_7^1}{b_1^1 b_2^2} t_1^2 t_3,\; \frac{b_4^1}{b_1^1} t_1 t_2 t_3,\; \frac{b_5^2 b_7^1}{b_1^1 b_2^2} t_1^2 t_2 t_3,\; \frac{b_9^1}{b_1^1} t_1 t_2 t_3,\; \frac{b_{10}^2 b_7^1}{b_1^1 b_2^2} t_1^2 t_2 t_3,\; t_1 t_2,\; t_2\right)\,. \end{aligned} \tag{4.15}$$

Recall that the values b_j^i *are polynomials in the rate constants shown in the display of the vectors* b^1 *and* b^2*. Finally, note that none of the calculations in this example depends on the specific values of the rate constants; in particular, one partition works for all systems, so the hypothesis of Corollary 4.2.1 holds. In fact, as Condition 4.2.3 does not impose any constraints on the rate constants, it follows that all 2-site phosphorylation systems admit positive steady states. Actually, a stronger result holds: each stoichiometric compatibility class contains a steady state in its relative interior [23, 170].*

4.2.1 More general sufficient conditions

We show in Example 4.2.3 below, extracted from [144], that the conditions in Theorem 4.2.2 are not necessary for a chemical reaction system to have toric steady states; in other words, the converse of Theorem 4.2.2 does not hold. However, the condition for the steady state ideal to be generated by binomials always can be checked algorithmically via a Gröbner basis computation, as stated in the following lemma.

Lemma 4.2.2 (Proposition 1.1.(a) of [43])**.** *Let I be a binomial ideal, let $\prec$ be a monomial order, and let G be the reduced Gröbner basis of I for that ordering. Then G consists of binomials.*

Lemma 4.2.2 is a basic result about binomial ideals which is due to Eisenbud and Sturmfels [43]; it is a result concerning polynomial linear combinations. Note however that Theorem 4.2.2 requires only *linear algebra computations over* $\mathbb{R}$. We make use of Lemma 4.2.2 in the following example. We will return to it later to show that Theorem 4.2.4 below can be used to prove that this system has toric steady states, without needing to compute a Gröbner basis.

Example 4.2.3 (Shinar and Feinberg network)**.** *This example demonstrates that Condition 4.2.1 is not necessary for a chemical reaction system to have toric steady states. The network in Example (S60) of the Supporting Online Material of the recent article of Shinar and Feinberg is the following [144]:*

$$\begin{aligned} XD \underset{\kappa_{21}}{\overset{\kappa_{12}}{\rightleftarrows}} X \underset{\kappa_{32}}{\overset{\kappa_{23}}{\rightleftarrows}} XT \overset{\kappa_{34}}{\to} X_p \\ X_p + Y \underset{\kappa_{65}}{\overset{\kappa_{56}}{\rightleftarrows}} X_pY \overset{\kappa_{67}}{\to} X + Y_p \\ XT + Y_p \underset{\kappa_{98}}{\overset{\kappa_{89}}{\rightleftarrows}} XTY_p \overset{\kappa_{9,10}}{\to} XT + Y \\ XD + Y_p \underset{\kappa_{12,11}}{\overset{\kappa_{11,12}}{\rightleftarrows}} XDY_p \overset{\kappa_{12,13}}{\to} XD + Y \end{aligned} \tag{4.16}$$

We denote by $x_1, x_2, \ldots, x_9$ the concentrations of the species as follows:

$$x_{XD} = x_1,\ x_X = x_2,\ x_{XT} = x_3,\ x_{X_p} = x_4\ ,$$

$$x_Y = x_5,\ x_{X_pY} = x_6,\ x_{Y_p} = x_7,\ x_{XTY_p} = x_8,\ x_{XDY_p} = x_9\ .$$

Note that the numbering of the 13 complexes in the network is reflected in the names of the rate constants κ_{ij}. The chemical reaction system is the following:

$$\begin{aligned} \tfrac{dx_1}{dt} &= -\kappa_{12}x_1 + \kappa_{21}x_2 - \kappa_{11,12}x_1x_7 + (\kappa_{12,11} + \kappa_{12,13})x_9 \\ \tfrac{dx_2}{dt} &= \kappa_{12}x_1 + (-\kappa_{21} - \kappa_{23})x_2 + \kappa_{32}x_3 + \kappa_{67}x_6 \\ \tfrac{dx_3}{dt} &= \kappa_{23}x_2 + (-\kappa_{32} - \kappa_{34})x_3 - \kappa_{89}x_3x_7 + (\kappa_{98} + \kappa_{9,10})x_8 \\ \tfrac{dx_4}{dt} &= \kappa_{34}x_3 - \kappa_{56}x_4x_5 + \kappa_{65}x_6 \\ \tfrac{dx_5}{dt} &= -\kappa_{56}x_4x_5 + \kappa_{65}x_6 + \kappa_{9,10}x_8 + \kappa_{12,13}x_9 \\ \tfrac{dx_6}{dt} &= \kappa_{56}x_4x_5 + (-\kappa_{65} - \kappa_{67})x_6 \\ \tfrac{dx_7}{dt} &= \kappa_{67}x_6 - \kappa_{89}x_3x_7 + \kappa_{98}x_8 - \kappa_{11,12}x_1x_7 + \kappa_{12,11}x_9 \\ \tfrac{dx_8}{dt} &= \kappa_{89}x_3x_7 + (-\kappa_{98} - \kappa_{9,10})x_8 \\ \tfrac{dx_9}{dt} &= \kappa_{11,12}x_1x_7 + (-\kappa_{12,11} - \kappa_{12,13})x_9 \end{aligned} \tag{4.17}$$

The reduced Gröbner basis with respect to the lexicographical order $x_1 > x_2 > x_4 > x_5 > x_6 > x_8 > x_9 > x_3 > x_7$ *consists of the following binomials:*

$$\begin{aligned}
g_1 &= [\kappa_{89}\kappa_{12}\kappa_{23}\kappa_{9,10}(\kappa_{12,11}+\kappa_{12,13})+\kappa_{11,12}\kappa_{21}\kappa_{12,13}(\kappa_{98}+\kappa_{9,10})(\kappa_{32}+\kappa_{34})]x_3x_7+\\
&\quad +[-\kappa_{23}\kappa_{34}\kappa_{12}(\kappa_{12,11}+\kappa_{12,13})(\kappa_{98}+\kappa_{9,10})]x_3\\
g_2 &= [-\kappa_{11,12}\kappa_{21}\kappa_{34}(\kappa_{98}+\kappa_{9,10})(\kappa_{32}+\kappa_{34})]x_3+\\
&\quad +[\kappa_{11,12}\kappa_{21}\kappa_{12,13}(\kappa_{98}+\kappa_{9,10})(\kappa_{32}+\kappa_{34})+\kappa_{12}\kappa_{23}\kappa_{89}\kappa_{9,10}(\kappa_{12,11}+\kappa_{12,13})]x_9\\
g_3 &= [-\kappa_{23}\kappa_{34}\kappa_{89}\kappa_{12}(\kappa_{12,11}+\kappa_{12,13})]x_3+\\
&\quad +[\kappa_{23}\kappa_{9,10}\kappa_{89}\kappa_{12}(\kappa_{12,11}+\kappa_{12,13})+\kappa_{11,12}\kappa_{21}\kappa_{12,13}(\kappa_{98}+\kappa_{9,10})(\kappa_{32}+\kappa_{34})]x_8\\
g_4 &= \kappa_{67}x_6-\kappa_{34}x_3\\
g_5 &= \kappa_{56}\kappa_{67}x_4x_5+\kappa_{34}(-\kappa_{65}-\kappa_{67})x_3\\
g_6 &= \kappa_{23}x_2+(-\kappa_{32}-\kappa_{34})x_3\\
g_7 &= -\kappa_{21}(\kappa_{32}+\kappa_{34})x_3+\kappa_{12}\kappa_{23}x_1
\end{aligned} \tag{4.18}$$

Therefore, the network has toric steady states (for any choice of positive reaction rate constants) because the steady state ideal can be generated by $g_1,\ g_2,\ \ldots,\ g_7$*. However, we claim that this chemical reaction system does not satisfy Condition 4.2.1. In fact, for any rate constants, it is not possible to find a partition* $I_1, I_2, \ldots, I_6 \subseteq \{1, 2, \ldots, 13\}$ *such that* $\ker(\Sigma)$ *has a basis* $\{b^1, b^2, \ldots, b^6\}$ *with* $\operatorname{supp}(b^i) = I_i$*. This can be seen by noting that the kernel of* Σ *can be generated as follows:*

$$\begin{aligned}
\ker(\Sigma) = \Bigg\langle & e_4,\ e_7,\ e_{10},\ e_{13},\ \left(\frac{\kappa_{21}\kappa_{12,13}(\kappa_{32}+\kappa_{34})}{\kappa_{23}\kappa_{34}\kappa_{12}}\right)e_1+\left(\frac{\kappa_{12,13}(\kappa_{32}+\kappa_{34})}{\kappa_{23}\kappa_{34}}\right)e_2+\left(\frac{\kappa_{12,13}}{\kappa_{34}}\right)e_3+\\
&+\left(\frac{(\kappa_{65}+\kappa_{67})\kappa_{12,13}}{\kappa_{67}\kappa_{56}}\right)e_5+\left(\frac{\kappa_{12,13}}{\kappa_{67}}\right)e_6+\left(\frac{(\kappa_{12,11}+\kappa_{12,13})}{\kappa_{11,12}}\right)e_{11}+e_{12},\\
&\left(\frac{\kappa_{21}\kappa_{9,10}(\kappa_{32}+\kappa_{34})}{\kappa_{23}\kappa_{34}\kappa_{12}}\right)e_1+\left(\frac{\kappa_{9,10}(\kappa_{32}+\kappa_{34})}{\kappa_{23}\kappa_{34}}\right)e_2+\left(\frac{\kappa_{9,10}}{\kappa_{34}}\right)e_3+\\
&+\left(\frac{(\kappa_{65}+\kappa_{67})\kappa_{9,10}}{\kappa_{67}\kappa_{56}}\right)e_5+\left(\frac{\kappa_{9,10}}{\kappa_{67}}\right)e_6+\left(\frac{\kappa_{98}+\kappa_{9,10}}{\kappa_{89}}\right)e_8+e_9\Bigg\rangle\ .
\end{aligned} \tag{4.19}$$

Our next result, Theorem 4.2.4, will generalize Theorem 4.2.2 by giving a stronger condition that guarantees that the steady state locus is generated by binomials. We first need to generalize Conditions 4.2.1, 4.2.2, and 4.2.3 to any (finite) polynomial system.

First we must introduce some notation. For polynomials $F_1, F_2, \ldots, F_{s'} \in \mathbb{R}[x_1, x_2, \ldots, x_s]$, we denote by $x^{y_1}, x^{y_2}, \ldots, x^{y_{m'}}$ the monomials that occur in these polynomials; that is, there exist $F_{ij} \in \mathbb{R}$ such that $F_i(x) = \sum_{j=1}^{m'} F_{ij}x^{y_j}$ for $i = 1, 2, \ldots, s'$. We can write the polynomial system $F_1(x) = F_2(x) = \cdots = F_{s'}(x) = 0$ as

$$\Sigma' \cdot \Psi'(x) \ = \ 0\ , \tag{4.20}$$

where $\Sigma' = (F_{ij}) \in \mathbb{R}^{s' \times m'}$ is the coefficient matrix and $\Psi'(x) = (x^{y_1}, x^{y_2}, \ldots, x^{y_{m'}})^{\dagger}$. We will let d' denote the dimension of $\ker(\Sigma')$.

Condition 4.2.4. *We say that the polynomial system* (4.20) *satisfies Condition 4.2.4 if there exists a partition* $I_1, I_2, \ldots, I_{d'}$ *of* $\{1, 2, \ldots, m'\}$ *and a basis* $b^1, b^2, \ldots, b^{d'} \in \mathbb{R}^{m'}$ *of* $\ker(\Sigma')$ *such that* $\operatorname{supp}(b^i) = I_i$*.*

Condition 4.2.5. *Consider a polynomial system* (4.20) *that satisfies Condition 4.2.4 for the partition* $I_1, I_2, \ldots, I_{d'}$ *of* $\{1, 2, \ldots, m'\}$ *and a basis* $b^1, b^2, \ldots, b^{d'} \in \mathbb{R}^{m'}$ *of* $\ker(\Sigma')$ *(with* $\mathrm{supp}(b^i) = I_i$*). We say that the system satisfies* ***additionally*** *Condition 4.2.5, if for all* $j \in \{1, 2, \ldots, d'\}$*, the nonzero entries of* b^j *have the same sign.*

As before, we collect the differences of exponent vectors as columns of a matrix

$$\Delta' := \left[(y_{j'} - y_{j_0})^\dagger\right]_{\forall j' \in I_j, j' \neq j_0, \forall 1 \leq j \leq d'} \tag{4.21}$$

and define the (row) vector

$$\Theta' := \left[\ln \frac{b^j_{j_0}}{b^j_{j'}}\right]_{\forall j' \in I_j, j' \neq j_0, \forall 1 \leq j \leq d'} . \tag{4.22}$$

Condition 4.2.6. *Consider a polynomial system* (4.20) *which satisfies Conditions 4.2.4 and 4.2.5. Let* U' *be a matrix with integer entries whose columns form a basis of the kernel of* Δ'*. We say that this system satisfies* ***additionally*** *Condition 4.2.6, if the following holds:*

$$\Theta' U' = 0 .$$

We then have the following sufficient conditions:

Theorem 4.2.4. *Consider a chemical reaction system with* m *complexes and assume that there exist monomials* $\mathbf{x}^{\alpha_1}, \mathbf{x}^{\alpha_2}, \ldots, \mathbf{x}^{\alpha_\ell}$ *and indices* $i_1, i_2, \ldots, i_\ell$*, with* $\{i_1, i_2, \ldots, i_\ell\} \subseteq \{1, 2, \ldots, s\}$*, such that Condition 4.2.4 holds for the enlarged polynomial system*

$$f_1 = \cdots = f_s = \mathbf{x}^{\alpha_1} f_{i_1} = \cdots = \mathbf{x}^{\alpha_\ell} f_{i_\ell} = 0.$$

Then the steady state ideal $J_{\Sigma\psi}$ *is binomial.*

Moreover, the system has positive (toric) steady states if and only if Conditions 4.2.5 and 4.2.6 hold additionally for the enlarged system.

This theorem can be proved following the lines of the proof of Theorem 4.2.2 for the enlarged system defined in the statement. It is important to note that the ideal $\langle f_1, f_2, \ldots, f_s \rangle$ equals the ideal $\langle f_1, \ldots, f_s, \mathbf{x}^{\alpha_1} f_{i_1}, \ldots, \mathbf{x}^{\alpha_\ell} f_{i_\ell} \rangle$.

With similar proof as in Theorem 4.2.3, we moreover have:

Theorem 4.2.5. *Under the hypotheses of Theorem 4.2.4, the steady state locus can be parametrized by monomials in the concentrations.*

We end this section by returning to Example 4.2.3.

Example 4.2.4 (Shinar and Feinberg network, continued)**.** *Consider the system of equations:*

$$\begin{cases} f_1 = 0 \\ f_2 = 0 \\ \vdots \\ f_9 = 0 \\ x_7 f_1 = 0 \\ x_7 f_3 = 0 \\ x_7 f_8 = 0 \\ x_7 f_9 = 0 \end{cases} , \tag{4.23}$$

This enlarged system satisfies Conditions 4.2.4 and 4.2.5 for the following partition:

$$I_1 = \{4\},\ I_2 = \{10\},\ I_3 = \{13\},\ I_4 = \{14, 15\},\ I_5 = \{16, 17\}, I_6 = \{1, 2, 3, 5, 6, 7, 8, 9, 11, 12\}$$

and the following basis $b^1, b^2, \ldots, b^6$ of its kernel verifying $\operatorname{supp}(b^j) = I_j$*:*

$$b^1 = \mathbf{e_4}\ , \quad b^2 = \mathbf{e_{10}}\ , \quad b^3 = \mathbf{e_{13}}\ ,$$

$$b^4 = (k_{12,11} + k_{12,13})\mathbf{e_{14}} + k_{11,12}\mathbf{e_{15}}, \quad b^5 = (k_{98} + k_{910})\mathbf{e_{16}} + k_{89}\mathbf{e_{17}},$$

$$\begin{aligned} b^6 = {} & (k_{12}k_{23}k_{89}k_{9,10}(k_{12,11} + k_{12,13}) + k_{21}k_{11,12}k_{12,13}(k_{32} + k_{34})(k_{98} + k_{9,10}))k_{21}(k_{32} + k_{34})k_{56}k_{67}\mathbf{e_1} + \\ & (k_{12}k_{23}k_{89}k_{9,10}(k_{12,11} + k_{12,13}) + k_{21}k_{11,12}k_{12,13}(k_{32} + k_{34})(k_{98} + k_{9,10}))k_{12}(k_{32} + k_{34})k_{56}k_{67}\mathbf{e_2} + \\ & (k_{12}k_{23}k_{89}k_{9,10}(k_{12,11} + k_{12,13}) + k_{21}k_{11,12}k_{12,13}(k_{32} + k_{34})(k_{98} + k_{9,10}))k_{12}k_{23}k_{56}k_{67}\mathbf{e_3} + \\ & (k_{12}k_{23}k_{89}k_{9,10}(k_{12,11} + k_{12,13}) + k_{21}k_{11,12}k_{12,13}(k_{32} + k_{34})(k_{98} + k_{9,10}))k_{12}k_{23}k_{34}(k_{65} + k_{67})\mathbf{e_5} + \\ & (k_{12}k_{23}k_{89}k_{9,10}(k_{12,11} + k_{12,13}) + k_{21}k_{11,12}k_{12,13}(k_{32} + k_{34})(k_{98} + k_{9,10}))k_{12}k_{23}k_{34}k_{56}\mathbf{e_6} + \\ & k_{12}^2k_{23}k_{34}(k_{32} + k_{34})k_{56}k_{67}(k_{98} + k_{9,10})(k_{12,11} + k_{12,13})\mathbf{e_7} + \\ & k_{12}^2k_{23}^2k_{34}k_{56}k_{67}(k_{98} + k_{9,10})(k_{12,11} + k_{12,13})\mathbf{e_8} + k_{12}^2k_{23}^2k_{34}k_{56}k_{67}k_{89}(k_{12,11} + k_{12,13})\mathbf{e_9} + \\ & k_{12}k_{21}k_{23}k_{34}(k_{32} + k_{34})k_{56}k_{67}(k_{98} + k_{9,10})(k_{12,11} + k_{12,13})\mathbf{e_{11}} + \\ & k_{12}k_{21}k_{23}k_{34}(k_{32} + k_{34})k_{56}k_{67}(k_{98} + k_{9,10})k_{11,12}\mathbf{e_{12}}\ . \end{aligned}$$

In addition to the monomials already occurring in $f_1, f_2, \ldots, f_9$, the following 4 monomials are also in the augmented system: $x^{y_{14}} = x_1x_7^2$, $x^{y_{15}} = x_9x_7$, $x^{y_{16}} = x_3x_7^2$, and $x^{y_{17}} = x_8x_7$. By Theorem 4.2.4, the system has toric steady states. Recall that the binomials $g_1, g_2, \ldots, g_7$ in equation (4.18) *generate the ideal $\langle f_1,\ f_2,\ \ldots, f_9\rangle = \langle f_1,\ f_2,\ \ldots, f_9,\ x_7f_1,\ x_7f_3,\ x_7f_8,\ x_7f_9\rangle$. We can see immediately that there are positive steady states for any choice of positive rate constants, and so there is no need to check Condition 4.2.6.*

4.3 The n-site phosphorylation system has toric steady states

In this section we introduce the n-site phosphorylation system (under the assumption of a distributive and sequential mechanism). To show that these systems have toric steady states, we apply Theorem 4.2.2; this generalizes Example 4.2.2 (the $n = 2$ case). Further, we note that the parametrization of the steady state locus given by Theorem 4.2.3 is implicit in work of Wang and Sontag [170].

4.3.1 The n-site phosphorylation system

We now define the n-site phosphorylation system (also called a "multiple futile cycle") $\Sigma_n(\kappa, \mathcal{C})$, which depends on a choice of rate constants $\kappa \in \mathbb{R}^{6n}_{>0}$ and values of the conservation relations $\mathcal{C} = (E_{\text{tot}}, F_{\text{tot}}, S_{\text{tot}}) \in \mathbb{R}^3_{>0}$. As in the earlier example of the 1-site network (2.11) and the 2-site network (4.11), we will make the assumption of a "distributive" and "sequential" mechanism (see, for example, [25]). As discussed in the first section of this chapter, this n-site phosphorylation system is of great biochemical importance: it is a recurring network motif in many networks describing processes as diverse as intracellular signaling (e.g. MAPK signaling with $n = 2$ and $n = 3$), cell cycle control (e.g. Sic1 with $n = 9$), and cellular differentiation (e.g. NFAT with $n = 13$).

Following notation of Wang and Sontag [170], the n-site phosphorylation system arises from the following reaction network:

$$S_0 + E \underset{k_{\text{off}_0}}{\overset{k_{\text{on}_0}}{\rightleftarrows}} ES_0 \overset{k_{\text{cat}_0}}{\to} S_1 + E \qquad\qquad S_1 + F \underset{l_{\text{off}_0}}{\overset{l_{\text{on}_0}}{\rightleftarrows}} FS_1 \overset{l_{\text{cat}_0}}{\to} S_0 + F$$

$$\vdots \qquad\qquad \vdots$$

$$S_{n-1} + E \underset{k_{\text{off}_{n-1}}}{\overset{k_{\text{on}_{n-1}}}{\rightleftarrows}} ES_{n-1} \overset{k_{\text{cat}_{n-1}}}{\to} S_n + E \qquad\qquad S_n + F \underset{l_{\text{off}_{n-1}}}{\overset{l_{\text{on}_{n-1}}}{\rightleftarrows}} FS_n \overset{l_{\text{cat}_{n-1}}}{\to} S_{n-1} + F$$

We see that the n-site network has $3n + 3$ chemical species $S_0, \ldots, S_n$, $ES_0, \ldots, ES_{n-1}$, $FS_1, \ldots, FS_n$, E, and F, so we write a concentration vector as $x = (s_0, \ldots, s_n, c_0, \ldots, c_{n-1}, d_1, \ldots, d_n, e, f)$, which is a positive vector of length $3n + 3$. These species comprise $4n + 2$ complexes, and there are $6n$ reactions. Each reaction has a reaction rate, and we collect these in the vector of rate constants $\kappa = \left(k_{\text{on}_0}, \ldots, l_{\text{cat}_{n-1}}\right) \in \mathbb{R}^{6n}_{>0}$.

For our purposes, we will introduce the following numbering for the complexes (which is compatible with the numbering in Examples 2.1.2 and 4.2.2):

$$1 \rightleftarrows n+2 \to 2 \qquad\qquad 2n+3 \rightleftarrows 3n+3 \to 2n+2$$
$$2 \rightleftarrows n+3 \to 3 \qquad\qquad 2n+4 \rightleftarrows 3n+4 \to 2n+3$$
$$\vdots \qquad\qquad \vdots$$
$$n \rightleftarrows 2n+1 \to n+1 \qquad\qquad 3n+2 \rightleftarrows 4n+2 \to 3n+1$$

The conservation relations here correspond to the fact that the total amounts of free and bound enzyme or substrate remain constant. That is, the following three conservation values $\mathcal{C} = (E_{\text{tot}}, F_{\text{tot}}, S_{\text{tot}})$ remain unchanged as the dynamical system progresses:

$$\begin{aligned} E_{\text{tot}} &= e + \sum_{i=0}^{n-1} c_i \,, \\ F_{\text{tot}} &= f + \sum_{i=1}^{n} d_i \,, \\ S_{\text{tot}} &= \sum_{i=0}^{n} s_i + \sum_{i=0}^{n-1} c_i + \sum_{i=1}^{n} d_i \,. \end{aligned} \tag{4.24}$$

Any choice of these three values defines a stoichiometric compatibility class of dimension $3n$:

$$\mathcal{P}_{\mathcal{C}} \;=\; \left\{ x \in \mathbb{R}^{3n+3}_{\geq 0} \mid \text{the conservation equations (4.24) hold} \right\}$$

We will see in Theorem 4.3.1 that the steady state locus in this system is 3-dimensional. A forthcoming work will concern the question of how many times the steady state locus intersects a compatibility class $\mathcal{P}_{\mathcal{C}}$ for multisite phosphorylation systems [23].

4.3.2 Results

For the n-site phosphorylation system, we will call its complex-to-species rate matrix Σ_n, and we will let G_n denote the underlying digraph of the chemical reaction network. In order to apply the results of Section 4.2 to this system, we now aim to exhibit a specific basis of the kernel of Σ_n that satisfies Condition 4.2.1. We begin by describing the rows of $\Sigma_n := Y \cdot \mathcal{L}(G_n)$ as linear combinations of the rows of $\mathcal{L}(G_n)$. Recall that $\mathcal{L}(G_n)$ is minus the transpose of the Laplacian matrix of the associated digraph. Letting $R(i)$ represent the i-th row of $\mathcal{L}(G_n)$, we have:

$$\Sigma_n := Y \cdot \mathcal{L}(G_n) = \left[\begin{array}{c} R(1) + R(2n+2) \\ R(2) + R(2n+3) \\ \vdots \\ R(n+1) + R(3n+2) \\ \hline R(n+2) \\ \vdots \\ R(2n+1) \\ \hline R(3n+3) \\ \vdots \\ R(4n+2) \\ \hline R(1) + R(2) + \cdots + R(n+1) \\ R(2n+2) + \cdots + R(3n+2) \end{array}\right] \in \mathbb{R}^{(3n+3)\times(4n+2)} \tag{4.25}$$

Our next aim is to exhibit a submatrix of Σ_n that shares the same kernel as Σ_n. The only relations that exist among the rows of $\mathcal{L}(G_n)$ arise from the fact that the sum of the rows in each of the two blocks equals zero. Consequently, it is straightforward to check that

$$\operatorname{rank}(\Sigma_n) = 3n\,.$$

Moreover, if we delete any of the first $3n+1$ rows and the last two rows of Σ_n, we obtain a new matrix that has maximal rank. As we are interested in describing the kernel of Σ_n, we will discard the first and the last two rows, and we will focus on the resulting submatrix. Furthermore, as the $(n+1)$-st and $(2n+2)$-nd columns on Σ_n are equal to zero, we already know that e_{n+1} and e_{2n+2}, the $(n+1)$-st and $(2n+2)$-nd canonical basis vectors of $\mathbb{R}^{4n+2}$, belong to $\ker(\Sigma_n)$. Hence we can now focus on an even smaller submatrix of Σ_n obtained by deleting the first and the last two rows, and the $(n+1)$-st and $(2n+2)$-nd columns. We will call this submatrix Σ'_n, and we will denote by $C(j)$ the column of Σ'_n which corresponds to the j-th column of Σ_n after deleting the first row and the last two (for example, $C(n+2)$ will represent the $(n+1)$-st column of Σ'_n). Then, if we call Σ''_n the submatrix of Σ'_n formed by its first $3n$ columns, the system $\Sigma'_n v = 0$ is equivalent to the following one:

$$\Sigma''_n \begin{bmatrix} v_1 \\ \vdots \\ v_{3n} \end{bmatrix} = -\begin{bmatrix} C(3n+3) & \dots & C(4n+2) \end{bmatrix} \begin{bmatrix} v_{3n+1} \\ \vdots \\ v_{4n} \end{bmatrix}. \tag{4.26}$$

Let us call

$$D := \det(\Sigma''_n)\,. \tag{4.27}$$

If $D \neq 0$, then we can use Cramer's rule to solve system (4.26). In fact, we will show in Proposition 4.3.1 that this is the case and that we can find solutions to the system $\Sigma_n w = 0$ such that all the nonzero entries have the same sign.

Next we introduce a partition and a set of basis vectors b^i that will be used to show that the n-site system satisfies Condition 4.2.1. The partition $I_1, I_2, \ldots, I_{n+2}$ of $\{1, 2, \ldots, 4n+2\}$ is the following:

$$I_j = \{j,\, n+j,\, 2n+j+2,\, 3n+j+2\} \text{ (for } 1 \leq j \leq n), \quad I_{n+1} = \{n+1\}, \quad I_{n+2} = \{2n+2\}\,. \tag{4.28}$$

The entries in our vectors b^i will be certain determinants. More precisely, let $D_{\ell(j)}$ be minus the determinant of the matrix obtained by replacing $C(\ell(j))$ by $C(3n+j+2)$ in Σ''_n, for $\ell(j) = j,\ n+j+1,\ 2n+j+2$, where $1 \leq j \leq n$:

$$D_{\ell(j)} = -\det\left(\left[C(1)|\ldots|\overset{\ell(j)}{\overset{\downarrow}{C(3n+j+2)}}|\ldots|C(3n+2)\right]\right)\,. \tag{4.29}$$

Note that D, D_j, D_{n+j+1}, and D_{2n+j+2}, for $1 \leq j \leq n$, define polynomial functions of κ on $\mathbb{R}^{6n}_{>0}$. We will show in Proposition 4.3.1 that these functions D, D_j, D_{n+j+1}, and D_{2n+j+2} are nonzero and have the same sign, for $1 \leq j \leq n$.

Now we may define the vectors $b^1, b^2, \ldots, b^n$ of $\mathbb{R}^{4n+2}_{>0}$ by:

$$(b^j)_i = \begin{cases} D_j & \text{if } i = j \\ D_{n+j+1} & \text{if } i = n+j+1 \\ D_{2n+j+2} & \text{if } i = 2n+j+2 \\ D & \text{if } i = 3n+j+2 \\ 0 & \text{otherwise} \end{cases}\,, \tag{4.30}$$

for $1 \leq i \leq 4n+2$, where $1 \leq j \leq n$.

We are now equipped to state our main result in this section.

Theorem 4.3.1. *The n-site phosphorylation system has toric steady states. The steady state locus has dimension 3 and can be parametrized by*

$$\begin{aligned} \mathbb{R}^3 &\to \mathbb{R}^{3n+3} \\ (t_1,t_2,t_3) &\mapsto \left(t_3,\ \frac{D_{2n+3}}{D_1}t_1t_3,\ \ldots,\ \frac{D_{2n+3}}{D_1}\cdots\frac{D_{3n+2}}{D_n}t_1^n t_3,\ \frac{D_{n+2}}{D_1}t_1t_2t_3,\ \ldots,\right. \\ &\qquad \left.\frac{D_{n+2}}{D_1}\cdots\frac{D_{2n+1}}{D_n}t_1^n t_2t_3,\ \frac{D}{D_1}t_1t_2t_3,\ \ldots,\ \frac{D}{D_n}\frac{D_{2n+3}}{D_1}\cdots\frac{D_{3n+1}}{D_{n-1}}t_1^n t_2t_3,\ t_1t_2,\ t_2\right)\,. \end{aligned}$$

Moreover, the system satisfies Condition 4.2.1 with the partition $I_1, I_2, \ldots, I_{n+2}$ described in (4.28) *and the basis $\{b^1, \ldots, b^n\} \cup \{e_{n+1}, e_{2n+2}\}$ where the vectors b^j are defined in* (4.30) *and e_{n+1} and e_{2n+2} are the $(n+1)$-st and $(2n+2)$-nd vectors of the canonical basis of $\mathbb{R}^{4n+2}$. In addition, it satisfies Conditions 4.2.2 and 4.2.3.*

In particular,

$$\tilde{x} = \Bigg(1,\ \frac{D_{2n+3}}{D_1},\ \ldots,\ \frac{D_{2n+3}}{D_1}\cdots\frac{D_{3n+2}}{D_n},\ \frac{D_{n+2}}{D_1},\ \ldots,\ \frac{D_{n+2}}{D_1}\cdots\frac{D_{2n+1}}{D_n},\ \frac{D}{D_1},\ \ldots,\ \frac{D}{D_n}\frac{D_{2n+3}}{D_1}\cdots\frac{D_{3n+1}}{D_{n-1}},\ 1,\ 1\Bigg)$$

is an explicit positive steady state of the system.

We remark that the parametrization given in the statement of this theorem, which is one of the possible parametrizations provided by Theorem 4.2.3, gives systematically what Wang and Sontag obtained "by hand" in [170]. We note that the fact that this variety (the steady state locus) has a rational parametrization is a special case of a rational parametrization theorem for general multisite post-translational modification systems as analyzed by Thomson and Gunawardena [164].

4.3.3 Proof of Theorem 4.3.1

We start with the following proposition:

Proposition 4.3.1. *Let D be the determinant defined in* (4.27)*, and let D_j, D_{n+j+1}, and D_{2n+j+2} be as in* (4.29)*, for $1 \leq j \leq n$. Then each polynomial function $D, D_j, D_{n+j+1}, D_{2n+j+2} : \mathbb{R}^{6n}_{>0} \to \mathbb{R}$ for $1 \leq j \leq n$, never vanishes, and these functions all have the same constant sign on $\mathbb{R}^{6n}_{>0}$.*

Proof. For this proof, we will denote by $R(i)$ the i-th row of the matrix obtained from $\mathcal{L}(G_n)$ after deleting columns $n+1$ and $2n+2$. (Note that this notation differs slightly from that introduced in equation (4.25).) The proof has two steps: first we demonstrate that $D \neq 0$ on the positive orthant, and then we show that the other functions D_j, D_{n+j+1}, and D_{2n+j+2} are also nonzero on the positive orthant and that their signs coincide with that of D.

To prove that $D \neq 0$ on $\mathbb{R}^{6n}_{>0}$, we proceed by induction on n. First, if $n = 1$, we have:

$$\Sigma_1'' = \begin{bmatrix} 0 & k_{\mathrm{cat}_0} & -l_{\mathrm{on}_0} \\ k_{\mathrm{on}_0} & -k_{\mathrm{off}_0} - k_{\mathrm{cat}_0} & 0 \\ 0 & 0 & l_{\mathrm{on}_0} \end{bmatrix}.$$

In this case, $D = -k_{\mathrm{on}_0} k_{\mathrm{cat}_0} l_{\mathrm{on}_0} \neq 0$, as we wanted.

For the $n > 1$ case, we suppose now that the $D \neq 0$ result is valid for G_{n-1}, the network of the $(n-1)$-site phosphorylation system. In order to visualize the calculations, we will reorder the rows and columns of Σ_n'', placing $C(1)$, $C(n+2)$, and $C(2n+3)$ as the leftmost columns, and $R(2) + R(2n+3)$, $R(n+2)$, and $R(3n+3)$ as the uppermost rows. We notice that this ordering does not alter the sign of the determinants, hence we can write

$$D \;=\; \det\left(\left[\begin{array}{ccc|c} 0 & k_{\mathrm{cat}_0} & -l_{\mathrm{on}_0} & \cdots \\ k_{\mathrm{on}_0} & -k_{\mathrm{off}_0} - k_{\mathrm{cat}_0} & 0 & \mathbf{0} \\ 0 & 0 & l_{\mathrm{on}_0} & \mathbf{0} \\ \hline \mathbf{0} & \mathbf{0} & \mathbf{0} & \widetilde{D} \end{array}\right]\right) \;=\; -\,k_{\mathrm{on}_0} k_{\mathrm{cat}_0} l_{\mathrm{on}_0} \det(\widetilde{D})\,, \quad (4.31)$$

where $\widetilde{D}$ is a $(3n-3)\times(3n-3)$-submatrix of Σ''_n. This matrix $\widetilde{D}$ does not include either $C(1), C(n+2), C(2n+3)$, nor the first $(n+1)$-st or $(2n+1)$-st rows of Σ''_n. We next will see how the matrix $\widetilde{D}$ can be interpreted as the $3(n-1)\times 3(n-1)$-matrix Σ''_{n-1}, the corresponding matrix of the smaller network G_{n-1}. This interpretation will allow us to conclude by the inductive hypothesis that $D \neq 0$ in the positive orthant.

For the purpose of interpreting this submatrix of Σ''_n as the matrix of G_{n-1}, it is important to note that the deletion of $C(1), C(n+2)$, and $C(2n+3)$ from Σ''_n is equivalent to calculating Σ''_n after having deleted these columns from $\mathcal{L}(G_n)$ before calculating Σ_n. In turn, it is also equivalent to having deleted all the reactions that begin at the first, $(n+2)$-nd and $(2n+3)$-rd complexes of the network. Once we have additionally deleted the first, $(n+1)$-st, and $(2n+1)$-st rows (i.e. $R(2)+R(2n+3)$, $R(n+2)$, and $R(3n+3)$), we obtain a new submatrix of Σ_n whose entries we can rename as follows:

$$k_{\mathrm{on_j}} =: k'_{\mathrm{on_{j-1}}},\ k_{\mathrm{off_j}} =: k'_{\mathrm{off_{j-1}}},\ k_{\mathrm{cat_j}} =: k'_{\mathrm{cat_{j-1}}},\ l_{\mathrm{on_j}} =: l'_{\mathrm{on_{j-1}}},\ l_{\mathrm{off_j}} =: l'_{\mathrm{off_{j-1}}},\ l_{\mathrm{cat_j}} =: l'_{\mathrm{cat_{j-1}}}\ .$$

In fact, this new matrix is the corresponding complex-to-species rate matrix Σ'_{n-1} for the network G_{n-1}, with corresponding rate constants indicated by primes. We can also establish a correspondence between the nodes of the two networks: letting j' denote the j-th node of G_{n-1}, then j' corresponds to the following node of G_n:

$$j' \text{ corresponds to } \begin{cases} j+1 & \text{if } 1 \le j' \le n \quad (\text{complexes } S_0+E,\dots,S_{n-1}+E \text{ in } G_{n-1}) \\ j+2 & \text{if } n+1 \le j' \le 2n \quad (\text{complexes } ES_0,\dots,ES_{n-2} \text{ in } G_{n-1}) \\ j+3 & \text{if } 2n+1 \le j' \le 3n-1 \ (\text{complexes } S_0+F,\dots,S_{n-1}+F \text{ in } G_{n-1}) \\ j+4 & \text{if } 3n \le j' \le 4n-2 \quad (\text{complexes } FS_0,\dots,FS_{n-1} \text{ in } G_{n-1})\ . \end{cases}$$

From this correspondence, it follows that $\det(\widetilde{D})$ equals $\det(\Sigma''_{n-1})$, which is nonzero by inductive hypothesis, and therefore $D \neq 0$, which we wanted to prove.

We now complete the proof by verifying the following claim: the polynomial functions D_j, D_{n+j+1}, D_{2n+j+2} never vanish, and they all have the same constant sign as that of D on $\mathbb{R}^{6n}_{>0}$ (for $1 \le j \le n$).

We first prove this claim for the case $j=1$. We again reorder the entries of the matrices as described above, and as this ordering does not alter the sign of the determinants, we can write:

$$\begin{aligned} D_1 &= -\det\left(\left[\begin{array}{ccc|c} l_{\mathrm{off}_0} & k_{\mathrm{cat}_0} & -l_{\mathrm{on}_0} & \cdots \\ 0 & -k_{\mathrm{off}_0}-k_{\mathrm{cat}_0} & 0 & \mathbf{0} \\ -l_{\mathrm{cat}_0}-l_{\mathrm{off}_0} & 0 & l_{\mathrm{on}_0} & \mathbf{0} \\ \hline \mathbf{0} & \mathbf{0} & \mathbf{0} & \widetilde{D} \end{array}\right]\right) \\ &= -(k_{\mathrm{off}_0}+k_{\mathrm{cat}_0})l_{\mathrm{on}_0}l_{\mathrm{cat}_0}\det(\widetilde{D})\ , \end{aligned}$$

$$\begin{aligned} D_{n+2} &= -\det\left(\left[\begin{array}{ccc|c} 0 & l_{\mathrm{off}_0} & -l_{\mathrm{on}_0} & \cdots \\ k_{\mathrm{on}_0} & 0 & 0 & \mathbf{0} \\ 0 & -l_{\mathrm{cat}_0}-l_{\mathrm{off}_0} & l_{\mathrm{on}_0} & \mathbf{0} \\ \hline \mathbf{0} & \mathbf{0} & \mathbf{0} & \widetilde{D} \end{array}\right]\right) \\ &= -k_{\mathrm{on}_0}l_{\mathrm{on}_0}l_{\mathrm{cat}_0}\det(\widetilde{D})\ , \end{aligned}$$

$$\begin{aligned} D_{2n+3} &= -\det\left(\left[\begin{array}{ccc|c} 0 & k_{\mathrm{cat}_0} & l_{\mathrm{off}_0} & \cdots \\ k_{\mathrm{on}_0} & -k_{\mathrm{off}_0}-k_{\mathrm{cat}_0} & 0 & \mathbf{0} \\ 0 & 0 & -l_{\mathrm{cat}_0}-l_{\mathrm{off}_0} & \mathbf{0} \\ \hline \mathbf{0} & \mathbf{0} & \mathbf{0} & \widetilde{D} \end{array}\right]\right) \\ &= -k_{\mathrm{on}_0}k_{\mathrm{cat}_0}(l_{\mathrm{cat}_0}+l_{\mathrm{off}_0})\det(\widetilde{D})\,, \end{aligned}$$

where $\widetilde{D}$ is the same matrix we described in equation (4.31). That is, $\widetilde{D} = \Sigma''_{n-1}$. As we already know that $D \neq 0$, we deduce that $\det(\widetilde{D}) \neq 0$. By examining equation (4.31) and the display above, we conclude that the claim is true for $j = 1$.

For the $j > 1$ case, we will prove our claim by induction on n. The base case is $n = 2$ (as $j > 1$ is not possible when $n = 1$). In this case, the functions of interest are

$$\begin{aligned} D &= k_{\mathrm{on}_0}k_{\mathrm{cat}_0}l_{\mathrm{on}_0}k_{\mathrm{on}_1}k_{\mathrm{cat}_1}l_{\mathrm{on}_1}, & D_2 &= k_{\mathrm{on}_0}k_{\mathrm{cat}_0}l_{\mathrm{on}_0}(k_{\mathrm{off}_1}+k_{\mathrm{cat}_1})l_{\mathrm{on}_1}l_{\mathrm{cat}_1}, \\ D_5 &= k_{\mathrm{on}_0}k_{\mathrm{cat}_0}l_{\mathrm{on}_0}k_{\mathrm{on}_1}l_{\mathrm{on}_1}l_{\mathrm{cat}_1}, & D_8 &= k_{\mathrm{on}_0}k_{\mathrm{cat}_0}l_{\mathrm{on}_0}k_{\mathrm{on}_1}k_{\mathrm{cat}_1}(l_{\mathrm{cat}_1}+l_{\mathrm{off}_1}), \end{aligned}$$

all of which can be seen to be positive functions on $\mathbb{R}^{12}_{>0}$. Hence our claim holds for $n = 2$.

We now assume that the claim is true for G_{n-1}. As we did above, we view G_{n-1} as a subgraph of G_n, and if we call $D'_{\ell(j')}$ the corresponding determinant of the $(n-1)$-site system (for $\ell(j') = j',\ (n-1)+j'+1,\ 2(n-1)+j'+2,$ for $1 \leq j' \leq n-1$), then we have:

$$\begin{aligned} D_{\ell(j)} &= (-1)^{(n+1)+1}k_{\mathrm{on}_0}(-1)^{1+n}k_{\mathrm{cat}_0}(-1)^{(2n-1)+(2n-1)}l_{\mathrm{on}_0}D'_{\ell(j')} = \\ &= -k_{\mathrm{on}_0}k_{\mathrm{cat}_0}l_{\mathrm{on}_0}D'_{\ell(j')}\,, \end{aligned} \tag{4.32}$$

for $\ell(j') = j',\ (n-1)+j'+1,\ 2(n-1)+j'+2$, where $1 \leq j' \leq n-1$. By the inductive hypothesis, the claim holds for the $D'_{\ell(j')}$, so by equation (4.32), the claim holds for the $D_{\ell(j)}$ as well. This completes the proof. □

We now take care of the zero entries of the vectors b^j defined in (4.30). We start by defining $D_{u\leftrightarrow v}$ as minus the determinant of the matrix obtained by replacing column $C(u)$ by $C(v)$ in Σ''_n, for $1 \leq u \leq 3n+2$ such that $u \neq n+1$, $u \neq 2n+2$, and $3n+3 \leq v \leq 4n+2$:

$$D_{u\leftrightarrow v} := -\det\left(\left[C(1)|\ldots|\overset{u}{\overset{\downarrow}{C(v)}}|\ldots|C(3n+2)\right]\right)\,. \tag{4.33}$$

We will deduce from the following lemma that $D_{u\leftrightarrow v}$ is equal to zero unless $u = j,\ n+j+1,$ or $2n+j+2$ and $v = 3n+j+2$, for $1 \leq j \leq n$.

Lemma 4.3.1. *Fix $j \in \{1, 2, \ldots, n\}$ and call $\widehat{\Sigma'_n}$, the submatrix of Σ'_n obtained by deleting any two columns indexed by two elements of I_j. It holds that any $3n \times 3n$-minor of $\widehat{\Sigma'_n}$ is equal to zero.*

Proof. We will keep the notation $R(i)$ from the proof of Proposition 4.3.1. We now prove the lemma first for $j = 1$, then $j = n$, and then finally for $1 < j < n$.

For the case $j = 1$, we focus on the reactions $1 \rightleftarrows n+2 \to 2$, $2n+3 \rightleftarrows 3n+3 \to 2n+2$, and $3n+4 \to 2n+3$. If we delete $C(1)$ and $C(n+2)$, or $C(2n+3)$ and $C(3n+3)$, then the

rows of $\widehat{\Sigma'_n}$ corresponding to $R(n+2)$ or $R(3n+3)$ will be equal to zero and the minor will be zero.

If we delete $C(1)$ and $C(2n+3)$ (or $C(3n+3)$), or we delete $C(n+2)$ and $C(2n+3)$ (or $C(3n+3)$), the rows corresponding to $R(n+2)$ and $R(3n+3)$ will have only one entry different from zero and the determinant will be obviously zero if the column corresponding to any of this entries is not considered, or it will be the product of two constants and a $(3n-2)\times(3n-2)$-minor that does not include the columns $C(1), C(n+2), C(2n+3), C(3n+3)$ nor the rows $R(n+2), R(3n+3)$.

It is important to notice that the columns of $\mathcal{L}(G_n)$ carry the information of the reactions whose source (educt) is the corresponding complex, therefore, $C(\ell)$ carries the information of the reaction whose source is the ℓ-th complex. As the only complexes that generate reactions whose product is the $(n+2)$-nd or $(3n+3)$-rd complexes are the first and $(2n+2)$ complexes, respectively, it follows that the columns that are being considered in this new $(3n-2)\times(3n-2)$-minor carry the information of reactions that do not end in either the $(n+2)$-nd or the $(3n+3)$-rd complexes. Hence the sum of the rows in this new submatrix, and therefore the minor as well, is equal to zero.

For $j=n$, the analysis is similar.

For $1<j<n$ we focus on the reactions $j \rightleftarrows n+j+1 \to j+1$ and $2n+j+2 \rightleftarrows 3n+j+2 \to 2n+j+1$. If we delete $C(j)$ and $C(n+j+1)$, or $C(2n+j+2)$ and $C(3n+j+2)$, then the rows of $\widehat{\Sigma'_n}$ corresponding to $R(n+j+1)$ or $R(3n+j+2)$ will be equal to zero and the minor will be zero.

If we delete $C(j)$ and $C(2n+j+2)$ (or $C(3n+j+2)$), or we delete $C(n+j+1)$ and $C(2n+j+2)$ (or $C(3n+j+2)$), the rows corresponding to $R(n+j+1)$ and $R(3n+j+2)$ will have only one entry different from zero, and thus the determinant will be obviously zero if the column corresponding to any of these entries is not considered. Otherwise it will be the product of two nonzero rate constants and a $(3n-2)\times(3n-2)$-minor that does not include any of $C(j), C(n+j+1), C(2n+j+2), C(3n+j+2)$ nor any of $R(n+j+1), R(3n+j+2)$.

But deleting these columns is equivalent to not considering the reactions whose sources (educts) are the complexes $j, n+j+1, 2n+j+2$, or $3n+j+2$. This disconnects the graph into four linkage classes, so this new graph gives a Laplacian matrix formed by four blocks. The rows of Σ_n that we are considering in Σ'_n come from adding rows of the first and third blocks of $\mathcal{L}(G_n)$, or the second and fourth ones; and the last rows of Σ_n, which correspond to intermediary species, clearly belong to only one of the blocks. Then, this new submatrix of $\widehat{\Sigma'_n}$ can be reordered into a two-block matrix, for which the sums of the rows in each block are zero. Hence, the matrix obtained from $\widehat{\Sigma'_n}$ without these four columns and two rows has rank at most $3n-3$ and therefore any $(3n-2)\times(3n-2)$-minor will be zero. □

We are now ready to prove Theorem 4.3.1.

Proof of Theorem 4.3.1. Due to Lemma 4.3.1, for a $3n\times 3n$-minor of Σ'_n to be different from zero, we must obtain these $3n$ columns by choosing three from each group indexed by I_j, for $1\le j\le n$. In fact, any $3n\times 3n$-minor of Σ'_n that includes three columns from each group of four indexed by I_j, for $1\le j\le n$, is always nonzero due to Proposition 4.3.1.

We can now solve system (4.26) by applying Cramer's rule. Recall the notation from (4.33):

$$\begin{bmatrix} v_1 \\ \vdots \\ v_{3n} \end{bmatrix} = \frac{-1}{D} \begin{bmatrix} D_{1\leftrightarrow 3n+3} & \dots & D_{1\leftrightarrow 4n+2} \\ \vdots & & \vdots \\ D_{3n+2\leftrightarrow 3n+3} & \dots & D_{3n+2\leftrightarrow 4n+2} \end{bmatrix} \begin{bmatrix} v_{3n+1} \\ \vdots \\ v_{4n} \end{bmatrix}.$$

By Lemma 4.3.1, we already know that in the $3n \times n$-matrix in the right-hand side above, the only nonzero entries are D_j, D_{n+j+1}, and D_{2n+j+2}. This gives us a description of $\ker(\Sigma_n)$, which has a basis of the following form:

$$\{e_{n+1}, e_{2n+2}\} \cup \{b^1, b^2, \dots, b^n\}$$

for b^j as in (4.30).

This proves that the n-site phosphorylation system satisfies Condition 4.2.1 for the partition $I_1, I_2, \dots, I_{n+2}$ and the basis of $\ker(\Sigma_n)$, $\{b^1, b^2, \dots, b^n, e_{n+1}, e_{2n+2}\}$, described above.

We now prove that the n-site phosphorylation system additionally satisfies Conditions 4.2.2 and 4.2.3. Condition 4.2.2 is satisfied immediately by Proposition 4.3.1. With respect to Condition 4.2.3, we notice that the subspace spanned by the columns of the matrix Δ has the following basis:

$$\{e_{2n+j+1} - e_j - e_{3n+2},\ e_{2n+j+1} - e_{n+j+1},\ e_{2n+j+1} - e_{j+1} - e_{3n+3} \mid 1 \leq j \leq n\}. \quad (4.34)$$

Therefore, the dimension of the image of Δ is $3n$, so $\ker(\Delta) = 0$. Hence, equation (4.8) is trivially satisfied, as noted in Remark 4.2.4.

Then, by Theorem 4.2.2, it is immediate that the n-site phosphorylation system has toric steady states that are positive and real. Finally, for a parametrization of the steady state locus, let us consider the following matrix:

$$A = \left[\begin{array}{ccccc|cccc|cccc|cc} 0 & 1 & 2 & \dots & n & 1 & 2 & \dots & n & 1 & 2 & \dots & n & 1 & 0 \\ 0 & 0 & 0 & \dots & 0 & 1 & 1 & \dots & 1 & 1 & 1 & \dots & 1 & 1 & 1 \\ 1 & 1 & 1 & \dots & 1 & 1 & 1 & \dots & 1 & 1 & 1 & \dots & 1 & 0 & 0 \end{array}\right] \in \mathbb{R}^{3\times(3n+3)}.$$

It has maximal rank, and its kernel equals the span of all the differences $y_{j_2} - y_{j_1}$, for $j_1, j_2 \in I_j$, where $1 \leq j \leq n+2$, shown in (4.34). After applying Theorem 4.2.3, we are left to see that the point $\tilde{x}$ defined in the statement of the present theorem is a positive steady state of the system. But it is easy to check that $\tilde{x}$ is a positive steady state by applying Theorem 4.2.1 to the following binomials:
$Dx_j x_{3n+2} - D_j x_{2n+j+1}$, $Dx_{n+j+1} - D_{n+j+1} x_{2n+j+1}$, $Dx_{j+1} x_{3n+3} - D_{2n+j+2} x_{2n+j+1}$, for $1 \leq j \leq n$.

This completes the proof. □

4.4 Multistationarity for systems with toric steady states

In this section we focus on the capacity of a chemical reaction system with toric steady states to exhibit multiple steady states. Following prior work of Conradi *et al.* [24] and Holstein [78], we make use of an alternative notation for reaction systems to obtain a characterization of

steady states (Proposition 4.4.1). This result is used to prove a criterion for the existence of multistationarity for systems with toric steady states that satisfy Conditions 4.2.1, 4.2.2, and 4.2.3 (Theorem 4.4.1). At the end of this section, we make the connection to a related criterion of Feinberg.

Often a chemical reaction system has a continuum of steady states, as long as one steady state exists. However, as defined earlier (and as it is in Chemical Engineering), multistationarity refers to the existence of multiple steady states *within one and the same* stoichiometric compatibility class. In general one is interested in situations where the steady state locus intersects a stoichiometric compatibility class in a finite number of points [50]. In Computational Biology one is sometimes interested in situations where the steady state locus intersects an affine subspace distinct from translates of the stoichiometric subspace $\mathcal{S}$ [53]. Here we define multistationarity with respect to a linear subspace in the following way. Consider a matrix $Z \in \mathbb{R}^{s\times q}$, where q is a positive integer. We say that the chemical reaction system $\dot{x} = \Sigma\cdot\Psi(x)$ *exhibits multistationarity with respect to the linear subspace* $\ker(Z^\dagger)$ if and only if there exist at least two distinct positive steady state vectors x^1, $x^2 \in \mathbb{R}^s_{>0}$ such that their difference lies in $\ker(Z^\dagger)$; in other words the following equations must hold:

$$\Sigma\cdot\Psi(x^1) \;=\; 0 \tag{4.35a}$$

$$\Sigma\cdot\Psi(x^2) \;=\; 0 \tag{4.35b}$$

$$Z^\dagger\, x^1 \;=\; Z^\dagger\, x^2\;. \tag{4.35c}$$

Note that if the columns of Z form a basis for $\mathcal{S}^\perp$, one recovers the usual definition of multistationarity given before. In this case, Equation (4.35c) states that the steady states x^1 and x^2 belong to the same stoichiometric compatibility class, and we simply speak of multistationarity, omitting the linear subspace we are referring to.

4.4.1 Second representation of a chemical reaction system

We now introduce a second representation of the differential equations that govern a chemical reaction system (2.10); this will prove useful for the characterization of steady states (Proposition 4.4.1) and for establishing the capacity of a chemical reaction network for multistationarity. Letting r denote the number of reactions of a chemical reaction network G, we fix an ordering of these r reactions and define the *incidence matrix* $C_G \in \{-1, 0, 1\}^{m\times r}$ of the network to be the matrix whose i-th column has a 1 in the row corresponding to the product complex of the i-th reaction and a -1 for the educt (reactant) complex. Then the $(s \times r)$-matrix product

$$\Gamma \;:=\; Y\, C_G \tag{4.36}$$

is known as the *stoichiometric matrix*. Thus, the i-th column of Γ is the reaction vector corresponding to reaction i. Next we define the *educt-complex matrix*

$$\mathcal{Y} \;:=\; [\tilde{y}_1,\, \tilde{y}_2,\, \ldots,\, \tilde{y}_r]\;, \tag{4.37}$$

where the column $\tilde{y}_i$ of $\mathcal{Y}$ is defined as the vector of the educt complex of the i-th reaction. Now we can define the vector of educt complex monomials

$$\phi(x) \;:=\; \left(x^{\tilde{y}_1},\, x^{\tilde{y}_2},\, \ldots,\, x^{\tilde{y}_r}\right)^\dagger\;. \tag{4.38}$$

We also define $k \in \mathbb{R}^r_{>0}$ to be the vector of reaction rate constants: k_i is the rate constant of the i-th reaction (that is, $k_i \;=\; \kappa_{i'j'}$ where the i-th reaction is from the complex $x^{y_{i'}}$ to $x^{y_{j'}}$). We now give a second formulation for a chemical reaction system (2.10) (cf. [55]):

$$\dot{x} \;=\; \Gamma \,\mathrm{diag}(k)\,\phi(x)\;. \tag{4.39}$$

Both formulations of a chemical reaction system given in equations (2.10) and (4.39) lead to the same system of ODEs and hence are equivalent. This can be made explicit by way of the *doubling matrix* D of dimension $m \times r$ which relates $\mathcal{Y}$ and Y via $\mathcal{Y} \;=\; Y\,D$. Here the i-th column vector of D is defined as the unit vector e_j of $\mathbb{R}^m$ such that y_j is the educt (reactant) complex vector of the i-th reaction. From

$$\dot{x} \;=\; \Gamma\,\mathrm{diag}(k)\,\phi(x) \;=\; Y\,C_G\,\mathrm{diag}(k)\,D^\dagger\,\Psi(x) \;=\; \Sigma\Psi(x)\;,$$

it follows that $\phi(x) \;=\; D^\dagger\,\Psi(x)$ and $\mathcal{L}(G_n)^t \;=\; C_G\,\mathrm{diag}(k)\,D^\dagger$.

Example 4.4.1. *For the 1-site phosphorylation network (2.11), one obtains the matrices*

$$C_G \;=\; \begin{bmatrix} -1 & 1 & 0 & 0 & 0 & 0 \\ 1 & -1 & -1 & 0 & 0 & 0 \\ 0 & 0 & 1 & 0 & 0 & 0 \\ 0 & 0 & 0 & -1 & 1 & 0 \\ 0 & 0 & 0 & 1 & -1 & -1 \\ 0 & 0 & 0 & 0 & 0 & 1 \end{bmatrix}, \quad D = \begin{bmatrix} 1 & 0 & 0 & 0 & 0 & 0 \\ 0 & 0 & 0 & 0 & 0 & 0 \\ 0 & 1 & 1 & 0 & 0 & 0 \\ 0 & 0 & 0 & 0 & 0 & 0 \\ 0 & 0 & 0 & 1 & 0 & 0 \\ 0 & 0 & 0 & 0 & 1 & 1 \end{bmatrix},$$

$$\mathcal{Y} = \left[y_1^\dagger,\, y_3^\dagger,\, y_3^\dagger,\, y_5^\dagger,\, y_6^\dagger,\, y_6^\dagger\right] \;=\; \begin{bmatrix} 1 & 0 & 0 & 0 & 0 & 0 \\ 0 & 0 & 0 & 1 & 0 & 0 \\ 0 & 1 & 1 & 0 & 0 & 0 \\ 0 & 0 & 0 & 0 & 1 & 1 \\ 1 & 0 & 0 & 0 & 0 & 0 \\ 0 & 0 & 0 & 1 & 0 & 0 \end{bmatrix},$$

and the monomial vector $\phi(x) \;=\; (x_1\,x_5,\, x_3,\, x_3,\, x_2\,x_6,\, x_4,\, x_4)^\dagger$.

It follows from the differential equations (4.39) that a positive concentration vector $x \in \mathbb{R}^s_{>0}$ is a steady state for the chemical reaction system defined by the positive reaction rate constant vector k if and only if

$$\mathrm{diag}(k)\,\phi(x) \;\in\; \ker(\Gamma) \cap \mathbb{R}^r_{>0}\;.$$

We now recognize that the set $\ker(\Gamma) \cap \mathbb{R}^r_{>0}$, if nonempty, is the relative interior of the pointed polyhedral cone $\ker(\Gamma) \cap \mathbb{R}^r_{\geq 0}$. To utilize this cone, we collect a finite set of *generators* (also called "extreme rays") of the cone $\ker(\Gamma) \cap \mathbb{R}^r_{\geq 0}$ as columns of a non-negative matrix M. Up to scalar multiplication, generators of a cone are unique and form a finite set; as the cone of interest arises as the intersection of an orthant with a linear subspace, the generators are the vectors of the cone with minimal support with respect to inclusion. (Background on polyhedral cones can be found in the textbook of Rockafeller [129].) Letting p denote the number of generators of the cone, we can use M to express the condition for a positive vector $x \in \mathbb{R}^s_{>0}$ to be a steady state of the chemical reaction system in the following way:

$$\mathrm{diag}(k)\,\phi(x) \;=\; M\,\lambda\;,\; \text{for some } \lambda \in \mathbb{R}^p_{\geq 0} \text{ with } M\,\lambda \in \mathbb{R}^r_{>0}\;. \tag{4.40}$$

Note that this proves the following result which appears in [24]:

Proposition 4.4.1 (Characterization of steady states of chemical reaction systems)**.** *For a chemical reaction network G, let M denote a corresponding generator matrix as defined above. Then a positive vector $x \in \mathbb{R}^s_{>0}$ is a steady state for the chemical reaction system defined by reaction rate vector $k \in \mathbb{R}^r_{>0}$, if and only if there exists a vector $\lambda \in \mathbb{R}^p_{\geq 0}$ such that*

$$k \;=\; \operatorname{diag}(\phi(x))^{-1}\, M\,\lambda \;\; \textit{and} \;\; M\,\lambda \in \mathbb{R}^r_{>0}\,. \tag{4.41}$$

We now note that outside of a degenerate case, any positive concentration vector can be a steady state for appropriately chosen rate constants k.

Remark 4.4.1. *We now comment on the degenerate case of a network for which the set $\ker(\Gamma) \cap \mathbb{R}^r_{>0}$ is empty. First, this case is equivalent to either of the following three conditions: (i) there is no positive dependence among the reaction vectors $(y_j - y_i)$, (ii) the cone $\ker(\Gamma) \cap \mathbb{R}^r_{\geq 0}$ is contained in a coordinate hyperplane, and (iii) the generator matrix M has at least one zero row. Now, in this degenerate case, it is clear that for any choice of reaction rate constants, the chemical reaction system has no positive steady states. This is because if $x^* \in \mathbb{R}^s_{>0}$ is a steady state for the system with reaction rate constants κ_{ij}, then the numbers $\alpha_{ij} := \kappa_{ij} \cdot (x^*)^{y_i}$ witness to the positive dependence among the reaction vectors $(y_j - y_i)$'s.*

Outside of this degenerate case, it follows from Proposition 4.4.1 that there exists a vector of reaction rate constants k for which the resulting chemical reaction system has a positive steady state. Moreover, in this case any positive vector x can be a steady state, by choosing k as in equation (4.41) for some valid choice of $\lambda \in \mathbb{R}^p_{\geq 0}$.

Using our new notation, we return to the question of existence of steady states.

Remark 4.4.2. *Recall the content of Corollary 4.2.1: for a chemical reaction network for which a single partition works to satisfy Condition 4.2.1 for all choices of positive rate constants, the set of rate constant vectors k that yield systems with positive steady states is the semialgebraic set of $\mathbb{R}^r_{>0}$ defined by Conditions 4.2.2 and 4.2.3. We now note that Proposition 4.4.1 implies that this set of rate constant vectors is the image of the following polynomial map:*

$$\begin{aligned} \beta: \quad \mathbb{R}^s_{>0} \times \Omega \;&\to\; \mathbb{R}^r_{>0} \\ (x, \lambda) \;&\mapsto\; \operatorname{diag}(\phi(x))^{-1}\, M\,\lambda\,, \end{aligned}$$

*where $\Omega \;:=\; \{\lambda \in \mathbb{R}^p_{\geq 0} \mid M\lambda \in \mathbb{R}^r_{>0}\}$. In the case that Condition 4.2.1 holds and Condition 4.2.3 is **trivially** satisfied (i.e. Δ has full row rank), the image of β is cut out by the inequalities defined by Condition 4.2.2.*

4.4.2 Main result on multistationarity

We now make use of Proposition 4.4.1 to examine which chemical reaction systems with toric steady states exhibit multistationarity. We first note that in the setting of Section 4.2, the set of differences $\ln x^1 - \ln x^2$, where x^1 and x^2 are positive steady states for the same system, form a linear subspace. As before, the notation "$\ln x$" for a vector $x \in \mathbb{R}^s_{>0}$ denotes the vector $(\ln x_1, \ln x_2, \ldots, \ln x_s) \in \mathbb{R}^s$; similarly we will make use of the notation "e^x" to denote component-wise exponentiation.

Our next theorem, the main result of this section, is a consequence of [24, Lemma 1]. It states that a network that satisfies Condition 4.2.1 has the capacity for multistationarity if and only if two subspaces, namely $\mathrm{im}(A^\dagger)$ and $\mathcal{S}$, both intersect non-trivially some (possibly lower-dimensional) orthant $\{x \in \mathbb{R}^s \mid \mathrm{sign}(x) = \omega\}$ defined by a sign vector $\omega \in \{-, 0, +\}^s$. We remark that this is a matroidal condition. Related ideas appear in work of Feinberg [51], and details on the connection between our work and Feinberg's appears at the end of this section.

Theorem 4.4.1 (Multistationarity for networks with toric steady states)**.** *Fix a chemical reaction network G with s species and m complexes, and let $Z \in \mathbb{Z}^{s\times q}$ be an integer matrix, for some positive integer q. Assume that the cone $\ker(\Gamma) \cap \mathbb{R}^r_{\geq 0}$ is not contained in any coordinate hyperplane. Assume moreover that there exists a partition $I_1, I_2, \ldots, I_d$ of the m complexes of G such that Condition 4.2.1 is satisfied for all rate constants.*

Recall the matrix A for this partition from the proof of Theorem 4.2.3. Then there exists a reaction rate constant vector such that the resulting chemical reaction system exhibits multistationarity with respect to the linear subspace $\ker(Z^\dagger)$ if and only if there exists an orthant of $\mathbb{R}^s$ that both subspaces $\mathrm{im}(A^\dagger)$ and $\ker\left(Z^\dagger\right)$ intersect nontrivially. More precisely, given nonzero vectors $\alpha \in \mathrm{im}(A^\dagger)$ and $\sigma \in \ker\left(Z^\dagger\right)$ with

$$\mathrm{sign}(\alpha) \;=\; \mathrm{sign}(\sigma)\,, \tag{4.42}$$

then two steady states x^1 and x^2 and a reaction rate constant vector k that witness multistationarity (that is, that satisfy equations (4.35a)*,* (4.35b)*, and* (4.35c)*) arise in the following way:*

$$\left(x^1_i\right)_{i=1,\ldots,s} \;=\; \begin{cases} \frac{\sigma_i}{e^{\alpha_i}-1}\text{, if } \alpha_i \neq 0 \\ \bar{x}_i > 0\text{, if } \alpha_i = 0\,, \end{cases} \tag{4.43}$$

where $\bar{x}_i$ denotes an arbitrary positive number, and

$$x^2 \;=\; \mathrm{diag}(e^\alpha)\, x^1 \tag{4.44}$$

$$k \;=\; \mathrm{diag}(\phi(x^1))^{-1}\, M\, \lambda\,, \tag{4.45}$$

for any non-negative vector $\lambda \in \mathbb{R}^p_{\geq 0}$ for which $M\lambda \in \mathbb{R}^r_{>0}$. Conversely, any witness to multistationarity with respect to $\ker\left(Z^\dagger\right)$ (given by some x^1, $x^2 \in \mathbb{R}^s_{>0}$, and $k \in \mathbb{R}^r_{>0}$) arises from equations (4.42)*,* (4.43)*,* (4.44)*, and* (4.45) *for some vectors $\alpha \in \mathrm{im}(A^\dagger)$ and $\sigma \in \ker\left(Z^\dagger\right)$ that have the same sign.*

Proof. Assume that there exist nonzero vectors $\alpha \in \mathrm{im}(A^\dagger)$ and $\sigma \in \ker\left(Z^\dagger\right)$ having the same sign. First note that the vectors x^1, x^2, and k defined by (4.43), (4.44), and (4.45), respectively, are positive because α and σ have the same sign and because the cone $\ker(\Gamma) \cap \mathbb{R}^r_{\geq 0}$ is not contained in a coordinate hyperplane. By Proposition 4.4.1, equation (4.45) implies that x^1 is a steady state of the system defined by k. We now claim that x^2 too is a steady state of the same system. This follows from Theorem 4.2.3 because the difference between $\ln x^1$ and $\ln x^2$ is in $\mathrm{im}(A^\dagger)$:

$$\ln x^1 - \ln x^2 \;=\; -\alpha \;\in\; \mathrm{im}(A^\dagger)\,.$$

Conversely, assume that vectors x^1, x^2, and k are a witness to multistationarity with respect to $\ker(Z^\dagger)$. Let us now construct appropriate vectors α and σ. By Theorem 4.2.3, the vector $\alpha := \ln x^2 - \ln x^1$ is in $\mathrm{im}(A^\dagger)$. Next, we define $\sigma \in \mathbb{R}^s$ by $\sigma_i = (e^{\alpha_i} - 1)x_i^1$ if $\alpha_i \neq 0$ and $\sigma_i = 0$ if $\alpha_i = 0$, so by construction, α and σ have the same sign. In addition, equations (4.43) and (4.44) easily follow for these values of α and σ. We also see that

$$-\sigma \;=\; x^1 - x^2 \;\in\; \ker(Z^\dagger)\;,$$

so $\sigma \in \ker(Z^\dagger)$. Finally, Proposition 4.4.1 implies that there exists a valid $\lambda \in \mathbb{R}^p_{\geq 0}$ that satisfies (4.45). □

Remark 4.4.3. *If a chemical reaction system defined by reaction rate constants k^* and a partition of its complexes satisfy Conditions 4.2.1, 4.2.2, and 4.2.3 (but not necessarily for other choices of rate constants), then the equations* (4.42)*,* (4.43)*,* (4.44)*, and* (4.45) *in Theorem 4.4.1 still characterize multistationarity. In other words, x^1 and x^2 are two steady states that demonstrate that the system defined by k^* has the capacity for multistationarity with respect to $\ker(Z^\dagger)$ if and only if there exist $\alpha \in \mathrm{im}(A^\dagger)$, $\sigma \in \ker(Z^\dagger)$, and $\lambda \in \mathbb{R}^p_{\geq 0}$ such that those four equations hold.*

Example 4.4.2 (Triangle network, continued)**.** *We return to the Triangle network analyzed in Examples 4.1.1 and 4.2.1. The stoichiometric subspace is*

$$\ker(\Sigma) \;=\; \mathcal{S} \;=\; \mathrm{span}\{(1,-1)\}\;.$$

In the toric setting (recall that this is when $\kappa_{31} = \kappa_{32}$), the partition for which the system satisfies Condition 4.2.1 is $\{1,2\},\{3\}$, so a matrix A for which

$$\ker(A) \;=\; \mathrm{span}\{y_2 - y_1\} \;=\; \mathrm{span}\{(2,-2)\}$$

is $A = [1\ 1]$. We can see that the subspaces $\ker(\mathcal{S})$ and $\mathrm{im}(A^\dagger) = \mathrm{span}\{(1,1)\}$ do not both intersect some orthant nontrivially. So Theorem 4.4.1 allows us to conclude that no system (for which $\kappa_{31} = \kappa_{32}$) arising from the Triangle network exhibits multistationarity.

Although the capacity of the Triangle network to exhibit multistationarity is easily determined directly, without the need to apply Theorem 4.4.1, it is more difficult in the case of the multisite phosphorylation system. Recall that we proved in Theorem 4.3.1 that any n-site phosphorylation system satisfies Condition 4.2.1 with the same partition (for fixed n). Hence, Theorem 4.4.1 can be used to compute the semialgebraic set of reaction rate constants k that give rise to multistationarity for the phosphorylation networks. This was performed by Conradi *et al.* (for the 2-site network) [24] and Holstein (for the general n-site network) [78]; multistationarity is possible only for $n \geq 2$. Results on the number of steady states of phosphorylation systems appeared in work of Wang and Sontag [170] and is the focus of a forthcoming work. [23].

4.4.3 Connection to related results on multistationarity

We now make the connection between our results on the capacity of a chemical reaction network to exhibit multistationarity and related results of Feinberg [51]. To state Feinberg's results, we must first give some definitions. Recall that a "linkage class" is a connected component of a network; a "terminal strong linkage class" is a maximal strongly connected subgraph

of a network in which there are no edges (reactions) from a complex in the subgraph to a complex outside the subgraph.

A *regular* network is a network for which (i) $\ker(\Gamma) \cap \mathbb{R}^r_{>0} \neq \emptyset$, (ii) each linkage class contains a unique terminal strong linkage class, and (iii) removing the reaction(s) between any two adjacent complexes in a terminal strong linkage class disconnects the corresponding linkage class. Recall from Remark 4.4.1 that condition (i) in this definition is simply the requirement that the reaction vectors $y_j - y_i$ are positively dependent, and that this condition is necessary for the existence of positive steady states.

We now can explain the relationship between Feinberg's result and ours. Feinberg examined regular deficiency-one networks, while we are concerned with networks for which there exists a partition that satisfies Condition 4.2.3 (for all rate constants). In these respective settings, both Theorem 4.1 and Corollary 4.1 of [51] and Theorem 4.4.1 in this chapter state that *a certain subset of $\mathbb{R}^s$ and the stoichiometric subspace both intersect the same orthant non-trivially if and only if the network has the capacity for multistationarity.* In the result of Feinberg, this set is a union of certain polyhedral cones, while in our case, this set is the image of $A^\dagger$. In both cases, this set consists of all vectors $\ln(x^*/x^{**})$, where x^* and x^{**} are steady states arising from the same rate constants. As an illustration, see Example 4.4.3 below.

Let us now explain how the two results are complementary. First, there are some networks for which only Feinberg's results apply. For example, consider any network for which the union of polyhedral cones obtained from Feinberg's results is not a linear space. Additionally, for some networks, only our results apply. As an example, the $n > 1$ multisite networks have deficiency greater than one. Finally, for some networks, both our results and Feinberg's apply, such as in the following example.

Example 4.4.3. *The 1-site phosphorylation network of Example 2.1.2 is regular and has deficiency one. In this case, both the image of $A^\dagger$ and Feinberg's union of cones are the subspace of $\mathbb{R}^6$ spanned by the three vectors $(e_1+e_2+e_3+e_4)$, $(e_2+e_3+e_4+e_5)$, and $(e_3+e_4+e_5+e_6)$. So in this instance, our Theorem 4.4.1 and Feinberg's Corollary 4.1 of [51] coincide.*

Finally we note that the proofs of both results make use of special structure of $\ker(\Sigma)$. In our case, we assume the existence of a basis with disjoint support. For Feinberg's results, there is a non-negative basis whose supports of the first L correspond exactly to the L terminal strong linkage classes, and the last basis vector is the all-ones vector (here L denotes the number of terminal strong linkage classes).

Chapter 5

How far is complex balancing from detailed balancing?

In this chapter we study the conditions in parameter space which ensure the existence of particularly well behaved dynamics in general (mass–action) kinetics chemical reaction systems and we compare from an algebraic perspective important classical notions.

Special cases of systems whose ideal of *positive* steady states is binomial are detailed and complex balanced systems. Throughout this chapter, and in particular in Theorem 5.1.1, we clarify the relation between the algebraic conditions that must be satisfied by the reaction constants in general mass–action kinetics systems for the existence of detailed or complex balanced equilibria. The main properties of these systems have been set by Horn, Jackson and Feinberg [45, 49, 50, 79–82]. These systems have remarkable dynamic properties and have a wide range of applications in chemistry and biology [31, 32, 60, 63–65, 112, 142, 146].

We plan to further apply this point of view to the study of biologically meaningful biochemical reaction networks, in particular those associated to enzymatic reactions as in [2,32,64,112], where we expect that tools from elimination theory in the framework of algebraic varieties (and in particular, toric varieties), together with results in algebraic combinatorics (as the Matrix-Tree Theorem), will contribute to generalize current approaches.

5.1 Setting and results

Here, we restate the precise definitions of detailed and complex balancing, and we show that a reversible Horn–Jackson general mass–action kinetics system satisfying Feinberg's circuit conditions is detailed balanced if and only if it is complex balanced. In other words, under formal balancing conditions for the cycles (of the underlying undirected graph) of the reaction graph, both notions coincide. We formulate this property in terms of the algebraic equations defining the corresponding varieties in rate constant space.

In order to illustrate some of the definitions and concepts along the chapter, we will recall Example 2.5.1, which represents a nonsequential multisite phosphorylation system with two

sites, under mass–action kinetics.

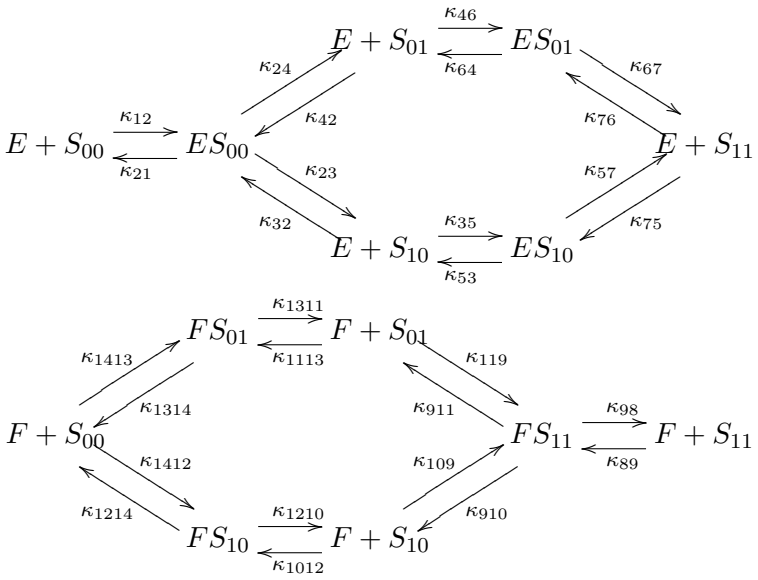

(5.1)

The four phosphoforms, S_{00}, S_{10}, S_{01}, S_{11}, are interconverted by the kinase E and the phosphatase F. There are other six *species* $ES_{00}, ES_{10}, ES_{01}, FS_{11}, FS_{10}, FS_{01}$.

Assuming mass–action kinetics, each reaction between two of the 14 *complexes* is annotated with the corresponding rate constant, indicated by a choice of numbering of the complexes. Although the rate constants κ_{32}, κ_{42}, κ_{75}, κ_{76}, κ_{109}, κ_{119}, κ_{1412}, κ_{1413}, are usually taken to be very small and so the corresponding reactions are omitted, we will not ignore them in this example because we are interested in special properties of the reaction constants in reversible networks.

In general, recalling Chapter 2, we will consider s species, with $x_1, x_2, \ldots, x_s$ representing their molar concentrations; a set of m complexes, and a numbered set $\mathscr{R}$ of r reactions between different complexes. The associated *chemical reaction network* is the finite directed graph $G = (V, \mathscr{R}, Y)$, whose vertices V are labeled by the complexes $y_1, \ldots, y_m$ and whose edges $\mathscr{R}$ correspond to the reactions. We record the complexes by an $s \times m$-matrix of non-negative integers $Y = (y_{ji})$, which contains these stoichiometric coefficients. For instance, in the reaction diagram (5.1), we will name the 12 concentrations as $x_1, \ldots, x_{12}$ according to the following order of the species: S_{00}, S_{10}, S_{01}, S_{11}, E, F, ES_{00}, FS_{11}, ES_{10}, FS_{10}, ES_{01}, FS_{01}. The columns of the stoichiometric matrix $Y \in \{0,1\}^{12\times 14}$ are ordered according to the numbering of the complexes which is reflected in the names of the rate constants in diagram (5.1). For example, $y_1 = e_1 + e_5$, where e_i denotes the i-th canonical basis vector in $\mathbb{R}^{12}$, and the corresponding concentrations will be denoted by x_1, x_5.

In this chapter, in order to simplify the notation, we will refer to reaction $(y_i, y_j) \in \mathscr{R}$ as $(i, j) \in \mathscr{R}$.

We assume there is a non-negative continuous real-valued rate function $\mathcal{K}_{ij}(\mathbf{x})$ for each reaction (i, j) in the network, with the property that $\mathcal{K}_{ij}(\mathbf{x}) = 0$ if and only if $x_k = 0$ for some k in the support of y_i (that is, $y_{ik} \neq 0$). The reaction network $(V, \mathscr{R}, Y)$ endowed with a kinetics is called a *chemical reaction system* and we record this information in the notation as $G = (V, \mathscr{R}, \mathcal{K}, Y)$. In a mass–action kinetics chemical reaction system, we simply have $\mathcal{K}_{ij}(\mathbf{x}) = \kappa_{ij}\mathbf{x}^{y_i}$, where $\kappa_{ij} \in \mathbb{R}_{>0}$ are the rate constants, and in this case the notations $G =$

$(V, \mathscr{R}, \kappa, Y)$ and $G = (V, \mathscr{R}, \mathcal{K}, Y)$ will refer to the same system.

The instantaneous rate of change of the concentrations x_k is given by:

$$\frac{dx_k}{dt} = \sum_{(i,j)\in\mathscr{R}} \mathcal{K}_{ij}(\mathbf{x})\,(y_{jk} - y_{ik})\,, \quad k = 1, \ldots, s. \tag{5.2}$$

In what follows, we will assume *general mass–action kinetics*. In this case, the differential equations (5.2) can be written in the following form. Let $\mathcal{L}(G)$ denote the negative of the transpose of *Laplacian* of G. Hence $\mathcal{L}(G)$ is the $m \times m$-matrix whose off-diagonal entries are the κ_{ij} and whose column sums are zero. We denote by $\Psi(\mathbf{x})$ the vector $\Psi(\mathbf{x}) = (\mathbf{x}^{y_1}, \mathbf{x}^{y_2}, \ldots, \mathbf{x}^{y_m})^\dagger$. For instance, in our example (5.1) we have

$\Psi(\mathbf{x}) = (x_5x_1, x_7, x_5x_2, x_5x_3, x_9, x_{11}, x_5x_4, x_6x_4, x_8, x_6x_2, x_6x_3, x_{10}, x_{12}, x_6x_1)^\dagger$.

Then, the dynamical mass–action kinetics system (5.2) equals:

$$\frac{d\mathbf{x}}{dt} = \left(\frac{dx_1}{dt}, \ldots, \frac{dx_s}{dt}\right)^\dagger = Y\mathcal{L}(G)\Psi(\mathbf{x}), \tag{5.3}$$

where $\mathbf{x}$ denotes the vector of species concentrations $(x_1(t), \ldots, x_s(t))^\dagger$.

Recall from Section 2.5 the definition of a complex balanced system.

Definition 5.1.1. *A* complex balanced *mass–action kinetics system is a dynamical system* (5.3) *for which the algebraic equations $\mathcal{L}(G)\Psi(\mathbf{x}) = 0$ admit a strictly positive solution $\mathbf{x}_0 \in \mathbb{R}^s_{>0}$. Such a solution $\mathbf{x}_0$ is a steady state of the system, i.e., the s coordinates of $Y\mathcal{L}(G)\Psi(\mathbf{x}_0)$ vanish.*

Remark 5.1.1. *Clearly, a mass–action kinetics system* (5.3) *being complex balanced depends on both the digraph G and the rate constants κ_{ij}. A main property of complex balanced systems is that* all *strictly positive steady states $\mathbf{x}$ satisfy $\mathcal{L}(G)\Psi(\mathbf{x}) = 0$. They are* quasi-thermostatic *[80], which in the terminology of [30] means that the positive steady state variety is* toric.

We will assume throughout the chapter that digraphs $G = (V, \mathscr{R}, Y)$ representing a chemical reaction network are *reversible*, i.e. if $(i, j) \in \mathscr{R}$, then $(j, i) \in \mathscr{R}$. We can thus identify G with the underlying undirected graph $\widetilde{G} = (V, \widetilde{\mathscr{R}}, Y)$, where $\widetilde{\mathscr{R}} = \{\{i, j\} : (i, j) \in \mathscr{R}\}$.

Definition 5.1.2. *A detailed balanced mass–action kinetics system is a dynamical system* (5.3) *for which the following algebraic equations admit a strictly positive solution $\mathbf{x}_0 \in \mathbb{R}^s_{>0}$:*

$$-\kappa_{ij}\mathbf{x}_0^{y_i} + \kappa_{ji}\mathbf{x}_0^{y_j} = 0, \quad \textit{for all} \quad \{i, j\} \in \widetilde{\mathscr{R}}. \tag{5.4}$$

As it is for complex balanced mass–action kinetics systems, the condition of being detailed balanced depends on the graph $\widetilde{G}$ and the constants κ_{ij}.

Note that $\mathcal{L}(G)$ decomposes as the sum of $m \times m$ matrices $\mathcal{L}(G)^{\{i,j\}}$ for each undirected edge $\{i, j\} \in \widetilde{\mathscr{R}}$ of the graph G, where in rows i, j and columns i, j the matrix $\mathcal{L}(G)^{\{i,j\}}$ equals

$$\begin{pmatrix} -\kappa_{ij} & \kappa_{ji} \\ \kappa_{ij} & -\kappa_{ji} \end{pmatrix},$$

and all other entries of the matrix $\mathcal{L}(G)^{\{i,j\}}$ are 0. Since the algebraic equation $-\kappa_{ij}\mathbf{x}_0^{y_i} + \kappa_{ji}\mathbf{x}_0^{y_j} = 0$ means that $\mathcal{L}(G)^{\{i,j\}}\Psi(\mathbf{x}_0) = 0$, we see that every detailed balanced mass–action

kinetics system is also complex balanced. The converse is not true in general. Again, a main property of a detailed balanced mass–action kinetics system is that *all* of its positive steady states $\mathbf{x}$ satisfy $-\kappa_{ij}\mathbf{x}^{y_i} + \kappa_{ji}\mathbf{x}^{y_j} = 0$ for every $\{i, j\} \in \widetilde{\mathscr{R}}$.

For instance, in our example (5.1), for *any* choice of first order rate constant κ_1 and second order rate constant κ_2 for which the value of κ_1 equals the value of κ_2 regardless of the corresponding units, the mass–action kinetics system with the following rate constants is complex balanced but not detailed balanced:

$$\begin{array}{l}
\kappa_{12} = \kappa_{46} = \kappa_{89} = \kappa_{1012} = \kappa_2 \\
\\
\kappa_{24} = \kappa_{53} = \kappa_{67} = \kappa_{910} = \kappa_{1214} = \kappa_{1311} = \kappa_1 \\
\\
\kappa_{32} = \kappa_{42} = \kappa_{75} = \kappa_{76} = \kappa_{109} = \kappa_{119} = \kappa_{1412} = \kappa_{1413} = \frac{1}{4}\kappa_2 \\
\\
\kappa_{35} = \kappa_{1113} = \frac{3}{4}\kappa_2,\ \kappa_{23} = \kappa_{57} = \kappa_{64} = \kappa_{911} = \kappa_{1314} = \frac{3}{4}\kappa_1,\ \kappa_{21} = \frac{23}{4}\kappa_1,\ \kappa_{98} = \frac{47}{4}\kappa_1, \\
\kappa_{1210} = \frac{69}{22}\kappa_1.
\end{array} \tag{5.5}$$

For any $\alpha \in \mathbb{R}_{>0}$, the real vector in $\mathbb{R}^{12}_{>0}$ of the values of the molar concentrations of the different species $\mathbf{x}_{0,\alpha} = \alpha\,(23, 17, 11, 47, 1, 2, 4, 8, 14, 11, 13, 16)$ is a positive steady state of the system for which $\mathcal{L}(G)\Psi(\mathbf{x}_{0,\alpha}) = 0$, and hence the system is complex balanced. On the other side, for this choice of rate constants the system is *not* detailed balanced since (5.4) does not hold, for instance, for both $i_1 = 1,\ j_1 = 2$ and $i_2 = 10,\ j_2 = 12$ simultaneously that is, for the pairs of reactions

$$E + S_{00} \underset{\frac{23}{4}\kappa_1}{\overset{\kappa_2}{\rightleftarrows}} ES_{00}\,, \qquad FS_{10} \underset{\kappa_2}{\overset{\frac{69}{22}\kappa_1}{\rightleftarrows}} F + S_{10}.$$

We now recall *Feinberg's circuit conditions* [49]. They correspond to linear relations which only depend on the structure of the reaction graph and not on the particular complexes. For every cycle $\widetilde{C}$ in $\widetilde{G}$, we will choose one direction and define C^+ as the cycle in G in that direction. C^- will be the cycle in the opposite direction. Although the directions are arbitrarily chosen, we will not worry about that since we will only need to distinguish between the two of them.

Definition 5.1.3. *A formally balanced mass–action kinetics system is a dynamical system* (5.3) *for which the following circuit condition holds for every cycle $\widetilde{C}$ of $\widetilde{G}$:*

$$\prod_{(i,j)\ in\ C^+} \kappa_{ij} = \prod_{(j,i)\ in\ C^-} \kappa_{ji}. \tag{5.6}$$

We will talk about formally balanced systems, although this definition can be applied to any digraph whose edges are reversible and labeled by constants κ_{ij}.

In our example (5.1), we can consider the cycle $\widetilde{C}$:

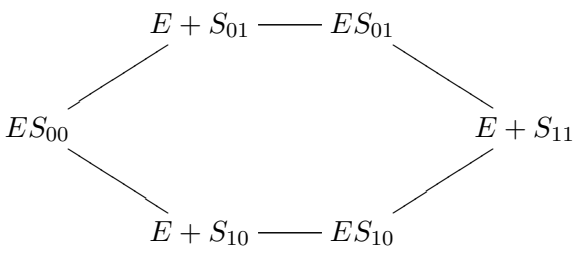

(5.7)

As (5.6) is not satisfied for $\widetilde{C}$, the system is not formally balanced.

Equations (5.6) show that the set

$$\mathcal{FB}_Y = \{\kappa = (\kappa_{ij})_{(i,j)\in\mathscr{R}} : G = (V, \mathscr{R}, \kappa, Y)\ is\ formally\ balanced\}$$

is an algebraic variety in $\mathbb{R}^r_{>0}$, i.e., it is cut out by polynomial equations in the rate constants.

We will review in §5.2.1 the known conditions for detailed balance, which are relations among the rate constants. Proposition 5.2.1 will recast the results in [49,137], which imply that the set

$$\mathcal{DB}_Y = \{\kappa = (\kappa_{ij})_{(i,j)\in\mathscr{R}} : G = (V, \mathscr{R}, \kappa, Y)\ is\ detailed\ balanced\}$$

is also an algebraic variety in $\mathbb{R}^r_{>0}$.

In turn, it follows from [30, Section 2] that the set

$$\mathcal{CB}_Y = \{\kappa = (\kappa_{ij})_{(i,j)\in\mathscr{R}} : G = (V, \mathscr{R}, \kappa, Y)\ is\ complex\ balanced\}$$

is a third algebraic subvariety of $\mathbb{R}^r_{>0}$ (see Proposition 5.3.2), called the *moduli space of toric dynamical systems* in [30].

As we have already remarked, $\mathcal{DB}_Y \subseteq \mathcal{CB}_Y$. In fact, the main Theorem in [49] shows that $\mathcal{DB}_Y \subseteq \mathcal{FB}_Y$.

In this chapter we prove the following result for a mass–action kinetics dynamical system associated to a reversible chemical reaction system $G = (V, \mathscr{R}, \kappa, Y)$:

Theorem 5.1.1. *Under the assumption of formal balancing, a reversible mass–action kinetics system is detailed balanced if and only if it is complex balanced. That is,*

$$\mathcal{CB}_Y \cap \mathcal{FB}_Y = \mathcal{DB}_Y. \tag{5.8}$$

Our result generalizes two particular situations in which it is known that the notions of detailed and complex balancing coincide: the case in which $\widetilde{G}$ has no cycles, and the case of deficiency zero networks for which $\mathcal{DB}_Y = \mathcal{FB}_Y$ ([49], see also Proposition 5.3.1 below).

Our algebraic approach follows the lines of [30]. Our arguments easily imply that (5.8) holds at the level of ideals (which are radical). We refrain from giving a more algebraic formulation since it is straightforward and our main concern is to clarify these notions in the framework of general mass–action kinetics systems.

In Section 5.2 we recall known results, mainly from [30,49,137], that we state in a language adapted to our setting. In Section 5.3, we introduce new quotient variables which allow us to characterize formal and complex balancing in terms of the rate constants, and which we use to organize the proof of Theorem 5.1.1 in Section 5.4.

In Section 5.5, following a suggestion of Martin Feinberg, we translate Theorem 5.1.1 to the setting of general kinetic systems in Theorem 5.5.1, and we express in Proposition 5.5.1 another necessary and sufficient condition for a complex balanced system to be detailed balanced.

5.2 Preliminaries for this chapter

In this section we only consider reversible mass–action kinetics systems. Given a chemical reaction network $G = (V, \mathscr{R}, Y)$, we will denote by $\widetilde{G} = (V, \widetilde{\mathscr{R}}, Y)$ the associated undirected graph. Since we assume that G is reversible, there is no loss of information in passing to $\widetilde{G}$.

Choose a numbering of the set of reactions, that is of the set of edges $\mathscr{R}$ of G and form the signed incidence matrix $C_G \in \{-1, 0, 1\}^{m\times r}$ whose column associated to the reaction (i, j) has a -1 on row i, a 1 on row j and all other entries equal to 0. We denote by

$$N \;=\; \ker_{\mathbb{Z}}(Y \cdot C_G) \;\subset \mathbb{Z}^r, \tag{5.9}$$

the kernel over $\mathbb{Z}$ of the product matrix $Y \cdot C_G$. Another name for the kernel of a matrix is the (right) nullspace of the matrix.

Clearly, the vector with a 1 on its (i, j)-th coordinate and on its (j, i)-th coordinate (and all other coordinates equal to zero) lies in N. We could instead choose one direction for each pair of reactions $(i, j), (j, i)$ in any way to get a directed subgraph G' of G, and consider the associated signed incidence matrix $C_{G'}$, with integer kernel

$$N' = \ker_{\mathbb{Z}}(Y \cdot C_{G'}) \subset \mathbb{Z}^{\frac{r}{2}}, \tag{5.10}$$

since we can clearly reconstruct N' from N and vice versa.

Remark 5.2.1. *For interested readers, we survey the different notations occurring in the literature for the nullspace N' in* (5.10)*. In [49], it is the subspace spanned by the vectors $(\alpha_{i\to j})_{i,j}$ with (i, j) reactions in G'. In [137], it is the subspace spanned by the columns of the matrix λ (there, $Y \cdot C_{G'}$ is called C). In [168], it is the subspace spanned by the vectors $(\varepsilon_w)_w$ with $w = \{i, j\} \in \widetilde{\mathscr{R}}$. Finally, it is the subspace spanned by the columns of the matrix B in [42], where N stands instead for the matrix $Y \cdot C_{G'}$.*

We introduce the following variables, which are usually known as *equilibrium constants*:

Definition 5.2.1. *Let $G = (V, \mathscr{R}, \kappa, Y)$ be a reversible chemical reaction system defining a dynamical system as in* (5.3)*. For each $(i, j) \in \mathscr{R}$ we define*

$$q_{ij} \;=\; \frac{\kappa_{ij}}{\kappa_{ji}}. \tag{5.11}$$

Clearly, $q_{ij}q_{ji} \;= 1$ for all $(i, j) \in \mathscr{R}$.

5.2.1 Detailed balanced systems

Detailed balanced systems have been broadly studied. In 1989, Feinberg ([49]) and Schuster and Schuster ([137]) described necessary and sufficient conditions for detailed balance to occur. The latter conceived these conditions as a *generalization of Wegscheider's condition*, which states that for cycles of monomolecular reactions the product of the equilibrium constants (q_{ij}, according to our notation) around these cycles must be equal to unity. Feinberg grouped these conditions more structurally into *circuit and spanning forest conditions* (see § 5.3.1).

In accordance to our notations, Theorem in [49, Section 3] and Theorem 1 in [137] can be restated as follows. As usual, for any $z = (z_1, \ldots, z_n) \in \mathbb{R}^n$ and $\lambda = (\lambda_1, \ldots, \lambda_n) \in \mathbb{Z}^n$, z^λ will denote the product $\prod_{i=1}^n z_i^{\lambda_i}$.

Proposition 5.2.1. *A chemical reaction system, $G = (V, \mathscr{R}, \kappa, Y)$, is detailed balanced if and only if*

$$q^\lambda = 1 \quad \text{for all } \lambda \in N, \tag{5.12}$$

where q denotes the vector $q = (q_{ij})_{(i,j)\in\mathscr{R}}$.

In fact, it is possible to derive a proof of this proposition using the following basic result [43]:

Proposition 5.2.2. *Let* $\mathbf{k}$ *be a field and* $a_1, \ldots, a_n \in \mathbb{Z}^s$. *Given a vector* $z = (z_1, \ldots, z_n) \in (\mathbf{k} - \{0\})^n$, *there exists* $x = (x_1, \ldots, x_s) \in (\mathbf{k} - \{0\})^s$ *such that* $z_i = x^{a_i}$ *for all* $i = 1, \ldots, n$ *if and only if* $z^\lambda = 1$ *for all* $\lambda \in \mathbb{Z}^n$ *such that* $\sum_{i=1}^n \lambda_i a_i = 0$.

When $\mathbf{k} = \mathbb{R}$ and $z \in \mathbb{R}^n_{>0}$, which will be our case, an easy proof of Proposition 5.2.2 can be given by taking logarithms.

Proof (of Proposition 5.2.1). A positive vector $\mathbf{x}_0$ satisfies a binomial equation $-\kappa_{ij}\mathbf{x}_0^{y_i} + \kappa_{ji}\mathbf{x}_0^{y_j} = 0$ if and only if $\mathbf{x}_0^{y_i - y_j} = q_{ij}$. The result follows from Proposition 5.2.2 for $n = r$ and $\{a_1, \ldots, a_n\} = \{y_i - y_j, (i,j) \in \mathscr{R}\}$. □

One can translate Conditions (5.12) into a finite number of equalities associated to a system of generators of N, as described in [49], or in general, by matrix algebra tools as in [137, 168]. In [42], a new formalism of *thermodynamic-kinetic modeling* is introduced, where detailed balanced is imposed.

5.2.2 The minors of $\mathcal{L}(G)$

We will recall in this section the shape of the minors of $\mathcal{L}(G)$, already seen in Section 2.2. This time, we work with a digraph not necessarily strongly connected.

Let G be a reversible digraph corresponding to a chemical reaction network and call G_t, $t = 1, \ldots, l$, the linkage classes of G, with corresponding sets of vertices V_t and edges $\mathscr{R}_t$. Up to renumbering, we can assume $\mathcal{L}(G)$ is block diagonal, with diagonal blocks the corresponding matrices $\mathcal{L}(G_t)$ for the components $G_1, \ldots, G_l$. Following [30], we introduce the following definition:

Definition 5.2.2. *Consider any directed subgraph* T *of* G *such that the underlying undirected graph of* T *is a spanning forest of the underlying undirected graph of* G. *We denote the set of vertices of* T *by* $V(T)$ *and its set of edges by* $\mathscr{R}(T)$. *Thus,* $\mathscr{R}(T)$ *consists of* $m - l$ *edges. Fix a connected component* G_t *of* G *and write* κ_t^T *for the product of the* $\#V_t - 1$ *rate constants which correspond to all edge labels of the edges in* $\mathscr{R}(T) \cap \mathscr{R}_t$. *Let* i *be one of the nodes of* G_t. *The directed tree obtained by the restriction* T_t *of* T *to* G_t *is called an* i*-tree if the node* i *is its unique sink, i.e., all edges are directed towards node* i. *We will write* κ^{T_t} *for the product of the* $\#V_t - 1$ *rate constants which correspond to all edge labels of the edges of* T_t. *We introduce the following constants, which are polynomials in the* (κ_{ij})*:*

$$K_i = \sum_{T_t \text{ an } i-tree} \kappa^{T_t}. \tag{5.13}$$

Note that each K_i *is a nonempty sum of positive terms because, as* G_t *is strongly connected, there exists at least one* i*-tree for every vertex* i *and each* $\kappa_{uv} > 0$ *for* $(u, v) \in \mathscr{R}_t$.

It follows from the Matrix-Tree Theorem [149] that for any $i \in V_t$, the absolute value of the determinant of the submatrix of $\mathcal{L}(G_t)$ obtained by deleting the i-th column and any one of

the rows, equals K_i. This (non-zero) minor is independent (up to sign) of the choice of rows because the row sums of $\mathcal{L}(G_t)$ are zero. Compare also with the statements in [100].

In Example 2.2.1 in Chapter 2 we showed how these minors look like.

5.2.3 The linear relations

We recall the structure of the nullspaces N and N' defined in (5.9) and (5.10). The statements that follow are all contained in [49] (with a different language).

The subsequent combinatorial arguments go back to Kirchoff. We can distinguish the following sublattice N'_1 of N'. It is the $\mathbb{Z}$-module spanned by the cycles of the underlying undirected graph $\widetilde{G}$. More precisely, given any oriented cycle $\mathcal{C}$ we form the vector $v_{\mathcal{C}} \in \{-1, 0, 1\}^{\frac{e}{2}}$ whose (i, j) coordinate equals 1 if the edge $(i, j) \in G'$ is in $\mathcal{C}$, -1 if instead the edge (j, i) lies in $\mathcal{C}$, and 0 if neither of the edges $(i, j), (j, i)$ is in $\mathcal{C}$.

The rank of N'_1 equals $\frac{r}{2} - m + l$, and a basis is formed by the *fundamental cycles* associated to a choice of a spanning forest T of G. The fundamental cycles associated to T are those (undirected) cycles which are created when we add an edge in the associated undirected graph $\widetilde{T}$ between any two vertices in the same connected component of G. Note that although the number of fundamental cycles in a graph is fixed, the cycles that become fundamental change with the spanning forest.

If we fix a spanning forest $\widetilde{T}$ of $\widetilde{G}$, we can moreover choose a direct complement N'_2 of N'_1 in N' as follows. Consider all vectors $v = (v_{ij},\ (i, j) \in \mathscr{R}(G'))$ in N' such that $v_{ij} \neq 0 \Rightarrow \{i, j\} \in \mathscr{R}(\widetilde{T})$. Call N'_2 the $\mathbb{Z}$-span of all these vectors v with support contained in $\mathscr{R}(\widetilde{T})$. Then

$$N' \ = \ N'_1 \oplus N'_2.$$

With our notations, the structural deficiency of the network G (see Section 2.4) equals $\delta_S = m - \dim \mathcal{S} - l$, where $\mathcal{S}$ is the stoichiometric linear subspace defined by

$$\mathcal{S} \ = \ \mathrm{span}\{y_i - y_j,\ (i, j) \in \mathscr{R}\}.$$

Thus, $\dim \mathcal{S} \ = \ \mathrm{rank}(Y \cdot C_{G'}) \ = \ \mathrm{rank}(Y \cdot C_G)$. As $\dim \mathcal{S} \ = \ \frac{r}{2} - \mathrm{rank}(N')$, we get that $\mathrm{rank}(N'_2) = \delta_S$, so that $N'_2 = 0$ if and only if $\delta_S = 0$, and for $\delta_S > 0$ we could choose a system of δ_S generators of N'_2.

In a similar way, we can decompose N as $N = N_0 \oplus N_1 \oplus N_2$, where N_0 is the lattice of rank $\frac{e}{2}$ spanned by the $0, 1$ vectors in N which express the fact that the (i, j)-th column of $Y \cdot C_G$ is minus its (j, i)-th column, and N_i for $i = 1, 2$ is isomorphic to N'_i (we simply add 0 coordinates for the entries corresponding to the edges not in G').

5.3 Characterizing formally balanced and complex balanced systems

We keep the notations of § 5.2.

5.3.1 Formally balanced systems

We recall that our definition of formally balanced systems reformulates with our notation Feinberg's circuit conditions, which in the case of monomolecular reactions are also equivalent to Wegscheider's condition.

We can use the description of the kernel N in § 5.2.3 to translate our definition of formal balancing, similarly to the characterization of detailed balanced systems in Proposition 5.2.1.

Proposition 5.3.1. *Given a chemical reaction system, $G = (V, \mathscr{R}, \kappa, Y)$, the following statements are equivalent:*

(i) The associated system is formally balanced,

(ii) For every cycle $\widetilde{C}$ of $\widetilde{G}$, it holds that

$$\prod_{(i,j)\ in\ C^+} q_{ij} \ = \ 1, \tag{5.14}$$

(iii) The vector $q = (q_{ij})_{(i,j)\in\mathscr{R}}$ verifies

$$q^\lambda = 1 \quad \text{for all } \lambda \in N_1. \tag{5.15}$$

Then, a formally balanced system G is detailed balanced if and only if Equations (5.12) hold for all λ in a set of generators of N_2. These are the *spanning forest conditions* in [49].

5.3.2 Complex balanced systems

We now characterize mass–action kinetics complex balanced chemical reaction systems. We introduce new variables which are suitable for our formulations.

Definition 5.3.1. *Let $G = (V, \mathscr{R}, \kappa, Y)$ be a reversible chemical reaction system defining a dynamical system as in* (5.3)*. For each $(i, j) \in \mathscr{R}$, we define*

$$Q_{ij} \ = \ \frac{K_j}{K_i}. \tag{5.16}$$

Remark 5.3.1. *The following equations hold*

$$Q_{ij}Q_{ji} \ = 1 \quad \text{for all } (i,j) \in \mathscr{R}.$$

We define Q_{ij} by the same formula for any pair i, j in $1, \ldots, m$ and then

$$Q_{ij}Q_{jk} \ = Q_{ik} \quad \text{for all } i,j,k \in \{1,\ldots,n\}.$$

It turns out that the existence of a positive steady state $\mathbf{x}_0$ satisfying $\mathcal{L}(G)\Psi(\mathbf{x}_0) = 0$ as in Definition 2.5.1, is again equivalent to algebraic conditions given purely in terms of the rate constants.

Proposition 5.3.2. *A chemical reaction system, $G = (V, \mathscr{R}, \kappa, Y)$, is complex balanced if and only if*

$$Q^\lambda = 1 \quad \text{for all } \lambda \in N. \tag{5.17}$$

Here, Q denotes the vector $Q = (Q_{ij})_{(i,j)\in\mathscr{R}}$.

Proof. We first claim that a system $G = (V, \mathscr{R}, \kappa, Y)$ defines a complex balanced system if and only if there exists a positive vector $\mathbf{x}_0 \in \mathbb{R}^s$ such that the following binomial equations are satisfied

$$K_i \mathbf{x}_0^{y_j} - K_j \mathbf{x}_0^{y_i} = 0, \text{ for all } (i,j) \in \mathscr{R}. \tag{5.18}$$

To prove this claim, we form as in [30] the following binomial ideals in $\mathbb{Q}[\mathbf{x}] := \mathbb{Q}[x_1, \ldots, x_s]$:

$$I = I_1 + \cdots + I_l, \quad I_t = \langle K_i \mathbf{x}^{y_j} - K_j \mathbf{x}^{y_i}, (i,j) \in \mathscr{R}_t \rangle, \; t = 1, \ldots, l. \tag{5.19}$$

Here $\mathscr{R}_1, \ldots, \mathscr{R}_l$ are the edges of the different connected components of G, as in Section 5.2. We moreover define the ideal T_G as the saturation

$$T_G = (I : (x_1 x_2 \ldots x_s)^\infty) = \{p \in \mathbb{Q}[\mathbf{x}] : \exists\, u \in \mathbb{Z}_{\geq 0} \text{ such that } p(x_1 x_2 \ldots x_s)^u \in I\}.$$

We denote by $V_{>0}(I)$ the positive variety of I, that is, the zeros of I in $(\mathbb{R}_{>0})^s$, and similarly for other ideals. As $T_G = (I : (x_1 x_2 \ldots x_s)^\infty) = (I_1 : (x_1 x_2 \ldots x_s)^\infty) + \cdots + (I_l : (x_1 x_2 \ldots x_s)^\infty)$, we deduce from display (8) in [30] that $V_{>0}(T_G) = \{\mathbf{x} \in \mathbb{R}^s_{>0} : \mathcal{L}(G)\Psi(\mathbf{x}) = 0\}$. But a point x with all non-zero coordinates is annihilated by T_G if and only if it is annihilated by I. We then have that

$$V_{>0}(I) = \{\mathbf{x} \in \mathbb{R}^s_{>0} : \mathcal{L}(G)\Psi(\mathbf{x}) = 0\},$$

and so the system G is complex balanced if and only if there exists a positive vector $\mathbf{x}_0$ satisfying Equations (5.18).

Now, we argue as in the proof of Proposition 5.2.1. These equations are equivalent to $x_0^{y_i - y_j} = Q_{ij}$ for all $(i,j) \in \mathscr{R}$. By Proposition 5.2.2, for $n = r$ and $\{a_1, \ldots, a_n\} = \{y_i - y_j, (i,j) \in \mathscr{R}\}$, these conditions are in turn equivalent to $Q^\lambda = 1$ for all $\lambda \in N$, as stated. □

Remark 5.3.2. *From the definition of the vector Q, it is clear that the equalities $Q^\lambda = 1$ always hold for any $\lambda \in N_0 \cup N_1$. Therefore, it is enough to check Equalities* (5.17) *for λ in a basis of N_2. For instance, the rank of N_2 in* (5.1) *is* 3*. It is straightforward to check that for any choice of constants as in* (5.5)*:*

$$Q^1_{12} \times Q^1_{24} \times Q^1_{1113} \times Q^1_{1314} = \frac{K_4 K_{14}}{K_1 K_{11}} = 1$$

$$Q^1_{12} \times Q^1_{23} \times Q^1_{1012} \times Q^1_{1214} = \frac{K_3 K_{14}}{K_1 K_{10}} = 1$$

$$Q^1_{35} \times Q^1_{57} \times Q^1_{89} \times Q^1_{910} = \frac{K_7 K_{10}}{K_3 K_8} = 1,$$

which proves again that the system is complex balanced (without needing to show a complex balanced steady state).

5.4 Proof of Theorem 5.1.1

Consider a reversible mass–action kinetics chemical reaction system $G = (V, \mathscr{R}, \kappa, Y)$ which is formally balanced. By Propositions 5.2.1, 5.3.1 and 5.3.2, we need to show that if the constants q_{ij} satisfy Equations (5.14), then

$$Q^\lambda = 1 \quad \text{for all } \lambda \in N$$

if and only if

$$q^\lambda = 1 \quad \text{for all } \lambda \in N.$$

These relations possibly involve constants associated to edges in several connected components of G. In fact, it holds that, modulo the formal balancing relations, an algebraic dependency relation $P(K) = 0$ among the (invertible) variables Q_{ij} holds for a polynomial P in r variables if and only if the "same" algebraic relation $P(q) = 0$ is true for the (invertible) variables q_{ij}. This is an immediate consequence of the following proposition.

Proposition 5.4.1. *Let $G = (V, \mathscr{R}, \kappa, Y)$ be a reversible mass–action kinetics system which is formally balanced. Then,*

$$Q_{ij} \;=\; q_{ij} \quad \text{for all } (i,j) \in \mathscr{R}. \tag{5.20}$$

Proof. Since Equations (5.14) relate variables q_{uv} for (u, v) in a single connected component of G, and since for given $(i, j) \in \mathscr{R}$, i, j belong to the same component, we can assume G is connected.

Fix $(i, j) \in \mathscr{R}$. We define a bijection between the set of j-trees and the set of i-trees as follows (see Example 5.4.1 for an illustration). Let T be any j-tree.

(i) If the edge $(i, j) \in \mathscr{R}(T)$, then let T' be the tree obtained by replacing (i, j) by the opposite edge (j, i).

(ii) If the edge $(i, j) \notin \mathscr{R}(T)$, let $\mathcal{C}_{ij}$ be the *undirected* fundamental cycle which is created in $\widetilde{T}$ by adding the edge (i, j). Call $\mathcal{C}_{ij}^+$ the corresponding *oriented* cycle which contains (i, j). Then, let T' be the tree obtained by giving to the edges of T which "lie" on $\mathcal{C}_{ij}$ the direction in $\mathcal{C}_{ij}^+$ (that is, we "reverse" all these edges in T).

It is straightforward to check that in both cases T' is, in fact, an i-tree and that the map $T \mapsto T'$ is a bijection. So, we have established a bijection between the terms in K_i and the terms in K_j.

Let T be a j-tree. We compare the term κ^T in K_j with the corresponding term $\kappa^{T'}$ in K_i. If $(i, j) \in \mathscr{R}(T)$, we clearly have that

$$\kappa^T \;=\; q_{ij}\, \kappa^{T'}.$$

If instead we have that $(i, j) \notin T$ then

$$\kappa^T = \left(\prod_{(u,v) \in \mathcal{C}_{ij}^+, (u,v) \neq (i,j)} q_{vu} \right) \kappa^{T'}.$$

By the assumption of formal balance, we have that $\prod_{(u,v)\in\mathcal{C}_{ij}^{+}} q_{uv} = 1$ and so

$$\prod_{(u,v)\in\mathcal{C}_{ij}^{+},(u,v)\neq(i,j)} q_{vu} = q_{ij}.$$

Therefore,

$$Q_{ij} = \frac{K_j}{K_i} = q_{ij},$$

as wanted. □

Example 5.4.1 (Example 2.2.1 continued)**.** *Considering the network*

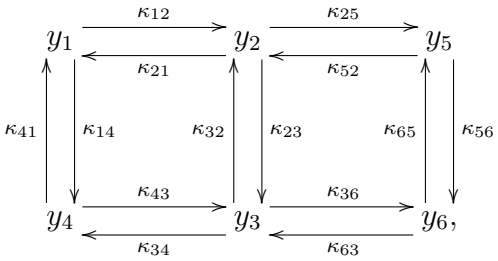

choose the following 1*-tree* T*:*

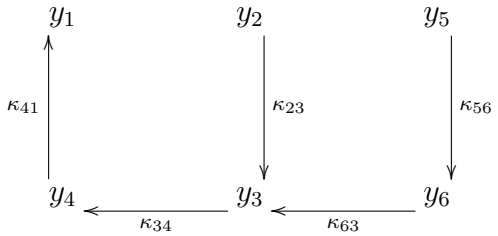

Let $(i,j) = (4,1)$*. It is clear that by reversing the edge* $(4,1) \in \mathscr{R}(T)$ *one gets a* 4*-tree.*

Let now $(i,j) = (2,1)$*, which does not lie in* $\mathscr{R}(T)$*, and* $\mathcal{C}_{12}^{+}$ *be the corresponding oriented fundamental cycle:*

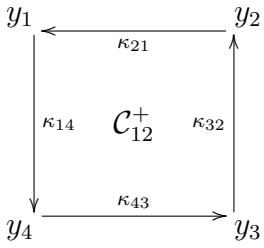

Then, reversing the arrows in the cycle gives the following 2*-tree* T'

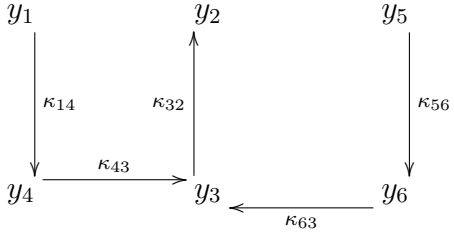

5.5 General kinetic systems

In this section we generalize Theorem 5.1.1 to non–necessarily mass–action kinetic systems in the sense of [48], see also [142, Section 2].

Let $G = (V, \mathscr{R}, \mathcal{K}, Y)$ be a kinetic system as in the introduction of this chapter. The differential equations (5.2) that describe the corresponding dynamics can be written as

$$\frac{d\mathbf{x}}{dt} = Y C_G \mathcal{K}, \tag{5.21}$$

where $\mathcal{K}$ is the $e \times 1$ matrix with entries $\mathcal{K}_{ij}$, and $C_G^\dagger$ is the (transpose of) the corresponding signed incidence matrix we considered in Subsection 5.2.3.

Remark 5.5.1. *It might be useful to compare our notation with the notation in [2, 56]. For instance,*

$$\frac{d\mathbf{x}}{dt} = \Gamma \mathcal{K}(\mathbf{x}), \quad \textit{where } \Gamma = Y.C_G \in \mathbb{Z}^{s\times r}.$$

Assume we have a mass–action kinetics system. We denote by K the $r\times m$ real matrix with entry equal to κ_{ij} in column indicated by complex i and row indicated by the reaction edge (i, j), and equal to zero elsewhere. Then, $\mathcal{K}(\mathbf{x}) = K\Psi(\mathbf{x})$, the Laplacian matrix equals $\mathcal{L}(G) = C_G K$ and we have

$$\frac{d\mathbf{x}}{dt} = Y\mathcal{L}(G)\Psi(\mathbf{x}) = Y(C_G K)\Psi(\mathbf{x}) = \Gamma\mathcal{K}(\mathbf{x}).$$

In the notation of [56], Y is called Y_s, and the incidence matrices are denoted by $C_G = I_a, K^\dagger = I_K$.

In this general context, we adapt the previous definitions.

Definition 5.5.1. *A* complex balanced *kinetic system is a dynamical system* (5.21) *associated with the data $G = (V, \mathscr{R}, \mathcal{K}, Y)$ for which the equations $C_G\mathcal{K} = 0$ admit a strictly positive solution $\mathbf{x}_0 \in \mathbb{R}^s_{>0}$. Such a solution $\mathbf{x}_0$ is a steady state of the system, i.e., the s coordinates of $YC_G\mathcal{K}$ vanish. We call $\mathbf{x}_0$ a complex balancing equilibrium.*

As before, we will assume that the digraph G is reversible, and thus identify G with the underlying undirected graph $\widetilde{G}$.

Definition 5.5.2. *A* detailed balanced *kinetic system is a dynamical system* (5.21) *associated with the data $G = (V, \mathscr{R}, \mathcal{K}, Y)$ for which the equations $\mathcal{K}_{ij}(\mathbf{x}) - \mathcal{K}_{ji}(\mathbf{x}) = 0$, for all $\{i, j\} \in \widetilde{\mathscr{R}}$, admit a strictly positive steady state $\mathbf{x}_0 \in \mathbb{R}^s_{>0}$. We call $\mathbf{x}_0$ a detailed balancing equilibrium.*

Again, every detailed balanced kinetic system is also complex balanced. To define formal balancing, we need to start from a particular positive steady state:

Definition 5.5.3. *Given a complex balanced system at the positive steady state $\mathbf{x}_0 \in \mathbb{R}^s_{>0}$ corresponding to the data $G = (V, \mathscr{R}, \mathcal{K}, Y)$, we say the kinetic system is* formally balanced at $\mathbf{x}_0$ *(or that $\mathbf{x}_0$ is a formally balancing equilibrium) if the following condition holds for every cycle $\widetilde{C}$ of $\widetilde{G}$:*

$$\prod_{(i,j)\ in\ C^+} \mathcal{K}_{ij}(\mathbf{x}_0) = \prod_{(j,i)\ in\ C^-} \mathcal{K}_{ji}(\mathbf{x}_0). \tag{5.22}$$

We can now reformulate Theorem 5.1.1:

Theorem 5.5.1. *Consider a kinetic system* (5.21) *associated to the data* $G = (V, \mathscr{R}, \mathcal{K}, Y)$ *with a complex balancing positive steady state* $\mathbf{x}_0 \in \mathbb{R}^s_{>0}$. *We have that* $\mathbf{x}_0$ *is a detailed balancing equilibrium if and only if it the system is formally balanced at* $\mathbf{x}_0$.

Proof. Given the complex balancing steady state $\mathbf{x}_0 \in \mathbb{R}^s_{>0}$, we define constants

$$\kappa_{ij} = \mathcal{K}_{ij}(\mathbf{x}_0)\mathbf{x}_0^{-y_i}$$

for each $(i,j) \in \mathscr{R}$ and we consider the mass–action kinetics dynamical system $\frac{d\mathbf{x}}{dt} = Y\mathcal{L}(G)\Psi(\mathbf{x})$ associated with $G = (V, \mathscr{R}, \kappa, Y)$. As $\mathcal{K}_{ij}(\mathbf{x}_0) = \kappa_{ij}\mathbf{x}_0^{y_i}$, we have $\mathcal{L}(G)\Psi(\mathbf{x}_0) = 0$, and so this new mass–action kinetics system is complex balanced in the previous sense.

Moreover, as the kinetic system is formally balanced at $\mathbf{x}_0$, we have that

$$\prod_{(i,j)\ in\ C^+} \kappa_{ij} = C \prod_{(i,j)\ in\ C^+} \mathcal{K}_{ij}(\mathbf{x}_0) = C \prod_{(j,i)\ in\ C^-} \mathcal{K}_{ji}(\mathbf{x}_0) = \prod_{(j,i)\ in\ C^-} \kappa_{ji},$$

where $C = x_0^{-\sum_{i\in\mathscr{R}(\widetilde{C})} y_i} \neq 0$. Then, the mass–action kinetics system associated with $G = (V, \mathscr{R}, \kappa, Y)$ is formally balanced. By Theorem 5.1.1 it is detailed balanced. This means that every binomial $\kappa_{ij}\mathbf{x}^{y_i} - \kappa_{ji}\mathbf{x}^{y_j}$ vanishes at $\mathbf{x}_0$, implying $\mathcal{K}_{ij}(\mathbf{x}_0) - \mathcal{K}_{ji}(\mathbf{x}_0) = 0$, and so the kinetic system associated with $G = (V, \mathscr{R}, \mathcal{K}, Y)$ is detailed balanced at $\mathbf{x}_0$. The other implication is clear. □

We end the chapter by showing another necessary and sufficient condition for a complex balanced kinetic system to be detailed balanced.

Proposition 5.5.1 (Feinberg)**.** *Given a kinetic system* (5.21) *associated to the data* $G = (V, \mathscr{R}, \mathcal{K}, Y)$ *with a complex balancing positive steady state* $\mathbf{x}_0 \in \mathbb{R}^s_{>0}$, *the following statements are equivalent:*

(i) The equilibrium $\mathbf{x}_0$ *is detailed balancing.*

(ii) For every cycle $\widetilde{C}$ *in* $\widetilde{G}$ *there exists an edge* $\{i_{\widetilde{C}}, j_{\widetilde{C}}\} \in \mathscr{R}(\widetilde{C})$ *such that*

$$\mathcal{K}_{i_{\widetilde{C}}j_{\widetilde{C}}}(\mathbf{x}_0) - \mathcal{K}_{j_{\widetilde{C}}i_{\widetilde{C}}}(\mathbf{x}_0) = 0.$$

(iii) Property (ii) holds for every basic *cycle associated to any spanning forest of* $\widetilde{G}$.

Proof. The equivalence between (ii) and (iii) is clear, as well as the implication from (i) to (ii). To see that (iii) implies (i), let G' be the digraph obtained from G by "deleting" all edges $(i_{\widetilde{C}}, j_{\widetilde{C}}), (j_{\widetilde{C}}, i_{\widetilde{C}})$ in the corresponding directed cycle C, together with their labels, for all basic cycles $\widetilde{C}$. Then, the associated undirected graph $\widetilde{G'}$ has no cycles and so any positive complex balancing equilibrium $\mathbf{x}_0$ for G' is automatically also detailed balancing. Call $\mathcal{L}(G)(\mathbf{x}_0)$ (respectively, $\mathcal{L}(G)'(\mathbf{x}_0)$) the Laplace matrices of the mass–action kinetics system associated with G (resp. G') with reaction constants $\kappa_{ij} = \mathcal{K}_{ij}(\mathbf{x}_0)\mathbf{x}_0^{-y_i}$ for each $(i,j) \in \mathscr{R}$

(resp. $\kappa_{ij} = \mathcal{K}_{ij}(\mathbf{x}_0)\mathbf{x}_0^{-y_i}$ for each $(i,j) \in \mathscr{R} - \{(i_{\widetilde{C}}, j_{\widetilde{C}}), (j_{\widetilde{C}}, i_{\widetilde{C}}),\ \widetilde{C}$ a basic cycle of $\widetilde{G}\}$). But if $\mathbf{x}_0$ satisfies the conditions in (iii), it follows that

$$\mathcal{L}(G)'(\mathbf{x}_0)\Psi(\mathbf{x}_0) \;=\; \mathcal{L}(G)(\mathbf{x}_0)\Psi(\mathbf{x}_0) = 0.$$

Therefore, $\mathbf{x}_0$ is detailed balancing for G', which together with the equalities in (iii) implies that $\mathbf{x}_0$ is detailed balancing for G, as wanted. □

Chapter 6

Finding absolute concentration robustness with tools from computational algebra

We address in this chapter the determination of Absolute Concentration Robustness (ACR, defined in [144]), using more advanced tools from computational algebra. We make clear throughout these pages that, when dealing with the steady states of a chemical reaction system under mass–action kinetics, we are not only working with the zeros of a certain polynomial ideal, but we are necessarily faced with the *positive* zeros. It is inevitable, then, to eventually introduce tools from real algebraic geometry for describing and analyzing the properties of the positive steady states of a mass–action kinetics system.

In [144], Shinar and Feinberg define that a biological system shows absolute concentration robustness (ACR) for an active molecular species if the concentration of that species is identical in every positive steady state the system might admit. We use here tools from computational algebra, algebraic geometry and real algebraic geometry to detect if a chemical reaction system shows absolute concentration robustness for a certain chemical species. We comment on the difficulties for a general algorithm and present some sufficient conditions for a system to have absolute concentration robustness.

6.1 Setting

All the chemical reaction systems here will be considered under mass–action kinetics.

We keep throughout this chapter the notions and notations from previous chapters, which will be briefly presented in the subsequent paragraphs.

Recall that a chemical reaction system under mass–action kinetics is a finite directed graph $G = (V, \mathscr{R}, \kappa, Y)$, with vertices labeled by $y_1, \ldots, y_m$ and edges called "reactions", endowed with a kinetics such that each reaction takes place at a rate that is proportional to the product of the concentrations of the species being consumed in that reaction. In other words, the rate of the reaction from y_i to y_j has the form $\kappa_{ij}\mathbf{x}^{y_i}$, where κ_{ij} is a positive number called the reaction rate constant, and $\mathbf{x} = (x_1, \ldots, x_s)^\dagger$ is the vector whose ℓ-th coordinate contains the molar concentration of the ℓ-th species. Recall that † denotes transpose.

A reaction system defines differential equations that describe the evolution of the molar

concentrations of the species

$$\frac{d\mathbf{x}}{dt} = f(\mathbf{x}).$$

In the case of mass–action systems, the coordinate functions $f_1, \ldots, f_s$ are polynomials in $\mathbb{Q}[\kappa][x_1, \ldots, x_s]$, where $\kappa = (\kappa_{ij})$.

We will call I the ideal generated by the polynomials $f_1, \ldots, f_s$:

$$I = \langle f_1, \ldots, f_s \rangle = \{ \sum_{i=1}^{s} g_i f_i,\ g_i \in \mathbb{R}[x_1, \ldots, x_s], i = 1, \ldots, s \}. \tag{6.1}$$

This ideal was also called $J_{\Sigma\Psi}$ in Section 2.2.

A steady state of the reaction system will be a point $\mathbf{x} \in \mathbb{R}^s_{\geq 0}$ such that $f(\mathbf{x}) = 0$. A positive steady state is a zero of f that belongs to $\mathbb{R}^s_{>0}$. It is important to notice that the steady states of a system are the nonnegative zeros of the ideal I.

We define now ACR with a more "mathematical flavor", using the terminology above.

Definition 6.1.1. *Let $f_1, \ldots, f_s \in \mathbb{Q}[\kappa^0][x_1, \ldots, x_s]$, with reaction rate constants $\kappa^0 \in \mathbb{R}^r_{>0}$, and $i \in \{1, \ldots, s\}$. We say that the system $f_1 = \cdots = f_s = 0$ has* absolute concentration robustness (ACR) *in the i-th variable if there exists a* positive *constant c such that for any $\mathbf{x} \in \mathbb{R}^s_{>0}$ satisfying $f_1(\mathbf{x}) = \cdots = f_s(\mathbf{x}) = 0$, it holds that $x_i = c$. That is, the value of x_i is independent of $\mathbf{x}$ for any positive steady state of the system.*

Throughout this chapter, we will make no distinctions between a chemical reaction system and its corresponding ideal I, as we are only interested in the characteristics of the steady states. Neither will we separate the i-th species from the corresponding variable x_i. For instance, there should be no confusion if we say that the ideal I shows ACR in the variable x_i.

We will give in the following sections some sufficient conditions for a system to show ACR and some algorithms, but we will also explain why it is impossible to develop an algorithm for the general case without further hypotheses.

We will make use of results from commutative algebra, algebraic geometry and real algebraic geometry. The reader not familiar with the terminology is referred to [7, 29, 62, 147].

6.2 Some basic algebraic notions

This section presents some basic definitions from commutative algebra and algebraic geometry that can be found in [28]. We will need these notions and notation for our results.

Let k be a field. Throughout this chapter, k will be either $\mathbb{Q}$, $\mathbb{R}$, $\mathbb{C}$, or $\mathbb{Q}(\kappa)$, the field of the rational functions with coefficients over $\mathbb{Q}$ and variables determined by κ. If we consider a particular value $\kappa^0 \in \mathbb{R}^r_{>0}$ of κ, we obtain the field $\mathbb{Q}(\kappa^0) \subset \mathbb{R}$. And let X be a set, which for us will be $\mathbb{C}$, $\mathbb{C}^*$ (the complex numbers without zero), $\mathbb{R}$, $\mathbb{R}_{>0}$, or a real closed field R that we will mention later.

For the moment, we will work over any field k, and let $J \subset k[x_1, \ldots, x_s]$ be an ideal of polynomials over k. We can define the following sets:

- The *variety* of J over the set X is the set of zeros of the ideal that belong to X (for X a "suitable" set for k). We will denote it as $V_X(J)$.

$$V_X(J) := \{\mathbf{x} \in X^s : g(\mathbf{x}) = 0 \text{ for all } g \in J\}$$

- The *radical* of J is the ideal of the polynomials in $k[x_1, \ldots, x_s]$ that vanish over $V_{\overline{k}}(J)$, where $\overline{k}$ is the algebraic closure of k. This is in fact an equivalence stated by Hilbert's Nullstellensatz of the actual definition of the radical $\sqrt{J}$ of J:

$$\sqrt{J} := \{g \in k[x_1, \ldots, x_s] : g^n \in J \text{ for some } n \in \mathbb{N}\}.$$

  An ideal J is called radical if $J = \sqrt{J}$.

- Let h be a polynomial in $k[x_1, \ldots, x_s]$, the *saturation* of J with respect to h is the ideal $(J : h^\infty)$ defined by

$$(J : h^\infty) := \{g \in k[x_1, \ldots, x_s] : h^n g \in J \text{ for some } n \in \mathbb{N}\}.$$

  For us, h will be the monomial $\mathfrak{m}$ formed by the product of all the variables in the ring. For example, for the ring $k[x_1, \ldots, x_s]$, $\mathfrak{m} = x_1 \cdots x_s$. Notice that the zeros of J with nonzero coordinates are the zeros of $(J : \mathfrak{m}^\infty)$ with nonzero coordinates. Roughly speaking, $(J : \mathfrak{m}^\infty)$ allow us to "divide" the polynomials in J by monomials in the variables.

  It can be easily proved that if $J = \langle g_1, \ldots, g_t \rangle$, and z is a new variable, then

$$(J : h^\infty) = \langle g_1, \ldots, g_t, hz - 1 \rangle \cap k[x_1, \ldots, x_s].$$

Both, the saturation ideal and the radical ideal, can be computed from I with Gröbner basis methods, implemented for instance in the computer algebra systems Macaulay2 [61] or Singular [35]. In these systems, the output of each method is a set of generators of the corresponding ideal.

6.3 First sufficient conditions for ACR

Inspired in Example 4.2.3 of Chapter 4, from Shinar and Feinberg [144], we use the saturation of I with respect to the monomial $\mathfrak{m} = x_1 \cdots x_s$ to help us check if a given ideal shows ACR for a certain variable i. The following lemma goes in that direction.

Lemma 6.3.1. *If there exists $i \in \{1, \ldots, s\}$ and a polynomial $g \in \sqrt{(I : \mathfrak{m}^\infty)} \cap \mathbb{R}[x_i]$ with only one positive real root, then the system shows ACR for the i-th species.*

Proof. We need to show that there exists a positive c such that, for every positive steady state, the i-th coordinate equals c. Let i and g be as in the statement, and let c be the only positive real root of g. There exists n such that $\mathfrak{m}^n g^n \in I$. Let $\tilde{\mathbf{x}}$ be a positive steady state, it holds that $(\tilde{x}_1 \ldots \tilde{x}_s)^n g^n(\tilde{x}_i) = 0$. As $\tilde{x}_j \neq 0$ for $1 \leq j \leq s$, we have $g(\tilde{x}_i) = 0$, and therefore, as $\tilde{x}_i > 0$, it holds that $\tilde{x}_i = c$. And this is true for any positive steady state $\tilde{\mathbf{x}}$, which implies that the system shows ACR for the i-th species. □

We then have the following algorithm to detect if the conditions in Lemma 6.3.1 are satisfied. This algorithm may not be optimal, but it can yet lead to the detection of ACR.

Algorithm 6.3.1. INPUT: $f_1, \ldots, f_s \in k[x_1, \ldots, x_s]$ *and* $i \in \{1, \ldots, s\}$.
OUTPUT: *"Yes", if there exists a polynomial* g *as in Lemma 6.3.1, or "No" if it does not.*

Step 1: Compute the saturation ideal $(I : \mathfrak{m}^\infty)$.
Step 2: Compute the elimination ideal $I_i := (I : \mathfrak{m}^\infty) \cap k[x_i]$.
Step 3: Compute $\sqrt{I_i}$ *and pick a generator* g.
Step 4: Compute the number of positive real roots of g *(via Sturm's theorem).*

If g *has only one positive real root, return "Yes". Otherwise, return "No".*

Ideally, $k = \mathbb{R}$. For computational reasons, one may assume $k = \mathbb{Q}$ or $k = \mathbb{Q}(\kappa^0)$, but we will deal with some problems related to these kind of assumptions in Examples 6.5.1 and 6.5.2.

Note that Sturm's theorem counts all distinct real roots without counting their multiplicity. Once we consider the radical ideal, we can be sure that each root of its generators has multiplicity one. We do not compute the radical ideal until Step 3 because it is sufficient and cheaper to do the computations in one variable.

An important remark is that, if the answer to the algorithm is "Yes", then we can confirm ACR for the system in the i-th variable.

We apply the algorithm to the following example.

Example 6.3.1 (Shinar-Feinberg example, continued)**.** *Recall from Example 4.2.3 in Chapter 4 that using the lexicographical order* $x_1 > x_2 > x_4 > x_5 > x_6 > x_8 > x_9 > x_3 > x_7$*, the reduced Gröbner basis of the ideal of the system contained the polynomial* $g_1 = [k_{89}k_{12}k_{23}k_{910}(k_{12,11}+k_{12,13})+k_{11,12}k_{21}k_{12,13}(k_{98}+k_{9,10})(k_{32}+k_{34})]x_3x_7+[-k_{23}k_{34}k_{12}(k_{12,11}+k_{12,13})(k_{98}+k_{9,10})]x_3$*. So, this computation already gives a binomial, which ensures ACR in* x_7*. If we follow the steps of Algorithm 6.3.1, we obtain the polynomial* $g = g_1/x_3$*. It is important to notice that, in this case, the system exhibits ACR for any choice of rate constants* κ*.*

The ideal I *in this example is a* binomial ideal*: it can be generated by the binomials* $g_1, \ldots, g_7$*. Moreover, it can be proved that for* any *binomial ideal (not containing monomials) and* any *term order, the reduced Gröbner basis is composed of binomials (Proposition 1.1.(a) of [43]). In particular, we could read the binomial* g_1*. However, it is not true that if there is a binomial of the form* $p = \mathfrak{m}\, x_i - \mathfrak{m}\, c$ *in a given ideal, the computation of any Gröbner basis will show any binomial nor will easily allow to deduce the existence of such* p*. But this will be always achieved from the steps in Algorithm 6.3.1.*

Using the saturation of I with respect to $\mathfrak{m} = x_1 \cdots x_s$, we can also prove the following proposition related to the results in Chapter 4, generalizing the Shinar-Feinberg Theorem for ACR [144].

Proposition 6.3.1. *Consider a mass–action system that admits a positive steady state and suppose that the system satisfies Condition 4.2.1 defined in Section 4.2, for the partition* $I_1, I_2, \ldots, I_d$ *of* $\{1, 2, \ldots, m\}$*. If, in the network, there are two different complexes* y_{j_1} *and* y_{j_2} *with* $j_1 \neq j_2, j_1, j_2 \in I_j$ *for some* $j \in \{1, 2, \ldots, d\}$*, that differ only in the* i*-th species, then the system has ACR in the* i*-th species.*

Proof. As the system admits a positive steady state and satisfies Condition 4.2.1, according to Theorem 4.2.1, any steady state satisfies the binomial $b^j_{j_1}x^{y_{j_2}} - b^j_{j_2}x^{y_{j_1}}$ for some positive $b^j_{j_1}, b^j_{j_2}$. Let us assume, without loss of generality, that $(y_{j_2})_i > (y_{j_1})_i$, then the polynomial $x_i^{(y_{j_2})_i} - \frac{b^j_{j_2}}{b^j_{j_1}}$ belongs to the ideal $(I : \mathfrak{m}^\infty)$. As the zeros of I with nonzero coordinates are the zeros of $(I : \mathfrak{m}^\infty)$ with nonzero coordinates, in particular, all the positive steady states are positive zeros of $(I : \mathfrak{m}^\infty)$. Hence, if we call c the $(y_{j_2})_i$-th root of $\frac{b^j_{j_2}}{b^j_{j_1}}$, we have $x_i = c\,(> 0)$ for all $\mathbf{x}$ positive steady state of the system, which is what we wanted to prove. □

6.4 ACR vs. CACR

Many chemical reaction systems are classified according to special characteristics in their *positive* equilibria. We focus here on ACR, but we can recall, for example, detailed balance from Chapter 5. Let us come back to Example 4.1.1 from Chapter 4.

Example 6.4.1 (Triangle network, continued)**.** *We have the network*

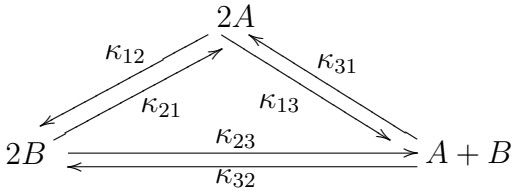

We label the three complexes as $x^{y_1} = x_1^2$, $x^{y_2} = x_2^2$, $x^{y_3} = x_1x_2$, and we define κ_{ij} to be the (real positive) rate constant of the reaction from complex y_i to complex y_j. The resulting mass-action kinetics system equals

$$\frac{dx_1}{dt} \;=\; -\frac{dx_2}{dt} \;=\; (-2\kappa_{12} - \kappa_{13})x_1^2 + (2\kappa_{21} + \kappa_{23})x_2^2 + (\kappa_{31} - \kappa_{32})x_1x_2\ .$$

The steady state locus in $\mathbb{R}^2_{\geq 0}$ is defined by this single trinomial. As only the coefficient of x_1x_2 can be zero, this system has toric steady states if and only if $\kappa_{31} = \kappa_{32}$.

But if we fix $\kappa_{31} = \kappa_{23} = 2$, $\kappa_{13} = \kappa_{32} = \kappa_{12} = 1$, $\kappa_{21} = 4$, the system does not have toric steady states ($\kappa_{31} = 2 \neq 1 = \kappa_{32}$) since $f_1 = (3x_1 + 5x_2)(2x_2 - x_1)$. However, all positive steady states satisfy the binomial equation $2x_2 - x_1 = 0$. In fact, we have that the ideal of polynomials vanishing on the positive roots of the ideal $\langle f_1\rangle$ is $\langle 2\,x_2 - x_1\rangle$, which is binomial. This system is an example of a detailed balanced system (recall Definition 5.1.2 in Chapter 5) which is not binomial.

If we widen our scope to the (algebraically closed field of the) complex numbers $\mathbb{C}$, we may lose chemical significance in principle, but we can gain much from the theoretical and computational point of view. Let us start by introducing a generalization of the notion of absolute concentration robustness. It is simply an extension of this particular quality from the positive zeros to the complex zeros with nonzero coordinates.

Definition 6.4.1. *Let $f_1, \ldots, f_s \in \mathbb{Q}[\kappa^0][x_1, \ldots, x_s]$, with reaction rate constants $\kappa^0 \in \mathbb{R}^r_{>0}$, and $i \in \{1, \ldots, s\}$. We say that the system $f_1 = \cdots = f_s = 0$ has* complex absolute concentration robustness (CACR) *in the i-th variable if there exists a constant c such that for any $\mathbf{x} \in (\mathbb{C}^*)^s$ satisfying $f_1(\mathbf{x}) = \cdots = f_s(\mathbf{x}) = 0$, it holds that $x_i = c$. That is, the value of x_i is independent of $\mathbf{x}$.*

Remark 6.4.1. *Assume a system $f_1 = \cdots = f_s = 0$ has CACR in the i-th variable. If $c \in \mathbb{R}_{>0}$ then the system has ACR in the i-th species (and for any positive steady state, its i-th coordinate equals c), but if $c \notin \mathbb{R}_{>0}$, then the system cannot have any positive steady state.*

What we gain from this new definition is *necessary* and sufficient conditions for CACR to occur. Moreover, CACR can be detected algorithmically. We record our claim in the following proposition and algorithm.

Proposition 6.4.1. *Let $I = \langle f_1, \ldots, f_s \rangle \subset \mathbb{R}[x_1, \ldots, x_s]$ as in* (6.1)*. The system has CACR in the i-th variable if and only if there exists a binomial of the form $x_i - c$ in $\sqrt{(I : \mathfrak{m}^\infty)}$, where $\mathfrak{m}$ is the monomial $x_1 \cdots x_s$, and c is a rational function of the coefficients of the polynomials $f_1, \ldots, f_s$.*

Proof. First assume that the system has CACR in the i-th variable, and $x_i = c$ for all $\mathbf{x} \in (\mathbb{C}^*)^s$ satisfying $f_1(\mathbf{x}) = \cdots = f_s(\mathbf{x}) = 0$. Then, $\mathfrak{m}\,(x_i - c)$ is identically zero over all the zeros of I in $\mathbb{C}^s$. We deduce from the Nullstellensatz that there exists a natural number n such that $\mathfrak{m}^n\,(x_i - c)^n \in I$. Thus, $(x_i - c)^n \in (I : \mathfrak{m}^\infty)$ and only depends on x_i. This implies that $x_i - c \in \sqrt{(I : \mathfrak{m}^\infty)}$.

Now assume that there exists a binomial of the form $x_i - c$ in $\sqrt{(I : \mathfrak{m}^\infty)}$. Then there exists n big enough such that $\mathfrak{m}^n(x_i - c)^n \in I$. If $\tilde{\mathbf{x}} \in V_{\mathbb{C}^*}(I)$, then $(\tilde{x}_1 \ldots \tilde{x}_s)^n(\tilde{x}_i - c)^n = 0$. As $(\tilde{x}_1 \ldots \tilde{x}_s)^n \neq 0$, we have $(\tilde{x}_i - c)^n = 0$, and then $x_i = c$ for all $\tilde{\mathbf{x}}$ zero of I in $(\mathbb{C}^*)^s$, as we wanted to prove. □

This algorithm detects if there is CACR in a certain variable x_i.

Algorithm 6.4.1. INPUT: $f_1, \ldots, f_s \in k[x_1, \ldots, x_s]$ *and* $i \in \{1, \ldots, s\}$.
OUTPUT: *c, if the system has CACR, or "No" if it does not.*

Step 1: Compute the saturation ideal $(I : \mathfrak{m}^\infty)$.
Step 2: Compute the elimination ideal $I_i := (I : \mathfrak{m}^\infty) \cap k[x_i]$.
Step 3: Compute $\sqrt{I_i}$ and pick a generator g.

If g has degree 1, return its root. Otherwise, return "No".

As in Algorithm 6.3.1, ideally $k = \mathbb{R}$ but sometimes $k = \mathbb{Q}$ or $k = \mathbb{Q}(\kappa^0)$ is assumed (see Examples 6.5.1 and 6.5.2 below). We do not compute the radical ideal until Step 3 because it is sufficient and cheaper to do the computations in one variable. As before, this algorithm may not be optimal, but it still can lead us to CACR.

Example 6.4.2 (Shinar-Feinberg example, continued)**.** *We come back to this example where using the lexicographical order $x_1 > x_2 > x_4 > x_5 > x_6 > x_8 > x_9 > x_3 > x_7$, the reduced Gröbner basis of the ideal of the system contained the polynomial $g_1 = [k_{89}k_{12}k_{23}k_{910}(k_{12,11} +$*

$k_{12,13})+k_{11,12}k_{21}k_{12,13}(k_{98}+k_{9,10})(k_{32}+k_{34})]x_3x_7+[-k_{23}k_{34}k_{12}(k_{12,11}+k_{12,13})(k_{98}+k_{9,10})]x_3$, *which ensures CACR in* x_7. *If we follow the steps of Algorithm 6.4.1, we again obtain the polynomial* $g = g_1/x_3$. *Notice that this system also exhibits CACR for* any *choice of rate constants* κ.

Even though detecting CACR is possible, there are systems that show ACR but do not have CACR. We capture this situation in the following example.

Example 6.4.3. *Consider the polynomials in two variables:*

$$f_1(\mathbf{x}) := (x_1-2)(x_1-3)(x_1^2+1), \quad f_2(\mathbf{x}) := (x_1-2)(x_1-3)(x_2^2-x_2)+(x_1^2+1)(2-x_2).$$

Here $s = 2$ *and there are two positive solutions:* $(2,2)$ *and* $(3,2)$, *so the system has ACR in the second variable. However, there are two complex solutions with nonzero entries, with second coordinate equal to* 1, *and therefore the system does not show CACR in this variable.*

Note that the polynomials f_1, f_2 *have the following shape:* $f_i = p_i - x_i q_i, i = 1, 2$, *where all the coefficients of* p_i, q_i *are non negative. It follows from [68, Theorem 3.2], as we mentioned at the end of Section 2.1, that it is possible to find a reaction network modeled with mass–action kinetics, such that the associated system is* $dx_1/dt = f_1, dx_2/dt = f_2$.

6.5 Towards detecting ACR with tools from real algebraic geometry

We finally need to face the fact that we are not actually interested in *all* the complex zeros of a given chemical reaction system, but we are looking for the real non-negative ones. Moreover we are usually interested in the positive equilibria. We are then looking for a polynomial $g(\mathbf{x}) := x_i - c \in \mathbb{R}[x_i]$ that equals zero on *any* positive steady state.

In other words, we want to state that, given $i \in \{1, \ldots, s\}$, there exists $c > 0$ such that, for all $x_i > 0$ such that there exist $x_1 > 0, \ldots, x_{i-1} > 0, x_{i+1} > 0, \ldots, x_s > 0$ satisfying $f_1(\mathbf{x}) = \cdots = f_s(\mathbf{x}) = 0$ for $\mathbf{x} = (x_1, \ldots, x_s)$, then $x_i = c$. This is a formula in the language of ordered fields, that is equivalent to the projection of a semialgebraic set onto the i-th coordinate. There are results from quantifier elimination theory ([7, Chapter 2]) that allow us to decide this existence algorithmically. The first result is due to Tarski and Seidenberg [138, 156, 157] and there are more recent improvements [5, 6, 71–73, 127] related to the complexity of this algorithm, which is usually quite expensive. There are some implementations of quantifier elimination based on the method of Cylindrical Algebraic Decomposition (CAD) proposed by Collins [13, 21, 22, 152].

In this section we address this issue from a different approach, which is more demanding but serves as a starting point for the development of other computational tools from real algebraic geometry for the analysis of steady states of biochemical reaction systems.

Recall now the ideal $I = \langle f_1, \ldots, f_s \rangle \in \mathbb{Q}[\kappa^0][x_1, \ldots, x_s]$ generated by the equations of the mass–action chemical reaction system with rate constants $\kappa^0 \in \mathbb{R}^r_{>0}$. One thing we could do is try to find the ideal $P \subseteq \mathbb{R}[x_1, \ldots, x_s]$ of all the polynomials that vanish on the positive real zeros of I, then ACR for the i-th species would be equivalent to $x_i - c \in P$ for some

positive c. But an algorithm to find this ideal P in a generic case would imply computing the factorization of polynomials over the field $\mathbb{R}$, which is impossible.

Considering this dilemma, we will give some heuristics and further sufficient conditions to decide whether a specific chemical reaction system shows ACR, using tools from algebraic geometry, real algebraic geometry and computational algebra.

As we are interested in the positive zeros among the real ones, we can focus on the ideal $J \in \mathbb{Q}[\kappa^0][x_1, \ldots, x_s, z_1, \ldots, z_s]$ defined as

$$J := \langle I, x_1 z_1^2 - 1, x_2 z_2^2 - 1, \ldots, x_s z_s^2 - 1 \rangle.$$

This basic yet ingenious trick was suggested to us by Daniel Perrucci. Notice that the zeros of J have nonzero coordinates. Moreover, if $(x_1, x_2, \ldots, x_s, z_1, z_2, \ldots, z_s)$ belongs to the *real* variety of J, then x_i must be positive for $1 \leq i \leq s$ as it satisfies the equation $x_i z_i^2 = 1$, with $z_i \in \mathbb{R}$.

As we are only interested in a description of the (positive real) variety of the ideal, we can focus on its radical ideal $\sqrt{J}$ which we will denote $\tilde{I}$.

$$\tilde{I} := \{g \in \mathbb{Q}[\kappa^0][x_1, \ldots, x_s] : g^n \in J \text{ for some } n \in \mathbb{N}\}. \tag{6.2}$$

We will focus then on the real zeros of $\tilde{I}$, as we can recover the positive zeros of I by projecting $V_{\mathbb{R}}(\tilde{I})$ onto the first s coordinates. Moreover, there is no impediment in studying $\tilde{I}$ since it can be computed effectively.

We can also notice that $\tilde{I}$ is equal to its saturation with respect to the monomial $\mathfrak{m} = x_1 \cdots x_s z_1 \cdots z_s$.

Lemma 6.5.1. *Let $\tilde{I}$ as in* (6.2)*, then we have $\tilde{I} = (\tilde{I} : \mathfrak{m}^\infty)$.*

Proof. One inclusion is obvious (we take $n = 1$). For the other one, let $g \in (\tilde{I} : \mathfrak{m}^\infty)$, then there exists $n \in \mathbb{N}$ such that $g.\mathfrak{m}^n \in \tilde{I}$. Let $(\tilde{\mathbf{x}}, \tilde{\mathbf{z}})$ be a zero of $\tilde{I}$, then $\tilde{x}_i \tilde{z}_i^2 = 1$ for all $i \in \{1, \ldots, s\}$ and this implies $\tilde{x}_i \neq 0$, $\tilde{z}_i \neq 0$ for all i, and therefore $(\tilde{x}_1 \ldots \tilde{x}_s \tilde{z}_1 \ldots \tilde{z}_s)^n \neq 0$. Then, necessarily $g(\tilde{\mathbf{x}}, \tilde{\mathbf{z}}) = 0$ and by the Nullstellensatz, g belongs to the radical of $\tilde{I}$, but $\tilde{I}$ is a radical ideal; hence, $g \in \tilde{I}$. □

Let us see now how we can recover ACR even if the system does not have CACR. Recall from Example 6.4.3 the polynomials $f_1(\mathbf{x}) := (x_1 - 2)(x_1 - 3)(x_1^2 + 1)$, $f_2(\mathbf{x}) := (x_1 - 2)(x_1 - 3)(x_2^2 - x_2) + (x_1^2 + 1)(2 - x_2)$ that can be considered as $dx_1/dt = f_1, dx_2/dt = f_2$ for a chemical reaction system. We can find

$$\tilde{I} = \langle (x_1-2)(x_1-3)(x_1^2+1), (x_1-2)(x_1-3)(x_2^2-x_2)+(x_1^2+1)(2-x_2), x_1z_1^2-1, x_2z_2^2-1 \rangle.$$

This ideal can be decomposed as $\tilde{I} = P_1 \cap P_2$, where $P_1 = \langle (x_1 - 2)(x_1 - 3), (x_1^2 + 1)(2 - x_2), x_1 z_1^2 - 1, x_2 z_2^2 - 1 \rangle$ and $P_2 = \langle (x_1^2 + 1), (x_1 - 2)(x_1 - 3)(x_2^2 - x_2), x_1 z_1^2 - 1, x_2 z_2^2 - 1 \rangle$.

As P_2 has no real zeros ($V_{\mathbb{R}}(P_2) = \emptyset$), we deduce that the real variety of $\tilde{I}$ coincides with the real variety of P_1. This last ideal shows CACR in the second variable, with $c = 2 > 0$. Therefore, this way we can also see that the system shows ACR for the second variable. In general, we will give a sufficient condition to find ACR when there is no CACR in the following lemma:

Lemma 6.5.2. *Let $\tilde{I}$ be as in* (6.2)*. If $\tilde{I}$ can be written as the intersection of two ideals P_1 and P_2:*

$$\tilde{I} = P_1 \cap P_2,$$

such that $V_{\mathbb{R}}(P_2) = \emptyset$ and there exists a positive c such that $x_i - c \in P_1$, for some $i \in \{1, \ldots, s\}$, then the system shows ACR in the i-th species.

Proof. Immediate since $V_{\mathbb{R}}(\tilde{I}) = V_{\mathbb{R}}(P_1)$. □

This would lead us to a sufficient condition that could be checked algorithmically as in Algorithm 6.4.1 if we could compute effectively the ideals P_1 and P_2 in the decomposition. Notice that what we did in Example 6.4.3 is a factorization of f_1 into $f_1 = g.h$ with g such that all its roots are real, and h with all roots nonreal. In practice, this is impossible without further hypotheses. For example, suppose that we want to factor the polynomial $x_1^3 - 2$. We would like to isolate the factor $x_1 - \sqrt[3]{2}$. A computer can either approximate the irrational number $\sqrt[3]{2}$ or give us a representation of the form $x_1 - \alpha = 0$, $\alpha^3 - 2 = 0$, which is informative but not quite sufficient. Moreover, even if we were satisfied with this type of factorization, a description on the roots of a polynomial in the form $x_i^n - C = 0$ would imply the polynomial is solvable by radicals, which is rare for univariate polynomials of degree bigger than four.

Many authors in real algebraic geometry have addressed the issue of finding the polynomials that vanish in the real zeros of a certain ideal [7, 10, 106, 123, 131, 147, 148]. In [10, 123], Becker and Neuhaus present algorithms to compute τ-radicals, in particular $\sqrt[\mathbb{R}]{J}$. These algorithms work if certain specified computational requirements for k are satisfied. The τ-radical of an ideal J in $k[x_1, \ldots, x_s]$ is $\sqrt[\tau]{J} = \{g \in k[x_1, \ldots, x_s]; g^{2t} + \sum_{i=1}^{N} a_i h_i^2 \in J \text{ for some } t, N, a_i \in \tau, h_i \in k[x_1, \ldots, x_s]\}$, where k is a field and $\tau \subset k$ a preordering, i.e. τ is a subset of k, closed under addition and multiplication such that $k^2 \subseteq \tau, -1 \notin \tau$. The smallest preordering $\tau_0 = k^2$ gives $J = \sqrt[\mathbb{R}]{J}$ which is called the real radical. Analogous to Hilbert's Nullstellensatz, it holds that $\sqrt[\mathbb{R}]{J}$ is the ideal in $k[x_1, \ldots, x_s]$ of the polynomials that vanish on the real variety $V_{\mathbb{R}}(J)$ of J. The requirements, in order to cope with an arbitrary univariate polynomial $f \in k(\kappa_1, \ldots, \kappa_r)[x]$ are the following computational assumptions: The preordered field (k, τ) should be effectively given and it should allow

(F) polynomial factorization of multivariate polynomials over k as well as

(R) an algorithm to test if a given irreducible polynomial $p \in k[\kappa_1, \ldots, \kappa_r, x]$ is τ-real over $k(\kappa_1, \ldots, \kappa_r)$, i.e. if $\sqrt[\tau]{(p)} = (p)$ in $k(\kappa_1, \ldots, \kappa_r)[x]$.

In the case of $k = \mathbb{R}$ with the usual order, (F) would mean effective factorization over $\mathbb{R}$.

We could bypass this difficulty working on a field different from $\mathbb{R}$. For instance, even though for a fixed $\kappa^0 \in \mathbb{R}^r_{>0}$, $\mathbb{Q}(\kappa^0) \subset \mathbb{R}$, we can think the polynomials in $\mathbb{Q}(\kappa)[x_1, \ldots, x_s]$, where absolute factorization can be implemented [20]. However, we must return to the specialization $\mathbb{Q}(\kappa^0)$ for the specific system we are working with. Once we are back in $\mathbb{R}$ we face two problems. The first one is whether the specialized polynomials are still irreducible. It follows from Hilbert's irreducibility theorem that the set of all irreducible specialization, called Hilbert set, is Zariski dense in $\mathbb{Q}^r$, so we may be lucky to have κ^0 in this Hilbert's set. The second problem is related to the strong dependence of ACR on the specific constants of the system. We show in the following example why this might be inconvenient.

Example 6.5.1. *Consider the following polynomials in two variables:*

$$f_1 = (x_1 - (\kappa_1 - 1))(x_1 - (\kappa_2 - 2))$$
$$f_2 = (x_2 - 3)(x_2 - 4)$$

- *If $\kappa_1 > 1$ and $\kappa_2 > 2$, then there is no ACR in any variable.*
- *If $\kappa_1 \leq 1$ and $\kappa_2 \leq 2$, then there are no positive solutions to the system and ACR holds vacuously for the first species.*
- *If $\kappa_1 > 1$ and $\kappa_2 \leq 2$, then it holds that $x_1 - (\kappa_1 - 1) = 0$ for all (x_1, x_2) positive steady state, and hence there is ACR in the first species.*
- *If $\kappa_1 \leq 1$ and $\kappa_2 > 2$, then it holds that $x_1 - (\kappa_2 - 2) = 0$ for all (x_1, x_2) positive steady state, and hence there is ACR in the first species.*

  Visually, this is

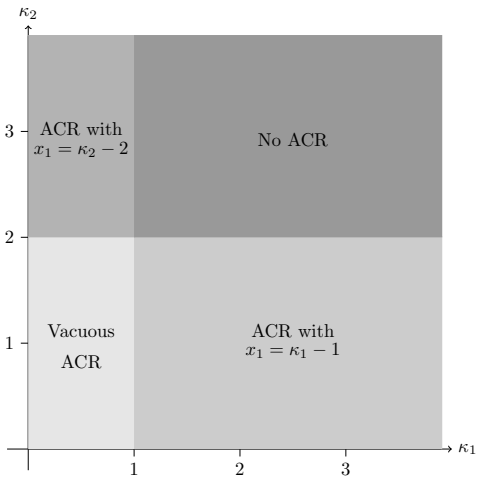

We can see from this example how unstable the system can be.

Another option is to assume $\kappa^0 \in \mathbb{Q}^r$. This is a sensible assumption since one cannot deal with irrational numbers on a computer. However, we have to be careful at approximating our real constants, as the following example points out.

Example 6.5.2. *Consider the following polynomials in two variables:*

$$f_1 = (x_1 - (\kappa - \pi))(x_1 - (\kappa - 3.1415))$$
$$f_2 = (x_2 - 3)(x_2 - 4)$$

Notice that if we approximate κ by 3.1416 or any number bigger than π, then there is no ACR. If we chose instead a number smaller than or equal to 3.1415, the system shows ACR vacuously, since there are no positive steady states for that choice. Finally, if we approximate κ by a number in the interval $(3.1415, \pi]$ then $x_1 = \kappa - 3.1415 > 0$, for all positive steady states (x_1, x_2).

In the literature mentioned above, with the notions of pre-orderings, orderings, real closed fields and real closure, the authors develop the theory for finding the real radical ideal. For instance, a first approach to compute it comes from a result present in Bochnack et al. [12], where with the extra notion of a non-singular point of an ideal they state a criterion that can help us isolate the components of the ideal decomposition that eventually lead us to describe the real zeros.

Definition 6.5.1. *Let R be a real closed field and $P = \langle g_1, \ldots, g_t \rangle$ be a prime ideal of $R[x_1, \ldots, x_s]$ of dimension d. A point $\mathbf{x}$ in $V_R(P)$ is called a* non-singular *point of P when* $\operatorname{rank}\left(\left[\frac{\partial g_i}{\partial x_j}(\mathbf{x})\right]\right) = s - d$.

The following proposition is deduced from Proposition 3.3.15 and Corollary 4.1.8 in [12]:

Proposition 6.5.1. *Let $P = \langle g_1, \ldots, g_t \rangle$ be a prime ideal of $R[x_1, \ldots, x_s]$ of dimension d, with R a real closed field. If P has a non-singular zero in R^s, then $P = \sqrt[R]{P}$.*

This implies that if we could, *in theory*, find the decomposition in prime ideals over $\mathbb{R}$, then we could check for the existence of a non-singular point in each component, and if there is one such point, finding ACR is equivalent to finding CACR in that component. This last procedure is computable (although its complexity is very high [7, Chapter 13]), and in case there is no non-singular point, then all such zeros are in the ideal of the singular points of the corresponding component and the procedure could be repeated in this new ideal of lower dimension. This paragraph roughly describes an algorithm that could be implemented if it were possible to factor over $\mathbb{R}$. For a better understanding of this theoretical algorithm, we refer the reader to Example 6.5.3.

We come back to the assumption of $f_i \in \mathbb{Q}[x_1, \ldots, x_s]$, keeping in mind the warning from Example 6.5.2. We arrive to the following propositions whose proofs are immediate from the discussion above.

Proposition 6.5.2. *Let $f_i \in \mathbb{Q}[x_1, \ldots, x_s]$ for $i = 1, \ldots, s$. Let $\tilde{I}$ be as in* (6.2)*, and assume $\tilde{I} = P_1 \cap P_2$, with $P_1,\ P_2 \subseteq \mathbb{Q}[x_1, \ldots, x_s]$, $V_{\mathbb{R}}(P_2) = \emptyset$. If P_1 shows CACR, then $\tilde{I}$ shows ACR.*

This proposition is similar to Lemma 6.5.2. The main difference is that over the ground field $\mathbb{Q}$ the decomposition of $\tilde{I}$ into $P_1 \cap P_2$ with $P_1,\ P_2 \subseteq \mathbb{Q}[x_1, \ldots, x_s]$ is computable. More in general,

Proposition 6.5.3. *Let $I = \langle f_1, \ldots, f_s \rangle \subseteq \mathbb{Q}[x_1, \ldots, x_s]$. Let $\tilde{I}$ be as in* (6.2)*, if we can write $\tilde{I} = \bigcap_{i=1}^{\ell} Q_i$ with $Q_i \subseteq \mathbb{Q}[x_1, \ldots, x_s]$ prime ideals over $\mathbb{Q}[x_1, \ldots, x_s]$. Assume also that we can regroup these ideals as $P_1 = \bigcap_{i=1}^{\ell'} Q_i$ and $P_2 = \bigcap_{i=\ell'+1}^{\ell} Q_i$ such that $V_{\mathbb{R}}(P_2) = \emptyset$ and $V_{\mathbb{R}}(Q_i) \neq \emptyset$ for $i = 1, \ldots, \ell'$.*

We add two ***main hypotheses****:*

1. *$Q_i \subseteq \mathbb{Q}[x_1, \ldots, x_s]$ is prime over $\mathbb{R}[x_1, \ldots, x_s]$ for $i = 1, \ldots \ell'$,*
2. *for all $i \in \{1, \ldots \ell'\}$, there exists $\mathbf{x} \in V_{\mathbb{R}}(Q_i)$ non-singular.*

Then $\tilde{I}$ shows ACR if and only if P_1 shows CACR.

It is important to notice that every assumption in the statement is checkable/computable except for the first main hypothesis 1.

We end this chapter with an example that shows what could be an algorithm to compute and detect ACR if all the steps involved could be done effectively.

Example 6.5.3. *Consider the following polynomials in two variables:*

$$f_1(\mathbf{x}) = x_1[(x_1-1)^2 + (x_2-2)^2]$$
$$f_2(\mathbf{x}) = x_2[(x_1-1)^2 + (x_2-2)^2].$$

Notice that these polynomials also have the shape: $f_i = p_i - x_i q_i, i = 1, 2$, where all the coefficients of p_i, q_i are non negative. As we mentioned before, it is possible to find a reaction network modeled with mass–action kinetics, such that the associated system is $dx_1/dt = f_1, dx_2/dt = f_2$.

It is easy to see in this example that the system shows ACR for both variables, since the only positive solution is $x_1 = 1$, $x_2 = 2$. However, we will ignore this obvious fact and use a procedure inspired by our previous discussion. All the computations here can be checked using any computer algebra system, such as Macaulay2 [61] and Singular [35].

We consider the ideal $\tilde{I} = \langle f_1, f_2, x_1z_1^2 - 1, x_2z_2^2 - 1\rangle$, which can be decomposed as

$$\tilde{I} = Q_1 \cap Q_2 \cap Q_3 \cap Q_4,$$

with $Q_1 = \langle (x_1-1)^2 + (x_2-2)^2, x_1z_1^2 - 1, x_2z_2^2 - 1\rangle$, $Q_2 = \langle x_1, (x_1-1)^2 + (x_2-2)^2, x_1z_1^2 - 1, x_2z_2^2 - 1\rangle$, $Q_3 = \langle x_2, (x_1-1)^2 + (x_2-2)^2, x_1z_1^2 - 1, x_2z_2^2 - 1\rangle$ and $Q_4 = \langle x_1, y, x_1z_1^2 - 1, x_2z_2^2 - 1\rangle$.

We can easily see that $V_{\mathbb{C}}(Q_2) = V_{\mathbb{C}}(Q_3) = V_{\mathbb{C}}(Q_4) = \emptyset$, hence, we deduce that the real variety of $\tilde{I}$ coincides with the real variety of Q_1 (in symbols, $V_{\mathbb{R}}(\tilde{I}) = V_{\mathbb{R}}(Q_1)$). This ideal Q_1 does not show CACR in any variable, but we could try to use Proposition 6.5.1. As Q_1 is a prime ideal over $\mathbb{R}[x_1, \ldots, x_s, z_1, \ldots, z_s]$ with dimension 1, and $\mathbb{R}$ is a real closed field, we can check if there exists a non-singular point in the real variety of Q_1. We have the generators $g_1 = x_1^2 - 2x_1 + x_2^2 - 4x_2 + 5$, $g_2 = x_1z_1^2 - 1$, $g_3 = x_2z_2^2 - 1$, and let us consider the matrix of partial derivatives:

$$\begin{bmatrix} 2x_1 - 2 & 2x_2 - 4 & 0 & 0 \\ z_1^2 & 0 & 2x_1z_1 & 0 \\ 0 & z_2^2 & 0 & 2x_2z_2 \end{bmatrix}.$$

A real zero is non-singular if this matrix has rank 3 when specialized in that zero. In other words, a real zero is non-singular if there exists a 3×3 minor of this matrix that does not vanish on this zero of the ideal Q_1. All the 3×3 minors of this matrix are $h_1 = (x_1-1)x_1z_1z_2^2$, $h_2 = (x_2-2)x_2z_1^2z_2$, $h_3 = (x_1-1)x_1x_2z_1z_2$, $h_4 = (x_2-2)x_1x_2z_1z_2$. If w_1, w_2, w_3, w_4 are new variables, we can form the ideals $J_i = \langle g_1, g_2, g_3, h_iw_i - 1\rangle$, and finding a non-singular real zero is equivalent to checking if any of the varieties $V_{\mathbb{R}}(J_i)$ is nonempty (we refer the reader to [7, Chapter 13]). Once checked that $V_{\mathbb{R}}(J_i) = \emptyset$ for all $i = 1, \ldots, 4$, we define the ideal $Q_1^{(1)} = \langle g_1, g_2, g_3, h_1, h_2, h_3, h_4\rangle$, whose real variety then coincides with the real variety of $\tilde{I}$,

and has dimension 0 (< 1). We repeat the reasoning for $Q_1^{(1)}$. This ideal can be decomposed in several prime ideals over $\mathbb{R}[x_1, \ldots, x_s]$, most of which can be easily seen to have an empty complex variety, except for the ideal

$$Q_1^{(2)} := \langle x_1 - 1, x_2 - 2, x_1 z_1^2 - 1, x_2 z_2^2 - 1 \rangle,$$

and so $V_{\mathbb{R}}(\tilde{I}) = V_{\mathbb{R}}(Q_1^{(1)}) = V_{\mathbb{R}}(Q_1^{(2)})$. The matrix of partial derivatives for this new ideal is

$$\begin{bmatrix} 1 & 0 & 0 & 0 \\ 0 & 1 & 0 & 0 \\ z_1^2 & 0 & 2x_1 z_1 & 0 \\ 0 & z_2^2 & 0 & 2x_2 z_2 \end{bmatrix},$$

which has full rank at, for example, $(1, 2, 1, \frac{1}{\sqrt{2}})$. Hence, $Q_1^{(2)}$ has ACR if and only if it has CACR, and this is the case for both variables, x_1 and x_2.

In this chapter we started dealing with interesting mathematical questions that have already appeared in other contexts, but now can be located inside the framework of chemical reaction systems. Even assuming mass–action kinetics, the special shape of the equations does not provide much information for finding positive zeros of the system. For instance, if we have two polynomials g_1, g_2 in two variables x_1, x_2, we can build the system $dx_1/dt = x_1 g_1, dx_2/dt = x_2 g_2$, which has the shape $f_i = p_i - x_i q_i, i = 1, 2$, where all the coefficients of p_i, q_i are non negative. As we have done before, it is possible from [68, Theorem 3.2] (see Section 2.1), to find a reaction network modeled with mass–action kinetics, such that the associated system is this one.

Nevertheless, there are systems with special characteristics that may allow to perform the computations needed to be able to describe the real zeros of the polynomial ideal associated to the system.

Chapter 7

A discrete model for the NF-κB module

7.1 Introduction

In this chapter we focus on the NF-κB regulatory module. NF-κB is a ubiquitously expressed family of transcription factors that regulates the expression of numerous genes that play important roles in cellular responses, cell growth, survival and inflammatory and immune responses [57, 70, 110]. It is also involved in numerous sterile and non-sterile diseases such as autoimmunity, cancer and sepsis [130]. Therefore the comprehension of the mechanisms that govern NF-κB responsive gene expression is indispensable for understanding these pathologies and to identify appropriate drug targets.

In mammals, five related gene products participate in NF-κB functions (p50, p52, RelA/p65, RelB and cRel) forming various homo- and heterodimeric complexes with different transcriptional activities and tissue specificities [15, 69]. Among them, p65-p50 heterodimers are the predominant species in many cell types [76].

In resting cells, p65-p50 heterodimers (referred herein as NF-κB) are normally held inactive in the cytoplasm by being bound to a family of proteins called inhibitory κB (IκB) that includes IκBα, -β and -ϵ [58]. Most of the inhibitory potential of this family is carried out by IκBα which is evidenced by the fact that its absence, but not of the other two isoforms, is lethal in mice [11, 101]. In response to various extracellular signals such as tumor necrosis alfa, IL-1 and several pathogens associated molecular patterns, IκB kinase (IKK) complex is transformed from its neutral form into its active form, a form capable of phosphorylating and inducing IκB degradation by the 26S proteasome. Degradation of IκB releases the main activator NF-κB which then translocates to the nucleus, by exposing its nuclear localization signal, where it recognizes DNA elements with the consensus sequence 5'-GGGRNYYYCC-3' (R is any purine, Y is any pyrimidine, and N is any nucleotide) and triggers transcription of numerous genes including IκB [18, 89, 91, 105, 154]. The newly synthesized IκB enters the nucleus leading NF-κB to the cytoplasm by means of the nuclear export signal present in IκB [84]. NF-κB regulation of IκB transcription represents a delayed negative feedback loop that drives oscillations in NF-κB translocation to the nucleus [85, 86, 122].

The NF-κB signaling pathway has an additional negative regulation step mediated by the protein A20, a zinc finger deubiquitylating enzyme that inactivates the regulatory subunit of the IKK complex, IKK$_\gamma$/NEMO, as well as several transducing proteins that link receptor activation to IKK activation such as TRAF6, RIP1 and RIP2. A20, as IκB, is also induced by NF-κB,

participating in a negative feedback loop that blocks IKK signaling and renders the complex inactive following initial NF-κB translocation to the nucleus [26, 109, 155, 172]. A sketch of these interactions can be seen in Figure 7.1.

This chapter presents the core regulatory network of this pathway, reconstructed from published molecular data. It is the product of joint work with Juan Ignacio Fuxman Bass and Abdul Salam Jarrah. The reconstructed network was modeled incorporating an approach different from the one used in the previous chapters: we model it as a *discrete dynamical system*, with a qualitative deterministic approach. This type of modeling has been previously applied to various regulatory networks [1, 115]. The network encompasses 11 nodes, namely S (the stimulus), IKKneutral, IKKactive, IKKinactive, IκB, IκB|NF-κB, IκBnuclear, IκBtranscript, A20transcript, A20, as well as their cross-regulatory interactions. The strategy used is based on a bottom-up approach, starting with an extensive overview of published molecular data to reconstruct the underlying biological network. The NF-κB signaling pathway has also been approached with models of differential equations: the level of mRNAs, proteins, and other components are assumed to be continuous functions of time, and the evolution of these components within a cell is modeled by differential equations with mass–action kinetics or other rate laws for the production and decay of all components [110]. Our work will be mostly based upon the molecular data present at Lee et al. [109] and Hoffmann et al. [76], and the continuous model developed by Lipniacki et al. [110].

7.2 Background on modeling tools

Modeling tools in mathematical biology include a spectrum of methods beyond the traditional and very successful continuous models, with the introduction of Boolean network models in the 1960s and the more general so-called logical models in the 1980s. Since then, other methods have been added, in particular Petri nets as models for metabolic and molecular regulatory networks. More recently, agent-based, or individual-based models, long popular in social science, have been used increasingly in areas ranging from molecular to population biology. Discrete models such as these have many useful features. Qualitative models of molecular networks such as logical models, do not require kinetic parameters but can still provide information about network dynamics and serve as tools for hypothesis generation. Structural and qualitative analysis is emerging as a feasible and useful alternative [124, 134, 171]. On the other hand, quantitative dynamic models are usually difficult to construct and validate because of the scarcity of known mechanistic details and kinetic parameters. Moreover, discrete models have the advantage of being more intuitive than models based on differential equations, so they have added appeal for researchers without a strong mathematical background.

Most models can be classified by three dimensions of modeling: continuous and discrete; quantitative and qualitative; stochastic and deterministic. However, these dimensions are not entirely independent nor are they exclusive. Many modeling approaches are hybrid as they combine continuous and discrete, quantitative and qualitative, stochastic and deterministic aspects.

With respect to time, in synchronous models, the state of each node is updated simultaneously at multiples of a common time step. Thus the future state means the state at the next time step. Asynchronous models, however, update the state of each node individually. Syn-

chronous models have deterministic state transitions, asynchronicity introduces stochasticity (update order dependence) in the dynamics.

For many biological networks, and in particular genetic control or regulatory networks, detailed information on the kinetic rates of protein-protein or protein-DNA interactions is rarely available. However, for many biological systems, evidence shows that regulatory relationships can be modeled as sigmoidal and be well approximated by step functions. In this case, Boolean models, where every variable has only two states (ON/OFF), and the dynamics is given by a set of logical rules, are frequently appropriate descriptions of the network of interactions among genes and proteins. First proposed by Kauffman [94], Boolean network models have the advantage of being more intuitive than ODE models. He used Boolean networks to study the dynamics of gene regulatory networks [93–95]. A gene is assumed to be in one of two states, expressed or not expressed, and is modeled by a binary value 1, 0, respectively. The next state of a gene is determined by a Boolean function in terms of the current states of the gene and its immediate neighbors in the network.

An important (continuous) model for *Drosophila melanogaster* segment polarity genes was first developed in von Dassow et al. [169], where a thorough investigation of the parameter space showed that the system is very robust with respect to variations in the kinetic constants. They concluded that the topology of the network is more important than the fine-tuning of the kinetic parameters, since its results are robust for a large region of parameter (scaling factor, activation threshold) space. To investigate this, Albert and Othmer [1] proposed and analyzed a Boolean model of the network of regulatory interactions throughout several stages of embryonic development of the *Drosophila* segment polarity genes. It was based on a binary ON/OFF representation of mRNA and protein levels, and the interactions were formulated as logical functions. The spatial and temporal patterns of gene expression were determined by the topology of the network and whether components were present or absent, rather than the absolute levels of the mRNAs and proteins and the functional details of their interactions. The model was able to reproduce the wild-type gene expression patterns, as well as the ectopic expression patterns observed in overexpression experiments and various mutants. Furthermore, they computed explicitly all steady states of the network and identified the basin of attraction of each steady state. Both the continuous model and the discrete model agree in their overall conclusions regarding the robustness of the segment polarity gene network.

In the work of Chaves et al. [17], they apply two methods for adapting qualitative models to incorporate the continuous-time character of regulatory networks to the Boolean model of the segment polarity gene network of *Drosophila melanogaster* in [1]. The first method consists of introducing asynchronous updates in the Boolean model. In the second method, they adopt the approach introduced by L. Glass [59] to obtain a set of piecewise linear differential equations which continuously describe the states of each gene or protein in the network. They analyze the dynamics of the model, and provide a theoretical characterization of the model's gene pattern prediction as a function of the timescales of the various processes.

In many cases, the biological information about a particular network node might not be sufficient, however, to construct a logical function governing regulation. In the case of a continuous model, the remedy would be to insert a differential equation of specified form, e.g., mass action kinetics, with unspecified parameters. If experimental time course data for the network is available, then one can use one of several existing inference methods to estimate a function that will result in a model that fits the data. Data fit is determined by model simulation,

using numerical integration of the equations in the model. Note, however that parameters are not always identifiable from the dynamics [33].

The software package described in [41] addresses the need for a discrete analogue of this process. In the case of missing information about a particular node in the network to be modeled, one can insert a general Boolean function, maybe of a specified type, e.g., a nested canalyzing function. This is most easily done by viewing the Boolean function as a general polynomial, with undetermined (0/1) coefficients. This function in addition satisfies a specified optimality criterion, similar to the optimality criterion for the fitting of continuous parameters. This process might be considered the discrete analogue of parameter estimation. The software package described there integrates several different inference methods to accomplish this purpose. It furthermore couples parameter estimation with extensive simulation capabilities. For instance, it is increasingly likely that Boolean models using sequential update of the variables are more realistic than parallel update systems. Moreover, it has been shown that stochastic models are sometimes more appropriate than deterministic ones. The software package Polynome has the capability of simulating models deterministically as well as stochastically. The stochastic features can arise either through random update schedule choice or random choice of functions at each update. Update-stochastic networks are common in the general framework of logical models, and function-stochastic models have been introduced and used by Shmulevich and collaborators [145].

One of the disadvantages of the Boolean network modeling framework is the need to discretize real-valued expression data into an ON/OFF scheme, which loses a large amount of information. In response to this deficiency, multi-state discrete models and hybrid models have been developed. The most complex one [158, 159, 161] uses multiple states for the genes in the network corresponding to certain thresholds of gene expression that make multiple gene actions possible. The authors are most interested in the modeling and function of feedback loops. The model includes a mixture of multi-valued logical and real-valued variables, as well as the possibility of asynchronous updating of the variables. While this modeling framework is capable of better capturing the many characteristics of gene regulatory networks than Boolean networks, it also introduces substantially more computational complications from a reverse-engineering point of view.

Other examples of logical models include models of genetic networks in the fruit fly *Drosophila melanogaster* [135] and the flowering plant *Arabidopsis thaliana* [44, 116].

Milo et al. [118] show that certain graph theoretic motifs appear far more often in the topology of regulatory network graphs than would be expected at random. In [97, 98, 120] it was shown that a certain type of Boolean regulatory logic has the kind of dynamic properties one would expect from molecular networks. And in [67] it was shown that logical rules that appear in published Boolean models of regulatory networks are overwhelmingly of this type. These rules, so-called nested canalyzing rules, are a special case of canalyzing rules, and they have been broadly studied [88, 121]. In [128], Ribba et al. present a multiscale model of cancer growth and examine the qualitative response to radiotherapy. The mathematical framework includes a Boolean description of a genetic network relevant to colorectal oncogenesis, a discrete model of the cell cycle and a continuous macroscopic model of tumor growth and invasion.

A major drawback that discrete models of biological systems have is the relative lack of mathematical analysis tools. While methods like bifurcation, sensitivity, and stability analysis

are available for differential equations models, the principal tool in the discrete case is simulation. This is very effective for small models, but it becomes impossible for larger models, since the size of the phase space is exponential in the number of variables in the model. Thus, problems like the identification of steady states for a Boolean network model become difficult once the model contains many more than 20 or 30 nodes, unless one makes use of high performance computation capabilities. An added complication is the heterogeneity of the different discrete model types so that tools developed for one type are unlikely to apply to another one.

Agent-based models are a class of computational models for simulating the actions and interactions of autonomous agents with a view to assessing their effects on the system as a whole. A natural way to approximate them by state space models that are grounded in a richer mathematical theory and satisfies the constraints discussed above is to construct an algebraic model specification, that is, a discrete time, discrete state dynamical system whose state space represents exactly the dynamic properties of the agent-based models. Algebraic models can be described by polynomial functions over finite fields, which provides access to the rich algorithmic theory of computer algebra and the theoretical foundation of algebraic geometry. In Hinkelmann et al. [75], they propose such a framework, which preserves all features of agent-based models and provides access to mathematical analysis tools and they demonstrate the added value that is gained from such a mathematical description through a collection of examples.

The mathematical framework is that of polynomial dynamical systems over a finite field, which provides access to theoretical and computational tools from computer algebra and discrete mathematics. An algebraic structure of addition and multiplication is imposed on the set of possible states of the model variables to obtain a field. (This has long been made in the case of Boolean networks, where the choice of underlying field is the Galois field $\mathbb{F}_2 = \{0, 1\}$.) This is possible whenever the number of states for a given variable is a power of a prime number.

A finite dynamical system is a time-discrete dynamical system on a finite state set. That is, it is a mapping from a cartesian product of finitely many copies of a finite set to itself. Dynamics is generated by iteration of the mapping. Once we choose such an algebraic structure $\mathbb{F}$, then the set function description of an agent-based model turns into a mapping between vector spaces over the finite field $\mathbb{F}$, which can be described in terms of polynomial coordinate functions.

More explicitly,let A be the set of possible states of the network nodes, and we assume that A is a finite set. Consider

$$f : A^n \to A^n,$$

iteration of f results in a time-discrete dynamical system over A of dimension n. And f can be described in terms of its coordinate functions $f_i : A^n \to A$, for $i = 1, \ldots, n$. This is, if $\mathbf{x} = (x_1, \ldots, x_n) \in A^n$ is a state, then $f(\mathbf{x}) = (f_1(\mathbf{x}), \ldots, f_n(\mathbf{x}))$. We will refer to such a system as *finite dynamical system*. [1]

If A has $q = p^r$ elements, for some prime p, we can render the structure of a finite field to A (we denote it as $\mathbb{F} := A$), and then any coordinate function $f_i : \mathbb{F}^n \to \mathbb{F}$ can be described by a unique polynomial in $\mathbb{F}[x_1, \ldots, x_n]$ of degree less than q in each variable.

As mentioned in [75], polynomials are neither intuitive nor are they simple functions. But *they provide an exact representation of the dynamics of the model that is more compact than the*

[1] For those readers who are familiar with the notation from the previous chapters, notice that here f_i describes the "trajectory" of the i-th node, and not the "derivative". Actually, f_i describes the state of node i at the following time step, depending on the present state of all nodes.

state space, which is not feasible to describe for most realistic models. Any computer algebra system can be used to analyze a polynomial system, independent of a particular software or implementation. The polynomials can be generated in an almost automatic way: a simple script is provided to generate the polynomials that interpolates a given truth table, and tables are easily generated from the description of the model.

The rigorous mathematical language is another advantage of the framework: the rich algorithmic theory from computer algebra and the theoretical foundation of algebraic geometry are available to analyze algebraic models. Furthermore, in [166], it was shown that logical models [160] as well as Petri nets [150] could be viewed and analyzed as algebraic models.

But, unless all the correspondences are known, the polynomials f_i cannot be determined. For general networks only a few *transition pairs* are known. This means, the data available is of the form $\mathbf{s}_1, \dots \mathbf{s}_m, \mathbf{t}_1, \dots, \mathbf{t}_m \in \mathbb{F}^n$, where $f(\mathbf{s}_i) = \mathbf{t}_i$, and usually $m << q^n$. Hence, there are many options for possible models after applying any reverse-engineering method.

In [107], Laubenbacher and Stigler describe the dynamics of the network from data of this form. They find for each coordinate a minimal interpolator polynomial, in the sense that there is no nonzero polynomial $g_i \in \mathbb{F}[x_1, \dots, x_n]$, that arises from reodering and regrouping the terms of f_i, such that $f_i = h_i + g_i$ and $g_i(\mathbf{s}_j) = 0$ for all $j = 1, \dots, m$, $i = 1, \dots, n$. For this, they choose the normal form of some interpolator with respect to a Gröbner basis for the ideal of $\{\mathbf{s}_1, \dots, \mathbf{s}_m\}$. One of the biggest problems for this choice is that it strongly depends on the particular monomial order chosen for computing the Gröbner basis. Different orderings of the monomials can give rise to different polynomial models, since the algorithm uses such an order for multivariate polynomial division, and there is no canonical choice for monomial orderings.

In [40], Dimitrova et al. present a systematic method for selecting most likely polynomial models for a given data set, using the Gröbner fan of the ideal of the input data. The Gröbner fan of a polynomial ideal [119, 153] is a combinatorial structure, which is a polyhedral complex of cones in which every point encodes a monomial ordering. The cones are in bijective correspondence with the distinct Gröbner bases of an ideal. (To be precise, the correspondence is to the marked reduced Gröbner bases of the ideal.) Therefore, it is sufficient to select exactly one monomial ordering per cone and, ignoring the rest of the orderings, still guarantees that all distinct reduced models are generated.

Some methods aim to discover only the network topology, that is, which genes regulate which others, with a directed graph or "wiring diagram" as output, possibly signed to indicate activation or inhibition. This static network is a directed graph showing the influence relationships among the components of the network, where an edge from node y to node x implies that changes in the concentration of y could change the concentration of x. The goal of other methods is to describe the dynamics of the network, which describes how exactly the concentration of x is affected by that of y. Due to the fact that biological networks are not well-understood and the available data about the network is usually limited, many models end up fitting the available information and the criteria for choosing a particular model are usually not biologically motivated but rather a consequence of the modeling framework.

The model in [87] is based on the primary decomposition of a monomial ideal generated from the data. Here they are only interested in describing the causal relations among the nodes of the network. This is why the aim is to find, for each coordinate, minimal (according to inclusion) sets of variables for which there exists an interpolator.

So far, we have presented a general overview of what discrete modeling concerns. We develop in subsequent sections a *discrete qualitative deterministic algebraic model* for the NF-κB regulatory module. To be more precise, it is a polynomial dynamical system over the ground field $\mathbb{F}_3$.

Before introducing our model, we review a continuous model of this regulatory network done by Lipniacki et al. [110].

7.3 A continuous model for the NF-κB module

In this section, we summarize the modeling considerations presented in Lipniacki et al. [110], and we add some analysis of our own, regarding the steady states of the system they present and the conservation relations that arise from the equations. The results of their work will be presented later, together with our discrete model results.

They apply ordinary differential equations to model the NF-κB regulatory network. A model is constructed that includes two regulatory feedback loops; the first involving the protein IκBα and the second involving the protein A20. The kinetics considered involves formation and dissociation of complexes, catalysis, mRNA synthesis and translations as well as transport between the nucleus and the cytoplasm (considering their respective volumes). The proposed model involves a very restricted number of components: RNA transcripts, proteins and complexes, which were found to be the most important ones. Using this limited number of components they attempted to model the NF-κB regulatory module, which in fact involves a much larger set of components, and whose true kinetics is much more complicated. There are two main reasons for the simplifications they made. First, they did not have enough data, second a more elaborate model would be possibly too difficult to analyze; at least the parameter fitting would be both very difficult and ambiguous.

The main simplifications and implicit assumptions of the model were firstly that they neglected the formation of NF-κB and IKK, which are protein complexes themselves, as the kinetics leading to their formation are complicated. Secondly, the inhibitory proteins A20 and IκBα were considered to mimic a collective action of groups of inhibitors. Particularly, they approximated the collective action of all IκB isoforms by the IκBα; which is the most active and abundant one, and the knockout of which, in contrast to the other two isoforms, is lethal. Finally, they assumed that all other proteins, some known, some unknown, which they do not account for in the pathway, remain at their normal levels.

The authors amend the model in Hoffmann et al. [76] taking into account the difference between the nuclear and the cytoplasmic volume generating a two-compartment kinetics; they also impose an upper bound for the amount of free IκBα; and finally they re-estimate the mRNA transcription and translation coefficients.

Because of a large number of undetermined parameters they decided to carry out the fit "manually" rather than to try to quantify the data, which are in the form of blots (which are a method of transferring proteins, DNA or RNA, onto a carrier that can be, for example, a nylon membrane), and then to apply one of the fitting engines available. The first reason they considered was that such quantification is by no means unique, the second was that when fitting, they would have had to take into account diverse, usually not precise, information coming from different researchers and their own intuitive understanding of the process. For the fitting, the

authors start from a reasonable set of parameters, which produces a correct steady state in the absence of stimulus. Secondly, they proceed with the signal initiated by the stimulus along the autoregulation loop. Finally, they iterate the second step until the fit to all the data is satisfactory.

They note that although it is not easy to find a fitting set of parameters, once the satisfactory fit is found, it is not difficult to find other sets which are almost equivalent for rendering approximately the same trajectories.

To reach the resting cell equilibrium state, they start the simulation 101 hours prior to the signal being turned on. At t = 1 hour, the rectangular signal of the stimulus is turned on for 6 hours to the end of the simulation time.

Typical available experimental data consist of measurements made in time points that are not uniformly distributed. The non-uniform distribution reflects the fact that during the first hour, the oscillations are more rapid and more measurements are needed to accurately trace the dynamic. Therefore, to compare their solutions with experimental data, Lipniacki et al. rescaled the time coordinate. The total amount of NF-κB is kept constant in the course of simulation, and it is set by assuming the initial concentration of cytoplasmic complexes IκB—NF-κB.

After parameter fitting, the proposed model in [110] is able to properly reproduce time behavior of all variables for which the data are available: NF-κB, cytoplasmic IκBα, A20 and IκB mRNA transcripts, IKK and IKK catalytic activity in both wild-type and A20-deficient cells. The model allowed detailed analysis of kinetics of the involved proteins and their complexes and gave the predictions of the possible responses of the whole kinetics to the change in the level of a given activator or inhibitor.

There is also a mathematical model in [174] but the authors disregard the influence of A20, whose inhibitory potential was demonstrated by Lee et al. [109], who found that the knockout of A20 in mice dramatically alters the cells response to TNF stimulation due to persistent IKK activity, and causes A20-/- deficient mice to die prematurely.

Using tools from the previous chapters, we analyze below the steady states arising from the equations in [110] considering the stimulus (TNF) as persistent (that is, TNF$\equiv$1), and the constants listed in their Appendix.

Making the correspondence: $x_1 =$ IKKn, $x_2 =$ IKKa, $x_3 =$ IKKi, $x_4 =$ IKKa|IκBα, $x_5 =$ IKKa|IκBα|NF-κB, $x_6 =$ NF-κB, $x_7 =$ IκBα|NF-κB, $x_8 =$ NF-κB$_n$, $x_9 =$ IκBα_n, $x_{10} =$ IκBα_n|NF-κB$_n$, $x_{11} =$ A20, $x_{12} =$ A20$_t$, $x_{13} =$ IκBα, $x_{14} =$ IκBα_t, and considering the parameters in the Appendix of [110] we can describe the differential equations in this paper as follows.

$\dot{x}_1 = \frac{25}{1000000} - (\frac{125}{1000000} + \frac{25}{10000})x_1;$
$\dot{x}_2 = \frac{25}{10000}x_1 + \frac{1}{10}x_4 - (\frac{125}{1000000} + \frac{15}{10000})x_2 - \frac{2}{10}x_2x_{13} - \frac{1}{10}x_2x_{11} - x_2x_7 + \frac{1}{10}x_5;$
$\dot{x}_3 = \frac{15}{10000}x_2 + \frac{1}{10}x_2x_{11} - \frac{125}{1000000}x_3;$
$\dot{x}_4 = -\frac{1}{10}x_4 + \frac{2}{10}x_2x_{13};$
$\dot{x}_5 = x_2x_7 - \frac{1}{10}x_5;$
$\dot{x}_6 = \frac{1}{10}x_5 - \frac{5}{10}x_{13}x_6 + \frac{2}{100000}x_7 - \frac{25}{10000}x_6;$
$\dot{x}_7 = -x_2x_7 + (\frac{5}{10})x_{13}x_6 - \frac{2}{100000}x_7 + \frac{1}{100}x_{10};$
$\dot{x}_8 = -\frac{5}{10}x_9x_8 + \frac{125}{10000}x_6;$

$\dot{x}_9 = -\frac{5}{10}x_9x_8 - \frac{25}{10000}x_9 + \frac{5}{1000}x_{13}$;
$\dot{x}_{10} = -\frac{5}{100}x_{10} + \frac{5}{10}x_9x_8$;
$\dot{x}_{11} = \frac{5}{10}x_{12} - \frac{3}{10000}x_{11}$;
$\dot{x}_{12} = \frac{5}{10000000}x_8 - \frac{4}{10000}x_{12}$;
$\dot{x}_{13} = -\frac{2}{10}x_2x_{13} - \frac{5}{10}x_{13}x_6 + \frac{5}{10000}x_9 - (\frac{1}{1000} + \frac{1}{10000})x_{13} + \frac{5}{10}x_{14}$;
$\dot{x}_{14} = \frac{5}{10000000}x_8 - \frac{4}{10000}x_{14}$;

The polynomials on the right-hand side have the following shape: $f_i = p_i - x_iq_i, i = 1, 2$, where all the coefficients of p_i, q_i are non negative. It follows from [68, Theorem 3.2], as we mentioned at the end of Section 2.1, that it is possible to find a reaction network modeled with mass action kinetics, such that the associated system is $dx_i/dt = f_i$, $i = 1, \ldots, 14$. This encourages us to examine the system as the mass–action systems we studied in the previous chapters.

Lemma 7.3.1. *When the stimulus is persistent (TNF≡1), the system of differential equations in [110] (with the reaction constants listed in their Appendix) has a positive steady state if and only if the concentration of IKKa satisfies* $0 < [IKKa] < \frac{4}{273}$. *Moreover, for each* $[IKKa] \in (0, \frac{4}{273})$ *there is a unique positive steady state.*

Proof. By elimination, using the computer algebra system Singular [35], we find the following polynomials in the ideal generated by the equations of the system in [110].

$g_1 = 105x_1 - 1$
$g_3 = 21x_3 + 21x_2 - 4$
$g_4 = x_4 - 2x_{13}x_2$
$g_5 = x_5 - 10x_7x_2$
$g_6 = x_6 - 32000x_9x_{12}$
$g_7 = (1254400x_2^2(273x_2 - 4)(50000x_2 + 1)^2)x_7^2 - (448x_2(50000x_2 + 1)(2744000000x_2^4 - 71036000x_2^3$
$-1024849x_2^2 + 10612x_2 - 80))x_7 - ((56000x_2^2 - 245x_2 + 4)(-4 + 273x_2)^2)$
$g_8 = x_8 - 800x_{12}$
$g_9 = 49x_9x_2 - 2x_9 + 175x_{13}x_2$
$g_{10} = x_{10} - 8000x_9x_{12}$
$g_{11} = 3x_{11} - 5000x_{12}$
$g_{12} = 28000000x_{12}x_2 + 273x_2 - 4$
$g_{13} = (5600000x_2(-4+273x_2))x_{13}^2+(11200x_2(49000x_2^2-1293x_2-11))x_{13}+((-4+273x_2)(49x_2-2))$
$g_{14} = x_{14} - x_{12}$

From g_{12}, we notice that x_2 has to be less than $\frac{4}{273}$ in order to have a positive twelfth coordinate. And then, analyzing in detail g_7 and g_{13}, we find that if $x_2 \in \left(0, \frac{4}{273}\right)$, there exists only one positive solution for the seventh and thirteenth coordinates. We can then solve for the other coordinates i using the corresponding g_i. □

It can be shown that there is a single conservation relation arising from the equations in [110]:

$5[\text{IKKa}|\text{I}\kappa\text{B}|\text{NF-}\kappa\text{B}] + 5[\text{NF-}\kappa\text{B}] + 5[\text{I}\kappa\text{B}|\text{NF-}\kappa\text{B}] + [\text{NF-}\kappa\text{B}_n] + [\text{I}\kappa\text{B}_n|\text{NF-}\kappa\text{B}_n] = \text{C}$.

Moreover, using Singular [35], it can be seen that the dimension of the ideal generated by the equations of the system and the conservation relation has dimension zero.

The continuous model has numerous unknown parameters. In fact, according to [99], in the case of the NF-κB signaling module, one-third of the parameters are known with a high degree of confidence, one-third are significantly constrained by literature data, and the remaining third has to be derived from parameter fitting (note that we took in Lemma 7.3.1 the values proposed in [110] after fitting and adjusting to the literature.)

7.4 Algebraic modeling of the network

As we mentioned, we propose a *discrete qualitative deterministic algebraic model* for the NF-κB regulatory module. In this section we present our model and how it was built.

7.4.1 A toy model

To illustrate how our model was built, let us start with a toy example that will introduce us to the reasoning used while building a discrete model. Let us assume that we have two nodes x_1 and x_2 (two chemical species, for example), and we somehow know that each one influentiate the other positively, i.e. each one leads to the formation (or activation) of the other one. We could represent this network as

$$x_1 \rightleftarrows x_2.$$

If we discretize the quantities of each species into three levels (0,1 and 2), we have 3^{18} possible models $f = (f_1, f_2) : \mathbb{F}_3^2 \to \mathbb{F}_3^2$ that describe the behavior of each node.

We can start reducing the spectrum of possible models by assuming in this case that, if there is no x_1 nor x_2, then there will not be any at any moment. In other words, if f_1 and f_2 describe the behavior of x_1 and x_2, respectively, then $f_1(0,0) = f_2(0,0) = 0$ (which can be abbreviated to $(0,0) \mapsto (0,0)$).

We may also want to adjust our model to the mass–action kinetics system:

$$x_1 \underset{\kappa_2}{\overset{\kappa_1}{\rightleftarrows}} x_2.$$

This leads to the system of differential equations

$$\begin{cases} \frac{dx_1}{dt} &= -\kappa_1 x_1 + \kappa_2 x_2 \\ \frac{dx_2}{dt} &= \kappa_1 x_1 - \kappa_2 x_2 \end{cases}$$

The only conservation relation for this system is

$$x_1(t) + x_2(t) = x_1(0) + x_2(0) \text{ for all } t \geq 0, \tag{7.1}$$

and its unique equilibrium is $\tilde{x}_1 = (x_1(0)+x_2(0))\frac{\kappa_2}{\kappa_1+\kappa_2}$, $\tilde{x}_2 = (x_1(0)+x_2(0))\frac{\kappa_1}{\kappa_1+\kappa_2}$. Moreover, as this system of ODEs is linear, we can solve the equations and we get

$$\begin{aligned} x_1 &= \frac{x_1(0)+x_2(0)}{\kappa_1+\kappa_2}\kappa_2 - \frac{\kappa_2 x_2(0) - \kappa_1 x_1(0)}{\kappa_1+\kappa_2} exp(-(\kappa_1+\kappa_2)t), \\ x_2 &= \frac{x_1(0)+x_2(0)}{\kappa_1+\kappa_2}\kappa_1 + \frac{\kappa_2 x_2(0) - \kappa_1 x_1(0)}{\kappa_1+\kappa_2} exp(-(\kappa_1+\kappa_2)t). \end{aligned}$$

Therefore, the derivatives are:

$$\dot{x}_1 = (\kappa_2 x_2(0) - \kappa_1 x_1(0))exp(-(\kappa_1 + \kappa_2)t),$$
$$\dot{x}_2 = (\kappa_1 x_1(0) - \kappa_2 x_2(0))exp(-(\kappa_1 + \kappa_2)t).$$

Returning to our discrete model, if we want it to reproduce the results from the continuous mass–action kinetics model, we can do our parameter fitting to reduce the model space, adding the following assumptions.

We want to translate into the discrete setting the fact that the total amount of x_1 and x_2 remains constant at all times, by the conservation relation in (7.1). One could expect that there exists a function $\varphi : \mathbb{F}_3 \times \mathbb{F}_3 \to \mathbb{F}_3$ such that $\varphi(f_1, f_2) = \varphi(x_1, x_2)$ and also

$$\begin{aligned}\varphi(0,0) =& 0\\ \varphi(1,0) =& \varphi(0,1) = 1\\ \varphi(2,y) =& \varphi(x,2) = 2 \text{ for all } x, y \in \{0,1,2\}\\ \varphi(1,1) =& \alpha \in \{1,2\}.\end{aligned}$$

Then, as all functions from $\mathbb{F}_3 \times \mathbb{F}_3$ to $\mathbb{F}_3$ can be described with polynomials in two variables with degree at most 2 in each variable, we interpolate and find that the shape of φ is

$$\varphi_\alpha(x,y) = x + y + xy + \alpha(xy + x^2y + xy^2 + x^2y^2). \tag{7.2}$$

We call such a function a *pseudo conservation relation*.

Let us, for the moment assume $\kappa_1 \approx 0$ and $\kappa_2 \gg \kappa_1$. This is similar to assuming that the reaction $x_1 \xrightarrow{\kappa_1} x_2$ does not exist, and hence we could ask

$$\begin{aligned}f_1(x,0) =& x \text{ for all } \ x \in \{0,1,2\}\\ f_1(2,y) =& 2 \text{ for all } \ y \in \{0,1,2\}\\ f_2(x,y) =& c_y \text{ for all } \ x, y \in \{0,1,2\} \text{ and } c_0 = 0.\end{aligned}$$

If we start at $(1,1)$, one would expect $\kappa_2 x_2(0) > \kappa_1 x_1(0)$, and therefore x_1 would be increasing and x_2 decreasing, leading us to assume $f_1(1,1) \neq 0$ and $c_1 \leq 1$.

We can summarize the case $\kappa_1 \approx 0$ and $\kappa_2 \gg \kappa_1$ in the following *transition table* (or truth table), where $c_1, \ldots, c_6$ are parameters to be determined:

x_1	x_2	f_1	f_2
0	0	0	0
1	0	1	0
2	0	2	0
0	1	c_3	c_1
1	1	c_4	c_1
2	1	2	c_1
0	2	c_5	c_2
1	2	c_6	c_2
2	2	2	c_2

As we mentioned above, we want $c_1 \leq 1$, $f_1(1,1) \geq 1$ (that is, $c_4 \geq 1$), and all the parameters should also satisfy more restrictions arising from the condition $\varphi(f_1, f_2) = \varphi(x_1, x_2)$.

By now, we have reduced the space of possible models, but we still have many options satisfying the conditions above. To narrow down the search to one model, it is necessary to add more criteria for the discrete model to satisfy. One sensible choice for our toy example with $\kappa_1 \approx 0$ and $\kappa_2 \gg \kappa_1$ could be

x_1	x_2	f_1	f_2
0	0	0	0
1	0	1	0
2	0	2	0
0	1	1	0
1	1	2	0
2	1	2	0
0	2	2	0
1	2	2	0
2	2	2	0

This model satisfies the pseudo conservation relation $\varphi_\alpha(f_1, f_2) = \varphi(x_1, x_2)$ for $\alpha = 2$.

With a similar analysis, a sensible model for $0 < \epsilon < \kappa_1 \ll \kappa_2$ could be

x_1	x_2	f_1	f_2
0	0	0	0
1	0	1	0
2	0	2	1
0	1	1	0
1	1	2	0
2	1	2	1
0	2	2	0
1	2	2	0
2	2	2	1

And for $\kappa_1 \approx \kappa_2$ it would be

x_1	x_2	f_1	f_2
0	0	0	0
1	0	1	0
2	0	1	1
0	1	0	1
1	1	1	1
2	1	1	2
0	2	1	1
1	2	2	1
2	2	2	2

One can check that in both cases, the resulting functions f_1, f_2 satisfy $\varphi_\alpha(f_1, f_2) = \varphi_\alpha(x_1, x_2)$ for $\alpha = 2$.

7.4.2 Coming back to NF-κB: our model

The model

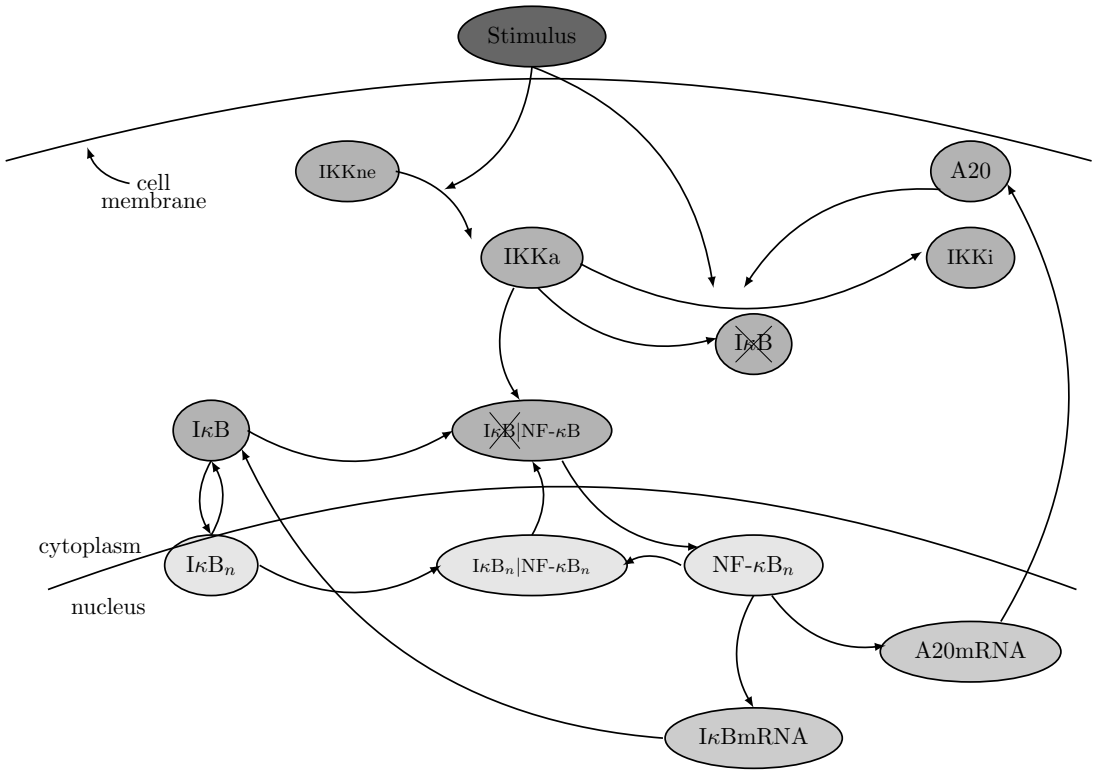

Figure 7.1: A sketch of the NF-κB regulatory module. Upon stimulation, neutral IKKne is transformed into its active form IKKa. Active IKKa forms complexes with IκB and IκB|NF-κB; and strongly catalyzes IκB degradation. Liberated NF-κB enters the nucleus where it binds to κB motifs in A20, IκB or other gene promoters. The newly synthesized IκB enters the nucleus and leads NF-κB again to cytoplasm, while newly synthesized A20 triggers transformation of IKKa into inactive IKKi.

In order to describe the dynamics between the components of the NF-κB signaling pathway, we construct a discrete model from published molecular data. We conceive these components in a network with eleven nodes which can take at most three levels (i.e., we discretize the data into the levels $\{0, 1, 2\}$) and we then build a polynomial dynamical system $f : \mathbb{F}_3^{11} \to \mathbb{F}_3^{11}$. The corresponding transition tables that lead us to the 11 polynomials are present in Appendix 1. These tables were derived from experimental data and completed by considerations discussed in Section 7.4.2. We formed the eleven functions corresponding to each node using the computer algebra system Singular [35].

To be precise, the eleven nodes are S (the stimulus), IKKneutral (IKKne), IKKactive (IKKa), IKKinactive (IKKi), IκB, IκB|NF-κB, IκBnuclear (IκB$_n$), IκBtranscript (IκB$_t$), A20transcript (A20$_t$), and A20. We discretized the observed quantities of each molecule in the data into two or three levels. Nine of the eleven nodes in the network have three associated levels ("low", "medium" and "high"), whereas the other nodes have only two. The notation is equivalent to assigning values 0, 1 and 2 in the first case, and 0 and 1 in the second. The stimulus has been

assigned two levels corresponding to its presence or absence. According to the observed western blots, A20 can also be discretized into two levels (either it is present, or it is not). The rest of the nodes have been assigned three levels according to the different results they could lead to in the observed experimental data. We can summarize this information in the following figure.

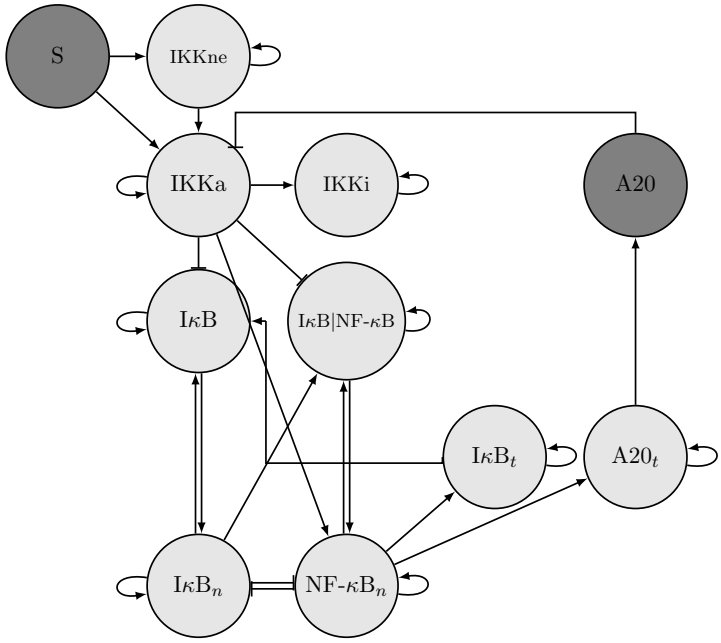

Light gray circles show the nodes that are modeled as ternary variables, whereas dark gray circles correspond to the nodes modeled as binary variables. The activatory interactions are represented by pointed arrows, and the inhibitory interactions by terminating segments.

Notation Guide:

- IKKne–cytoplasmic level of the neutral form of IKK,
- IKKa–cytoplasmic level of the active form of IKK,
- IKKi–cytoplasmic level of the inactive form of IKK,
- IκB–cytoplasmic level of IκBα,
- IκB$_n$–nuclear level of IκBα,
- IκB$_t$–IκB mRNA transcript level,
- IκB|NF–κB–cytoplasmic level of IκB|NF-κB complexes,
- A20–cytoplasmic level of A20 protein,
- A20$_t$–A20 mRNA transcript level,
- NF-κB$_n$–nuclear level of NF-κB,
- S–stimulus.

Justification

In this section we discuss how the transition tables present in Appendix 1 were derived from experimental data, and present the considerations that were used to complete these tables.

IKK activation and inactivation:

The cytoplasmic complex IKK may exist in one of three forms:

1. neutral (denoted by IKKne), which is specific to resting cells without any extracellular stimuli like TNF-α or IL-1.
2. active (denoted by IKKa),
3. inactive, but different from the neutral form, possibly overphosphorylated (denoted by IKKi) [36].

- **IKKne:** In resting cells all the IKK is in the neutral form. Upon stimulation all IKKne is transformed intro IKKa, but there is a constant basal transcription and translation of new IKKne [36].
- **IKKa:** It is formed only from IKKne upon signal activation (S), and all the IKKne becomes active. We consider some IKKa is preserved between two time steps, and the rest of the existing becomes inactive. We also take into consideration the induced inactivation by A20 [3,36,109,175]. As IKK is very active in phosphorylating IκB, we considered the mild bands of IKKa observed in experimental data after peak activation to be of medium level as they are capable of phosphorylating a considerable amount of IκB.
- **IKKi:** We assumed that IKK can only be transformed into IKKi from IKKa form, that is independent of stimulus and that is triggered by the cytoplasmic protein A20 [26, 36].

A20 protein:

Since we are only interested in the existence of this protein, it will have two possible states, and it will be 1 or 0 according to the existence of $A20_t$ in the previous time step.

IκB:

We focus on IκBα, postponing the inclusion of the other isoforms to a further study. More precisely, we approximate the collective action of these three isoforms by the action of the most active and abundant inhibitor, i.e. IκBα, the knock out of which, in contrast to the other two, is lethal [11, 101, 114]. We refer to it as IκB.

In resting wild-type cells, IκB is observed only in the cytoplasm where it remains bound to NF-κB.

Upon TNF-α stimulation, IKK is transformed into its active form IKKa and forms complexes with IκB and IκB|NF-κB, which leads to IκB phosphorylation, ubiquitination, and degradation. The free NF-κB rapidly enters the nucleus where it may bind to specific κB sites in the A20 and IκB promoters and activate their expression. The newly synthesized A20 enhances IKK inhibition, while the newly synthesized IκB enters the nucleus, binds to NF-κB and takes it out into cytoplasm. Then the cycle may be repeated, but since the IKK activity is already lowered by A20, the amplitude of the subsequent cycles is smaller [18, 58, 84–86, 105, 154].

Free cytoplasmic IκB protein:

We consider its dependence on itself, IκB$_n$, IκB$_t$ and IKKa. We disregard the influence of free cytoplasmic NF-κB as it rapidly enters the nucleus. Moreover, compared to the induced degradation by IKKa, the spontaneous degradation of IκB is negligible [125]. We assume the half-life of IκB is longer than the time steps we considered; hence it will have a positive influence on its future level. IκB$_n$ will also contribute to the level of its free cytoplasmic form as the IκB protein shuttles between nucleus and cytoplasm as it contains nuclear export signals as well as nuclear localization signals [133]. IκB$_t$ will also contribute to the level of IκB due to translation. We considered that in the case where IKKa is 1, the only contribution to IκB comes from its transcript. When IKKa is 2, even the newly synthesized IκB is degraded immediately.

Free nuclear IκB protein:

We consider its dependence on itself, on cytosolic IκB and on nuclear NF-κB. As IκB shuttles between cytoplasm and nucleus (where it is more concentrated [16]), cytosolic and nuclear IκB influence its level. Nuclear NF-κB also influences nuclear IκB as they associate and the resulting complex exported to the cytoplasm.

Cytoplasmic IκB|NF-κB complexes:

As we did with cytoplasmic IκB protein, we consider its dependence on itself and IKKa, we disregard its formation and spontaneous dissociation in the cytoplasm and its spontaneous degradation as these processes are much slower than the induced degradation by IKKa and the contribution of the nuclear IκB|NF-κB complex [110]. We incorporate the contribution of the nuclear complex IκB|NF-κB, but as it is rapidly transported out of the nucleus, we actually consider the influence of the level of the nuclear proteins IκB and NF-κB. When IKKa is 1, there is a mild decrease on the level of the existing cytoplasmic IκB|NF-κB and there may be contribution from the nuclear complex. If IKKa is 2, we will only consider the contribution from the nucleus as active IKK will almost completely induce IκB phosphorylation and degradation releasing NF-κB and disrupting the complex.

IκB and A20 transcripts:

IκB and A20 transcripts are dependent on NF-κB$_n$ as both genes contain κB elements and are highly responsive to NF-κB [104], and are also self regulatory as we consider the half lives of the transcripts to be of approximately 1 time step.

Free nuclear NF-κB:

We consider the income due to the liberation of NF-κB from IκB|NF-κB complexes, induced by IKKa in the cytoplasm. We also take into account the existing nuclear NF-κB and the transport to cytoplasm from the formation of the complex with IκB$_n$. With respect to the income from the cytoplasm, IKKa is necessary, and if there is just 1 of it there only will be freed some of the NF-κB present in the IκB|NF-κB complexes; whereas, if there is 2 of IKKa, all the NF-κB will be liberated. Regarding the nuclear contribution, if IκB$_n$ equals 2, all the existing NF-κB$_n$ will be transported out of the nucleus, while if IκB$_n$ equals 1, the decrease in the level is only noticed if NF-κB$_n$ equals 1.

7.5 Results

7.5.1 Comparison with experimental data and the continuous model

In order to validate our model, we present in this section our results, and compare them with existing data. We show in each case what is conserved and explain some structural features that our model infers. We also record other features that this discrete model is not able to reproduce.

Using Singular [35] we perform a simulation for the wild-type cells using our polynomial dynamical system. We consider persistent stimulation (S=1) and our initial state consisted of:

- S=1: as the simulation starts with a stimulus activating resting cells.
- IKKne=2, IKKa=0 and IKKi=0: as all IKK is in the neutral form before activation
- IκB|NF-κB=2: since maximum amount of the complex is seen in resting cells.
- IκB$_n$=1, IκB=0: As in resting cells there is some free IκB that is mainly localized in the nucleus.
- A20=0: as protein A20 is mainly induced by NF-κB and is not observed in resting cells.
- A20$_t$=0 and IκB$_t$=0: as it is not observed in resting cells [109].
- NF-κB$_n$=0: as NF-κB is retained in the cytoplasm by IκB in resting cells.

The wild type case:

The evolution of the system in the wild type case, from this initial state is depicted in figure 7.2.

We can compare our results for the wild type case with the ones in [110]. In Figure 3 [110], Lipniacki et al. show the numerical solution corresponding to wild-type cells; at the first hour the stimulus (TNF) starts and persists; and the concentrations of the different molecules and their complexes(vertical axis) are given in μM, while time (horizontal axis) is in hours. If we discretize the vertical axis into 3 levels (or 2 levels for the graph corresponding to A20), and assign certain times for each time step in our model, then we can compare both results through the graphs shown in Figure 7.4. The discretization of the concentrations is depicted in Figure 7.3, where dark orange corresponds to 2; light orange, to 1; and yellow, to 0.

Notice that the dynamics of our discrete model (including time, when time steps are replaced by minutes, comparing with kinetics model) is conserved for NF-κB$_n$, IKKa, IκB$_t$, A20, A20$_t$, IκB and IκB$_n$. The dynamics of IκB—NF-κB is also conserved, except for a transient rise at min 25. We miss the damped oscillation for NF-κB$_n$. However, if we transform the results of the kinetics model or the experimental data into discrete values, the oscillation is lost and coincides with our result. Another drawback is that our model is not additive: for example, it is not possible to calculate total IκB, from IκB, IκB—NF-κB and IκB$_n$, but, as we will see below, there is a pseudo conservation relation between NF-κB$_n$ and IκB—NF-κB that somehow coincides with the conservation relation we found for the continuous model of Lipniacki et al. (see the following section for details). Moreover, we cannot reproduce the time of IκB downregulation either, but just for little time.

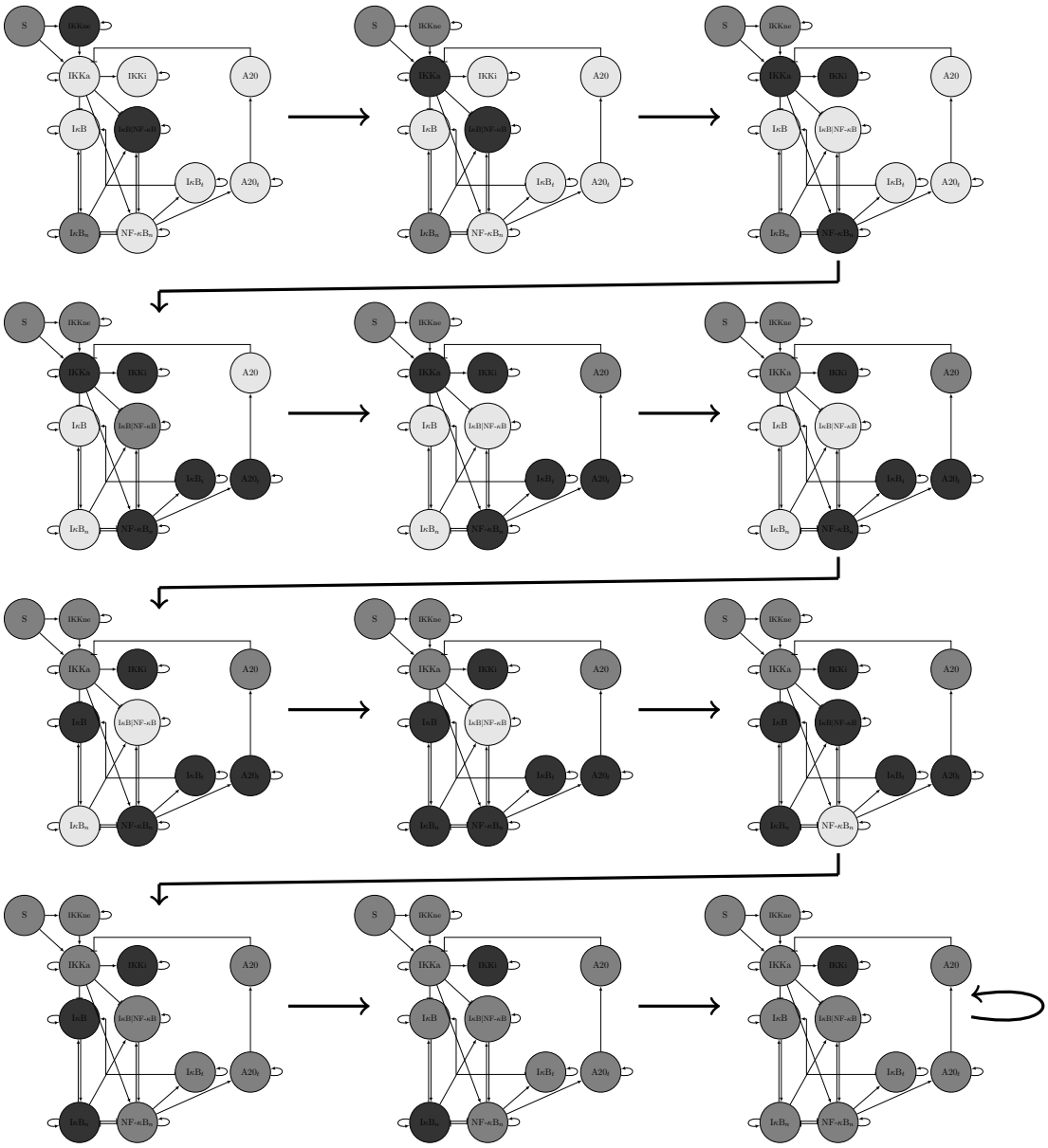

Figure 7.2: Evolution of the wild type system with persistent stimulus. The different states are encoded as:

.

Further insights into the NF-κB signaling pathway can be obtained from the simulation of single or multiple null mutations, over-activations, or any combination thereof.

The A20 knock-out (A20-/-) case:

We computed the evolution of the A20 knock-out system by setting $f_{A20} \equiv 0$, $f_{A20_t} \equiv 0$. The result is depicted in figure 7.5

In our discrete model, IKKa remains high, as well as in the continuous model. NF-κB$_n$ and IκB$_t$ also remain high, as it is seen in the data. The times of the dynamics, if we assume the same times in minutes as in the wild type case, are also conserved. In this discrete model, however, in the steady state there is no IκB nor IκB—NF-κB but in the kinetics model there is about half of the maximum of the total IκB. Nevertheless, in our favor, in experimental data [109], no total IκB is detected in A20 -/- mice after activation with TNF-a (stimulus).

The case when the stimulus is removed at different time steps:

We also computed the evolution of the system in the wild-type case when the stimulus is removed at different time steps. We show the result when we remove the stimulus at steady state in figure 7.6. We should remark that our model reaches a final state without NF-κB$_n$, as observed in experimental data. Moreover we can point out that this final state is different from the initial state without stimulus.

In figure 7.7 we represent the evolution of NF-κB$_n$ in the wild-type case when the stimulus is removed at different time steps. As observed in experimental data, if we remove the stimulus during the first NF-κB$_n$ peak, the intensity and duration of the NF-κB$_n$ peak remains unchanged compared to persistent stimulus, then NF-κB$_n$ disappears and never increases again.

When IKKa is inhibited at steady state:

We also studied how the system evolves when IKKa is inhibited in the steady state. The evolution is depicted in Figure 7.8. If we inhibit IKK at the steady state, NF-κB$_n$ drops to zero. In experimental data, IKK inhibition lowers NF-κB activity, reduces NF-κB dependent transcription, and reduces the impact of chronic inflammation. [136]

7.5.2 Conservation and final states

In the first chapters of this work we have focused on the steady states of continuous chemical reaction systems and also on the conservation relations they may satisfy. We now make analogue studies for this discrete model.

We start by the concept of conservation. Our model satisfies the pseudo conservation relation $\varphi_2(x, y) = x + y + 2x^2y + 2xy^2 + 2x^2y^2$ for IκB—NF-κB and NF-κB$_n$. This is, it verifies $\varphi_2(f_{I\kappa B|NF-\kappa B}, f_{NF-\kappa B_n}) = \varphi_2(x_{I\kappa B|NF-\kappa B}, x_{NF-\kappa B_n})$. Notice that $\varphi_2(x, y) = 2$ if $x.y \neq 0$, $\varphi_2(1, 0) = 1,\ \varphi_2(0, 1) = 1,\ \varphi_2(0, 0) = 0$. This means that, if $x_{I\kappa B|NF-\kappa B}$ (or $x_{NF-\kappa B_n}$) is nonzero, then $\varphi_2(x_{I\kappa B|NF-\kappa B}, x_{NF-\kappa B_n}) = 2$; and if we start with a few of IκB—NF-κB or NF-κB$_n$ ($x_{I\kappa B|NF-\kappa B} = 1$ and $x_{NF-\kappa B_n} = 0$, or $x_{I\kappa B|NF-\kappa B} = 0$ and $x_{NF-\kappa B_n} = 1$) then $\varphi_2(x_{I\kappa B|NF-\kappa B}, x_{NF-\kappa B_n}) = 1$; finally, if we start with no IκB—NF-κB nor NF-κB$_n$, then there will not be any in the next time steps, either. Recall that, in the continuous model [110], there was a conservation relation among the complexes involving NF-κB. Namely, it was

5[IKKa|IκB|NF-κB] + 5[NF-κB] + 5[IκB|NF-κB] + [NF-κB$_n$] + [IκB$_n$|NF-κB$_n$] =C.

In our discrete model, we only consider IκB|NF-κB and NF-κB$_n$ and could be expected that

the respective concentrations satisfied a pseudo conservation relation involving [IκB|NF-κB] and [NF-κB$_n$],which is a situation similar to the one in the toy example. Therefore, it is sensible to expect that our model satisfies the pseudo conservation relation $\varphi_2(f_{I\kappa B|NF-\kappa B}, f_{NF-\kappa B_n}) = \varphi_2(x_{I\kappa B|NF-\kappa B}, x_{NF-\kappa B_n})$ prescribed by φ_2. Note, however, that the functions corresponding to IκB|NF-κB and NF-κB$_n$ depend on more proteins.

We now analyze the fixed points of the system and its cycle. We found 16 fixed points for persistent stimulus (S=1). We present them in the following tables. The last column shows how many initial states evolve towards that fixed point.

IκB	IκB|NF-κB	IKKa	NF-κB$_n$	IκB$_n$	IκB$_t$	S	A20	A20$_t$	IKKi	IKKne	Total
0	0	1	0	0	0	1	0	0	2	1	204
0	0	1	0	1	0	1	0	0	2	1	3603
0	0	2	0	0	0	1	0	0	2	1	39
0	0	2	0	1	0	1	0	0	2	1	528

These first fixed points are the final states for initial ones with neither IκB|NF-κB nor NF-κB$_n$. (This can be deduced from the pseudo conservation relation.) Initializations without the presence of NF-κB are not of biological interest for this study.

IκB	IκB|NF-κB	IKKa	NF-κB$_n$	IκB$_n$	IκB$_t$	S	A20	A20$_t$	IKKi	IKKne	Total
1	1	1	1	1	1	1	1	1	2	1	14127
1	2	1	1	1	1	1	1	1	2	1	132
2	1	1	1	1	2	1	1	2	2	1	48
2	1	1	1	2	2	1	1	2	2	1	24
2	2	1	1	1	2	1	1	2	2	1	540
2	2	1	1	2	2	1	1	2	2	1	10983
1	1	1	1	1	1	1	1	2	2	1	84
1	2	1	1	1	1	1	1	2	2	1	66
2	1	1	1	1	2	1	1	1	2	1	84
2	1	1	1	2	2	1	1	1	2	1	48
2	2	1	1	1	2	1	1	1	2	1	60
2	2	1	1	2	2	1	1	1	2	1	48

We can notice the robustness of the system. When the stimulus is persistent (S=1), there are basically 3 attractors with more than 20% of attraction, and they together collect the 86% of the cases. The principal attractor is the one that we identified with the initial state proposed, and shows correlation with the literature. Those attractors that do not come from initial states without IκB|NF-κB nor NF-κB$_n$, have NF-κB$_n$=1, and this is a key fact in the biological function.

The steady states for the system without stimulus are shown in Appendix 2. With respect to $S = 0$, all the fixed points show NF-κB$_n$=0, and almost all of them have IKKa=0. This coud be interpreted as, for any initial state, once the stimulus is removed, the system turns off.

There is only one cycle consisting of two states, and a total of 8748 initial states terminate here.This cycle, represented in the two rows of the table below, shows an oscillation in NF-κB$_n$, similar to what is seen in most experiments. However, the damped oscillation is expected to be seen a constant level in a discrete model.

IκB	IκB|NF-κB	IKKa	NF-κB$_n$	IκB$_n$	IκB$_t$	S	A20	A20$_t$	IKKi	IKKne
1	0	1	1	1	0	1	1	0	2	1
0	1	1	0	1	1	1	0	1	2	1

7.6 Discussion for this chapter and future work

We introduced in this model the discretization of time and concentrations of the different proteins and their complexes. By the discretization on three states of most of the molecules involved in this process, we could reproduce the dynamics observed in the wild-type case with persistent stimulation and also in the A20 knock-out.

This model does not depend on affinity and catalytic constants, which are usually difficult to determine and require a deep understanding of the system (which, except for the NF–κB regulatory module and some other special cases, is rare). It can be built with the information biologists normally handle: IκB binds to NF–κB and prevents it from entering the nucleus, IKKa induces IκB degradation, etc.

And despite it simply requires this kind of data, it can render even more information, such as predictions in mutant cases.

We expect to introduce, in the near future, some stochasticity into this model, and we would also like to study its interaction with other systems within the context of a bigger model of a cellular process.

However, there are also some open questions in our minds about the relations between discrete models and continuous models. Which would be a correct way to compare the results from both approaches?

In this model that we present here, we were faced to fitting parameters while completing the transition (or truth) tables. Our parameters belong to the finite set $\{0, 1, 2\}$, and were fitted using different data from the bibliography and our intuition. As we mentioned before, in [110] the authors decided to carry out their fit "manually" rather than to try to quantify the data, and then to apply one of the fitting engines available, claiming that such quantification is by no means unique, and because, when fitting, they would have to take into account diverse, usually not precise, information coming from different researchers and their own intuitive understanding of the process. They in [110] remark that if there were no feedback loops in the pathway, the proposed method would be quite efficient, but since they exist it was necessary to iterate the signal tracing several times, until the fit was satisfactory. They say that it is not obvious whether the method, in general, converges, but it seemed to them so, provided they started from a relatively accurate set of parameters and provided that the model approximates the true regulatory mechanism reasonably well.

As we did, they made some drastic simplifications, as it is usually inevitable. They alleged that they did not have enough data, and that a more elaborate model would be possibly too difficult to analyze; at least the parameter fitting would be both very difficult and ambiguous.

We must point out that all these assumptions and considerations made by the authors in [110] are the usual ones in the context of continuous modeling, given the inherent difficulty of these systems.

Besides, with respect to continuous models, particularly those where mass–action kinetics is assumed, in most cases, only the identity of the chemical species present in the network

is known, and the exact structure of the chemical reactions, as well as the reaction rate constants are unknown; in other cases, the set of chemical reactions (i.e., the reaction network) is also known, and only the reaction rate constants are unknown. And even though a great variety of computational methods have been developed for the identification of chemical reaction networks and their reaction rate constants from time-dependent measurements of chemical species concentrations, two different reaction networks might generate identical dynamical system models, making it impossible to discriminate between them, even if we are given experimental data of perfect accuracy and unlimited temporal resolution. In [33], Craciun and Pantea describe necessary and sufficient conditions for two reaction networks under mass–action kinetics to give rise to the same dynamical system model. Also, they show that, even if we knew the reaction network that gives rise to the chemical dynamics under study, there might exist multiple sets of reaction rate constants that provide perfect fit for the data since they give rise to identical dynamical system models.

Here are two specific mathematical questions that we expect to address in the near future:

Question 7.6.1. *We would like to dig through the relationship between continuous and discrete models.*

As we mentioned in the background, for many biological systems that have been modeled using both the continuous and the discrete frameworks, it has been shown that both models have similar dynamical properties. Furthermore, it has been hypothesized that the dynamics of biochemical networks are constrained by the topological structure of the wiring diagram. This in turn suggests that mathematical models describing the same biochemical phenomena should have similar behavior, even if they come from different frameworks. These connections between the discrete and the continuous models have been studied by several authors, [96, 117]. In [167], Veliz-Cuba et al. provide mathematical proofs about the relationship between steady states of continuous and discrete models, where the continuous model is "sigmoidal enough" and has the same qualitative features of a discrete model. Their results generalize some previous results and their proofs also show why the relationship between continuous and discrete models is likely to occur even when continuous models are not very sigmoidal.

Is it possible to develop more mathematical theory to validate the coincidences that are usually found between discrete and continuous models of the same system?

Question 7.6.2. *We would also like to formalize and generalize the notion of pseudo conservation relations introduced in* (7.2)*. The steady states of a dynamical system strongly depend on the initial conditions. In the case of systems that can be modeled under mass–action kinetics, this dependence is reflected in the conservation relations.*

Is it possible to establish a formal correspondence between conservation relations in continuous models and pseudo conservation relations in discrete models?

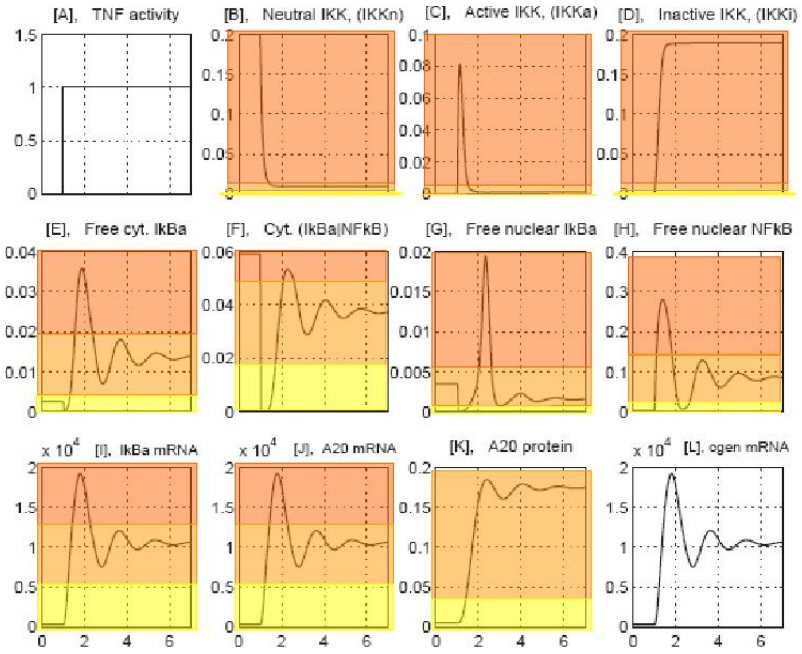

Figure 7.3: Discretization of concentrations of molecules and their complexes in Figure 3 in [110]. Dark orange corresponds to 2; light orange, to 1; and yellow, to 0.

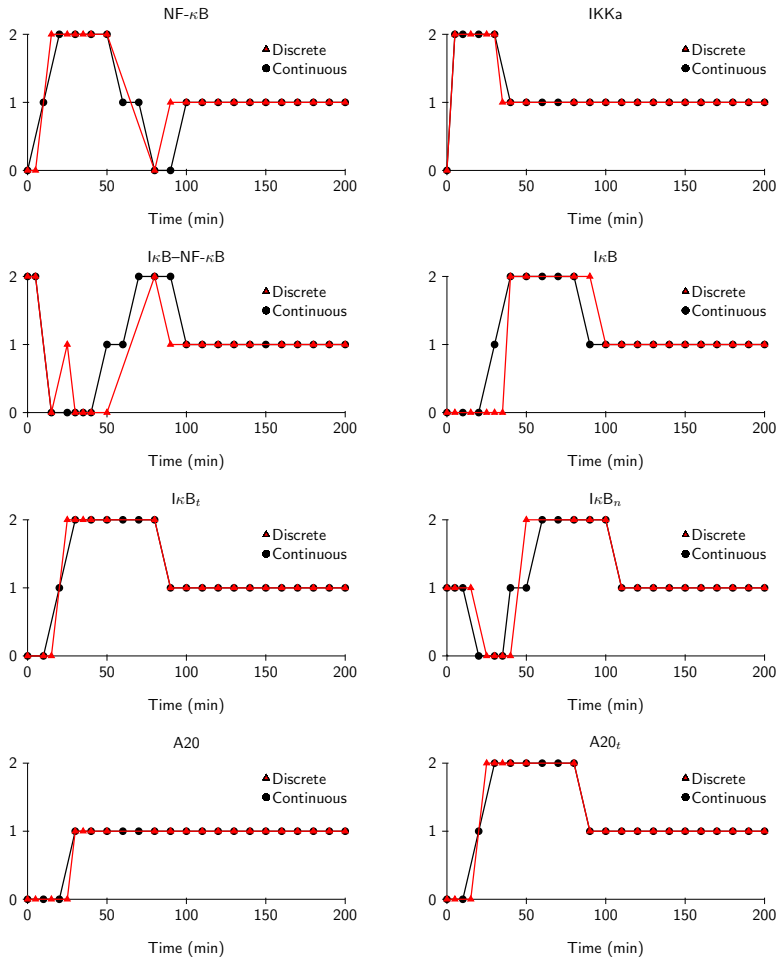

Figure 7.4: Comparison between the continuous model [110] and the discrete model for the wild type with persistent stimulus. For this, we discretized the results of the first model and assigned a certain time for the time steps of the second one.

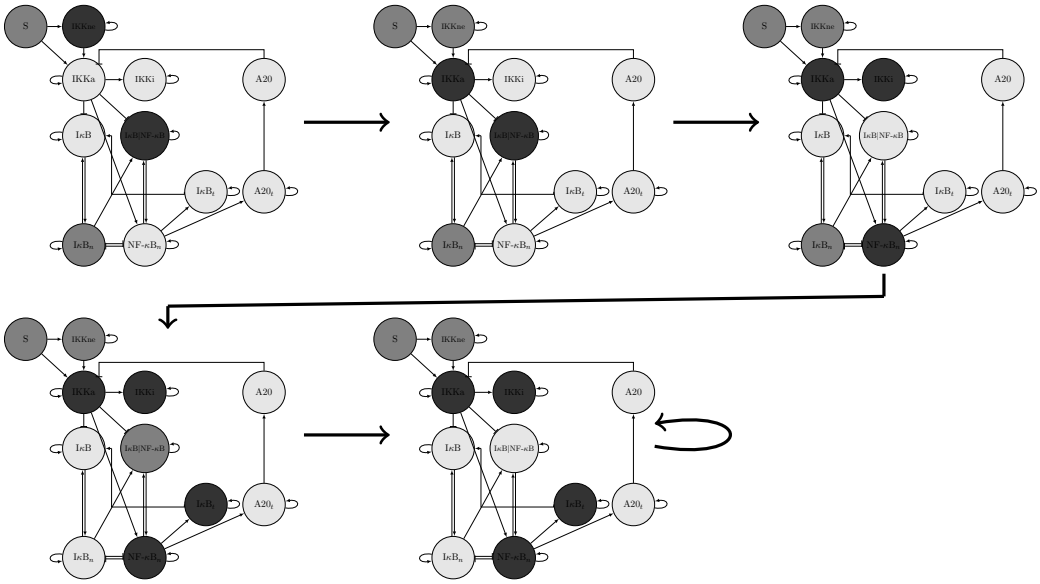

Figure 7.5: Evolution of the A20 knock-out system. NF-κB$_n$ and IκB$_t$ remain high, as seen in the literature.

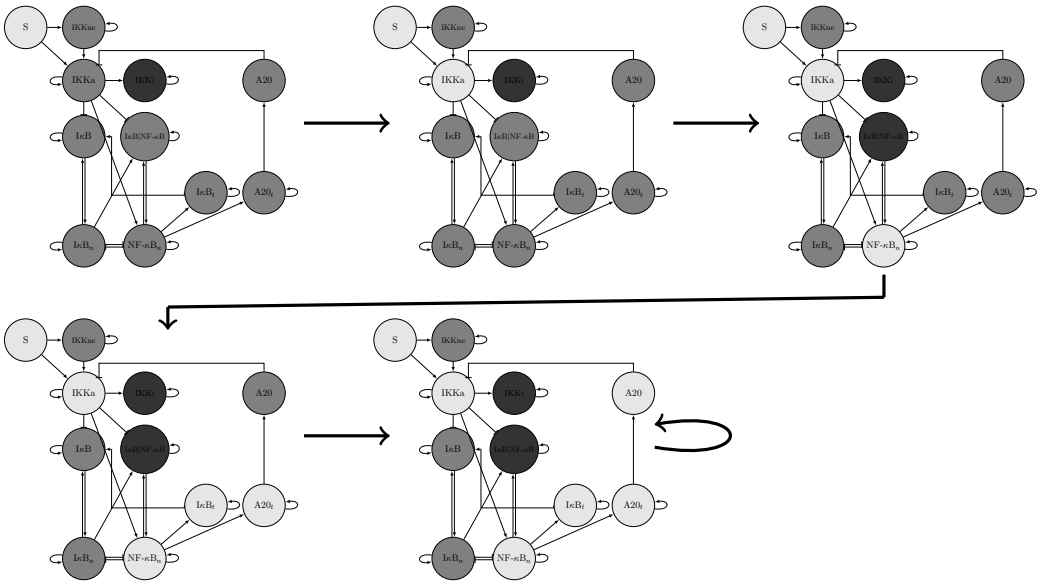

Figure 7.6: Evolution of the system when the stimulus is removed at steady state. A final state without NF-κB$_n$ is reached, as observed in experimental data, moreover this final state differs from the basal state without stimulus.

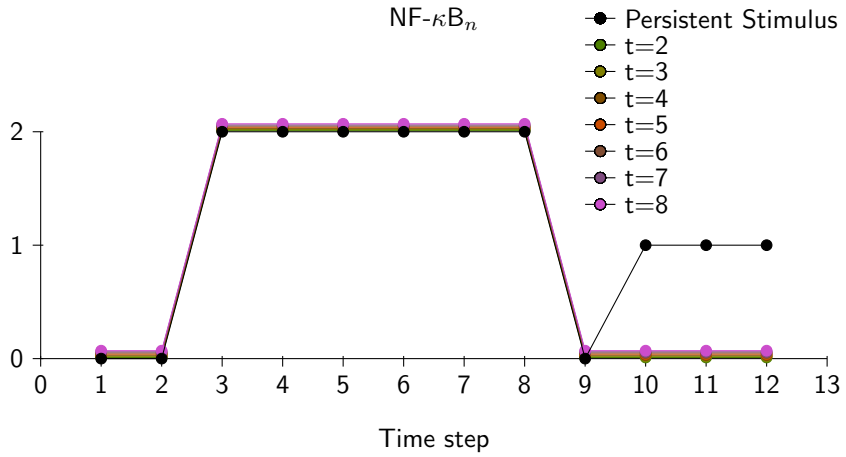

Figure 7.7: Evolution of NF-κB$_n$ when the stimulus is removed at different time steps. When the stimulus is removed within the maximum peak of NF-κB$_n$ there is no change in the amplitude of the peak nor in its length, as observed in experimental data.

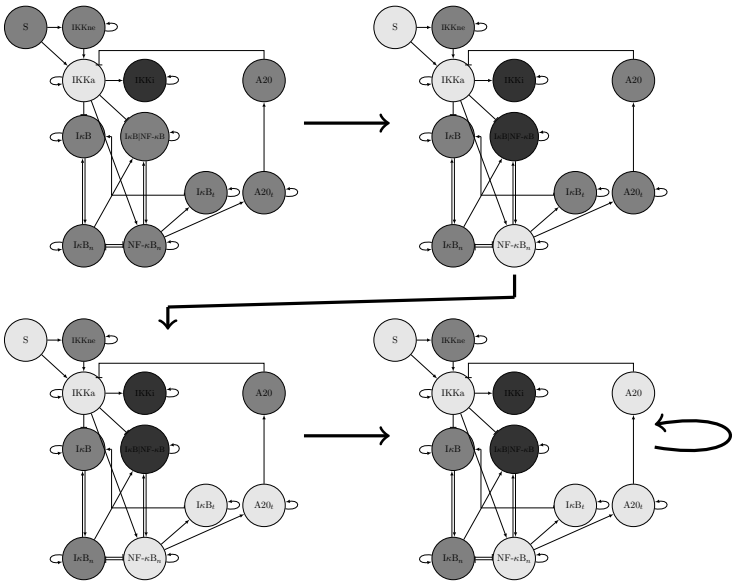

Figure 7.8: Evolution of the system when IKKa is inhibited at steady state. A final state without NF-κB$_n$ is reached.

Bibliography

[1] Albert R., Othmer H. G., (2003), The topology of the regulatory interactions predicts the expression pattern of the drosophila segment polarity genes J. Theor. Biol. 223:1–18.

[2] Angeli D., de Leenheer P., Sontag E. D., (2007), A Petri net approach to the study of persistence in chemical reaction networks, Mathematical Biosciences, 210:598–618.

[3] Arvelo M. B., Cooper J. T., Longo C., Soizic D., Grey S. T., Mahiou J., Czismadia E., Abu-Jawdeh G., Ferran C., (2002), A20 protects mice from d-galactosamine/lipopolysaccharide acute toxic lethal hepatitis, Hepatology 35, 535–543.

[4] Barkai N., Leibler S., (1997), Robustness in simple biochemical networks, Nature, 387:913–917.

[5] Basu S., (1999), New results on quantifier elimination over real closed fields and applications to constraint databases, Journal of the ACM, 46(4):537–555.

[6] Basu S., Pollack R., Roy M. -F., (1996), On the combinatorial and algebraic complexity of Quantifier elimination, J. A. C. M., 43, 1002–1045.

[7] Basu S., Pollack R., Roy M. -F., (2006), Algorithms in Real Algebraic Geometry Algorithms and Computation in Mathematics Series (A. M. Cohen, H. Cohen, D. Eisenbud, M. F. Singer, B. Sturmfels, eds.), vol. 10 (2nd ed.), Springer-Verlag.

[8] Batchelor E., Goulian M., (2003), Robustness and the cycle of phosphorylation and dephosphorylation in a two-component regulatory system. Proc. Natl. Acad. Sci. USA 100:691–6.

[9] Battogtokh D., Tyson J. J., (2004), Bifurcation analysis of a model of the budding yeast cell cycle, Chaos 14(3), 653–661.

[10] Becker E., Neuhaus R., (1993), Computation of real radicals of polynomial ideals. Progr. Math., -Vol.109, Birkhäuser Boston, Boston, MA, 1–20.

[11] Beg A. A., Sha W. C., Bronson R. T., Baltimore D., (1995), Constitutive NF-kappa B activation, enhanced granulopoiesis, and neonatal lethality in I kappa B alpha-deficient mice, Genes Dev. 9, 2736–2746.

[12] Bochnak J., Coste M., Roy M. -F., (1987), Géométrie algébrique réelle, Ergebnisse der Mathematik und ihrer Grenzgebeite, 3 Folge, Band 12, Springer-Verlag, Berlin, Heidelberg, and New York.

[13] Brown C., (2003), Qepcad b: a program for computing with semi-algebraic sets using cads, ACM SIGSAM , 37(4):97–108, http://www.cs.usna.edu/ qepcad/B/QEPCAD.html.

[14] Burack W. R., Sturgill T., (1997), The Activating Dual Phosphorylation of MAPK by MEK Is Nonprocessive, Biochemistry, 36(20):5929–5933.

[15] Caamano J., Hunter C. A., (2002), NF-κB family of transcription factors: central regulators of innate and adaptive immune functions, Clin. Microbiol. Rev. 15, 414–429.

[16] Carlotti F., Dower S. K., Qwarnstrom E. E., (2000), Dynamic shuttling of nuclear factor kappa B between the nucleus and cytoplasm as a consequence of inhibitor dissociation, J. Biol. Chem. 275, 41028–41034.

[17] Chaves M., Sontag E. S., Albert R., (2006), Methods of robustness analysis for Boolean models of gene control networks, IEE Proceedings in Systems Biology 153, 154–167.

[18] Chen F. E., Huang D., Chen Y., Ghosh G., (1998), Crystal structure of p50/p65 heterodimer of transcription factor NF-kB bound to DNA, Nature 391, 410–413.

[19] Chen K. C., Calzone L., Csikasz-Nagy A., Cross F. R., Novak B., Tyson J. J., (2004), Integrative analysis of cell cycle control in budding yeast, Mol. Biol. Cell 15(8), 3841–3862.

[20] Chèze G., Lecerf G., (2007), Lifting and recombination techniques for absolute factorization, Journal of Complexity, 23(3):380–420.

[21] Collins G. E., (1975), Quantifier Elimination for the Elementary Theory of Real Closed Fields by Cylindrical Algebraic Decomposition, Lect. Notes Comput. Sci. 33, 134–183.

[22] Collins G. E., (1998), Quantifier Elimination by Cylindrical Algebraic Decomposition–Twenty Years of Progress, In Quantifier Elimination and Cylindrical Algebraic Decomposition (Ed. B. F. Caviness and J. R. Johnson). New York: Springer-Verlag, pp. 8–23.

[23] Conradi C., Dickenstein A., Pérez Millán M., Shiu A., (2011), Counting positive roots of polynomials with applications for biochemical systems, In preparation.

[24] Conradi C., Flockerzi D., Raisch J., (2008), Multistationarity in the activation of a MAPK: Parametrizing the relevant region in parameter space, Math. Biosci. 211(1), 105–131.

[25] Conradi C., Saez-Rodriguez J., Gilles E.-D., Raisch J., (2005), Using Chemical Reaction Network Theory to discard a kinetic mechanism hypothesis, IEE Proc. Systems Biology (now IET Systems Biology) 152(4), 243–248.

[26] Coornaert B., Carpentier I., Beyaert R., (2009), A20: Central Gatekeeper in Inflammation and Immunity, J. Biol. Chem., 284, 8217–8221.

[27] Cornish-Bowden A, (1995), Fundamentals of Enzyme Kinetics (Portland Press, London, UK), 2nd edition.

[28] Cox D., Little J., O'Shea D., (1992) Ideals, varieties, and algorithms: an introduction to computational algebraic geometry and commutative algebra, Springer-Verlag, New York.

[29] Cox D. A., Little J., O'Shea D., (2005), Using algebraic geometry. Graduate Texts in Mathematics, -Vol.185,Second Edition,Springer, New York.

[30] Craciun G., Dickenstein A., Shiu A., Sturmfels B., (2009), Toric dynamical systems, Journal of Symbolic Computation, 44:1551–1565.

[31] Craciun G., Feinberg M., (2006), Multiple Equilibria in Complex Chemical Reaction Networks: II. The Species-Reactions Graph, SIAM Journal on Applied Mathematics, 66(4): 1321–1338.

[32] Craciun G., Tang Y., Feinberg M., (2006), Understanding bistability in complex enzymedriven reaction networks, Proc. Natl. Acad. Sci., 103(23):8697–8702.

[33] Craciun G., Pantea C., (2008), Identifiability of chemical reaction networks. J. Math. Chem. 44:244–59.

[34] Dasgupta T., Croll D. H., Vander Heiden M. G. , Locasale J. W., Alon U., Cantley L. C., Gunawardena J., (2010), Bifunctionality in PFK2/F2,6BPase confers both robustness and plasticity in the control of glycolysis. Submitted.

[35] Decker W., Greuel G.-M., Pfister G., Schönemann H., (2011), SINGULAR 3-1-3 — A computer algebra system for polynomial computations. http://www.singular.uni-kl.de.

[36] Delhase M., Hayakawa M., Y. Chen Y., and M. Karin, (1999), Positive and negative regulation of IkB kinase activity through IKKb subunit phosphorylation, Science 284, 309–313.

[37] Deshaies R. J., Ferrell J. E., (2001), Multisite phosphorylation and the countdown to S phase, Cell 107(7), 819–822.

[38] Dickenstein A., (2009), A world of binomials, London Math. Soc. Lecture Note Ser., 363, Foundations of computational mathematics, Hong Kong 2008, 42–67.

[39] Dickenstein A., Pérez Millán M., (2011), How far is complex balancing from detailed balancing? Bulletin of Mathematical Biology 73(4):811–828.

[40] Dimitrova E. S., Jarrah A. S., Laubenbacher R., Stigler B., (2007), A Gröbner fan method for biochemical network modeling, In Proceedings of the 2007 international Symposium on Symbolic and Algebraic Computation (Waterloo, Ontario, Canada, July 29 - August 01, 2007). ISSAC '07. ACM, New York, NY.

[41] Dimitrova E., García-Puente L. D., Hinkelmann F., Jarrah A. S., Laubenbacher R., Stigler B., Stillman M., Vera-Licona P., (2011), Parameter estimation for Boolean models of biological networks, Theoretical Computer Science, 412(26), 2816–2826.

[42] Ederer M., Gilles E. D., (2007), Thermodynamically feasible kinetic models of reaction networks, Biophysical Journal, 92(6):1846–1857.

[43] Eisenbud D., Sturmfels B., (1996), Binomial ideals, Duke J. Math., 84(1):1–45.

[44] Espinosa-Soto C., Padilla-Longoria P., and E. R. Alvarez-Buylla E. R., (2004), A gene regulatory network model for cell-fate determination during arabidopsis thaliana flower development that is robust and recovers experimental gene expression profiles, Plant Cell, 16, 2923–2939.

[45] Feinberg M., (1972), Complex balancing in general kinetic systems, Arch. Rational Mech. Anal. 49(3), 187–194.

[46] Feinberg M., Horn F., (1977), Chemical mechanism structure and the coincidence of the stoichiometric and kinetic subspaces. Arch. Rational Mech. Anal., 66: 83–97.

[47] Feinberg M., (1977), Mathematical Aspects of Mass Action Kinetics, Chapter 1 in Chemical Reactor Theory: A Review (eds. N. Amundson and L. Lapidus) Prentice-Hall.

[48] Feinberg M., (1979), Lectures on chemical reaction networks, Notes of lectures given at the Mathematics Research Center of the University of Wisconsin in 1979, available at: http://www.che.eng.ohio-state.edu/˜FEINBERG/LecturesOnReactionNetworks.

[49] Feinberg M., (1989), Necessary and sufficient conditions for detailed balancing in mass action systems of arbitrary complexity, Chem. Eng. Sci. 44(9), 1819–1827.

[50] Feinberg M., (1995), The existence and uniqueness of steady states for a class of chemical reaction networks, Arch. Rational Mech. Anal., 132(4):311–370.

[51] Feinberg M., (1995), Multiple steady states for chemical reaction networks of deficiency one, Arch. Rational Mech. Anal. 132(4), 371–406.

[52] Ferrell Jr. J. E., Bhatt R., (1997), Mechanistic Studies of the Dual Phosphorylation of Mitogenactivated Protein Kinase, The Journal of Biological Chemistry, 272(30):19008–19016.

[53] Flockerzi D., Conradi C., (2008), Subnetwork analysis for multistationarity in mass-action kinetics, J. Phys. Conf. Ser. 138(1), 012006.

[54] Gatermann K., (2001), Counting stable solutions of sparse polynomial systems in chemistry, Contemporary Mathematics, Volume 286, Symbolic Computation: Solving Equations in Algebra, Geometry and Engineering, (Editors E. Green et al.), 53–69.

[55] Gatermann K., Huber B., (2002), A family of sparse polynomial systems arising in chemical reaction systems, J. Symbolic Comput. 33(3), 275–305.

[56] Gatermann K., Wolfrum M., (2005), Bernstein's second theorem and Viro's method for sparse polynomial systems in chemistry, Advances in Applied Mathematics, 34(2):252–294.

[57] Gerondakis S., Grossmann M., Nakamura Y., Pohl T., Grumont R., (1999), Genetic approaches in mice to understand Rel/NF-kappaB and IkappaB function: transgenics and knockouts, Oncogene 18, no. 49, 6888–95.

[58] Ghosh S., May M. J., Kopp E. B., (1998), NF-κB and rel proteins: Evolutionarily Conserved Mediators of Immune Responses, Annu. Rev. Immunol. 16, 225–260.

[59] Glass L., (1975), Classification of biological networks by their qualitative dynamics, J. Theor. Biol., 54, 85–107.

[60] Gnacadja G., (2009), Univalent positive polynomial maps and the equilibrium state of chemical networks of reversible binding reactions. Advances in Applied Mathematics, 43(4):394–414.

[61] Grayson D. R., Stillman M. E., Macaulay2, a software system for research in algebraic geometry. Available at http://www.math.uiuc.edu/Macaulay2/

[62] Greuel G.-M., Pfister G., (2008), A **Singular** introduction to commutative algebra. Springer-Verlag, Berlin. With contributions by Olaf Bachmann, Christoph Lossen and Hans Schönemann, With 1 CD-ROM (Windows, Macintosh, and UNIX).

[63] Gunawardena J., (2003), Chemical reaction network theory for in-silico biologists, Technical Report, Available at: http://vcp.med.harvard.edu/papers/crnt.pdf.

[64] Gunawardena J., (2007), Distributivity and processivity in multisite phosphorylation can be distinguished through steady-state invariants, Biophys. J., 93:3828–34.

[65] Gunawardena J., (2010), Models in systems biology: the parameter problem and the meanings of robustness, in H. Lodhi, S. Muggleton (editors), Elements of Computational Systems Biology, John Wiley and Sons, New York.

[66] Gunawardena J., (2011), A linear framework for nonlinear biochemical systems at steady state, Submitted.

[67] Harris S. E., Sawhill B. K., Wuensche A., Kauffman S., (2002), A model of transcriptional regulatory networks based on biases in the observed regulatory rules, Complexity 7 (4), 23–40.

[68] Hárs V., Tóth J., (1979), On the inverse problem of reaction kinetics, Colloquia Mathematica Societatis János Bolyai 30. Qualitative Theory of Differential Equations. Szeged (Hungary), pp. 363–379.

[69] Hayden M. S., Ghosh S., (2004), Signaling to NF-κB, Genes Dev.18, 2195–2224.

[70] Hayden M. S., West A. P., Ghosh S., (2006), NF-kappaB and the immune response, Oncogene 25, no. 51, 6758–80.

[71] Heintz J., Roy M. -F. , Solerno P., (1990), Sur la complexité du principe de Tarski-Seidenberg Bulletin de la SMF 118: 101–126.

[72] Heintz J., Roy M. -F. , Solerno P., (1993), On the theoretical and practical complexity of the existential theory of the reals, The Computer Journal, 36 (5): 427–431.

[73] Heintz J., Roy M. -F. , Solerno P., (1994), Description of the connected components of a semi-algebraic set in single exponential time, Discrete and Computational Geometry 11: 121–140.

[74] Hermann-Kleiter N., Baier G., (2010), NFAT pulls the strings during cd4+ t helper cell effector functions, Blood 115(15), 2989–2997.

[75] Hinkelmann F., Murrugarra D., Jarrah A. S., Laubenbacher R., (2011), A Mathematical Framework for Agent Based Models of Complex Biological Networks, Bulletin of Mathematical Biology, 73(7), 1583–1602.

[76] Hoffmann A., Levchenko A., Scott M. L., Baltimore D., (2002), The IκBα- NF-κB signaling module: temporal control and selective gene activation, Science 298,1241–1245.

[77] Hogan P. G., Chen L., Nardone J., Rao A., (2003), Transcriptional regulation by calcium, calcineurin, and NFAT, Gene Dev. 17(18), 2205–2232.

[78] Holstein K., (2008), Mathematische analyse der n-fachen Phosphorylierung eines Proteins: Existenz mehrfach stationärer Zustände. Master's thesis, Diplomarbeit, Universität Magdeburg.

[79] Horn F., (1972), Necessary and sufficient conditions for complex balancing in chemical kinetics, Arch. Ration. Mech. Anal. 49(3), 172–186.

[80] Horn F., Jackson R., (1972), General mass action kinetics, Arch. Ration. Mech. Anal. 47(2), 81–116.

[81] Horn F., (1973), Stability and complex balancing in mas–action systems with three short complexes, Proc. Roy. Soc. (London) Ser. A 334:331–342.

[82] Horn F., (1974), The dynamics of open reaction systems, in Mathematical aspects of chemical and biochemical problems and quantum chemistry (Proc. SIAM-AMS Sympos. Appl. Math., New York, 1974), 125–137. SIAM–AMS Proc., Vol. VIII. Amer. Math. Soc., Providence, RI.

[83] Huang C.-Y. F., Ferrell J. E., (1996), Ultrasensitivity in the Mitogen-Activated Protein Kinase Cascade, PNAS 93(19), 10078–10083.

[84] Huang T. T., Miyamoto S., (2001), Postrepression activation of NF-kappaB requires the amino-terminal nuclear export signal specific to IkappaBalpha, Mol. Cell Biol. 21, no. 14, 4737–47.

[85] Huxford T., Huang D. B., Malek S., Ghosh G., (1998), The crystal structure of the IκB/NF-κB complex reveals mechanisms of NF-κB inactivation, Cell 95, 759–770.

[86] Jacobs M. D., Harrison S. C., (1998), Structure of an IκB/NF-κB complex, Cell 95, 749–758.

[87] Jarrah A. S., Laubenbacher R., Stigler B., Stillman M., (2007), Reverse-engineering of polynomial dynamical systems, Adv. Appl. Math., 39, 477–489.

[88] Jarrah A. S., Raposa B., Laubenbacher R., (2007), Nested canalyzing, unate cascade, and polynomial functions, Physica D: Nonlinear Phenomena, 233(2): 167–174.

[89] Jimi E., Aoki K., Saito H., D'Acquisto F., May M. J., Nakamura I., Sudo T., Kojima T., Okamoto F., Fukushima H., Okabe K., Ohya K., Ghosh S., (2004), Selective inhibition of NF-κB blocks osteoclastogenesis and prevents inflammatory bone destruction in vivo, Nature Medicine 10, no. 6, 617–624.

[90] Kapuy O., Barik D., Sananes M. R.-D., Tyson J. J., Novák B., (2009), Bistability by multiple phosphorylation of regulatory proteins, Prog. Biophys. Mol. Bio. 100(1-3), 47–56.

[91] Karin M., Yamamoto Y., Wang Q. M., (2004), The IKK NF-κB system: a treasure trove for drug development, Nature Reviews Drug Discovery 3, 17–26.

[92] Karp R., Pérez Millán M., Dasgupta T., Dickenstein A., Gunawardena J., (2011), Complex–linear invariants of biochemical networks, Submitted.

[93] Kauffman S. A., (1969), Homeostasis and differentiation in random genetic control networks, Nature 224, 177–178.

[94] Kauffman S. A., (1969), Metabolic stability and epigenesis in randomly constructed genetic nets, Journal of Theoretical Biology, 22, 432–467.

[95] Kauffman S. A., (1993), The Origins of Order: Self–Organization and Selection in Evolution, Oxford University Press, New York; Oxford.

[96] Kauffman S., Glass K., (1973), The logical analysis of continuous, nonlinear biochemical control networks, J. Theor. Biol., 39:103–129.

[97] Kauffman S., Peterson C., Samuelsson B., Troein C., (2003), Random boolean network models and the yeast transcriptional network, Proceedings of the National Academy of Sciences of the United States of America, 100(25): 14796–14799.

[98] Kauffman S., Peterson C., Samuelsson B., Troein C., (2004), Genetic networks with canalyzing boolean rules are always stable, Proceedings of the National Academy of Sciences of the United States of America, 101(49):17102â17107, 2004.

[99] Kearns J. D., Hoffmann A., (2009), Integrating Computational and Biochemical Studies to Explore Mechanisms in NF-κB Signaling, Journal of Biological Chemistry 284, no. 9, 5439–5443.

[100] King E. L., Altman C., (1956), A Schematic Method of Deriving the Rate Laws for Enzyme-Catalyzed Reactions, J. Phys. Chem., 60(10):1375–1378.

[101] Klement J. F., Rice N. R., Car B. D., Abbondanzo S. J., Powers G. D., Bhatt P. H., Chen C. H., Rosen C. A., Stewart C. L., (1996), IkappaBalpha deficiency results in a sustained NF-kappaB response and severe widespread dermatitis in mice, Mol. Cell. Biol. 16, 2341–2349.

[102] Krambeck F. J., (1970), The mathematical structure of chemical kinetics in homogeneous single phase systems, Arch. Rational Mech. Anal., 38(5), 317–347.

[103] Kramer B. P., Usseglio Viretta A., Daoud-El Baba M., Aubel D., Weber W., Fussenegger M., (2004), An engineered epigenetic transgene switch in mammalian cells. Science 22:867–70.

[104] Krikos A., Laherty C. D., DixitV. M., (1992), Transcriptional activation of the tumor necrosis factor alpha-inducible zinc finger protein, A20, is mediated by kappa B elements, J. Biol. Chem. 267, no. 25, 17971–6.

[105] Kunsch C., Ruben S. M., Rosen C. A., (1992), Selection of optimal kappa B/Rel DNA-binding motifs: interaction of both subunits of NF-kappa B with DNA is required for transcriptional activation, Mol. Cell Biol. 12, 4412–4421.

[106] Lasserre J. B., Laurent M., Rostalski P., (2008), Semidefinite characterization and computation of zero-dimensional real radical ideals, Foundations of Computational Mathematics 8, 607–647.

[107] Laubenbacher R., Stigler B., (2004), A computational algebra approach to the reverse-engineering of gene regulatory networks. Journal of Theoretical Biology, 229, 523–537.

[108] Laurent M., Kellershohn N., (1999), Multistability: a major means of differentiation and evolution in biological systems. Trends Biochem. Sci. 24:418–22.

[109] Lee E. G., Boone D. L., Chai S., Libby S. L., Chien M., Lodolce J. P., Ma A., (2000), Failure to regulate TNF-induced NF-κB and cell death responses in A20-deficient mice, Science 289, 2350–2354.

[110] Lipniacki T., Paszek P., Brasier A. R., Luxon B., Kimmel M., (2004), Mathematical model of NF-κB regulatory module, Journal of Theoretical Biology 228, 195–215.

[111] Macian F., (2005), Nfat proteins: key regulators of t-cell development and function, Nat. Rev. Immunol. 5(6), 472–484.

[112] Manrai A. K., Gunawardena J., (2008), The geometry of multisite phosphorylation, Biophys. J. 95(12), 5533–5543.

[113] Markevich N. I., Hoek J. B., Kholodenko B. N., (2004), Signaling switches and bistability arising from multisite phosphorylation in protein kinase cascades, J. Cell Biol. 164(3), 353–359.

[114] Mémet S., Laouini D., Epinat J. -C., Whiteside S. T., Goudeau B., Philpott D., Kayal S., Sansonetti P. J., Berche P., Kanellopoulos J., Israël A., (1999), IκBϵ-Deficient Mice: Reduction of One T Cell Precursor Subspecies and Enhanced Ig Isotype Switching and Cytokine Synthesis, J. Immunol. 163, 5994–6005.

[115] Mendoza L., (2006), A network model for the control of the differentiation process in Th cells, BioSystems 84:101–114.

[116] Mendoza L., Thieffry D., Alvarez-Buylla E. R., (1999), Genetic control of flower morphogenesis in arabidopsis thaliana: a logical analysis, Bioinformatics, 15, 593–606.

[117] Mendoza L., Xenarios I., (2006), A method for the generation of standardized qualitative dynamical systems of regulatory networks, Theoretical Biology and Medical Modelling, 3(13):1–18.

[118] Milo R., Itzkovitz S., Kashtan N., Levitt R., Shen-Orr S., Ayzenshtat I., Sheffer M., U., (2004), Superfamilies of evolved and designed networks, Science 303: 1538–1542.

[119] Mora T., Robbiano L., (1988), The Gröbner fan of an ideal, J. Symb. Comp. 6, 183–208.

[120] Murrugarra D., Laubenbacher R., (2011), Regulatory patterns in molecular interaction networks, Journal of Theoretical Biology, 288, 66–72.

[121] Murrugarra D., Laubenbacher R., (2011), The number of multistate nested canalyzing functions, Available at arXiv:1108.0206

[122] Nelson D. E., Ihekwaba A. E. C., Elliott M., Johnson J. R., Gibney C. A., Foreman B. E., Nelson G., See V., Horton C. A., Spiller D. G., Edwards S. W., McDowell H. P., Unitt J. F., Sullivan E., Grimley R., Benson N., Broomhead D., Kell D. B., White M. R. H., (2004), Oscillations in NF–κB Signaling Control the Dynamics of Gene Expression, Science 306, 704–708.

[123] Neuhaus R., (1998), Computation of real radicals of polynomial ideals. II. J. Pure Appl. Algebra, 124, No. 1-3, 261–280.

[124] Pandey S., Wang R. -S., Wilson L., Li S., Zhao Z., Gookin T. E., Sarah M Assmann S. M., Albert R., (2010), Boolean modeling of transcriptome data reveals novel modes of heterotrimeric G-protein action, Molecular Systems Biology, 6:372.

[125] Pando M. P., Verma I. M., (2000), Signal-dependent and -independent degradation of free and NF-kB-bound IkBa, J. Biol. Chem. 275, 21278–21286.

[126] Pérez Millán M., Dickenstein A., Shiu A., Conradi C., (2011), Chemical reaction systems with toric steady states, Accepted for publication at the Bulletin of Mathematical Biology, Available online at DOI: 10.1007/s11538-011-9685-x.

[127] Renegar J., (1992), On the computational complexity and geometry of the first-order theory of the reals I-III, J. Symbolic Comput., 13(3):255–352.

[128] Ribba B., Colin T., Schnell S., (2006), A multiscale mathematical model of cancer, and its use in analyzing irradiation therapies, Theoretical Biology and Medical Modelling, 3(7)

[129] Rockafellar R. T., (1970) Convex Analysis, Princeton University Press, Princeton NJ.

[130] Roshak A. K., Jackson J. R., McGough K., Chabot-Fletcher M., Mochan E., Marshall L. A., (1996), Manipulation of distinct NF-kappaB proteins alters interleukin-1beta-induced human rheumatoid synovial fibroblast prostaglandin E2 formation, J. Biol. Chem. 271, 31496–501.

[131] Rostalski P., (2009), Algebraic Moments - Real Root Finding and Related Topics, PhD Thesis. Available at http://e-collection.ethbib.ethz.ch/view/eth:1

[132] Russo FD, Silhavy TJ (1993), The essential tension: opposed reactions in bacterial two-component regulatory systems, Trends Microbiol. 1, 306–10.

[133] Sachdev S., Bagchi S., Zhang D. D., Mings A. C., Hannink M., (2000), Nuclear import of IkappaBalpha is accomplished by a ran-independent transport pathway, Mol. Cell Biol. 20, 1571–82.

[134] Saez-Rodriguez J., Alexopoulos L. G., MingSheng Zhang MS., Morris M. K., Lauffenburger D. A., Sorger P. K., (2011), Comparing Signaling Networks between Normal and Transformed Hepatocytes Using Discrete Logical Models, Cancer Res., 71, 5400–5411.

[135] Sánchez L., Thieffry D., (2001), A logical analysis of the drosophila gap-gene system, J. Theor. Biol., 211:115–141.

[136] Schopf L., Savinainen A., Anderson K., Kujawa J., DuPont M., Silva M., Siebert E., Chandra S., Morgan J., Gangurde P., Wen D., Lane J., Xu Y., Hepperle M., Harriman G., Ocain T., Jaffee B., (2006), IKKβ inhibition protects against bone and cartilage destruction in a rat model of rheumatoid arthritis, Arthritis & Rheumatism 54, no. 10, 3163–3173.

[137] Schuster S., Schuster R., (1989), A generalization of Wegscheider's condition. Implications for properties of steady states and for quasi-steady-state approximation, Journal of Mathematical Chemistry, 3:25–42.

[138] Seidenberg A., (1954), A new decision method for elementary algebra, Annals of Mathematics, 60:365–374.

[139] Sha W., Moore J., Chen K., Lassaletta A. D., Yi C.-S., Tyson J. J., Sible J. C., (2003), Hysteresis drives cell-cycle transitions in xenopus laevis egg extracts, PNAS 100(3), 975–980.

[140] Shaul Y. D., Seger R., (2007), The mek/erk cascade: From signaling specificity to diverse functions, Biochim. Biophys. Acta. 1773(8), 1213–1226.

[141] Shinar G., Milo R., Martínez M. R., Alon U., (2007), Input-output robustness in simple bacterial signaling systems. Proc. Natl. Acad. Sci. USA, 104:19931–19935.

[142] Shinar G., Alon U., Feinberg M., (2009), Sensitivity and robustness in chemical reaction networks, Siam J. Appl. Math., 69(4):977–998.

[143] Shinar G., Rabinowitz J. D., Alon U., (2009), Robustness in glyoxylate bypass regulation. PLoS Comp. Biol. 5:e1000297.

[144] Shinar G., Feinberg M., (2010), Structural sources of robustness in biochemical reaction networks, Science 327(5971), 1389–1391.

[145] Shmulevich I., Dougherty E. R., Kim S., Zhang W., (2002), Probabilistic boolean networks: a rule-based uncertainty model for gene regulatory networks, Bioinformatics 18 (2), 261–274.

[146] Sontag E., (2001), Structure and stability of certain chemical networks and applications to the kinetic proofreading model of T-cell receptor signal transduction, IEEE Trans. Automat. Control, 46:1028–1047.

[147] Spang S. J., (2007), On the computation of the real radical, Diploma Thesis, Technical University of Kaiserslautern, Germany.

[148] Spang S. J., (2008), A zero-dimensional approach to compute real radicals Comput. Sci. J. Moldova, 16(1): 64–92.

[149] Stanley R. P., (1999), Enumerative combinatorics. Vol. 2, volume 62 of Cambridge Studies in Advanced Mathematics, Cambridge University Press, Cambridge. With a foreword by Gian-Carlo Rota and Appendix 1 by Sergey Fomin.

[150] Steggles L. J., Banks R., Shaw O., Wipat A., (2007), Qualitatively modelling and analysing genetic regulatory networks: a Petri net approach, Bioinformatics, 23, 336–343.

[151] Strang G., (1976) Linear Algebra and its Applications, Academic Press, New York.

[152] Strezebonski A., (2000), Solving systems of strict polynomial inequalities, Journal of Symbolic Computation, 29(3):471–480.

[153] Sturmfels B., (1996), Gröbner bases and convex polytopes, Vol. 8 of University Lecture Series. American Mathematical Society, Providence, RI.

[154] Sun S. C., Ganchi P. A., Ballard D. W., Greene W. C., (1993), NF-κB controls expression of inhibitor IκBα:evidence for an inducible autoregulatory pathway, Science 259, 1912–1915.

[155] Sun S. C., (2008), Deubiquitylation and regulation of the immune response, Nature Reviews Immunology 8, 501–511.

[156] Tarski A., (1931), Sur les ensembles définissables de nombres réels, Fund. Math. 17, 210–239.

[157] Tarski A., (1951), A decision method for elementary algebra and geometry, University of California Press, Berkeley and Los Angeles, Calif. 2nd ed.

[158] Thieffry D., Thomas R., Kaufman M., (1995), Dynamical behaviour of biological regulatory networksâI. Biological role of feedback loops and practical use of the concept of the loop-characteristic state, Bull. Math. Biol. 57, 247–276.

[159] Thieffry D., Thomas R., (1998), Qualitative analysis of gene networks. Proceedings of the Pacific Symposium on Biocomputing, World Scientific, Singapore, pp. 77–88.

[160] Thomas R., (1973), Boolean formalisation of genetic control circuits, Journal of Theoretical Biology, 42, 565–583.

[161] Thomas R., (1991), Regulatory networks seen as asynchronous automata: a logical description, J. Theor. Biol., 153, 1–23.

[162] Thomas R., Kaufman M., (2001), Multistationarity, the basis of cell differentiation and memory. I. Structural conditions of multistationarity and other nontrivial behavior, Chaos 11(1), 170–179.

[163] Thomas R., Kaufman M., (2001), Multistationarity, the basis of cell differentiation and memory. II. Logical analysis of regulatory networks in terms of feedback circuits, Chaos 11(1), 180–195.

[164] Thomson M., Gunawardena J., (2009), The rational parameterisation theorem for multisite post-translational modification systems, J. Theor. Biol. 261(4), 626–636.

[165] Thomson M., Gunawardena J., (2009), Unlimited multistability in multisite phosphorylation systems, Nature 460(7252), 274–277.

[166] Veliz-Cuba A., Jarrah A., Laubenbacher R., (2010), Polynomial algebra of discrete models in systems biology, Bioinformatics, 26(13):1637–1643.

[167] Veliz-Cuba A., Arthur J., Hochstetler L., Klomps V., Korpi E. (2011), On the relationship of steady states of continuous and discrete models, Available at http://arxiv.org/pdf/1109.5197.pdf

[168] Vlad M. O., Ross J., (2009), Thermodynamically based constraints for rate coefficients of large biochemical networks, Wiley Interdisciplinary Reviews: Systems Biology and Medicine, 1(3):348–358.

[169] von Dassow G., Meir E., Munro E. M., Odell G. M., (2000), The segment polarity network is a robust developmental module, Nature, 406:188–192.

[170] Wang L., Sontag E., (2008), On the number of steady states in a multiple futile cycle, J. Math. Biol. 57(1), 29–52.

[171] Wang R. -S., Albert R., (2011), Elementary signaling modes predict the essentiality of signal transduction network components BMC Systems Biology 5:44.

[172] Werner S. L., Kearns J. D., Zadorozhnaya V., Lynch C., O'Dea E., Boldin M. P., Ma A., Baltimore D., Hoffmann A., (2008), Encoding NF-κB temporal control in response to TNF: distinct roles for the negative regulators IκBα and A20, Genes Dev. 22, 2093–2101.

[173] Xu Y., Gunawardena J., (2011) Realistic enzymology for post-translational modification: zero-order ultrasensitivity revisited, Submitted.

[174] Yue H., Brown M., Knowles J., Wang H., Broomhead D. S., Kell D. B., (2006), Insights into the behaviour of systems biology models from dynamic sensitivity and identifiability analysis: a case study of an NF-κB signalling pathway, Mol. BioSyst., 2, 640–649.

[175] Zhang S. Q., Kovalenko A., Cantarella G., Wallach D., (2000), Recruitment of the IKK Signalosome to the p55 TNF receptor: RIP and A20 bind to Nemo (IKKg) upon receptor stimulation, Immunity 12, 301–311.

Notation

$\mathfrak{s}_1, \ldots, \mathfrak{s}_s$	species
$x_1, \ldots, x_s$	molar concentration of the species
s	number of species
$y_1, \ldots, y_m$	complexes
m	number of complexes
κ_{ij}	constant for the reaction from complex y_i to complex y_j
r	number of edges (reactions)
G	directed graph
V	set of vertices of the digraph G
$\mathscr{R}$	set of edges (reactions) of the digraph G
$\mathscr{S}$	set of species
$\mathscr{C}$	set of complexes
x^{y_i}	$x_1^{y_{i1}} x_2^{y_{i2}} \cdots x_s^{y_{is}}$
$\mathcal{K}_{y \to y'}$	rate function for reaction $y \to y'$
$\mathbb{R}$	the field of real numbers
$\mathbb{R}_{\geq 0}$	the nonnegative real numbers
$\mathbb{R}_{>0}$	the positive real numbers
$\mathbb{C}$	the field of complex numbers
$\mathbb{Z}$	the ring of integers
$\mathbb{Z}_{\geq 0}$	the nonnegative integers
$\mathbb{N}$	the positive integers
$\mathbb{Q}$	the field of rational numbers
$G = (V, \mathscr{R}, Y)$	chemical reaction network
$G = (V, \mathscr{R}, \mathcal{K}, Y)$	chemical reaction system with kinetics $\mathcal{K}$
$y' - y$	reaction vector corresponding to reaction $y \to y'$
$\kappa_{y \to y'}$	rate constant for the reaction $y \to y'$
f	species formation rate function
$\dot{\mathbf{x}}$	derivative of $\mathbf{x}$ with respect to time
$f_1, \ldots, f_s$	derivatives of $x_1, \ldots, x_s$ with respect to time: $\dot{x_1}, \ldots, \dot{x_s}$
$\mathcal{L}(G)$	the Laplacian matrix of the digraph G
†	transpose
$\Psi(x)$	$(x^{y_1}, \cdots, x^{y_m})^\dagger$
Y	$s \times m$ matrix of non-negative integers (y_{ji})
Σ	complex-to-species rate matrix $Y \cdot \mathcal{L}(G)$

E	kinase
F	phosphatase
S_i	substrate with i phosphate groups attached
$J_{\Sigma\Psi}$	ideal generated by $f_1, \ldots, f_s$
T	spanning tree of a strongly connected graph
$V(T)$	vertices of the tree T
$\mathscr{R}(T)$	edges of the tree T
K_i	a special polynomial in the rate constants (defined in §2.2)
l	number of linkage classes
ρ_G	generator of the kernel of $\mathcal{L}(G)$ for the strongly connected graph G
$\overline{G}$	directed graph with the strong linkage classes of G as nodes
G_u	strong linkage class
$G_1, \ldots, G_{\mathfrak{t}}$	terminal strong linkage classes of G
$\mathfrak{t}$	number of terminal strong linkage classes
$\rho^1, \ldots, \rho^T$	generators of the kernel of $\mathcal{L}(G)$, with $support(\rho^i) = G_i$
$\mathcal{S}$	stoichiometric subspace
$\mathcal{P}_{x^0}$	stoichiometric compatibility class
δ_D	dynamic deficiency ($\dim(\ker Y \cap \text{Image } \mathcal{L}(G))$)
δ_S	structural deficiency ($m - \dim \mathcal{S} - l$)
$\mathcal{S}^\perp$	orthogonal complement of the stoichiometric subspace
$\mathcal{I}_k$	vector space of type 1 complex-linear invariants on $y_1, \ldots, y_k$
d	dimension of $\ker(\Sigma)$
B	$m \times d$ matrix whose columns form a basis of $\ker(\Sigma)$
B'	$k \times d$ sub-matrix of B consisting of the first k rows
$\mathfrak{d}$	$\text{rank}(B')$
$I_1, I_2, \ldots, I_d$	partition of $\{1, 2, \ldots, m\}$
l_i	cardinality of I_i
$b^1, b^2, \ldots, b^d$	basis of $\ker(\Sigma)$ with $\text{supp}(b^i) = I_i$
κ^*_{ij}	particular choice of rate constants
j_0	$\min I_j$
$\ln x$	$(\ln(x_1), \ln(x_2), \ldots, \ln(x_s))$
Δ	a matrix whose columns are the differences $(y_{j_1} - y_{j_2})^\dagger$
Θ_κ	a (row) vector with $\left(\ln \frac{b^j_{j_1}}{b^j_{j_2}}\right)_{\forall j_1, j_2 \in I_j, \forall 1 \le j \le d}$ as entries
U	matrix with entries in $\mathbb{Z}$ whose columns form a basis of $\ker(\Delta)$
A	matrix of maximal rank in $\mathbb{Z}^{w \times s}$ with $\ker(A) = \langle y_{j_2} - y_{j_1} \rangle_{j_1, j_2 \in I_j,\, 1 \le j \le d}$
w	rank of A
A_i	i-th column of A
$\tilde{x}$	particular positive steady state
$\mathfrak{t}$	vector in $\mathbb{R}^w$
E_{tot}	total amount of kinase E in the n-site phosphorylation system
F_{tot}	total amount of phosphatase F in the n-site phosphorylation system
S_{tot}	total amount of substrate in the n-site phosphorylation system
$\mathcal{C}$	$(E_{\text{tot}}, F_{\text{tot}}, S_{\text{tot}}) \in \mathbb{R}^3_{>0}$
$\mathcal{P}_\mathcal{C}$	stoichiometric compatibility class for the conservation relations defined by $\mathcal{C}$

Σ_n	complex-to-species rate matrix for the n-site phosphorylation system
Σ'_n	submatrix of Σ_n obtained by deleting the first and the last two rows, and the $(n+1)$-st and $(2n+2)$-nd columns
$C(j)$	the column of Σ'_n which corresponds to the j-th column of Σ_n after deleting the first row and the last two
Σ''_n	the submatrix of Σ'_n formed by its first $3n$ columns
D	$\det(\Sigma''_n)$
$D_{\ell(j)}$	minus the determinant of the matrix obtained by replacing $C(\ell(j))$ by $C(3n+j+2)$ in Σ''_n
C_G	incidence matrix of the graph G
Γ	$Y\,C_G$
$\mathcal{Y}$	educt-complex matrix
$\phi(x)$	vector of educt complex monomials
M	matrix whose columns generate the cone $\ker(\Gamma) \cap \mathbb{R}^r_{\geq 0}$
$\widetilde{G} = (V, \widetilde{\mathscr{R}}, Y)$	the associated undirected graph of G
$\widetilde{C}$	cycle of $\widetilde{G}$
C^+	the cycle in G in a certain direction
C^-	the cycle in the opposite direction (with respect to C^+)
$\mathcal{FB}_Y$	the algebraic variety of $\mathbb{R}^r_{>0}$ for which the system is formally balanced
$\mathcal{DB}_Y$	the algebraic variety of $\mathbb{R}^r_{>0}$ for which the system is detailed balanced
$\mathcal{CB}_Y$	the algebraic variety of $\mathbb{R}^r_{>0}$ for which the system is complex balanced
N	$\ker_{\mathbb{Z}}(Y \cdot C_G)$
G'	directed subgraph of G with only one direction for each pair of reactions (i,j), (j,i)
N'	$\ker_{\mathbb{Z}}(Y \cdot C_{G'})$
q_{ij}	$\frac{\kappa_{ij}}{\kappa_{ji}}$
N'_1	the $\mathbb{Z}$-module spanned by the cycles of the underlying undirected graph $\widetilde{G}$
N'_2	a direct complement of N'_1 in N' constructed in § 5.2.3
N_0	the lattice which expresses the fact that the (i,j)-th column of $Y \cdot C_G$ is minus its (j,i)-th column
N_i	the $\mathbb{Z}$-module in N isomorphic to N'_i for $i = 1, 2$
$\mathbb{Q}(\kappa)$	the field of the rational functions with coefficients over $\mathbb{Q}$ and variables determined by κ
$\mathbb{C}^*$	the complex numbers without zero
R	a real closed field
$V_X(J)$	the variety of the ideal J over the set X
$\sqrt{J}$	the radical of the ideal J
$(J : h^\infty)$	the saturation of the ideal J with respect to the polynomial h
$\mathfrak{m}$	the monomial formed by the product of all the variables in the polynomial ring
IKKne	cytoplasmic level of the neutral form of IKK
IKKa	cytoplasmic level of the active form of IKK
IKKi	cytoplasmic level of the inactive form of IKK

IκB	cytoplasmic level of IκBα
IκB$_n$	nuclear level of IκBα
IκB$_t$	IκB mRNA transcript level
IκB|NF-κB	cytoplasmic level of IκB|NF-κB complexes
A20	cytoplasmic level of A20 protein
A20$_t$	A20 mRNA transcript level
NF-κB$_n$	nuclear level of NF-κB
S	stimulus

Appendix 1: The functions

The transition functions ($f_{X,T+1}$, where X represents a node in the network and T stands for time) were built using Singular [35], via interpolation over the finite field of three elements $\mathbb{F}_3$. Each function was based on the corresponding table shown below, where X_T denotes the state of node X at time T. The last column of each table exhibits the image of the function for the values shown in the columns on the left.

IκB function:

We separate the transition table into two parts. First, we consider the case IKKa=0, and build the function $f_{I\kappa B,1}$. We then consider the case IKKa=1 and form the function $f_{I\kappa B,2}$. And, finally, we build the function $f_{I\kappa B,T+1}$ as a function of $f_{I\kappa B,1}$ and $f_{I\kappa B,2}$, considering all the levels of IKKa. We repeat a similar reasoning for the rest of the functions.

If IKKa=0:

$I\kappa B_T$	$(I\kappa B_n)_T$	$(I\kappa B_t)_T$	$f_{I\kappa B,1}$
0	0	0	0
1	0	0	0
2	0	0	1
0	1	0	0
1	1	0	1
2	1	0	1
0	2	0	1
1	2	0	1
2	2	0	2
0	0	1	1
1	0	1	1
2	0	1	2
0	1	1	1
1	1	1	1
2	1	1	2
0	2	1	1
1	2	1	2
2	2	1	2
0	0	2	2
1	0	2	2
2	0	2	2
0	1	2	2
1	1	2	2
2	1	2	2
0	2	2	2
1	2	2	2
2	2	2	2

If there is no IKKa then the level of cytoplasmic IκB depends on the previous level of IκB (considering a half life of one time step), the previous level of IκB$_n$ considering that it can shuttle to and from the nucleus and that is generally more concentrated in the nucleus, and the level of IκB$_t$.

If IKKa=1:
$f_{I\kappa B,2} = (I\kappa B_t)_T$;

$f_{I\kappa B,T+1} = (1 + IKKa_T)((1 + 2IKKa_T)f_{I\kappa B,1} + 2IKKa_T f_{I\kappa B,2})$;

Notice that, if $IKKa_T = 0$, then $f_{I\kappa B} = f_{I\kappa B,1}$; if $IKKa_T = 1$, then $f_{I\kappa B} = f_{I\kappa B,2}$; and if $IKKa_T = 2$, then $f_{I\kappa B} = 0$.

IκB|NF-κB:

We consider first the income from the nucleus, and form the function $f_{I\kappa B|NF-\kappa B,1}$:

$(NF-\kappa B_n)_T$	$(I\kappa B_n)_T$	$f_{I\kappa B\|NF-\kappa B,1}$
0	0	0
1	0	0
2	0	0
0	1	0
1	1	1
2	1	1
0	2	0
1	2	1
2	2	2

$f_{I\kappa B|NF-\kappa B,T+1}$:

$I\kappa B\|NF-\kappa B_T$	$IKKa_T$	$f_{I\kappa B\|NF-\kappa B,1}$	$f_{I\kappa B\|NF-\kappa B,T+1}$
0	0	0	0
1	0	0	1
2	0	0	2
0	1	0	0
1	1	0	0
2	1	0	1
0	2	0	0
1	2	0	0
2	2	0	0
0	0	1	1
1	0	1	2
2	0	1	2
0	1	1	1
1	1	1	1
2	1	1	2
0	2	1	1
1	2	1	1
2	2	1	1
0	0	2	2
1	0	2	2
2	0	2	2
0	1	2	2
1	1	2	2
2	1	2	2
0	2	2	2
1	2	2	2
2	2	2	2

If there is some IKKa the contribution of the nuclear components to the IκB|NF-κB complex in the cytoplasm depends on the minimum of IκB$_n$ and NF–κB$_n$.

The level of IκB|NF-κB complex in the cytoplasm depends on the previous level of the complex (non enzymatic degradation is considered much lower than degradation triggered by IKKa), the level of IKKa that triggers degradation of IκB from the complex and the contribution

of complex from the nucleus.

IKKa:

With Stimulus:

$IKKa_T$	$A20_T$	$IKKne_T$	$f_{IKKa,1}$
0	0	0	0
1	0	0	0
2	0	0	1
0	1	0	0
1	1	0	0
2	1	0	0
0	0	1	1
1	0	1	1
2	0	1	2
0	1	1	1
1	1	1	1
2	1	1	1
0	0	2	2
1	0	2	2
2	0	2	2
0	1	2	2
1	1	2	2
2	1	2	2

If there is stimulus IKKa level depends on:

- **the previous level of IKKa considering spontaneous inactivation.**
- **the previous level of IKKn that can be transformed to IKKa through activation by the stimulus.**
- **The previous level of A20 that inactivates all previous IKKa but not the new one that is generated from IKKn in the presence of stimulus.**

Without Stimulus:

$IKKa_T$	$A20_T$	$f_{IKKa,2}$
0	0	0
1	0	0
2	0	2
0	1	0
1	1	0
2	1	1

In the absence of stimulus IKKa level depends on the previous level of IKKa and the level of A20 that inactivates IKKa, but not on IKKn.

$f_{IKKa,T+1} = S_T f_{IKKa,1} + (S_T + 2)^2 f_{IKKa,2}$;

Notice that, if $S_T = 1$, then $f_{IKKa,T+1} = f_{IKKa,1}$; and if $S_T = 0$, then $f_{IKKa,T+1} = f_{IKKa,2}$.

NF-κB$_n$:

We consider first the income of NF-κB from the cytoplasm:

$(I\kappa B\|NF-\kappa B)_T$	$IKKa_T$	$f_{NF-\kappa B,1}$
0	0	0
1	0	0
2	0	0
0	1	0
1	1	1
2	1	1
0	2	0
1	2	1
2	2	2

The income of NF-κB from the cytoplasm to the nucleus depends on the level of complex in the cytoplasm and the activity of IKKa that triggers IκB degradation. Full activation of IKK induces complete degradation of IκB and translocation of NF-κB to the nucleus.

If $f_{NF-\kappa B,1}$=0 (there is no income of NF-κB):

$(NF-\kappa B_n)_T$	$(I\kappa B_n)_T$	$f_{NF-\kappa B,2}$
0	0	0
1	0	1
2	0	2
0	1	0
1	1	0
2	1	2
0	2	0
1	2	0
2	2	0

If there is no income of NF-κB to the nucleus, the level of NF-κB$_n$ depends on the previous level of NF-κB$_n$ and IκB$_n$ that can shuttle NF-κB$_n$ to the cytoplasm. If IκB$_n$=1 it does not reduce NF-κB$_n$ content significantly if NF-κB$_n$=2, but if IκB$_n$ =2 it takes out all the NF-κB$_n$.

$f_{NF-\kappa B,T+1} = 2 + (f_{NF-\kappa B,1}+1)(f_{NF-\kappa B,2}+1)(2f_{NF-\kappa B,1}f_{NF-\kappa B,2}+1)$;

If $f_{NF-\kappa B,1} = 0$, $f_{NF-\kappa B,T+1} = f_{NF-\kappa B,2}$; if $f_{NF-\kappa B,1} = 2$, $f_{NF-\kappa B,T+1} = 2$; if $f_{NF-\kappa B,1} = 1$, $f_{NF-\kappa B,T+1} = (f_{NF-\kappa B,2})^2 + 1$. That is: if there is no income of NF-κB from the cytosol, then NF-κB$_n$ only depends on the existing NF-κB$_n$ and IκB$_n$; if the income is maximal, then the state of NF-κB will be two (disregarding the previous nuclear state); if the income equals 1, then the state of NF-κB$_n$ will be just 1, if there is no contribution from the nucleus, or 2, if there is any nuclear contribution.

IκB$_n$:

$I\kappa B_T$	$(I\kappa B_n)_T$	$(NF-\kappa B_n)_T$	$f_{I\kappa B_n,T+1}$
0	0	0	0
1	0	0	1
2	0	0	2
0	1	0	1
1	1	0	1
2	1	0	2
0	2	0	1
1	2	0	2
2	2	0	2
0	0	1	0
1	0	1	1
2	0	1	2
0	1	1	0
1	1	1	1
2	1	1	1
0	2	1	1
1	2	1	1
2	2	1	2
0	0	2	0
1	0	2	1
2	0	2	2
0	1	2	0
1	1	2	1
2	1	2	2
0	2	2	0
1	2	2	1
2	2	2	2

The level of IκB$_n$ is influenced by the free shuttle of IκB between nucleus and cytoplasm considering a preference of IκB to be in the nucleus, and the previous level of NF-κB$_n$ as it is taken out to the cytoplasm by IκB$_n$.

IκB$_t$:

$(NF-\kappa B_n)_T$	$(I\kappa B_t)_T$	$f_{I\kappa B_t,T+1}$
0	0	0
1	0	1
2	0	2
0	1	0
1	1	1
2	1	2
0	2	1
1	2	2
2	2	2

IκB$_t$ depends on the previous level of IκB$_t$ considering a half life of one time step, and the level of NF-κB$_n$ that triggers transcription of the IκB gene. The contribution of NF-κB$_n$ is considered proportional to

its level.

A20:

$f_{A20,T+1} = ((A20_t)_T)^2$;

The level of A20 depends on the presence of its transcript. We only consider presence or absence of A20.

That is: there will be A20 if and only if there is $A20_t$.

$A20_t$:

$f_{A20_t,T+1}$ is like $f_{I\kappa B_t,T+1}$, but instead of $(I\kappa B_t)_T$ we consider $(A20_t)_T$. The regulation of A20 expression was considered similar to the IκB expression.

IKKi:

$IKKa_T$	$IKKi_T$	$f_{IKKi,T+1}$
0	0	0
1	0	1
2	0	2
0	1	1
1	1	2
2	1	2
0	2	2
1	2	2
2	2	2

The level of IKKi depends on the previous level of IKKi and the IKKa that can be subject to inactivation.

IKKne:

$IKKne_T$	S_T	$f_{IKKne,T+1}$
0	0	1
1	0	1
2	0	2
0	1	1
1	1	1
2	1	1

The level of IKKn depends on the previous level of IKKn (considering that IKKn is constantly translated form its transcript) and the presence of a signal that activates IKK transforming all previous IKKn to IKKa.

Appendix 2: Fixed points for S=0

In this appendix we list the fixed points of the system for S=0. The last column shows how many initial states terminate in the corresponding fix point.

IκB	IκB|NF-κB	IKKa	NF-κB$_n$	IκB$_n$	IκB$_t$	S	A20	A20$_t$	IKKi	IKKne	Total
0	0	0	0	0	0	0	0	0	0	1	12
0	0	0	0	0	0	0	0	0	0	2	6
0	0	0	0	0	0	0	0	0	1	1	24
0	0	0	0	0	0	0	0	0	1	2	12
0	0	0	0	0	0	0	0	0	2	1	108
0	0	0	0	0	0	0	0	0	2	2	54
0	0	0	0	1	0	0	0	0	0	1	36
0	0	0	0	1	0	0	0	0	0	2	18
0	0	0	0	1	0	0	0	0	1	1	96
0	0	0	0	1	0	0	0	0	1	2	48
0	0	0	0	1	0	0	0	0	2	1	750
0	0	0	0	1	0	0	0	0	2	2	375
0	0	2	0	0	0	0	0	0	2	1	18
0	0	2	0	0	0	0	0	0	2	2	9
0	0	2	0	1	0	0	0	0	2	1	144
0	0	2	0	1	0	0	0	0	2	2	72
0	1	0	0	0	0	0	0	0	0	1	12
0	1	0	0	0	0	0	0	0	0	2	6
0	1	0	0	0	0	0	0	0	1	1	12
0	1	0	0	0	0	0	0	0	1	2	6
0	1	0	0	0	0	0	0	0	2	1	12
0	1	0	0	0	0	0	0	0	2	2	6
0	1	0	0	1	0	0	0	0	0	1	48
0	1	0	0	1	0	0	0	0	0	2	24
0	1	0	0	1	0	0	0	0	1	1	108
0	1	0	0	1	0	0	0	0	1	2	54
0	1	0	0	1	0	0	0	0	2	1	444
0	1	0	0	1	0	0	0	0	2	2	222
0	2	0	0	0	0	0	0	0	0	1	12
0	2	0	0	0	0	0	0	0	0	2	6
0	2	0	0	0	0	0	0	0	1	1	12

Fixed points for S=0 (continued).

IκB	IκB|NF-κB	IKKa	NF-κB$_n$	IκB$_n$	IκB$_t$	S	A20	A20$_t$	IKKi	IKKne	Total
0	2	0	0	0	0	0	0	0	1	2	6
0	2	0	0	0	0	0	0	0	2	1	12
0	2	0	0	0	0	0	0	0	2	2	6
0	2	0	0	1	0	0	0	0	0	1	60
0	2	0	0	1	0	0	0	0	0	2	30
0	2	0	0	1	0	0	0	0	1	1	108
0	2	0	0	1	0	0	0	0	1	2	54
0	2	0	0	1	0	0	0	0	2	1	156
0	2	0	0	1	0	0	0	0	2	2	78
1	0	0	0	1	0	0	0	0	0	1	72
1	0	0	0	1	0	0	0	0	0	2	36
1	0	0	0	1	0	0	0	0	1	1	168
1	0	0	0	1	0	0	0	0	1	2	84
1	0	0	0	1	0	0	0	0	2	1	408
1	0	0	0	1	0	0	0	0	2	2	204
1	0	0	0	2	0	0	0	0	0	1	36
1	0	0	0	2	0	0	0	0	0	2	18
1	0	0	0	2	0	0	0	0	1	1	84
1	0	0	0	2	0	0	0	0	1	2	42
1	0	0	0	2	0	0	0	0	2	1	132
1	0	0	0	2	0	0	0	0	2	2	66
1	1	0	0	1	0	0	0	0	0	1	204
1	1	0	0	1	0	0	0	0	0	2	102
1	1	0	0	1	0	0	0	0	1	1	552
1	1	0	0	1	0	0	0	0	1	2	276
1	1	0	0	1	0	0	0	0	2	1	2364
1	1	0	0	1	0	0	0	0	2	2	1182
1	1	0	0	2	0	0	0	0	0	1	36
1	1	0	0	2	0	0	0	0	0	2	18
1	1	0	0	2	0	0	0	0	1	1	36
1	1	0	0	2	0	0	0	0	1	2	18
1	1	0	0	2	0	0	0	0	2	1	36
1	1	0	0	2	0	0	0	0	2	2	18
1	2	0	0	1	0	0	0	0	0	1	336
1	2	0	0	1	0	0	0	0	0	2	168
1	2	0	0	1	0	0	0	0	1	1	768
1	2	0	0	1	0	0	0	0	1	2	384
1	2	0	0	1	0	0	0	0	2	1	1404
1	2	0	0	1	0	0	0	0	2	2	702
1	2	0	0	2	0	0	0	0	0	1	36
1	2	0	0	2	0	0	0	0	0	2	18
1	2	0	0	2	0	0	0	0	1	1	36

Fixed points for S=0 (continued).

IκB	IκB|NF-κB	IKKa	NF-κB$_n$	IκB$_n$	IκB$_t$	S	A20	A20$_t$	IKKi	IKKne	Total
1	2	0	0	2	0	0	0	0	1	2	18
1	2	0	0	2	0	0	0	0	2	1	36
1	2	0	0	2	0	0	0	0	2	2	18
2	0	0	0	2	0	0	0	0	0	1	168
2	0	0	0	2	0	0	0	0	0	2	84
2	0	0	0	2	0	0	0	0	1	1	276
2	0	0	0	2	0	0	0	0	1	2	138
2	0	0	0	2	0	0	0	0	2	1	384
2	0	0	0	2	0	0	0	0	2	2	192
2	1	0	0	2	0	0	0	0	0	1	348
2	1	0	0	2	0	0	0	0	0	2	174
2	1	0	0	2	0	0	0	0	1	1	588
2	1	0	0	2	0	0	0	0	1	2	294
2	1	0	0	2	0	0	0	0	2	1	1032
2	1	0	0	2	0	0	0	0	2	2	516
2	2	0	0	2	0	0	0	0	0	1	1500
2	2	0	0	2	0	0	0	0	0	2	750
2	2	0	0	2	0	0	0	0	1	1	2964
2	2	0	0	2	0	0	0	0	1	2	1482
2	2	0	0	2	0	0	0	0	2	1	10056
2	2	0	0	2	0	0	0	0	2	2	5028